Effects of hypoxia and hypercapnia on thermal tolerance: an integrative assessment on the green abalone (*Haliotis fulgens*).

Auswirkungen von Hypoxie und Hyperkapnie auf Temperaturtoleranz: Eine integrative Bewertung der Grünen Abalone (*Haliotis fulgens*)

Dissertation
zur Erlangung des akademischen Grades
Dr. rer.nat.

Dem Fachbereich 2 Biologie/Chemie
der Universität Bremen
vorgelegt von

Miguel Ángel Tripp Valdez

Bremen

- **Gutachter:** Prof. Dr. Hans O. Pörtner
  Alfred Wegener Institute Helmholtz Centre for Polar and Marine Research
  Integrative Ecophysiology
  Am Handelshafen 12
  27570 Bremerhaven, Germany

- **Gutachter:** Prof. Dr. Wilhelm Hagen
  Marine Zoology
  University of Bremen (NW2A)
  28334 Bremen, Germany

- **Prüfer:** Dr. Reinhard Saborowski
  Alfred Wegener Institute Helmholtz Centre for Polar and Marine Research
  Functional Ecology
  Am Handelshafen 12
  27570 Bremerhaven, Germany

- **Prüfer:** Prof. Dr. Matthias Wolff
  Leibniz-Center for Tropical Marine Ecology (ZMT)
  Theoretical Ecology and Modelling
  Fahrenheitstr. 6
  28359 Bremen, Germany

Tag des Promotionskolloquiums: 14.12.2018

TABLE OF CONTENTS

LIST OF FIGURES

LIST OF TABLES

ABBREVIATIONS

AWI	Alfred Wegener Institute
CIBNOR	Centro de Investigaciones Biológicas del Noroeste, S.C.
COX	Cytochrome c oxidase
CS	Citrate synthase
CSR	Cellular stress response
CT_{max}	Critical thermal maximum
DTNB	5,5′-Dithiobis(2-nitrobenzoic acid)
ENO	Enolase
ETS	Electron transport system
GADPH	Glyceraldehyde 3-phosphate dehydrogenase
GLR	Glutathione reductase
GST	Glutathione-S-transferase
HK	Hexokinase
HR	Heart rate
Hsp	Heat shock proteins
LDH	Lactate dehydrogenase
NAD	Nicotinamide adenine dinucleotide
OCLTT	Oxygen- and capacity- limited thermal tolerance
PEPCK	Phosphoenolpyruvate carboxykinase
pH_{NBS}	pH measurement on The National Bureau of Standards scale
PK	Pyruvate kinase
qPCR	quantitative polymerase chain reaction
T_c	Critical temperature
T_d	Denaturation temperature
T_p	*Pejus* temperature
TCA	Tricarboxylic acid cycle
TDH	Tauropine dehydrogenase
$\dot{M}O_2$	Oxygen consumption rate

SUMMARY

With the rise in atmospheric concentration of greenhouse gases, most marine ecosystems are facing increasing seawater temperatures, ocean acidification and a higher frequency or intensity of extreme warming events. Moreover, rising seawater temperature is expected to interact more frequently with falling oxygen levels (hypoxia) and increased CO_2 concentration (hypercapnia). Both drivers may impose constraints on physiological mechanisms that define thermal limits thereby increasing the vulnerability towards warming in marine ectotherms.

The green abalone *Haliotis fulgens* is an economically important marine gastropod at the Pacific Coast of Mexico. In recent years, an increased frequency and intensity of environmental extremes, such as El Niño events and upwelling of highly hypoxic or hypercapnic water, has been associated with mass mortality events, threatening natural populations. Within this framework, the present study aimed at investigating the thermal tolerance and the underlying metabolic and molecular response in multiple tissues of *H. fulgens* under conditions of hypoxia and hypercapnia. Juvenile abalone (25.05 ± 2.57 mm shell length) were exposed to a temperature ramp (from 18 °C to 32 °C; +3 °C day^{-1}) under hypoxia (50% air saturation) and hypercapnia (~1000 µatm PCO_2), both individually and in combination; the conditions are based on natural oxygen declines occurring along the Baja California Peninsula and PCO_2 values predicted by the end of the century, respectively.

Hypoxia constrained the whole-organism oxygen consumption at moderate temperature (27 °C) paralleled by the accumulation of anaerobic metabolites (succinate, lactate, and alanine) in gill and hepatopancreas, suggesting a limitation in the aerobic capacity and reduced thermal tolerance. On the contrary, warming under hypercapnic exposure did not constrain oxygen consumption, but the higher Q_{10} in metabolic rate and the increased levels of anaerobic metabolites at the warmest temperature (32 °C) indicate some stimulatory effect on metabolism. Finally, warming under combined hypoxia and hypercapnia resulted in negative synergistic impacts with an accumulation of anaerobic metabolites at a lower temperature (24 °C), followed by a depletion of metabolites, declining whole animal oxygen consumption indicating some hypometabolic state, and finally, the onset of muscular failure and death at the warmest temperature.

Further analyses of the cellular metabolic state in abalone musculature showed that the anaerobic capacities for energy production, evidenced by lactate dehydrogenase (LDH) and tauropine dehydrogenase (TDH) enzymes capacities, was largely unaffected by temperature with or without additional drivers. Besides, limited accumulation of lactate and tauropine indicates an unchanged mode of energy production. Under exposure to either hypoxia or hypercapnia, capacities of the mitochondrial key enzyme citrate synthase (CS) decreased with initial warming, in line with basic compensatory adjustment to warming, but returned to control levels at 32 °C. Under exposure to warming combined with both hypoxia and hypercapnia concomitantly, CS overcame thermal compensation and remained stable throughout the warming ramp. This indicates active mitochondrial regulation to sustain aerobic energy production through the warming ramp, despite a hypometabolic state. Valine accumulated at the highest temperature in all analyzed tissues, which may suggest increased rates of protein degradation and use of the released amino acids to fuel the tricarboxylic acid cycle.

A de novo transcriptome assembly for *H. fulgens* was constructed using a pool of multiple tissues from two animals: one unstressed (18 °C under normoxic normocapnia) and one stressed (32 °C under hypoxic hypercapnia). The comparison of these transcriptomes and subsequent qPCR analyses of genes involved in the cellular stress response showed a strong induction of the molecular chaperones (Hsp70), antioxidant genes and apoptosis inhibitors, indicating that protein synthesis is shifted towards damage prevention and repair systems. A strong and coordinated induction of several Hsp70 isoforms already at 30 °C in gill and muscle matches with limits of long-term performance and resistance to acute thermal stress in natural populations. Genes involved in energy metabolism were mostly down-regulated with warming under all experimental conditions. However, warming under combined hypoxia and hypercapnia kept the CS gene expression unchanged, reflected in a similar pattern in muscle enzyme capacity, thereby highlighting the active regulation of mitochondrial activity as a way to maintain aerobic energy production.

Altogether, the results from this thesis demonstrate that *H. fulgens* is able to tolerate short-term exposure to thermal stress for up to one week and 32 °C, involving a coordinated heat shock response, the antiapoptotic system, and an active mitochondrial regulation to sustain aerobic energy production. However, moderate hypoxia (50% air saturation) already increased the abalone thermal sensitivity by setting constraints in aerobic metabolism at the systemic level and stimulating anaerobiosis in the gill. Such thermal sensitivity was exacerbated under combined hypoxia and hypercapnia, as an overshoot of energy demand at a moderate temperature (24 °C) was followed by a hypometabolic state which finally led to muscular failure at the highest temperature.

The integrative approach from the molecular to the systemic levels and the use of different tissues in the present thesis allowed to identify promising indicators of physiological and metabolic traits responding sensitively to environmental challenges. Therefore, the identified traits and the approaches presented here represent a powerful tool in the assessment of the sensitivity of natural populations of green abalone to climate change.

ZUSAMMENFASSUNG

Mit dem Anstieg des Treibhausgases in der Atmosphäre sind die meisten marinen Ökosysteme ansteigenden Meerwassertemperaturen, Ozeanversauerung und einer erhöhten Frequenz und Intensität extremer Hitzeereignisse ausgesetzt. Darüber hinaus wird erwartet, dass es im Zuge steigender Wassertemperaturen zu einer verstärkten Überschneidung mit verminderten Sauerstoff- (Hypoxie) und erhöhten CO_2-Werten (Hyperkapnie) im Meerwasser kommen wird. Diese beiden Faktoren mögen physiologische Mechanismen, die die Temperaturgrenzen definieren, eingrenzen, und dadurch die Verletzlichkeit mariner ektothermer Tiere gegenüber Erwärmung verstärken.

Die grüne Abalone *Haliotis fulgens* ist ein ökonomisch wichtiger, mariner Gastropod an der pazifischen Küste Mexikos. In jüngster Vergangenheit wurden Massensterben, die zu einer Bedrohung der natürlichen Populationen führten, mit einer erhöhten Frequenz und Intensität von Umweltextrema, sei es El Niño oder der Auftrieb hypoxen oder hyperkapnischen Wassers, in Zusammenhang gebracht. Innerhalb dieses Rahmens diente die vorliegende Studie dem Zweck, das Temperaturtoleranzfenster der grünen Abalone unter dem Einfluss von Hypoxie und Hyperkapnie zu untersuchen und zugrundeliegende Mechanismen und molekulare Reaktionen in verschiedenen Geweben zu erarbeiten. Dazu wurden juvenile Abalone (20 – 30 mm Schalenlänge) einer Temperaturrampe (von 18 °C bis 32 °C, +3 °C Tag^{-1}) und zusätzlich Hypoxie (50% Luftsättigung) und Hyperkapmie (~1000 µatm PCO_2) jeweils einzeln oder in Kombination ausgesetzt. Die Sauerstoffwerte beruhten dabei auf natürliche Sauerstoff-Abnahmen entlang der Kalifornischen Halbinsel, während der PCO_2-Spiegel für das Ende des Jahrhunderts vorausgesagt wird.

Hypoxie schränkte den Sauerstoffverbrauch des Gesamttieres bei mittleren Temperaturen (27 °C) ein, was mit einer Akkumulation anaerober Metaboliten (Succinat, Lactat, Alanin) in den Kiemen und in der Mitteldarmdrüse einherging und eine Limitierung aerober Kapazitäten und eine reduzierte Temperaturtoleranz nahelegt. Im Gegensatz dazu schränkte Hyperkapnie den Sauerstoffverbrauch unter Erwärmung nicht ein, und ein erhöhter Q_{10} der metabolischen Rate und ein Anstieg anaerober Metaboliten bei der höchsten Temperatur (32 °C) deuten vielmehr auf eine Stimulation des Metabolismus hin. Die Kombination von Hypoxie und

Hyperkapnie schließlich resultierte in negativen synergistischen Effekten: einer Akkumulation anaerober Metaboliten bei niedriger Temperatur (24 °C) folgte eine Abreicherung der Metaboliten und eine Reduktion des Ganztier-Sauerstoffverbrauchs, die auf einen hypometabolen Zustand hindeutete und die schließlich in Muskelversagen und zum Tod bei der höchsten Temperatur mündeten.

Die weiteren Analysen des zell-metabolischen Status im Muskel der grünen Abalone ergaben, dass die Kapazitäten der anaeroben Energieproduktion, untersucht anhand der Enzymkapazitäten der Lactat-Dehydrogenase (LDH) und der Tauropin-Dehydrogenase (TDH), größtenteils nicht durch Temperatur oder die weiteren Faktoren beeinflusst waren. Daneben deuten die begrenzte Anreicherung von Lactat und Tauropin auf eine gleichbleibende Energieproduktion hin. Während der Exposition gegenüber jeweils einem der Faktoren Hypoxie oder Hyperkapnie verringerte sich die Kapazität des mitochondrialen Schlüsselenzyms Citratsynthase (CS) zunächst mit Erwärmung, im Einklang mit einer grundlegenden Temperaturkompensation, um dann bei 32 °C wieder auf Kontrollniveau zurückzukehren. Bei Wärmeexposition und gleichzeitiger Anwesenheit von Hypoxie und Hyperkapnie fehlte eine solche anfängliche Temperaturkompensation, und die CS-Kapazitäten blieben während der gesamten Wärmerampe konstant. Diese Ergebnisse weisen auf eine aktive Regulation der Mitochondrien zur Erhaltung einer aeroben Energieproduktion während der Temperaturrampe hin, trotz eines hypometabolischen Status. Valin wurde in allen analysierten Geweben bei der höchsten Temperatur angereichert, was auf einen verstärkten Proteinabbau und einer Nutzung der freigesetzten Aminosäuren als Brennstoff für den Citrat-Zyklus hindeutet.

Aus dem Pool verschiedener Gewebe wurden für zwei Tiere jeweils ein Transkriptom erstellt und de novo assembliert, eines von einem ungestressten Tier (18 °C ,Normoxie, Normokapnie) und eines von einem gestressten Tier (32 °C, Hypoxie zusammen mit Hyperkapnie). Anhand des Vergleichs beider Transkriptome und nachfolgender quantitativen Realtime-PCR von Genen der zellulären Stressantwort konnte eine starke Induktion molekularer Chaperone (Hsp70), anti-oxidativer Gene und von Apoptose-Inhibitoren nachgewiesen werden, was auf eine Verschiebung der Protein-Synthese hin zur Schadensvorbeugung und zu Reparatursystemen hindeutet. Eine ausgeprägte und koordinierte Induktion verschiedener Hsp70-Isoformen bereits bei 30 °C sowohl in Kieme als auch im Muskel steht mit der Limitierung der Langzeitleistungsfähigkeit und Resistenz natürlicher Populationen bei dieser Temperatur im Einklang. Gene, die am Energiestoffwechsel beteiligt sind, waren in der Wärme größtenteils herunterreguliert, unabhängig von der Anwesenheit der weiteren Faktoren. Allerdings blieb die Expression des CS-Gens unter den kombinierten Bedingungen -in Übereinstimmung mit den Enzym-Kapazitäten im Muskel- konstant, was eine aktive Regulation der mitochondrialen Kapazitäten zur Erhaltung einer aeroben Energieproduktion nochmals untermauert.

Zusammenfassend belegen die Ergebnisse der vorliegenden Arbeit, dass *H. fulgens* in der Lage ist, eine kurzzeitige Exposition gegenüber Temperaturstress von bis zu einer Woche und 32 °C zu tolerieren. Dabei sind eine koordinierte Hitzeschockantwort, das anti-apoptotische System, sowie die aktive Regulation der Mitochondrien zur Erhaltung einer aeroben Energieproduktion beteiligt. Allerdings erhöhte bereits eine moderate Hypoxie (50% Luftsättigung) die Temperaturempfindlichkeit der grünen Abalone, so dass Einschränkungen des aeroben Metabolismus auf systemischer Ebene manifestiert waren und es zu einer Stimulation der Anaerobiose in der Kieme kam. Diese Temperaturempfindlichkeit verschärfte sich in der Kombination von Hypoxie und Hyperkapnie, indem einem transient übersteigerten Energiebedarf bei moderaten Temperaturen (24 °C) ein hypometaboler Zustand folgte, der schließlich zu einem Muskelversagen bei der höchsten Temperatur führte.

Der in der vorliegenden Doktorarbeit verfolgte integrative Ansatz von der molekularen hin zur systemischen Ebene und die Verwendung verschiedener Gewebe erlaubte es, vielversprechende Indikatoren physiologischer und metabolischer Merkmale zu identifizieren, die auf Umwelteinflüsse sensitiv reagieren. Diese Merkmale und der verwendete Ansatz stellen somit ein leistungsfähiges Werkzeug dar, die Empfindlichkeit natürlicher Populationen gegenüber Klimawandel zu bemessen.

CHAPTER 1

INTRODUCTION

With the ongoing climate change, marine ecosystems are facing an increasingly interaction between multiple drivers, such as extreme temperature, reduction in O_2 availability (hypoxia), and high CO_2 concentration (hypercapnia). The present thesis investigates whether thermal tolerance of green abalone juveniles (*Haliotis fulgens*) –an economically important marine gastropod– is reduced under hypoxia and hypercapnia, independently and in combination, and identify physiological and molecular indicators of impacted thermal tolerance. The results from this work will contribute to the assessment of green abalone sensitivity to climate change and will deepen the understanding on the impacts of multiple stressors on the thermal tolerance in marine ectotherms.

1.1 Temperature and thermal tolerance

With the increasing concentration of anthropogenic CO_2 and other greenhouse gases in the atmosphere, many marine ecosystems are facing changes in their abiotic parameters beyond what is expected from their natural variability with negative impacts in their structure and functioning (Pörtner et al., 2014; Henson et al., 2017). Among the multiple environmental drivers influenced by climate change, temperature constitutes the main driving force causing changes in species distribution and abundance in marine ecosystems (Somero, 2005). Over the last 39 years, oceans have warmed at an average rate of >0.1 °C per decade in the upper 75 m (Pörtner et al., 2014). Furthermore, an increasing frequency and intensity of extreme warming events are expected as a response to greenhouse warming (Cai et al., 2014; Jacox et al., 2016). As progressive climate change intensifies the pressure on marine organisms, a mechanistic understanding on the organism's thermal limits and functional capacities is essential to address their vulnerability and adaptation potential to current and projected future conditions (Somero et al., 2016).

In ectothermic species, temperature controls virtually every aspect of their physiology, including the stability of macromolecules and the dynamics of chemical reactions (Hochachka

and Somero, 2002). Consequently, thermal optima and limits of thermal tolerance of a species are co-defined by the evolutionary adaptations in physiological, biochemical, and molecular traits to a certain thermal niche –and thermal variation therein (Hochachka and Somero, 2002; Somero, 2002, 2004). Investigations of the potential impacts of increasingly extreme seawater temperature, as projected in future scenarios, require addressing systemic to molecular mechanism and how these combine to shape the limits of thermal tolerance (Pörtner, 2002; Pörtner and Knust, 2007; Pörtner et al., 2017).

A framework linking such mechanisms is provided by the concept of **o**xygen- and **c**apacity-**l**imited **t**hermal **t**olerance (OCLTT). This concept has been developed in recent years based on studies in marine fishes and invertebrates and propose that the first line of thermal limitations in ectotherms is set at the highest level of organismal complexity, initiated by a limitation of the cardiorespiratory system to cover an increased temperature-dependent oxygen demand, resulting in declining levels of fluid PO_2 (Fig.1.1). The mismatch between oxygen demand and supply marks the reduction of aerobic performance in organisms exposed to temperatures beyond pejus (T_p) and extended thermal tolerance can be achieved by mechanisms which minimize energy costs, such as metabolic depression, the induction of the antioxidant systems and molecular chaperones, and the transition to anaerobic metabolism once the aerobic capacity vanishes at the critical temperature (T_c; Fig.1.1: Pörtner et al. 2017). These mechanisms can ensure survival at temperatures higher than upper T_p, but only for a limited time, as resources to counteract the progressive rise of oxidative and thermal stress are gradually depleted and energy becomes limiting once aerobic scope begins to fall (Sokolova, 2013).

Accordingly, thermal thresholds described by the OCLTT concept implies that functional limitations of organisms exposed to thermal extremes take place before the more conventional measures of upper thermal limits, such as the critical thermal maxima (CT_{max}) becomes relevant. CT_{max} is defined as the temperature at which the animal loses its ability to escape from conditions that will lead to its death and is characterized by the onset of muscular spams and loss of righting response (Lutterschmidt and Hutchison, 1997). While there is evidence of downward shift of CT_{max} with declining oxygen availability (Healy and Schulte, 2012; Verberk et al., 2013), these limits lie at the edge or outside of the aerobic power budget and from the thresholds described by OCLTT and therefore, the relationship between insufficient aerobic metabolism and CT_{max} remains obscure (Pörtner et al., 2017).

1.2 Metabolic response to thermal stress

In the context of the OCLTT concept, assessment of thermal thresholds indicating a transition from an optimum to a sublethal condition requires the measurement of physiological and

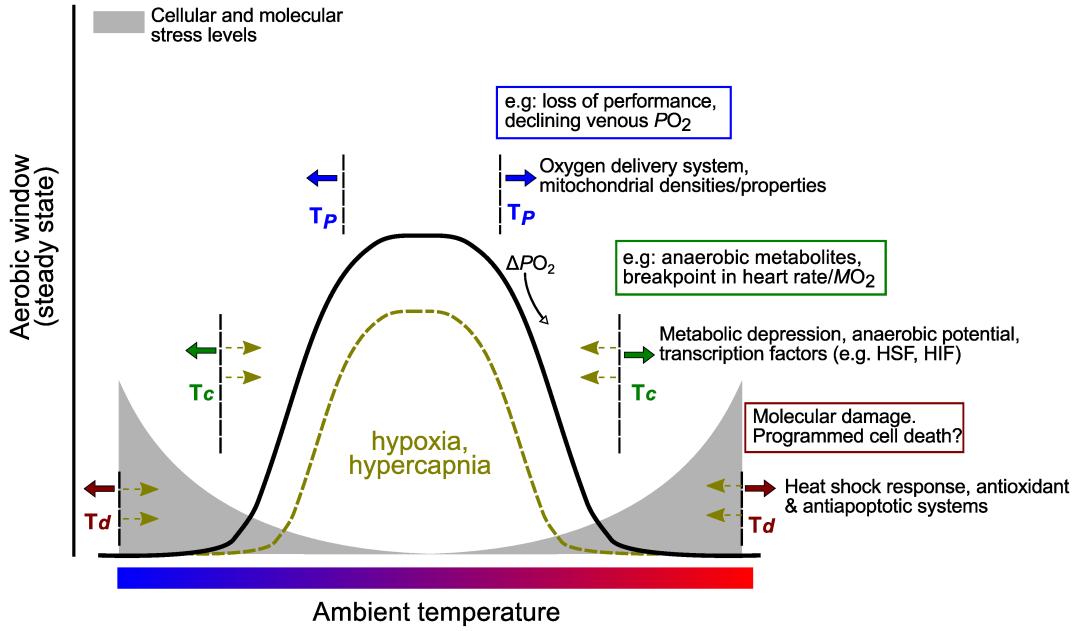

Figure 1.1 OCLTT conceptual model exemplified for a temperate aquatic animal under acute warming (After Pörtner et al. 2017). The range of active thermal tolerance is supported by optimized oxygen supply to tissues between low and high pejus temperatures (T_p). Towards the warmth, transition to passive thermal tolerance is indicated by the development of a mismatch between oxygen supply and temperature-dependent oxygen demand, leading to a decline in PO_2 in body fluids (solid black arrow) and increasing levels of cellular and molecular stress (grey area). With further warming, loss of aerobic capacity is indicated by the transition to anaerobic metabolism at the critical temperature (T_c). As increased levels of oxidative and thermal stress threaten to damage molecular structures, the activation of the heat shock response and induction of antioxidant and cellular repair systems support or extend the transition to acutely lethal conditions at T_d. Unidirectional shifts in thermal thresholds can be achieved by adjustments in mechanisms to sustain oxygen supply and tissue functional capacity as well as transcriptome and molecular adjustments to prevent and repair cellular damage and re-establish cellular homeostasis. Ambient hypoxia and hypercapnia can induce lower functional capacities and systemic oxygen tensions causing a narrowing of the thermal window (green arrows)

cellular parameters associated to the aerobic capacity of an organism (see Pörtner et al. 2017 for a review).

Oxygen consumption rate (MO_2) and cardiac performance are processes associated to the respiratory capacity, therefore, breakpoints in MO_2 and heart rate (HR) constitute early indicators of temperature-dependent constraints in oxygen supply beyond T_p (Frederich and Pörtner, 2000; Zittier et al., 2015; Chen et al., 2016; Han et al., 2017).

Cellular regulation upon environmental stress is accompanied by changes in the kinetic characteristic of regulatory enzymes important in certain metabolic pathways (Simpfendörfer et al., 1995; Hochachka and Somero, 2002). Capacities of key metabolic enzymes, such as

pyruvate kinase (PK), lactate dehydrogenase (LDH) and opine dehydrogenases also provide evidence of changes in the cellular metabolic state towards warming stress (Anestis et al., 2008; Feidantsis et al., 2009; Han et al., 2017). Adjustments in mitochondrial capacity for aerobic energy production represent another key functional trait (Lucassen et al., 2003; Windisch et al., 2011; Strobel et al., 2013). Consequently, modulation of mitochondrial enzymes such as citrate synthase (CS) and cytochrome- c- oxidase (COX) reflect changes in the aerobic capacity for energy production (Windisch et al., 2011; Vosloo et al., 2013a; Strobel et al., 2013), whereas increasing activities of glycolytic enzymes, such as PK and LDH at extreme warming would reflect a reorganization of the metabolic machinery with an enhanced dependence on carbohydrate metabolism and anaerobic pathways for energy production (Anestis et al., 2008; Feidantsis et al., 2009; Han et al., 2017).

Changes in the cellular metabolic state are accompanied by the depletion or accumulation of certain metabolic compounds, reflecting alterations of a given metabolic pathway (Aggio et al., 2010). Accordingly, the accumulation of anaerobic end products such as succinate, acetate and propionate during anaerobic mitochondrial ATP generation, and lactate or the opines by cytosolic glycolysis, constitutes early indicators of the onset of anaerobiosis when temperature surpass T_c (Frederich and Pörtner, 2000; Verberk et al., 2013; Zittier et al., 2015; Lu et al., 2016; Han et al., 2017; Clark et al., 2017). In this context, metabolomics constitute a powerful tool at identifying not only the accumulation of anaerobic metabolites, but also changes in amino acids composition and organic osmolytes which are also associated to the cellular response to heat stress (Viant et al., 2003).

In line with a systemic to molecular hierarchy of limitations of thermal tolerance (OCLTT), the transition to sublethal conditions triggers the induction of the heat shock response to avoid the loss of protein structural integrity and function at the borders of the thermal window (Feder and Hofmann, 1999). The heat shock proteins (Hsp) are a large subset of proteins termed molecular chaperones and play an important role in thermotolerance by preventing inappropriate protein aggregations and by folding or disassembly misfolded or aggregated proteins (Feder and Hofmann, 1999; Morris et al., 2013). Undoubtfully, such tasks of the molecular chaperones are essential under normal cellular conditions, preventing new proteins to form abnormal aggregations; however, stressful environmental conditions increase the potential of macromolecules to function irregularly, thereby impying higher demand for molecular chaperones which improves heat resistance of an organism for a limited time (Morris et al., 2013). Consequently, accumulation of Hsps, particularly from members of the Hsp70 family, are widely used as markers of cellular stress during extreme warming in a large number of species from different phylogenetic lineages including marine invertebrates (Piano et al., 2002; Anestis et al., 2008; Farcy et al., 2009; Ioannou et al., 2009; Katsikatsou et al., 2012).

1.3 Multiple environmental drivers: the effect of hypoxia and hypercapnia on thermal tolerance

With increasing concentration of anthropogenic CO_2, additional environmental drivers other than temperature are rapidly emerging as important threats to marine ecosystems. Among these, falling oxygen concentration (hypoxia) and increasing CO_2 (hypercapnia) –with the concomitant reduction in seawater pH– had received strong research attention during the last decade due their potential deleterious impacts on marine ecosystems (Pörtner et al., 2014; Gattuso et al., 2015; Henson et al., 2017).

Shoaling of hypoxic and hypercapnic/acidic water masses have being more frequently reported in many marine ecosystems, such as the California Current Large Marine Ecosystem (Feely et al., 2008; Hauri et al., 2009; Bakun et al., 2015) with negative consequences for benthonic marine organisms which cannot escape from such adverse conditions (e.g. Micheli et al. 2012). Additionally, with an increase in stratification from sea-surface warming, the lower oxygen solubility and enhanced respiration of animals due to higher metabolic rates results in the progressive development of hypoxia and increasing concentration of CO_2 (Gattuso et al., 2015; Henson et al., 2017). According to anthropogenic CO_2 emission scenarios, declining oxygen levels and a higher concentration of seawater CO_2 will not only continue, but there will be an increasing interaction between extreme warming, hypoxia, and hypercapnia events beyond the natural variability (Pörtner et al., 2014; Gattuso et al., 2015).

Both hypoxia and hypercapnia can negatively impact the energy metabolism of marine organisms affecting their sensitivity to temperature (Fig1.1; Pörtner 2010). Seawater hypoxia decreases oxygen availability and thereby causes a narrowing of the thermal windows due to exacerbated body fluid hypoxemia and compromising aerobic ATP generation below a critical threshold (Pörtner and Grieshaber, 1993). This finally results in metabolic depression to reduce the ATP-dependent cellular processes under conditions of reduced energy availability (Le Moullac et al., 2007b; Anestis et al., 2010). Moreover, reduced systemic oxygen levels have been associated to increased oxidative stress (Heise, 2006) and induce the activation of molecular chaperones to prevent protein damage (Anestis et al., 2010).

Similarly, high levels of CO_2 cause negative effects on energy homeostasis and disturbing acid-base homeostasis may also induce metabolic depression at high PCO_2 levels (Pörtner et al., 2000). At moderate PCO_2 levels, a stimulatory effect of CO_2 on HR and MO_2 has been described in the spider crab (*Hyas areneus*) and blue mussel (*Mytilus edulis*), but nevertheless, a breakpoint in both rates occurs at lower temperature than animals under normocapnia, indicating a negative effect on thermal tolerance (Walther et al., 2009; Zittier et al., 2015). Overall, hypoxia and hypercapnia can potentially induce constraints in active tolerance to

warming and, therefore, increase their vulnerability to thermal extremes (Walther et al., 2009; Lannig et al., 2010; Verberk et al., 2013; Zittier et al., 2015; Lu et al., 2016).

1.4 Transcriptional regulation in response to environmental factors

During adverse environmental conditions, organisms must be responsive through physiological and cellular adjustments to persist the environmental challenge which involves a constant feedback between the systemic and the molecular levels. The extent to which organisms are able to adjust their physiological capacities in response to changing environmental conditions is based on genomic mechanism, including altered patterns of gene expression (Hochachka and Somero, 2002; Buckley et al., 2006; Kassahn et al., 2009; Windisch et al., 2014).

With the development of new technologies in DNA sequencing and transcriptional profiling tools such as cDNA microarrays and RNA-seq, it is now possible to explore a large set of genes and pathways which are involved in acute stress and thermal acclimation (Buckley et al., 2006; Windisch et al., 2014). Most notably, the continuous improvements in bioinformatic tools for *de novo* transcriptome assembly procedures and transcript quantification provide highly-effective methods to simultaneously investigate changes in gene expression patterns from a wide range of cellular processes in non-model organisms or species were the genome is not yet available (Whitehead, 2012; Haas et al., 2013; Papetti et al., 2016).

A major complication with gene expression profiles to investigate the response to environmental insults comes with the integration –and attribution– of changes at gene expression level to functional changes at higher levels of biological organization, as not all increases in the amount of mRNA for a gene are reflected in the production of a protein encoded by that gene (addressed in Stillman and Armstrong 2015). Nonetheless, under extreme thermal stress, there is evidence of a correlation between mRNA and protein synthesis from molecular chaperones (Buckley et al., 2006). Additionally, studies in marine fishes have demonstrated that changes in expression patterns in mitochondrial genes match to fine-tuning of mitochondrial activity and changes in fuel utilization for the tricarboxylic acid cycle (TCA) (Lucassen, 2006; Eckerle et al., 2008; Windisch et al., 2011; Schiffer et al., 2014). Moreover, a *de novo* transcriptomic assembly from thermally challenged limpets (*Callana toreuma*) identified transcriptional changes leading to an enhanced glycolytic potential for anaerobic energy production near to the breakpoint temperature of cardiac performance (Han et al., 2017). Therefore, addressing transcriptional changes involved in energy metabolism, mitochondrial activity or protection mechanisms could be effectively used to access the cellular response of organisms during the transition to sublethal thresholds.

1.5 Green abalone as a model organism

1.5.1 Generalizations on abalone biology

Abalone (*Haliotis* spp.) are marine gastropods belonging to the family Haliotidae (Rafinesque 1815) inhabiting tropical and temperate waters around the world. The main characteristics of the family are the auriform and circular outline of the shell, a convex back which ranges from highly arched to extremely flattened, a row of rounded shell perforations overlying the respiratory cavity, and the enormous shell aperture (Fig.1.2; Cox 1962). Abalone are gonochoric, with no apparent sexual dimorphism. Minimum reproductive size varies according to the species and geographic zone, *e.g.* green abalone can reach sexual maturation at 95 or 110 mm shell length according to site (Shepherd et al., 1991).

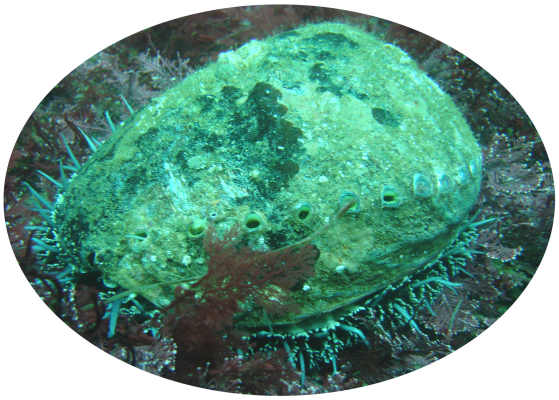

Figure 1.2 Green abalone (*Haliotis fulgens*). Photo credit: D. Vega, 2014.

In Mexico, abalone species occurs only at the Pacific coast of the Peninsula of Baja California but the main stock is located in the central part of the peninsula (Searcy-Bernal et al., 2010). Abalone distribution is associated to macroalgae beds such as *Macrocystis Sp.*, *Eisenia Sp.*, *Sargassum Sp.*, *Gelidium Sp.*, etc., as well as other benthic organisms like sea urchins establishing trophic relationship or protection and competition for substrate and food (Cox, 1962). Vertical distribution of the different species is determined by thermal tolerance in larvae and juveniles, and by food availability and wave action in adults (Cox, 1962).

Abalone have an open circulatory system but there is some degree of directionality and hemolymph can be shunted around the body to various organs under stressful conditions (Morash and Alter, 2015). Moreover, oxygen transport is extremely species specific, and this likely correlates to the diverse habitats and large latitudinal range over which abalone exist (tropical to temperate). The abalone's bipectinated gill is responsible for practically all oxygen

uptake under both normoxia and hypoxia (Taylor and Ragg, 2005), however, some studies indicate that only about 50% of oxygen extracted from the gills enters the hemolymph (Morash and Alter, 2015). At least in some abalone species, the aerobic metabolic scope appears to be met primarily by circulatory adjustments at the left gill, which at rest is highly perfusion limited (Ragg and Taylor, 2006).

The large muscular foot in abalone functions in attachment and locomotion. Although the foot region comprises approximately 66% of the body mass, it receives only 27% of the cardiac output (Jorgensen et al., 1984). Consequently, abalones are well known to frequently rely on anaerobic metabolism for energy production during periods of emersion or intense muscular activity (Gäde, 1983; Omolo et al., 2003; Venter et al., 2016, 2018a,b). LDH and tauropine dehydrogenase (TDH) are the main elements in anaerobic energy production in abalone; however, energy production through this pathways is a short-term mechanism to supplement additional energy which will be limited above certain temperatures (Morash and Alter, 2015).

1.5.2 Abalone fisheries and natural populations along the Baja California Peninsula

Total global landings from abalone fisheries have gradually decreased from almost 20,000 metric tons (mt) in the 1970s to only about 6,500 mt in 2015 (Cook, 2016). This phenomenon reflects a decline in natural populations, mainly due to overexploitation, illegal harvesting, increased predation, and habitat degradation (Morales-Bojórquez et al., 2008; Searcy-Bernal et al., 2010; Cook, 2016).

In the mexican Pacific, seven abalone species are distributed along the west coast of the Baja California Peninsula: *H. fulgens*, *H. corrugata*, *H. cracherodii*, *H. rufescens*, *H. sorenseni*, *H. assimilis* and *H. walallensis*. However, around 70% of the total catches are of *H. fulgens*, making it the most important commercial abalone species in Baja California, followed by *H. corrugata*, which comprise the remaining 30% of catches (Morales-Bojórquez et al., 2008)).

In line with global trends, the mexican abalone stock is in a critical state. Nonetheless, abalone fishery in Baja California remains a very lucrative activity worth approximately 5.7 million dollars in 2013. However, after dramatic declines in captures during the 1970s and 1980s, there is a great concern regarding the sustainability of the resource. If fisheries continue under current management models, there is a risk that these abalone species could be assigned as threatened species (e.g. as vulnerable, threated, endangered or critically endangered; Morales-Bojórquez et al. 2008.

Additionally, the impacts of climate variability have recently been recognized as a crucial factor in the dynamics of abalone populations in Baja California, particularly during strong El Niño events (Guzman del Proo et al., 2003; Rodríguez-Valencia et al., 2004; Searcy-Bernal

et al., 2010). Temperatures up to 31 °C (+4 °C anomaly from monthly average) were registered in abalone fisheries zones during a strong El Niño in 1997, severely reducing the population size of this species (Guzman del Proo et al., 2003). Similarly, declines in the physiological condition and lower recruitment of *H. fulgens* and *H. corrugata* were associated with severe El Niño conditions (Rodríguez-Valencia et al., 2004). In addition to the negative impacts of extreme warming events, important declines of abalone populations in the central region of Baja California have been associated to additional drivers, particularly due to frequent events of reduced oxygen availability. In 2010, oxygen concentration of 4.6 mgO_2 L^{-1} (~45% air saturation) were recorded for up to 23 days and concentrations below 2 mgO_2 L^{-1} (~20% air saturation) were recorded for 14 continuous hours in an abalone fishing zone. Such conditions were later associated with declines in abalone population around the area (Micheli et al., 2012). A subsequent study with *H. fulgens* from the same region, animals were kept inside cages in the field during summer of two consecutive years with constant food supply (kelp). Mortality rates were higher during a year with more strong hypoxic events (< 4 mgO_2 L^{-1}) compared to a year with less hypoxic events (Boch et al., 2018). Finally, increasing PCO_2 in seawater with concomitant acidification has also emerged as a detrimental challenge for benthic marine organisms along the California Current including abalone species (Turi et al., 2016).

1.5.3 Haliotis fulgens

Green abalone (*H. fulgens*: Philippi 1845; Fig.1.2) inhabits the coastal zone from Point Conception to Magdalena Bay along Baja California Peninsula (Fig.1.3). It is a shallow water species inhabiting the rocky areas from low intertidal to at least 9 m and with a maximum of 18 m (Cox, 1962). Several studies had addressed the effect of temperature of *H. fulgens*, focusing on its effect on larval and juvenile growth, with some variable results. At the coast of California, US, optimal temperature for larval fall in the range of 20 – 24 °C while juveniles display optimum growth in the range 24 – 28 °C (Leighton et al., 1981). Similarly, *H. fulgens* from the Pacific Coast of Mexico displayed higher growth rates in the range of 20 – 28 °C (Ponce-Díaz et al., 2004) and the critical thermal maxima was estimated at 33.6 °C, which was defined as the temperature, where attachment failed in 50% of the animals (Diaz et al., 2006). Beside the economic importance of the green abalone and the current environmental threats on natural stocks along the Peninsula of Baja California, the effects of additional drivers, like hypoxia and hypercapnia, and their impacts on thermal sensitivity has not been addressed as in other abalone species (Harris, 1999; Harris et al., 2005; Vosloo et al., 2013c,a; Kim et al., 2013).

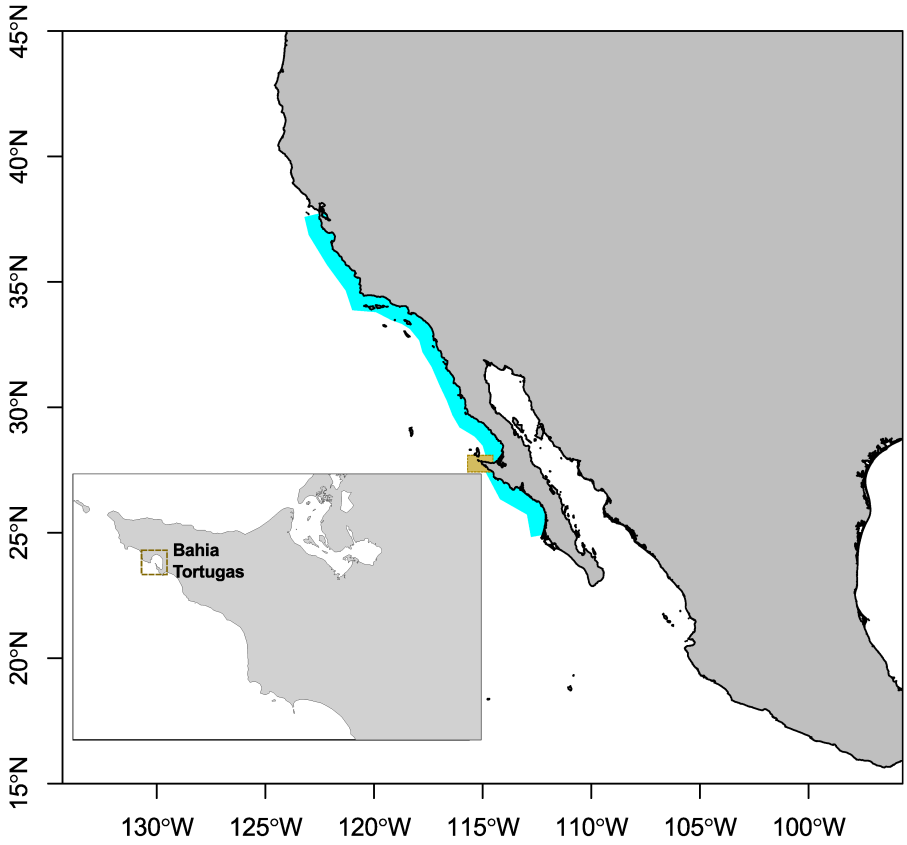

Figure 1.3 Distribution of *H. fulgens* (indicated in blue). A zoom-in is made for the region of Bahia Tortugas, Mexico, where abalone juveniles were obtained

1.6 Objectives of the study

With climate change, increasing seawater temperature is more frequently accompanied by declining oxygen availability and increasing CO_2 concentration, which can potentially constraint the mechanisms of thermal tolerance in marine ectotherms. Increasing thermal sensitivity due to hypoxia or hypercapnia have already been demonstrated in numerous organisms, however, impacts of the simultaneous presence of multiple drivers such as temperature, hypoxia, and hypercapnia considering the functional integration of several molecular to systemic levels are poorly addressed. This is of particular importance for natural populations of the economically important green abalone. Along the Pacific Coast of the Baja California Peninsula, extreme warming events, as well as anomalies in oxygen availability and seawater chemistry has been associated to numerous mass mortality events in the last two decades. This has raised serious concerns regarding the effects of climate change on abalone natural populations. Therefore, this study was designed to investigate the metabolic mechanisms involved in shaping the thermal tolerance window in *H. fulgens* from Baja California and assess the impacts of the

simultaneous presence of reduced oxygen concentration (hypoxia: 50% air saturation) and high PCO_2 (hypercapnia: 1,000 µatm PCO_2), both individually and in combination. The chosen oxygen and CO_2 values used in this study are based on reduced oxygen conditions that have been observed in some abalone fishery sites for several consecutive days (Micheli et al., 2012) and projected scenario of seawater PCO_2 reached by 2100 (Pörtner et al., 2014).

More specifically, this study aims to answer the following questions:

a) Will the presence of hypoxia and hypercapnia, as individual stressors and in combination, change the metabolic response of thermally challenged green abalone, resulting in a narrowing of the thermal window?

To address this question, green abalone juveniles (25.05 ± 2.57 mm shell length) were exposed to a temperature ramp under hypoxia and hypercapnia, independently and in combination. Whole-organism metabolic rate was used to assess temperature-induced limitation in the aerobic capacity whereas metabolic profiles of gill and hepatopancreas via ^{1}H-NMR were used as indicators of the onset of anaerobiosis and main impacts in the cellular metabolic state during the experimental conditions.

b) Is the reduction of the abalone sublethal and lethal thresholds and subsequent loss of muscular function related to impacted aerobic and anaerobic capacity or due to impacts in molecular protection mechanisms?

For this question, we focused on the muscular metabolic state and heat shock response to elucidate the downward shift in the upper thermal limit CT_{max}in green abalone during warming under combined hypoxia and hypercapnia. Changes in the cellular metabolic state and the aerobic and anaerobic potentials were assessed through changes in the activity of metabolic enzymes (CS, LDH and THD) and accumulation of anaerobic end products. The heat shock response was assessed through changes in expression patterns of six Hsp70 genes trough qPCR and Hsp70 protein induction trough immunoblot analysis.

c) Which are the transcriptional modifications in key regulatory processes involved in the warming-induced cellular and metabolic response of green abalone under the different experimental conditions?

A de novo transcriptome assembly of green abalone juveniles was constructed as a reference to explore the molecular bases involved in metabolic and cellular responses to stress. Changes in genes expression patterns of selected genes were evaluated in tissues which displayed contrasting metabolic responses (gill and muscle) through qPCR. Correlation networks

were constructed to identify tissue-specific and experiment-specific (hypoxia, hypercapnia, combination) patterns of gene expression.

CHAPTER 2

MATERIAL & METHODS

The following section includes the description of the experimental setup which was the base for all the publications derived from this thesis, as well as generalizations regarding the tissue samples analysis (i.e. metabolite extraction, protein extraction, RNA extraction, etc). Particularities regarding samples analysis and statistical methods are included in each publication.

2.1 Animal collection and maintenance

In March 2013, 224 juvenile green abalones (*Haliotis fulgens*) were provided by a fishery cooperative in Bahia Tortugas, an important abalone fishery site in Baja California Sur, Mexico (Fig.1.3), and transported in insulated boxes containing a bed of fresh kelp and frozen gel to the Northwest Biological Research Center (CIBNOR) in La Paz, Mexico. After arrival, abalones were cleaned from epibionts and kept at a density of one individual per liter in 100 L tanks with aerated filtered seawater at 12 °C and a salinity of 40 ppt. Every two days, water was renewed and abalones were fed *ad libitum* with rehydrated kelps. Photoperiod was set to a 12:12 hours light:dark cycle.

After pre-acclimation for 30 days, water temperature was increased from 12 °C to 18 °C (2 °C day^{-1}), which corresponds to the annual mean of the region of origin. At this point, feeding was switched to a commercial feed containing 35% protein, 10% fat, 3% raw fiber, 18% ash and 24% nitrogen-free extract, to exclude any possible effect of altered kelp nutritional status. During this acclimation period (73 days) no mortality was observed. Water temperature was constantly monitored by use of HOBO® pendant data loggers. Values of salinity and pH_{NBS} were monitored daily using an optic refractometer (Extech Instruments, Waltham, MA, USA) and a pH sensor (Neptune Systems, CA, USA). By the time of the experimental beginning, abalones were between 20 – 30 mm shell length and visual inspection of the gonads showed no signs of sexual maturation.

2.2 Experimental set-up

To investigate the impact of hypoxia (50% air saturation) and hypercapnia (1,000µatm PCO_2), individually and in combination on the thermal sensitivity of *H. fulgens*, four independent experiments were carried out consecutively. In each experiment, animals were exposed to an acute temperature ramp from 18 to 32 °C at 3 °C day^{-1} with a final temperature step of 2 °C only, as above 32 °C *H. fulgens* begin to lose the ability to attach to the ground (Diaz et al., 2006). The conditions for each experiment were as follows:

- **Experiment 1:** control exposure to normoxia (100% air saturation) and ambient normocapnia (400 µatm PCO_2)
- **Experiment 2:** hypoxia (50% air saturation) and normocapnia (400 µatm PCO_2)
- **Experiment 3:** normoxia (100% air saturation) and hypercapnia (1,000 µatm PCO_2)
- **Experiment 4:** Experiment 4: hypoxia (50% air saturation) and hypercapnia (1,000 µatm PCO_2)

Due to technical constraints and the limited number of green abalone juveniles available for this study, we treated individuals within tanks as independent samples. However, to account for any possible effect from the duration of the experiment or any potential variability in experimental conditions, each experiment was accompanied by incubation of a control group at 18 °C (Fig. 2.1). Experimental conditions were achieved by bubbling the water with air (normoxia) or with air mixed with N_2 (hypoxia) and/or CO_2 (hypercapnia). Dissolved oxygen (DO) levels were controlled by online monitoring using needle-type O_2-sensors (PreSens, GmbH, Regensburg, Germany) calibrated at the respective temperature. Water PCO_2 was controlled by measurements of water pH_{NBS} using a APEX Aquacontroller System (Neptune Systems, CA, USA). Temperature, salinity, pH_{NBS} and total alkalinity (TA) were determined twice a day. Total alkalinity was analyzed in triplicate water samples using potentiometric titration. Seawater PCO_2 was calculated from measured temperature, salinity, pH_{NBS} and TA values by use of the program CO_2Sys ver 01.05 (Lewis and Wallace, 1998) and equilibrium constants provided by Mehrbach et al. (1973) refitted by Dickson and Millero (1987), considering the formulation for KSO_4 by Dickson (1990).

In each of the experiments, a respirometry setup comprised 11 glass chambers for the experimental group (10 specimens and one blank) and seven respiration chambers for the control group (six specimens and one blank) all with 78 mL volume each. All chambers were mounted in a water bath with constant in- and outflow from two individual header tanks (250 L)

for the experimental and control groups, respectively. Individual abalones were placed inside each respiration chamber with a small plastic mesh grid to prevent the abalones from blocking the water flow. Water tanks were covered to minimize disturbances during experiments. After two hours of placing the animals in the chambers, the specific conditions (oxygen level and pH) in both header tanks were adjusted to intended values. Every two days, around 30% of the water from each tank was replaced to minimize the risk of toxic compounds accumulation. This was done using fresh seawater at the same temperature as in the experimental tank and with a slow inflow, to avoid strong fluctuations of oxygen and CO_2.

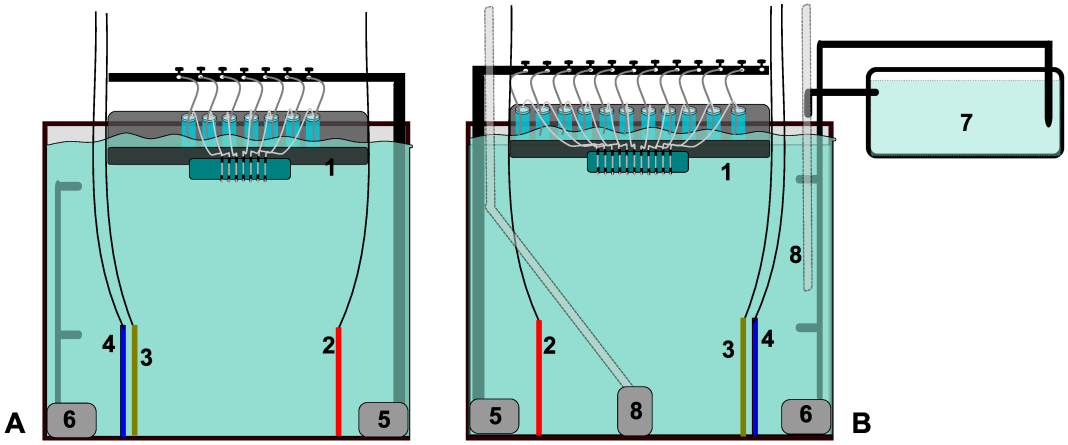

Figure 2.1 Graphic representation of the experimental set-up for A) control group at unchanged temperature and B) experimental group with the warming ramp. The systems consisted of 1) respirometry system submerse in the tank; 2) air diffuser, 3) N_2 diffuser, 4) CO_2 diffuser, 5) water pump directing seawater to the respirometry systems, 6) water pump for recirculation and to direct water to the side tank (7) and 8) water pump to direct seawater to the heating system and then back to the tank.

2.3 Metabolic rate

After 24 h of seawater adjustment in each experimental header tank (PO_2,pH) , standard metabolism of *H. fulgens* juveniles was determined via flow-through respirometry using microoptodes (PreSens, GmbH, Regensburg). The MO_2 from each animal was measured for 10 minutes in the morning (10:00 ± 1 h) and in the evening (22:00 ±1 h) by switching between animal chambers. The temperature in the experimental tank was increased every night (00:00 ±1 h) at a rate of 0.075 °C min^{-1} (Fig. 2.2). Oxygen microsensors were calibrated at each step of the temperature ramp using air-saturated seawater for 100% saturation and Na_2SO_3 (Fermont) saturated water for 0% saturation. Water flow was adjusted to 9 – 14 mL min^{-1} during MO_2 readings in a way that the animals consumed less than 25% of the oxygen from

the water. At the end of the experiment, abalones were removed from the chambers, and the soft body was isolated from the shells and freeze-dried (Telstar Mod Cryodos 50, Spain). The MO_2 was calculated with the formula:

$$MO_2 = (\Delta PO_2 * \beta O_2 * V_{\mathrm{fl}})/M_{0.79}$$

where MO_2 is oxygen consumption (µmol O_2 h^{-1} g DW^{-1}) normalized to dry soft tissue weight. ΔPO_2 is the difference in the partial pressure between inflowing and outflowing water. βO_2 is the temperature and salinity-specific oxygen capacity of water calculated from the Bunsen absorption coefficient considering vapor pressure according to the Campbell equation. V_{fl} is the flow rate (L h^{-1}), M is the dry soft mass (g), and 0.78 is the allometric coefficient

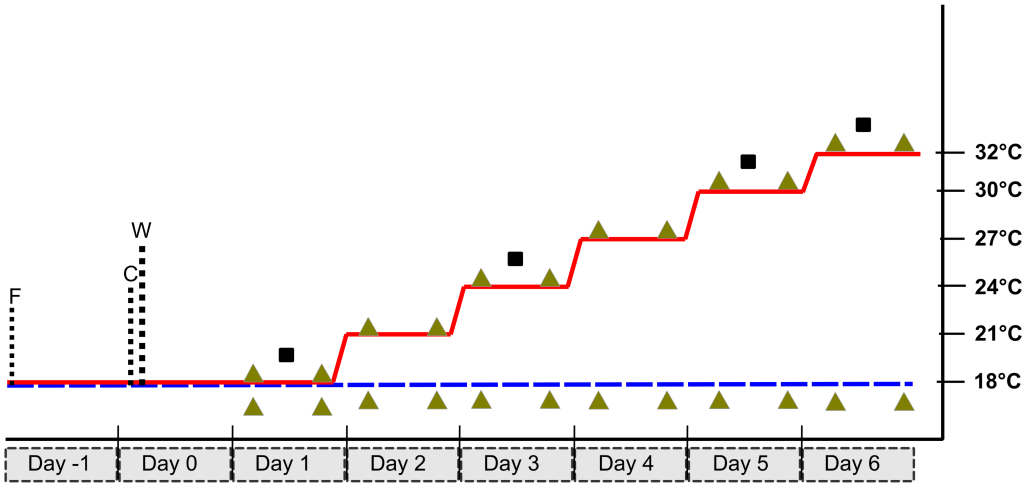

Figure 2.2 Graphic representation of the experimental design:The red line indicates the temperature (°C) for the experimental group; the blue line indicates the temperature (°C) for the control group (section 2.2); the triangles indicates the oxygen consumption measurements (2.3); the squares indicates tissue sampling (section 2.5).The F indicates the start of fasting; C indicates the point where organisms were placed inside the respiration chambers; W indicates the point where water parameters were adjusted according to the experiment (section 2.2).

2.4 Heart rate measurements

Heart rate in *H. fulgens* was assessed using a photoplethysmograph (isiTEC) connected to a digital recording device (PowerLab, Mountain View, CA, USA). The shell thickness of tested animals was reduced above the pericardial cavity region by grinding, and the plethysmograph

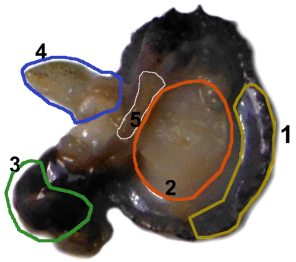

Figure 2.3 Collected *H. fulgens* tissues in this study: 1) epipodium, 2) muscle, 3) hepatopancreas, 4) mantle, 5) gills.

was glued to the shell with cyanoacrylate glue and covered with dental wax. To limit the movement of the animals and to prevent the sensor to detach from the shell, the animals were placed inside a histology cassette with a modified lid so that the sensor's cable was in a fixed position. Heart rate records were analyzed with the software LabChart Reader v8.09/30/2013. Care was taken to avoid pressure on the animal inside the cassette. However, the small size of the abalone juveniles (20 – 30 mm shell length) prevented an adequate use of this techniques and heart rate measurements were successful in only four animals: one under stable temperature (18 °C; normoxic normocapnia), one from experiment 3 (warming ramp; normoxic hypercapnia) and two from experiment 4 (warming ramp; hypoxic hypercapnia). Therefore, results from these measurements were not included in any of the published manuscripts but are included in the discussion.

2.5 Tissue collection

For evaluation of the impacts of warming under hypoxia, hypercapnia and their combination on cellular, biochemical and molecular process, each experimental setup contained an additional side tank of smaller capacity (50 L) with constant flow of seawater with the same conditions of temperature, oxygen and CO_2 as in the main tank (Fig. 2.1). Subsamples of 10 animals were taken at the 18 °C (day 1), 24 °C (day 3), 30 °C (day 5) and 32 °C (day 6) steps (Fig. 2.2). Samples of gill, muscle (adductor and foot), mantle, hepatopancreas, and epipodium were excised (Fig. 2.3) and immediately snap frozen in liquid nitrogen. Frozen samples were transported to the Alfred Wegener Institute (Bremerhaven, Germany) in boxes with dry ice and kept at -80 °C for further analyses. Tissue samples were used for the following analyses except for epipodium samples which are stored at -80 °C in the Alfred Wegener Institute.

2.6 Extraction of polar metabolites

Metabolomic analyses through proton nuclear magnetic resonance (^{1}H-NMR) were performed with polar metabolites extracted from the frozen tissues following the two-step methodology by

Wu et al. (2008). For gill samples (Publication I), pre-weighted frozen tissue was homogenized in 8 mL g^{-1} ice-cold methanol and 2.5 mL g^{-1} ice-cold water by one cycle of 20 s at 6,000 rpm using Precellys 24 (Bertin Technologies, France). This was followed by the addition of chloroform (8 mL g^{-1} tissue) and water (4 mL g^{-1} tissue). Afterward, the homogenate was vortexed for 20 seconds, incubated on ice for 10 minutes and centrifuged for 10 minutes at 3,000 rpm at 4 °C. For hepatopancreas (Publication I) and for muscle (Publication II) samples, frozen tissue was ground to a fine powder in liquid nitrogen followed by sonication in 4 mL g^{-1} ice-cold methanol and 0.85 mL g^{-1} ice-cold water for 5 min at 0 °C in a Branson Sonifier 450 (output control 8, duty cycle 50%) and addition of 4 mL g^{-1} chloroform and 2 mL g^{-1} water. Homogenate was vortexed for 20 seconds, incubated on ice for 10 minutes and centrifuged for 10 minutes at 3,000 rpm at 4 °C.

In all cases, the upper methanol layer containing the polar metabolites was transferred to a new 1.5 ml tube and dried overnight by a centrifugal vacuum concentration (RVC 2-18, Martin Christ Freeze dryers, GmbH, Germany) at room temperature. Prior to ^{1}H-NMR, dried samples were re-suspended in D_2O containing 0.05% Trimethylsilyl propionate (TSP; Sigma-Aldrich, St. Louis, USA) resulting in a final concentration of 0.3 g mL^{-1} of the initial tissue weight. D_2O provides a deuterium lock for the NMR spectrometer while the TSP acts as an internal standard. Samples were mixed and an aliquot of 50 µl was transferred to a 4 mm standard high resolution magic angle spinning (HRMAS) zirconia rotor.

2.7 ^{1}H-NMR spectroscopy

The ^{1}H-HRMAS NMR spectra for all tissue samples were acquired with a 9.4 T Avance III HD 400 WB spectrometer (Bruker Biospin GmbH, Germany). A Carr-Purcell-Meiboom-Gill (cpmg) sequence was used for gill and hepatopancreas samples (Publication I) while the Nuclear Overhauser Effect Spectroscopy (NOESY) sequence was used for muscle samples (Publication II). Spectra were analyzed for metabolite identification and quantification with Chenomx NMR suite 8.0 software (Chenomx Inc., Edmonton, Canada). Firstly, all the Fourier-transformed spectra were baseline corrected and calibrated to the internal reference (TSP at 0.0 ppm) followed by an exponential line broadening of 0.5 Hz. In all spectra, peaks were assigned with reference to chemical shift tables described for other abalone or related species (Viant et al., 2003; Rosenblum et al., 2005; Lu et al., 2016).

2.8 Enzyme activity measurements

Enzyme activities were determined for CS; involved in the aerobic capacity for energy production, and LDH and TDH representing anaerobic glycolysis, based on the following reactions:

$$\text{Acetyl}-\text{CoA} + \text{oxaloacetate} + \text{DNTB} + H_2O \xrightarrow{\text{CS}} \text{citrate} + \text{DNTB}-\text{S}-\text{CoA}$$

$$\text{NADH} + H^+ + \text{pyruvate} \xrightarrow{\text{LDH}} \text{lactate} + NAD^+ + H_2O$$

$$\text{NADH} + H^+ + \text{pyruvate} + \text{taurine} \xrightarrow{\text{TDH}} \text{tauropine} + NAD^+ + H_2O$$

Ground tissue subsamples were mixed in 10 volumes (w:v) of ice-cold extraction buffer (50mM imidazole-HCl, 1mM EDTA, 2 mM $MgCl_2$, pH 7.4) and sonicated for 5 min at 0 °C in a Branson Sonifier 450 (output control 8, duty cycle 50%). Homogenates were centrifuged at 4 °C for 20 min at 13,000 g, and the supernatant was transferred to a new tube and kept on ice for immediate assays. All enzymes were measured at 18 °C and 32 °C in a UV/VIS spectrophotometer (Beckman, Fullerton, CA, USA) in a total volume of 1 mL reaction buffer. Measurements were done in duplicate with different concentrations of the extract to ensure linearity. The final composition of the reaction mixtures for enzymes activities is listed in Table 2.1. Activity was calculated by recording the background activity of reaction buffer at specific absorbance for 1 min followed by the addition of the initiator to start the reaction. All enzyme activities were standardized to fresh tissue weight. Enzyme activities were calculated by the formula:

$$A_{FW} = \frac{\Delta E}{\Delta t * d * \varepsilon} * \frac{V_i}{V_{sample}} * \frac{V_{extract}}{FW}$$

where A_{FW} is the fresh tissue weight specific enzyme activity (µmol min^{-1} mg^{-1}), $\frac{\Delta E}{\Delta t}$ is the slope (min^{-1}), ε the extinction coefficient (µmol mL^{-1} cm^{-1}), d is the cuvette diameter (cm), V_i is cuvette volume (µL), V_{sample} the sample volume (mL), $V_{extract}$ the total volume of extract fraction (mL) and FW is the fresh tissue weight (mg).

Table 2.1 Reaction content for enzyme activity measurements

Enzyme	Reaction buffer (mmol L^{-1})	Initiator (mmol L^{-1})	Absorbance (nm)	Extinction coefficient (ε)
CS (EC.2.3.3.1)	Tris-HCl pH 8.0: 80 DTNB: 0.2 Acetyl-CoA: 0.3	oxaloacetate: 0.5	412	13.61
LDH (EC.1.1.1.27)	Imidazole-HCl pH 7.4: 80 EDTA: 1 $MgCl_2$:1 NADH: 0.15	pyruvate: 2.5	340	6.22
TDH (EC.1.5.1.23)	Imidazole-HCl pH 7.4: 80 EDTA: 1 $MgCl_2$:1 NADH: 0.15 taurine: 80	pyruvate: 2.5	340	6.22

2.9 Tauropine identification

Tauropine accumulation results from TDH activity, therefore it constitutes a good indicator of anaerobic glycolysis particularly in abalone musculature, where TDH activity is higher than in other tissues (Omolo et al., 2003; Venter et al., 2016). To identify the tauropine peak in green abalone muscle extracts (Publication II), we conducted a brief analysis using the product of the tauropine dehydrogenase enzyme activity described in section 2.8 by using four increasing concentrations of NADH and a fixed amount of taurine.

For this, three subsamples of *H. fulgens* muscle from 18 °C control experiment were used for determination of TDH activity as described in section 2.8. For each sample, three different concentrations of NADH were used: 0.15 mmol L^{-1}, 0.30 mmol $L^{1,}$ and 0.50 mmol L^{-1}. Taurine concentration remained constant at 80 mmol L^{-1} and samples without the addition of taurine (for lactate dehydrogenase determination) and without the addition of pyruvate (no reaction) were run in parallel as controls. All assays were conducted at 18 °C until all NADH was oxidized.

An aliquot of 200 µL from the resulting reaction of the enzyme assay was transferred into a new 1.5 mL tube. Polar metabolites were extracted following a modified method for fluid (Blackwell, A. et al., 2013. Agilent Technologies Inc. Technical Overview 5991-3528EN. USA). Briefly, 2 parts of ice-cold methanol and one part of ice-cold chloroform was added to the sample and vortexed for 10 s. This was followed by the addition of one part water and one part chloroform to a final solution ratio of 2:2:1.8. The homogenate was vortexed for 10 s and

centrifuged at 4 °C for 10 min at 3000 g. The supernatant was transferred to a new 1.5 mL tube and dried as described in section 2.8

The dried polar extract was re-suspended with 200 µL D_2O containing 0.05% TSP (Sigma-Aldrich, St. Louis, USA) and a 50 µL aliquot was transferred into a 4 mm zirconia rotor. The ^{1}H-HRMAS NMR was acquired using the NOESY sequence (protocol described in Publication II). All spectra were imported to the software Chenomx NMR suit 8.0 (Chenomx Inc. Edmonton, Canada) for metabolite identification.

An increasing double peak at 1.5 ppm were identified from the spectra, which matches the increasing concentration of NADH (R^2 = 0.88; P=0.001; Publication II: Supplementary material 1) of the enzyme activity reaction and which did not occur in the reaction without taurine and pyruvate, respectively. Furthermore, this double peak was absent in gill and hepatopancreas (Publication I), which matches with previous studies where low tauropine accumulation was observed in these tissues (Omolo et al., 2003), whereas muscle extracts displayed high levels of tauropine (Publication II).

2.10 RNA extraction

RNA was isolated from frozen tissue samples following two methodologies: i) using the Qiagen RNeasy kit according to the manufacturer's instruction (Qiagen, Hilden Germany) for gill, mantle and hepatopancreas samples and ii) by phase separation with chloroform and isopropanol precipitation, followed by two wash steps with 75% ethanol for the muscle samples. In both methods, RNA concentration was determined photometrically (NanoDrop ND-1000, Seqlab, Erlangen, Germany) at 260 nm and purity was determined from the ratios 260/280 nm and 260/230 nm. RNA integrity was assesed using capillary electrophoresis (Bioanalyzer, Agilent Technologies, Waldron, Germany). Similar to other invertebrate species, the 28S rRNA peak is not visible as a separate peak, and therefore calculation of the 28S/18S rRNA ratio is not possible. Therefore, RNA integrity was evaluated from the single peak around 41 s and the absence of any significant degradation products in the electropherogram (Fig. 2.4). To exclude genomic DNA contamination, all RNA extracts were treated with Turbo DNA-free Kit (Ambion, Darmstadt, Germany).

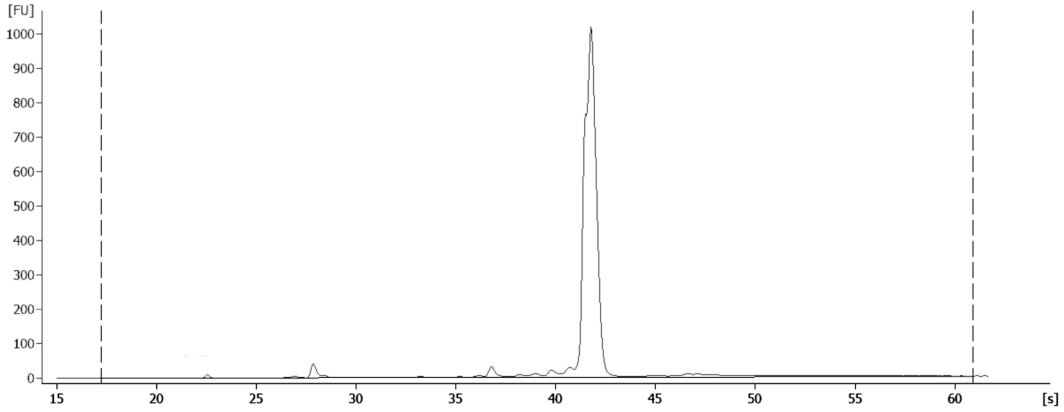

Figure 2.4 Representative electropherogram from isolated RNA from *H. fulgens*. A single peak at around 41 s indicate high quality RNA with no degradation or contamination.

2.11 Transcriptomic analysis

2.11.1 Library preparation and Illumina sequencing

To investigate the molecular basis of cellular processes shaping the thermal window of *H. fulgens*, a transcriptome was constructed de novo using two individuals: one under unstressed condition (18 °C under normoxic normocapnia) and one under stressed conditions (32 °C under hypoxic hypercapnia). From each individual, RNA from gill, mantle, and hepatopancreas was isolated and treated as described in section 2.10, thereafter, total DNA-free RNA from each tissue was pooled in equal amounts for the unstressed and stressed abalone individuals.

RNA pools were used for the preparation of random-primed and normalized cDNA libraries ready for Illumina TrueSeq sequencing by Vertis Biotechnologies AG (Freising, Germany). Preparation of the strand-specific cDNA started with enrichment of poly(A)+ RNA from total RNA using oligo(dt) chromatography followed by RNA fragmentation and synthesis of the first strand with an N6 random primer. Thereafter, Strand-specific sequencing adapters were ligated to the 3′ and 5′ ends of the first-strand cDNA followed by amplification using a proofreading enzyme for 10 – 15 cycles. The resulting libraries were size-fractioned and normalized using a kinetic denaturation/reassociation technique to reduce highly abundant clones. Sequencing of the libraries was performed on an Illumina MiSeq system in the Alfred Wegener Institute, Germany with the MiSeq Reagent Kit v3. (300 bp, pared end). Libraries properties and preparation for sequencing are described in Table A.1.

Table 2.2 Properties of the strand-specific normalized cDNA libraries

Sample	*unstressed* library	*stressed* library
Sample tag	Hf-7	Hf-159
Barcode i7	GGTAGC	CACGAT
Sample concentration (ng μL^{-1})	9.0	11.0
Volume (µL)	20	20
Size (bp)	400 – 700	400 – 700

2.11.2 Trascriptome assembly

A detailed description of the transcriptome assembly pipeline and gene annotation is included in Publication III. Further details regarding the transcriptome's quality, validation, and comparison with previously published transcriptome from other abalone species are included in the appendices.

2.12 Patterns of gene expression via qPCR

Patterns of gene expression were assessed to i) investigate the inducibility of members of the Hsp70 family in muscle of *H. fulgens* during warming (Publication II), and ii) to explore transcriptional changes in key regulatory process involved in the warming-induced cellular and metabolic response of *H. fulgens* under hypoxia, hypercapnia and their combination in gill and muscle samples (Publication III). Analyzed genes were selected from the resulting transcriptome from section 2.11. RNA was isolated and quality-checked (section 2.10). cDNA was synthesized with 0.4 µg of DNA-free RNA using the High-Capacity Reverse Transcription Kit (Applied Biosystems, Darmstadt, Germany), and qPCR reactions were conducted in a ViiA 7 Real-Time PCR System (Applied Biosystems) using SYBER Green PCR Master Mix (Applied Biosystems). Relative expression from each gene was evaluated using the R package MCMC.qpcr (Matz et al., 2013), using the genes 60s Ribosomal Protein L5 and E3 ubiquitin-protein ligase as reference genes. The detailed description of the qPCR protocol and statistical approaches are found in Publication II and Publication III.

CHAPTER 3

PUBLICATIONS

List of publications and authors' contribution

Publication I

Miguel A. Tripp-Valdez, Christian Bock, Magnus Lucassen, Salvador E. Lluch-Cota, M. Teresa Sicard, Gisela Lannig, Hans O. Pörtner (2017).Metabolic response and thermal tolerance of green abalone juveniles (*Haliotis fulgens*) under acute hypoxia and hypercapnia. *Journal of Experimental Marine Biology and Ecology*, 497 (2017), 11–18.

The concept of the study was elaborated by HOP, ML and myself. I performed the experiments in Mexico under the advisory of TS and SL. Data analysis and interpretation was done by CB, GL, ML and myself. I drafted the manuscript, which was revised by all co-authors.

Publication II

Miguel A. Tripp-Valdez, Christian Bock, Gisela Lannig, Nils Koschnick, Hans O. Pörtner, Magnus Lucassen. 2019. Assessment of muscular energy metabolism and heat shock response of the green abalone *Haliotis fulgens* (Gastropoda:Philipi) at extreme temperatures combined with acute hypoxia and hypercapnia . *Journal of Comparative Biochemestry and Physiology Part B*. 227. 1 – 11.

This manuscript was development by GL, CB, ML, HOP and myself. Metabolic profiles and enzymatic analysis were performed by myself, while relative quantification of proteins (western blots) were made by NK. Molecular analysis were made by ML and myself. I drafted the manuscript and revision were made by all co-authors

Publication III

Miguel A. Tripp-Valdez, Lars Harms, Hans O. Pörtner, M. Teresa Sicard, Magnus Lucassen (*submitted*).De novo transcriptome assembly and gene expression profile of thermally challenged green abalone (*Haliotis fulgens*:Gastropoda) under acute hypoxia and hypercapnia. *Marine Genomics*.

The ideas for this study were developed by ML, LH and myself. Biological material for experimental analysis were facilitated by TS. Bioinformatic analysis were made by LH, ML and myself. I drafted the manuscript and revision were made by all co-authors

3.1 Publication I

Metabolic response and thermal tolerance of green abalone juveniles (*Haliotis fulgens* : Gastropoda) under acute hypoxia and hypercapnia.

Miguel A. Tripp-Valdez, Christian Bock, Magnus Lucassen, Salvador E. Lluch-Cota, M. Teresa Sicard, Gisela Lannig & Hans O. Pörtner.

2017

Journal of Experimental Marine Biology and Ecology

Journal of Experimental Marine Biology and Ecology 497 (2017) 11–18

Contents lists available at ScienceDirect

Journal of Experimental Marine Biology and Ecology

journal homepage: www.elsevier.com/locate/jembe

Metabolic response and thermal tolerance of green abalone juveniles (*Haliotis fulgens:* Gastropoda) under acute hypoxia and hypercapnia

Miguel A. Tripp-Valdez[a,c,*], Christian Bock[a], Magnus Lucassen[a], Salvador E. Lluch-Cota[b], M. Teresa Sicard[b], Gisela Lannig[a], Hans O. Pörtner[a,c]

[a] Integrative Ecophysiology, Alfred Wegener Institute Helmholtz Centre for Polar and Marine Research, Am Handelshafen12, D-27570 Bremerhaven, Germany
[b] Centro de Investigaciones Biológicas del Noroeste (CIBNOR), Instituto Politécnico Nacional, 195, La Paz, Baja California Sur 23096, Mexico
[c] University Bremen, Bibliothekestraße 1, 28359, Germany

ARTICLE INFO

Keywords:
Critical temperature
Climate change
Energy metabolism $_1$H
NMR spectroscopy
Thermal tolerance

ABSTRACT

With ongoing climate change, rising ocean temperature is usually accompanied by falling oxygen levels (hypoxia) and increasing CO_2 concentration (hypercapnia). Both drivers may impose constraints on physiological mechanisms that define thermal limits resulting in increased vulnerability towards warming in marine ectotherms. The present study aimed to detect differences in thermal tolerance by investigating the underlying metabolic responses in the green abalone (*Haliotis fulgens*) under conditions of hypoxia and hypercapnia. Juvenile abalones were exposed to a temperature ramp (+3 °C day^{-1}) under hypoxia (50% air saturation) and hypercapnia (~1000 μatm pCO_2), both individually and in combination. Impacts on energy metabolism were assessed by analyzing whole animal respiration rates and metabolic profiles of gills and hepatopancreas via ^{1}H NMR spectroscopy. While hypercapnia had a minor impact on the results of the temperature treatment, hypoxia strongly increased the vulnerability to warming, indicated by respiration rates falling below values expected from an exponential increase and by the onset of anaerobic metabolism suggesting a downward shift of the upper critical temperature. Warming under combined hypoxia and hypercapnia elicited a severe change in metabolism involving a strong accumulation of amino acids, osmolytes and anaerobic end products at intermediate temperatures, followed by declining concentrations at warmer temperatures. This matched the limited capacity to increase metabolic rate, loss of attachment and mortality observed under these conditions suggesting a strong narrowing of the thermal window. In all cases, the accumulation of free amino acids identified proteins as a significant energy source during warming stress.

1. Introduction

With the ongoing rise in ocean temperature, changes in biogeography and biodiversity in marine ecosystems are expected if temperatures reach the thermal window limits of species (Pörtner et al., 2014; Sunday et al., 2012). Accordingly, the study of the biochemical and physiological processes shaping the limits of thermal tolerance of a species plays a key role in the assessment of its sensitivity to climate change (Pörtner, 2002; Verberk et al., 2016). Mechanisms that link systemic to molecular factors and shape limits at both ends of the thermal window in ectotherms have been explained through the concept of the oxygen- and capacity- limited thermal tolerance (OCLTT; Pörtner, 2002).

Under this conceptual model, the limited capacity to provide oxygen to tissue and cover temperature-dependent oxygen demand initiates thermal limitation. When temperature increases above the optimal range, the cardio-ventilatory capacity of the organism falls behind the rising demand as indicated by the development of systemic hypoxemia (Frederich and Pörtner, 2000). At the critical temperature (Tc) the exacerbated mismatch between oxygen supply and demand finally leads to the onset of anaerobic metabolism (Pörtner, 2010). Formation of anaerobic end products such as succinate during anaerobic mitochondrial ATP generation, and lactate or opines by cytosolic glycolysis constitute early indicators of Tc when thermal stress pushes an animal towards its lethal threshold (Frederich and Pörtner, 2000; Verberk et al., 2013; Zittier et al., 2015). With ongoing global climate change, additional drivers like ambient hypoxia and elevated CO_2 concentration are increasingly interacting with temperature in marine ecosystems. Both hypoxia and hypercapnia can negatively impact the same physiological mechanisms involved in thermal tolerance (Pörtner, 2010); hypoxia directly limits oxygen availability and compromises aerobic ATP generation below a critical threshold, causing metabolic

* Corresponding author at: Alfred Wegener Institute, Am Handelshafen 12, D-27570 Bremerhaven, Germany.
E-mail address: mtripp@awi.de (M.A. Tripp-Valdez).

http://dx.doi.org/10.1016/j.jembe.2017.09.002
Received 23 December 2016; Received in revised form 1 August 2017; Accepted 5 September 2017

depression in order to adjust ATP-dependent cellular processes to reduced energy availability (Guppy and Withers, 1999). Hypercapnia may also impose negative effects on energy homeostasis through dis-turbing acid-base regulation and thereby also inducing metabolic de-pression at high pCO_2 levels (Pörtner et al., 2000). Overall, both hy-poxia and hypercapnia can potentially induce constraints in metabolism and increase the vulnerability of the organism to thermal extremes (Lannig et al., 2010; Lu et al., 2016; Verberk et al., 2013; Zittier et al., 2015).

In this context, the use of metabolomic tools, like ^{1}H-Nuclear Magnetic Resonance (NMR) spectroscopy, has gained importance in environmental studies due to their ability to detect changes in a wide number of compounds (Verberk et al., 2013; Viant et al., 2003). Metabolomic studies of the abalone *H. diversicolor* found that exposure to warming and hypoxic stress not only affected energy metabolism but also osmoregulation and nucleotide metabolism (Lu et al., 2016). In nymphs of the aquatic stonefly, *Dinocras cephalotes*, exposed to different oxygen levels, hypoxia induced a downward shift of the critical temperature, evidenced by a lower energy status and accumulation of anaerobic end products at a lower temperature than under normoxia. Hyperoxia alleviated these effects, improving thermal tolerance (Verberk et al., 2013).

Green abalone (*Haliotis fulgens*; Philipi) is a marine gastropod with high economic importance along the Pacific coast of the Baja California, Mexico. Declines in natural populations have been attributed to overfishing and disease outbreaks. Additionally, the impacts of climate variability, particularly of strong El Niño events, have recently been recognized as a crucial factor in the dynamics of abalone populations (Guzman del Proo et al., 2003; Micheli et al., 2012). The increasing frequency and intensity of warming events (Robinson, 2016; Zaba and Rudnick, 2016), together with anomalies in oxygen availability and seawater chemistry along the California Current (Micheli et al., 2012; Stramma et al., 2010) have raised serious concern regarding the effects of climate change on abalone natural populations.

Accordingly, this study aimed to test the hypothesis that hypoxia and hypercapnia, as individual stressors and in combination, will modify the metabolic responses of thermally stressed *H. fulgens*, pos-sibly resulting in a downward shift of the critical temperature, and thus, increased thermal sensitivity. We tested this hypothesis in juveniles of *H. fulgens* exposed to a temperature ramp under normoxia, hypoxia (50% air saturation) or hypercapnia (1000 μatm pCO_2) as well as combined hypoxia and hypercapnia. Measurements of whole organism oxygen consumption were complemented by untargeted metabolic profiling of gill and hepatopancreas tissue extracts by use of ^{1}H NMR spectroscopy. The selected experimental conditions correspond to si-milar hypoxia conditions found in Baja California (Micheli et al., 2012) for several days, and mimic an IPCC (Intergovernmental Panel on Cli-mate Change) scenario of seawater CO_2 concentrations reached by 2100 (Pörtner et al., 2014).

2. Materials and methods

2.1. Animal maintenance

In March 2013, 224 juvenile green abalones (*Haliotis fulgens*) were provided by a fishery cooperative in Baja California Sur, Mexico, and transported to the Northwest Biological Research Center (Centro de Investigaciones BIológicas del Noroeste; CIBNOR) in La Paz, Mexico, in insulated boxes containing a bed of fresh kelp and frozen gel. After arrival, abalones were cleaned from epibionts and kept at a density of one individual per liter in 100 L tanks with aerated filtered seawater at 12 °C and a salinity of 40. Every two days, water was renewed and abalones were fed ad libitum with rehydrated kelps. Photoperiod was set to a 12:12 h light:dark cycle.

After pre-acclimation for 30 days, water temperature was increased from 12 °C to 18 °C (2 °C day^{-1}), which corresponds to the annual mean of the region of origin. During this acclimation period (73 days) no mortality was observed. Water temperature was constantly mon-itored by use of HOBO® pendant data loggers. Values of salinity and pH_{NBS} were monitored daily using an optic refractometer (Extech Instruments, Waltham, MA, USA) and a pH sensor (Neptune Systems, CA, USA). To exclude any possible effect of altered kelp nutritional status, feeding was switched to a commercial feed containing 35%protein, 10% fat, 3% raw fiber, 18% ash and 24% nitrogen-free extract (NFE). At the time of experimentation, abalones displayed between 20 and 30 mm shell lengths and visual inspection showed no signs of sexual maturation. Feeding was stopped two days prior to the start of the experiments.

2.2. Experimental setup and oxygen consumption measurements

To investigate the impact of hypoxia (50% air saturation) and hypercapnia (~1000 μatm pCO_2) – individually and in combination – on the thermal sensitivity of *H. fulgens*, four independent experiments were carried out consecutively. In each one, animals were exposed to an acute temperature ramp from 18 to 32 °C at 3 °C day^{-1} with a final temperature step of 2 °C only, as above 32 °C *H. fulgens* begin to lose the ability to attach to the substrate (Diaz et al., 2006). Treatments were: experiment 1: control exposure to normoxia (100% air saturation) and ambient normocapnia (400 μatm pCO_2); experiment 2: hypoxia (50%air saturation) and normocapnia (400 μatm pCO_2); experiment 3: nor-moxia (100% air saturation) and hypercapnia (~1000 μatm pCO_2); and finally experiment 4: hypoxia (50% air saturation) and hypercapnia (~1000 μatm pCO_2). Due to technical constraints and the limited number of green abalone juveniles available for this study, we treated individuals within tanks as independent samples. However, to account for possible effects of time duration of the experiments and any po-tential variability in experimental conditions, each experiment was accompanied by incubation of a control group at 18 °C (Supplementary Fig. 1). Experimental conditions were achieved by bubbling the water with air (normoxia) or with air mixed with N_2 (hypoxia) and/or CO_2 (hypercapnia). Dissolved oxygen (DO) levels were controlled by online monitoring using needle-type O_2-sensors (PreSens, GmbH, Regensburg, Germany) calibrated at the respective temperature (see below for calibration details). Water pCO_2 was controlled by measurements of water pH_{NBS} using a Neptune Aquacontroler Apex System (Neptune Systems, CA, USA). Temperature, salinity, pH_{NBS} and total alkalinity were determined twice a day. Total alkalinity was analyzed in triplicate water samples using potentiometric titration. Seawater pCO_2 was calculated from measured temperature, salinity, pH_{NBS} and TA values by use of the program CO_2Sys (*ver 01.05*; Lewis and Wallace, 1998) using the equilibrium constants from Mehrbach et al. (1973) refitted by Dickson and Millero (1987), considering the formulation for KSO_4 by Dickson (1990). Water parameters during experiments are shown in Supple-mentary Table 1.

In each of the experiments, the respirometry setup comprised 11 glass chambers for the experimental group (10 specimens and one blank) with 78 mL volume each, and seven respiration chambers for the control group (six specimens and one blank) at unchanged temperature, were mounted in a water bath with constant in- and outflow from two individual header tanks (250 L) for the experimental and control groups, respectively. Individual abalones were placed inside each re-spiration chamber with a small plastic mesh grid to prevent the aba-lones from blocking the water flow. Water tanks were covered to minimize disturbances during experiments. After 2 h, the specific con-ditions (oxygen level and pH) in both header tanks were adjusted to intended values. The following day and thereafter, standard metabo-lism of *H. fulgens* was determined via flow-through respirometry using microoptodes (PreSens, GmbH, Regensburg). Metabolic rate (MO_2) of each experimental animal was measured twice a day for 10 min in the morning (10:00 ± 1 h) and evening (22:00 ± 1 h) by switching be-tween animal chambers. Temperature in the experimental tank was

increased every night (00:00 ± 1 h) at a rate of 0.075 °C min^{-1} (Supplementary Fig. 1). Oxygen microsensors were calibrated at each temperature using air-saturated seawater for 100% saturation and Na_2SO_3 (Fermont) saturated water for 0% saturation. Water flow was adjusted to 9–14 mL min^{-1} during readings in a way that the animals consumed < 25% of the oxygen from the water. At the end of the experiment, abalones were removed from the chambers, and soft body was isolated from the shells and freeze-dried (Telstar Mod Cryodos 50, Spain). The MO_2 was calculated as follows: $MO_2 = (\Delta pO_2 * \beta O_2 * V_{fl})/M^{0.78}$ where MO_2 is oxygen consumption (μmol O_2 h^{-1} g DW^{-1}) normalized to a standard dry soft weight of 1 g. ΔpO_2 is the difference in the partial pressure between inflowing and outflowing water. βO_2 is the temperature and salinity-specific oxygen capacity of water calculated from the Bunsen absorption coefficient considering vapor pressure according to the Campbell equation. V_{fl} is the flow rate (1 h^{-1}), M is the dry soft mass (g), and 0.78 is the allometric coefficient. This was calculated from organisms at 18 °C ($n = 16$) and is similar to the value of 0.70 reported by Farías et al. (2003) for *H. fulgens* at 16 °C.

2.3. Tissue collection and metabolite extraction

To evaluate the impact of the different experimental conditions on the metabolite profile, additional specimens of *H. fulgens* were exposed to the same experimental protocol in separate tanks and sub-samples of 10 animals were taken at four temperatures (18, 24, 30 and 32 °C). Gill and hepatopancreas were excised and immediately snap-frozen in liquid nitrogen. Frozen samples were transported to the Alfred Wegener Institute (Bremerhaven, Germany) and kept at − 80 °C for further analyses.

Polar metabolites were extracted from frozen gill samples following the two step methodology for tissues < 50 mg (Wu et al., 2008). Briefly, pre-weighted frozen tissue was homogenized in 8 mL g^{-1} ice-cold methanol and 2.5 mL g^{-1} ice-cold water by one cycle of 20 s at 6000 rpm using Precellys 24 (Bertin Technologies, France). This was followed by the addition of chloroform (8 mL g^{-1} tissue) and water (4 mL g^{-1} tissue). Afterwards the homogenate was vortexed for 20 s, incubated on ice for 10 min and centrifuged for 10 min at 3000 rpm at 4 °C. After grinding to a fine powder in liquid nitrogen, hepatopancreas samples were sonicated in 4 mL g^{-1} ice-cold methanol and 0.85 mL g^{-1} ice-cold water for 5 min at 0 °C in a Branson Sonifier 450 (output control 8, duty cycle 50%), followed by the addition of 4 mL g^{-1} chloroform and 2 mL g^{-1} water. Thereafter, extraction and resuspension of polar metabolites proceeded as for gill tissue.

The upper methanol layer containing the polar metabolites was transferred to a new 1.5 mL tube and dried overnight in a centrifugal vacuum concentration (RVC 2-18, Martin Christ Freeze dryers, GmbH, Germany) at room temperature. Prior to analysis, dried samples were resuspended in D_2O containing 1% Thrymethylsilyl propionate (TSP; Sigma-Aldrich, St. Louis, USA) resulting in a final concentration of 0.3 g mL^{-1} of the initial tissue weight. D_2O provides a deuterium lock for the NMR spectrometer while the TSP acts as an internal standard and as a chemical shift reference. Samples were mixed and an aliquot of 50 μL was transferred to a 4 mm standard HRMAS (high resolution magic angle spinning) zirconia rotor. The ^{1}H-HRMAS NMR spectra were acquired with a 9.4 T Avance III HD 400 WB spectrometer (Bruker Biospin GmbH, Germany). A Carr-Purcell-Meiboom-Gill (cpmg) sequence was used with the following parameters: flip angle 90°, acquisition time 4.01 s, relaxation delay 4 s, sweep width 8.803 Hz, 64 scans with 4 dummy scans. Spectra were acquired and processed using TopSpin 3.2 (Bruker Biospin GmBH, Germany). All spectra were analyzed for metabolite identification and quantification with Chenomx NMR suite 8.0 software (Chenomx Inc., 2014). All the Fourier-transformed spectra were baseline corrected and calibrated to the internal reference (TSP at 0.0 ppm). An exponential line broadening of 0.5 Hz was applied to each spectrum. Peaks were assigned with reference to chemical shift tables described for other abalone or related species (Lu et al., 2016; Rosenblum et al., 2005; Viant et al., 2003).

2.4. Statistical analyses

All statistical analyses of MO_2 were performed with R software. Values were tested for normality (Shapiro-Wilk-Test) and homogeneity of variance (Bartlett Test). Datasets of the two MO_2 recordings (morning and evening) were pooled once a paired Student's *t*-test re-vealed no significant effect of time. Repeated measures ANOVA tested the differences in MO_2 with temperature followed by multiple com-parisons with Bonferroni correction. For each experiment, *t*-tests were carried out to compare means of individual data obtained from speci-mens in experimental and control tanks. Discontinuities (breakpoints) in the trajectories of temperature dependent MO_2 rates were defined as the points where curves leveled off or declined. Non-linear regressions were fitted to data by use of the equation ($y = y_0 + ae^{bx}$) with the package nls2 in R (Grothendieck, 2010). To detect patterns of meta-bolite accumulation, heatmaps were constructed using the scaled and centered metabolite concentration values using the Heatmap3 package in R. An ANOVA in combination with Tukey HSD test compared the means of the metabolite concentrations using the online program Me-taboAnalyst 3.0 (Xia et al., 2015).

3. Results

3.1. Animal performance and mortality

In experiments 1 (normoxia, normocapnia), 2 (hypoxia) and 3 (hypercapnia) no mortality was observed over the course of the experiment and abalone were firmly attached to the walls, irrespective of temperature change. Across the temperature ramp, organisms showed little activity with scattered spontaneous movements on the walls. In contrast, under combined exposure to hypoxia and hypercapnia in experiment 4, no activity was seen in animals constantly held at 18 °C whereas acute warming strongly impaired the wellbeing of green abalone. After 12 h at the final temperature (32 °C), five out of 16 animals lost their ability to remain attached to the wall and two of them also showed muscular spams. The rest of the animals were still fixed to the walls but had the mantle expanded and were continuously lifting their shells. All animals were weak and easily removed. After 20 h five animals had died, while the others had completely lost the ability to stay attached to the walls, with the mantle fully expanded. Therefore, oxygen consumption measurements were canceled at this time.

3.2. Oxygen consumption

Overall, progressive warming caused an increase in MO_2 of the green abalone; however, patterns differed between experiments (Fig. 1). Under exposure to hypoxia, hypercapnia and their combina-tion, MO_2 values at 18 °C were initially lower than in the control ex-periment (unpaired *t*-test $P < 0.05$). However, maximum MO_2 values were similar under all experimental conditions (control: 61.04 ± 20.46 μmol O_2 h^{-1} g DM^{-1}; hypoxia: 59.38 ± 10.44 μmo-l O_2 h^{-1} g DM^{-1}; hypercapnia: 61.51 ± 17.16 μmol O_2 h^{-1} g DM^{-1}; combined: 49.51 ± 14.25 μmol O_2 h^{-1} g DM^{-1}). Under control and hypercapnic conditions (experiments 1 and 3), MO_2 increased ex-ponentially over the whole temperature range resulting in a $Q_{10\ (18–32\ °C)}$ of 1.72 ± 0.60 ($N = 10$) and of 3.29 ± 0.94 ($N = 10$), re-spectively, and MO_2 values were significantly higher at 32 °C than at 18 °C ($P < 0.001$; Fig. 1A, C). Under hypoxia (experiment 2), the warming induced increase in MO_2 was much stronger, revealing sig-nificantly elevated metabolic rates already at temperatures above 24 °C ($P < 0.05$; Fig. 1B). The strong exponential rise in MO_2 up to 27 °C was characterized by a $Q_{10\ (18–27\ °C)}$ of 4.84 ± 2.28 ($N = 10$) and leveled off at higher temperatures. Finally, under combined hypoxic and hy-percapnic conditions in experiment 4, warming from 18 °C to 30 °C

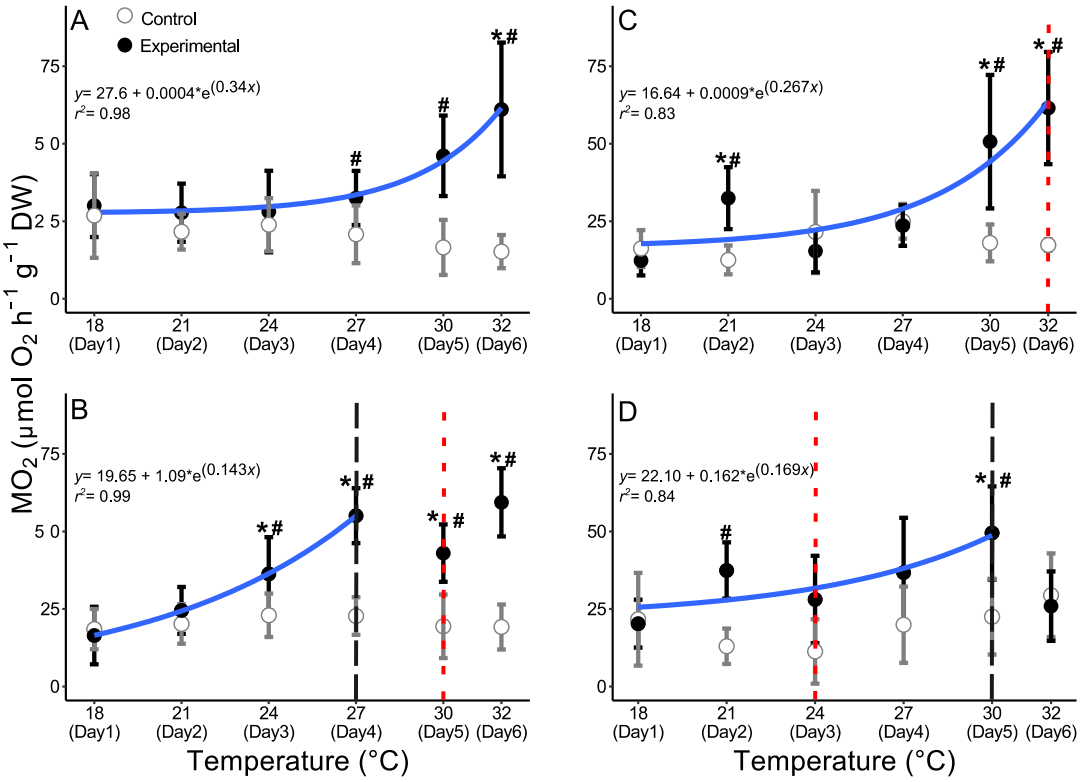

Fig. 1. Oxygen consumption rate of juvenile green abalone *Haliotis fulgens* under A) normoxic normocapnia; B) hypoxic normocapnia; C) normoxic hypercapnia; D) hypoxic hypercapnia. Experimental organisms were exposed to daily temperature increments while control organisms remained at 18 °C. * denotes significant differences from the respective data at the initial temperature (18 °C); # denotes significant differences from control organisms at the same day. Solid blue lines indicate a nonlinear regression fit of values following an exponential increment during warming (Section 2.4). The dashed black vertical line indicates the point where MO_2 failed to continue the exponential increase (Section 3.2) and the dotted red vertical line indicates the point where an increase of anaerobic end products was observed in gills (Section 3.3). Values are means ± S.D. with $N = 10$ for experimental and $N = 6$ for control.(For interpretation of the references to color in this figure legend, the reader is referred to the web version of this article.)

induced an exponential increase in MO_2 with a $Q_{10\ (18–30\ °C)}$ of 2.21 ± 0.72 leading to significantly higher rates at 30 °C. Further warming to 32 °C resulted in a drop in MO_2 to values similar to those determined at 18 °C (Fig. 1D).

Green abalone that were continuously kept under hypoxia, hypercapnia or combined hypoxia and hypercapnia at 18 °C displayed similar rates of MO_2 which remained more or less unchanged over time (Fig. 1).

3.3. Metabolic profiles by ^{1}H NMR spectroscopy

A representative one-dimensional ^{1}H NMR spectrum of branchial polar metabolites from *H. fulgens* under control conditions (18 °C; normoxia-normocapnia) is shown in Fig. 2. Twenty-one metabolites were identified including free amino acids (valine, leucine, isoleucine, threonine, alanine, arginine, lysine, glutamate, glutamine, glycine, aspartate, tyrosine and dimethylglycine), organic osmolytes (homarine, betaine and taurine) and energy-related compounds (succinate, lactate, acetate, ATP and carnitine). As in other invertebrates and abalone species, all spectra were dominated by the peaks of the organic osmolytes homarine, betaine and taurine (Viant et al., 2003; Rosenblum et al., 2005; Lu et al., 2016; Fig. 2). A similar metabolic profile was obtained from hepatopancreas and the same metabolites could be identified, except for ATP, whose peak was less clear in all spectra (data not shown).

Heat maps were constructed to easily visualize warming induced changes in metabolite concentrations. Under the control conditions of experiment 1, progressive warming led to increasing concentrations in

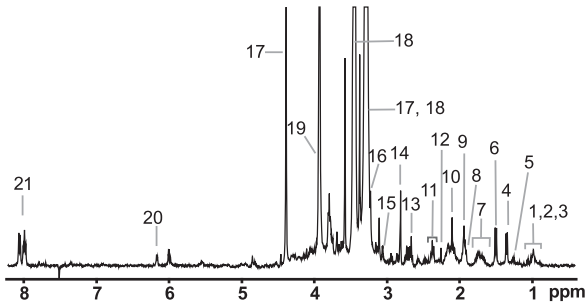

Fig. 2. Representative one-dimensional ^{1}H NMR spectrum from green abalone gill extracts under control conditions (18 °C, normoxic normocapnia); 1, 2, 3) leucine, isoleucine, valine (branched chain amino acids); 4) lactate; 5) threonine; 6) alanine; 7) arginine; 8) lysine; 9) acetate; 10) glutamate; 11) glutamine; 12) succinate; 13) aspartate; 14) dimethylglycine; 15) tyrosine; 16) carnitine; 17) betaine; 18) taurine; 19) glycine; 20) ATP; and 21) homarine.

various metabolites, particularly free amino acids (Figs. 3A, 4A). Among these, valine increased significantly at the highest temperature ($P < 0.05$). A different pattern was observed during warming under hypoxic conditions in experiment 2. In gills, warming to 30 °C elicited a significant accumulation of the anaerobic end products lactate, succinate ($P < 0.05$) and alanine ($P < 0.01$), however, succinate accumulation was only transient (Fig. 3B). In hepatopancreas succinate levels increased at 30 °C and remained elevated (Fig. 4B). Furthermore, valine increased significantly beyond 30 °C in both tissues

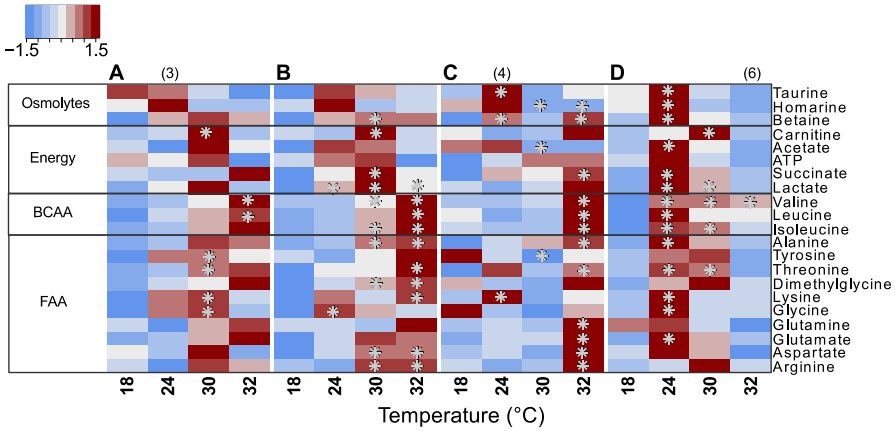

Fig. 3. Heatmaps with scaled and centered concentration values obtained from metabolite profiles of green abalone gill extracts under A) normoxic normocapnia; B) hypoxic normocapnia; C) normoxic hypercapnia; D) hypoxic hypercapnia. The * denotes significant differences in metabolite concentrations from their respective values at 18 °C. N = 7–9 per treatment or indicated in parenthesis if lower. BCAA = branched chain amino acids; FAA = free amino acids.

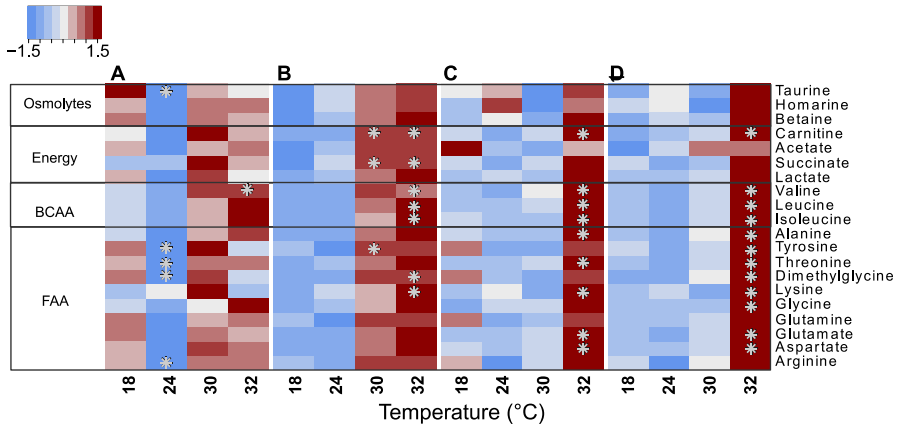

Fig. 4. Heatmaps with scaled and centered concentration values obtained from metabolite profiles of green abalone hepatopancreas extracts under A) normoxic normocapnia; B) hypoxic normocapnia; C) normoxic hypercapnia; D) hypoxic hypercapnia. The * denotes significant differences in metabolite concentrations from their respective values at 18 °C. N = 7–9. BCAA = branched chain amino acids; FAA = free amino acids.

($P < 0.001$).

Warming under hypercapnia in experiment 3 led to significant changes in the concentrations of only a few metabolites between 18 °C and 30 °C in both tissues. In gills, however, further warming to 32 °C caused a significant accumulation of succinate, alanine ($P < 0.05$), of the branched chain amino acids valine, leucine and isoleucine ($P < 0.001$) and of the amino acids glutamine, glutamate, aspartate and arginine ($P < 0.01$; Fig. 3C). A similar trend was observed in hepatopancreas, with the exception that anaerobic end products, arginine, and glutamine did not accumulate significantly (Fig. 4C).

Finally, concomitant hypoxia and hypercapnia in experiment 4 strongly affected the metabolite spectrum of gills at lower temperatures than in the other experiments. Warming to 24 °C already caused a significant accumulation of succinate, lactate, alanine, acetate, branched chain amino acids, of the organic osmolytes and of the amino acids threonine, lysine, glycine and glutamate ($P < 0.05$; Fig. 3D). Upon warming to 30 °C, however, levels of acetate, succinate, and alanine, of the osmolytes and the amino acids lysine, glycine and glu-tamate decreased to values as low as at 18 °C. At the highest tem-perature (32 °C), the concentration of all metabolites had decreased, except for that of valine, which remained at high levels ($P < 0.001$). A slightly different metabolic response was observed in hepatopancreas, where a delayed increase of most of metabolites was observed at 32 °C (Fig. 4D).

Fig. 5 highlights the warming-induced changes in alanine, succinate, lactate, valine and arginine levels of both tissues, also depicting their high variation at intermediate temperatures (24° and 30 °C) and some tissue-specific concentration differences.

4. Discussion

The present study investigated the effects of hypoxia (50% air saturation) and hypercapnia (~1000 µatm pCO_2) either separately or in combination, on metabolic patterns during acute warming of green abalone juveniles (*Haliotis fulgens*) from Baja California, Mexico, with the goal to determine potential shifts in thermal tolerance. We found that organisms under hypoxia surpassed their Tc at lower temperatures and were more sensitive to temperature change than animals that were only exposed to warming or to warming under hypercapnia. Under combined hypoxia and hypercapnia, warming resulted in a strong perturbation of energy metabolism already at 24 °C. In combination with the distress observed in the whole organism (e.g. loss of attach-ment and mortality), the present results indicate a strong synergistic impact of hypoxia and hypercapnia on the thermal tolerance of juvenile green abalone.

4.1. Warming induced responses under normoxia and normocapnia

Green abalone from Baja California is frequently exposed to warming events. In 1997 temperatures up to 31 °C (+4 °C anomaly from the monthly average) were registered in abalone fishery zones due to a strong El Niño event. Although the population was reduced (mainly affected by the depletion of food sources), *H. fulgens* was able to persist and recovered slowly (Guzman del Proo et al., 2003). This tolerance to warming is reflected in the present study, as warming from 18 °C to 30 °C induced only slight changes in MO_2 and a moderate accumulation of anaerobic metabolites. In fact, temperatures between 24 °C and 28 °C

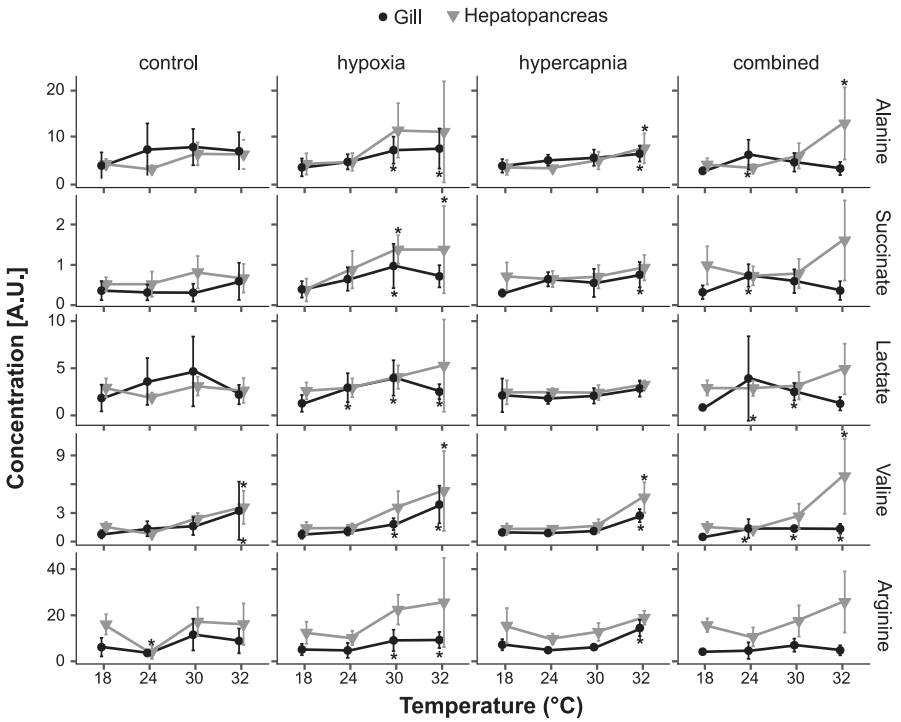

Fig. 5. Concentrations of alanine, succinate, lactate, valine and total arginine (sum of phospho-L-arginine and arginine). The * indicates significant differences from values at initial temperatures in gills (below error bar) and hepatopancreas (above error bar; ANOVA; Section 2.4). Control: normoxic normocapnia; hypoxia: hypoxic normocapnia; hypercapnia: normoxic hypercapnia; combined: hypoxic hypercapnia, values are means ± S.D.

have been estimated to be optimal for growth of green abalone juveniles (Diaz et al., 2006; Leighton et al., 1981). The accumulation of branched chain amino acids, especially valine, suggests a temperature driven shift to protein catabolism. Alternatively, the concentration of these amino acids may have changed to contribute to the regulation of intracellular osmolarity (Lu et al., 2016; Viant et al., 2003). However, the lack of concentration changes in the most abundant organic osmolytes taurine, betaine and homarine provide little support for this hypothesis. The higher metabolic rate (MO_2) observed at 32 °C probably induced higher rates of protein degradation to balance an increase in the energy demand for maintenance (Lu et al., 2016; Vosloo et al., 2013). As abalone tissues possess low lipid contents, their metabolism is driven mainly by the use of carbohydrates and proteins, thus protein breakdown likely provided free amino acids that were then used to fuel metabolism under stressful conditions (Lu et al., 2016; Rosenblum et al., 2005; Vosloo et al., 2013).

4.2. Effects of hypoxia

Reduced oxygen consumption and metabolic depression constitute a common response of *Haliotis* species to hypoxia (Harris, 1999). In this study, organisms under hypoxia displayed a slightly lower metabolic rate at initial condition (18 °C) compared to organisms under normoxia in experiment 1; however, control organisms that were held under hypoxia at constant temperature (18 °C) showed no signs of metabolic depression, suggesting that the chosen oxygen concentrations were still above a critical value that would trigger metabolic depression in juvenile *H. fulgens*. Acute warming under hypoxia, however, led to a pronounced exponential increase in MO_2 which failed to continue from 27 °C onwards (Fig. 1B). A similar warming induced limitation in MO_2 was observed in the blue mussel, *Mytilus edulis* from the North Sea, which was linked to a drop in the heart rate and in hemolymph pH, denoting the onset of impaired oxygen supply capacity (Zittier et al., 2015). Similarly, warming stress in the abalones *H. discuss hannai* and *H. gigantea* resulted in irregular heartbeats and reduced cardiac performance (Chen et al., 2016). Therefore, it is possible to infer from the MO_2 recordings that at 27 °C and temperatures beyond, the cardioventilatory capacity of hypoxia-exposed abalone became limited, reducing the amount of oxygen available to aerobic energy production.

As aerobic capacity reached its limits, the changing mode of metabolism was mirrored in the metabolic profile of *H. fulgens* tissues. At 30 °C, the accumulation of lactate, succinate and alanine in gills, and the accumulation of succinate in the hepatopancreas indicates an onset of anaerobic metabolism and the limited capacity of oxygen supply to meet the progressive rise in energy demand (Pörtner, 2010; Venter et al., 2016). It can be excluded that anaerobiosis was caused by ex-ercise, as this would result in the localized accumulation of anaerobic end products in the muscle (Venter et al., 2016). In addition, abalone behavior remained unchanged excluding intense muscular activity as an option to explain these changes. Hence, we conclude that the upper critical temperature (Tc) was shifted to lower temperatures, reflecting a higher thermal vulnerability of green abalone under hypoxia. At first sight, the accumulation of arginine in both tissues might have resulted from the breakdown of arginine phosphate, the main phosphagen in mollusks (Grieshaber et al., 1988). However, in ^{1}H NMR spectra it is not possible to distinguish between arginine and phosphoarginine (Viant et al., 2003), thus, a breakdown of phosphoarginine related to en-ergetics would not change the arginine NMR signal and is thus unlikely. In the oyster *Crassotrea virginica*, arginine is one of the most abundant amino acids, but its concentration is higher in digestive gland than in musculature, suggesting a function other than in energetics (Tikunov et al., 2010). As arginine is also the final intermediate in the urea cycle and is involved in ammonia detoxification (Tikunov et al., 2010), its accumulation may rather be associated with higher rates of protein degradation.

Tauropine is also commonly used as an indicator of anaerobic metabolism in *Haliotis* species (Omolo et al., 2003). However, an accumulation of tauropine mainly occurred in adductor muscle and was low in other tissues (Omolo et al., 2003). Moreover, taurine, a precursor of tauropine, followed the same pattern as the rest of the main osmolytes

(betaine and homarine), suggesting that at least in the tissues analyzed, the role of taurine is more related to osmoregulation than to energetics. Accordingly, no tauropine peak was found in the ^{1}H NMR spectra of gill and hepatopancreas.

With further warming, the anaerobic end products succinate and lactate, did not increase further in gills but continued to increase in the hepatopancreas (Fig. 5). These results suggest a transient use of anaerobic resources with an overshoot of warming-induced energy demand followed by a stabilization of metabolic conditions (Grieshaber et al., 1988). In contrast to abalone musculature, the digestive system receives a large hemolymph volume, and a high retention of hemolymph has been observed in this organ (Taylor and Ragg, 2005). Therefore, transport of metabolites into the hepatopancreas and their potential uptake would also explain the observed metabolic profiles (Rosenblum et al., 2005; Taylor and Ragg, 2005). An increased perfusion of the bipectinate gills may be involved in adjusting oxygen delivery to tissues and cells (Ragg and Taylor, 2006). This would allow higher protein turnover and use of free amino acids as an energy source, in line with the accumulation of valine observed under these conditions.

The observed metabolic response differs from previous metabolomic analyses of juvenile abalone that were starved for 28 and 56 days (Sheedy et al., 2016). Starvation caused a reduction of most metabolites, while the opposite was observed in the present study, indicating that an influence of starvation can be neglected in our experiments. Only *N*,*N*-dimethylglycine increased in both starved (Sheedy et al., 2016) and thermally challenged (present study) abalones. Further in-vestigations are thus necessary to unravel its role in the energy status of abalone.

4.3. Effects of hypercapnia

The effects of hypercapnia, associated with a reduction in water pH (ocean acidification) have not been studied widely in abalone species. Previous studies on marine mollusks demonstrated that moderate and high levels of hypercapnia have little or no impact on oxygen consumption at control temperature (Cunningham et al., 2016; Lannig et al., 2010; Zittier et al., 2015). This is in line with our observations, where control organisms under conditions of realistic ocean acidification scenarios displayed no metabolic response at constant temperature (18 °C). Furthermore, warming under hypercapnia caused MO_2 to increase exponentially and follow a similar pattern as under normocapnia (Exp. 1) denoting an unconstrained aerobic capacity. Changes in the metabolic profile of tissue samples after warming up to 30 °C were also minor and anaerobic metabolism was not involved. Although the MO_2 response during acute warming was similar and animals reached similar maximal MO_2 values in experiment 3 and 1, it is important to note that initial MO_2 was lower under hypercapnia (Exp. 3) than normocapnia. Thus, the Q_{10} was higher under hypercapnia than under normocapnia (3.29 vs. 1.72) indicating a stronger thermal stimulation of metabolism under hypercapnia. The metabolic profile of the gills and, to a lesser extent of hepatopancreas also reflects enhanced energy demand. The accumulation of succinate, alanine and free amino acids at 32 °C in hyper- but not normocapnia exposed abalones suggest the activation of anaerobic metabolism to cover the high energy demand and to maintain ATP levels under hypercapnia. An enhanced warming-induced rise in metabolic rate and energy demand under hypercapnia was also found in oyster (*Crassostrea gigas*: Lannig et al., 2010) and mussels (*Mytilus edulis*: Zittier et al., 2015), although the exact me-chanisms behind this stimulatory effect of hypercapnia during warming are not clear yet. Nonetheless, in the present study T*c* may not have been reached under hypercapnia, as aerobic respiration remained un-constrained.

In gill samples, a significant decrease in homarine and acetate levels with warming was only observed under hypercapnia (Fig. 3C). Homarine, which is an endogenously synthesized heteroaromatic quaternary ammonium compound, plays an important role as an organic osmolyte. Changes in its concentration have been related to stressful conditions like warming, hypoxia, starvation and pathogen infection (Lu et al., 2016; Rosenblum et al., 2005; Viant et al., 2003). As no significant changes in homarine concentrations were neither observed in the gill tissue of control (Exp. 1) and hypoxia exposed abalones (Exp. 2), nor in hepatopancreas samples under any of the experimental con-ditions, the observed drop in homarine under hypercapnia may be re-lated to a tissue-specific impact of hypercapnia on osmotic balance.

4.4. Effects of combined hypoxia and hypercapnia

Warming under combined hypoxia and hypercapnia cause a strong metabolic response (Exp. 4). Gills at 24 °C displayed a remarkable increase in most of the investigated metabolites including anaerobic end products, amino acids and osmolytes, suggesting that juveniles of *H. fulgens* became hypoxemic, and ATP production was sustained by the involvement of anaerobic metabolism at a lower temperature than in animals exposed to warming under hypoxia alone (Exp. 2). Nonetheless, MO_2 increased exponentially with warming until 30 °C. A possible stimulatory effect of hypercapnia as well as an enhanced per-fusion of gill may explain why whole organism metabolic rate did not collapse at a lower temperature and why valine did not accumulate in gills to the same extent as in experiments 1, 2 and 3, but rather re-mained stable during warming (Fig. 5). Nevertheless, the signs of anaerobiosis, together with the drop in MO_2 at 32 °C indicate that abalone juveniles had surpassed their T*c*. As the condition of abalone started to deteriorate (see below), metabolic activity of the gills became compromised and metabolites might be transported and accumulated in the hepatopancreas, explaining why this tissue showed an accumula-tion of these metabolites (Fig. 5).

The lifting of the shell by extension of the adductor muscle and sporadic 180° turns around the foot muscle observed in green abalone at 32 °C is a well-documented behavior in *Haliotis* species when they are close to their upper critical thermal limits (Diaz et al., 2006). In previous experiments with *H. fulgens* from the Baja California, the critical thermal maximum (CTmax) was found at 33.6 °C, and this was defined as the temperature where attachment failed in 50% of the animals (Diaz et al., 2006). Therefore, our observations in experiment 4 indicate that under combined hypoxia and hypercapnia green abalone juveniles not only surpassed their T*c*, but also reached CTmax at a lower temperature than reported in a previous study under temperature stress alone (Diaz et al., 2006). Observations of muscular spasms at 32 °C suggest that thermal limitation also affects the neural motor control (Verberk et al., 2013). However, these aspects need to be investigated further, in particular as spasms were only observed in animals exposed to warming under combined hypoxia and hypercapnia exposure and not in the other experiments.

5. Conclusion

Oxygen consumption measurements and the untargeted metabolic profiling of gill and hepatopancreas samples revealed differences in the metabolic responses of juvenile *H. fulgens* to warming when animals were additionally challenged by hypoxia, hypercapnia or their combination. Under hypoxia warming first stimulated but then constrained aerobic respiration and initiated anaerobic metabolism at somewhat lower temperatures than under normoxia indicating a narrowing of the thermal tolerance window, in line with the OCLTT concept. Hypercapnia did not induce any temperature dependent limitation in aerobic respiration and some impacts on energy metabolism became only evident at the highest temperature. Accordingly, present data revealed no potential narrowing of the thermal tolerance window due to hypercapnia exposure in juvenile abalones. Under exposure to combined hypoxia and hypercapnia, however, acute warming resulted in an early impairment of aerobic energy metabolism and stronger narrowing of the thermal tolerance range. Then, organisms not only surpassed T*c*

but also reached their CTmax. Under all conditions warming initiated protein degradation as indicated by the accumulation of branched chain amino acids. While amino acids constitute a significant energy source under adverse conditions, the hypothesis of an emerging imbalance of protein degradation and amino acid oxidation requires further investigation. Moreover, it remains to be explored whether the observed constraints on aerobic energy metabolism and increasing rates of protein degradation affect other important functions such as the immune response, reproductive potential, and growth performance of *H. fulgens*, such constraints may well contribute to the observed mass mortality events in Baja California during ambient extremes. In light of climate change, long-term exposures are necessary to assess the acclimation potential and to substantiate whether the observed rise in energy demand results in impaired development and performance of juvenile *H. fulgens* in the long run.

Supplementary data to this article can be found online at http://dx.doi.org/10.1016/j.jembe.2017.09.002.

Acknowledgements

The authors acknowledge the technical support provided by Gilberto Gonzales Soriano and Julio Felix Dominguez during the experiments in CIBNOR and to Rosa Linda Salgado Garcia for her support and advice during the experimental design; to Martín Gerardo Ruíz, from the Sociedad Cooperativa de Producción Pesquera de Bahía Tortugas S.C. de R.L. and their personnel for kindly providing the organisms. Financial support to Miguel A. Tripp-Valdez was granted by fellowship of the Deutscher Akademischer Austausdienst (DAAD) program: 57076385. This project was also supported by The Helmholtz Graduate School for Polar and Marine Research (POLMAR): VH-GS-200.

References

Chen, N., Luo, X., Gu, Y., Han, G., Dong, Y., You, W.-W., Ke, C., 2016. Assessment of the thermal tolerance of abalone based on cardiac performance in *Haliotis discus hannai*, *H. gigantea* and their interspecific hybrid. Aquaculture 465, 258–264. http://dx.doi.org/10.1016/j.aquaculture.2016.09.004.

Cunningham, S.C., Smith, A.M., Lamare, M.D., 2016. The effects of elevated pCO_2 on growth, shell production and metabolism of cultured juvenile abalone, *Haliotis iris*. Aquac. Res. 47, 2375–2392. http://dx.doi.org/10.1111/are.12684.

Diaz, F., Re, A.D., Medina, Z., Re, G., Valdez, G., Valenzuela, F., 2006. Thermal preference and tolerance of green abalone *Haliotis fulgens* (Philippi, 1845) and pink abalone *Haliotis corrugata* (Gray, 1828). Aquac. Res. 37, 877–884. http://dx.doi.org/10.1111/j.1365-2109.2006.01506.x.

Dickson, A.G., 1990. Thermodynamics of the dissociation of boric acid in synthetic seawater from 273.15 to 318.15 K. Deep Sea Res. Part A 37, 755–766. http://dx.doi.org/10.1016/0198-0149(90)90004-F.

Dickson, A.G., Millero, F.J., 1987. A comparison of the equilibrium constants for the dissociation of carbonic acid in seawater media. Deep-Sea Res. 34, 1733–1743. http://dx.doi.org/10.1016/0198-0149(87)90021-5.

Farías, A., García-Esquivel, Z., Viana, M.T., 2003. Physiological energetics of the green abalone, *Haliotis fulgens*, fed on a balanced diet. J. Exp. Mar. Biol. Ecol. 289, 263–276. http://dx.doi.org/10.1016/S0022-0981(03)00049-2.

Frederich, M., Pörtner, H.O., 2000. Oxygen limitation of thermal tolerance defined by cardiac and ventilatory performance in spider crab, *Maja squinado*. Am. J. Phys. Regul. Integr. Comp. Physiol. 279, R1531–8.

Grieshaber, M.K., Kreutzer, U., Pörtner, H.O., 1988. Critical PO_2 of euryoxic animals. In: Acker, H. (Ed.), Oxygen Sensing in Tissues. Springer, Berlin, Heidelberg, pp. 37–48. http://dx.doi.org/10.1007/978-3-642-83444-8_3.

Grothendieck, C., 2010. nls2: Non-linear Regression With Brute Force. R Package Version 0.1-3.

Guppy, M., Withers, P., 1999. Metabolic depression in animals: physiological perspectives and biochemical generalizations. Biol. Rev. 74, 1–40.

Guzman del Proo, S.A., Palau, L.C., Perez, J.B., Laguna, J.C., Fragoso, R.H., 2003. Effects of the "El Niño" event on the recruitment of benthic invertebrates in Bahia Tortugas, Baja California Sur. Geofis. Int. 42, 429–438.

Harris, J.O., 1999. Low dissolved oxygen reduces growth rate and oxygen consumption rate of juvenile greenlip abalone, *Haliotis laevigata* Donovan. Aquaculture 174, 265–278.

Lannig, G., Eilers, S., Pörtner, H.O., Sokolova, I.M., Bock, C., 2010. Impact of ocean acidification on energy metabolism of oyster, *Crassostrea gigas*—changes in metabolic pathways and thermal response. Mar. Drugs 8, 2318–2339. http://dx.doi.org/10.3390/md8082318.

Leighton, D.L., Byhower, M.J., Kelly, J.C., Hooker, G.N., Morse, D.E., 1981. Acceleration of development and growth in young green abalone (*Haliotis fulgens*) using warmed effluent seawater. J. World Maric. Soc. 12, 170–180. http://dx.doi.org/10.1111/j.1749-7345.1981.tb00253.x.

Lewis, E., Wallace, D.W.R., 1998. Program Developed for CO_2 System Calculations. ORNL/CDIAC-105. Carbon Dioxide Information Analysis Center, Oak Ridge National Laboratory, U.S. Department of Energy, Oak Ridge, Tennessee.

Lu, J., Shi, Y., Wang, S., Chen, H., Cai, S., Feng, J., 2016. NMR-based metabolomic analysis of *Haliotis diversicolor* exposed to thermal and hypoxic stresses. Sci. Total Environ. 545–546, 280–288. http://dx.doi.org/10.1016/j.scitotenv.2015.12.071.

Mehrbach, C., Culberson, C.H., Hawley, J.E., Pytkowicx, R.M., 1973. Measurement of the apparent dissociation constants of carbonic acid in seawater at atmospheric pressure. Limnol. Oceanogr. 18, 897–907. http://dx.doi.org/10.4319/lo.1973.18.6.0897. Micheli, F., Saenz-Arroyo, A., Greenley, A., Vazquez, L., Espinoza Montes, J.A., Rossetto, M., De Leo, G.A., 2012. Evidence that marine reserves enhance resilience to climatic impacts. PLoS One 7, e40832. http://dx.doi.org/10.1371/journal.pone.0040832.

Omolo, S.O., Gade, G., Cook, P., Brown, C., 2003. Can the end products of anaerobic metabolism, tauropine and D-lactate, be used as metabolic stress indicators during transport of live South African abalone *Haliotis Midae*? Afr. J. Mar. Sci. 25, 301–309. http://dx.doi.org/10.2989/18142320309504019.

Pörtner, H.O., 2002. Climate variations and the physiological basis of temperature dependent biogeography: systemic to molecular hierarchy of thermal tolerance in animals. Comp. Biochem. Physiol. A Mol. Integr. Physiol. 132, 739–761.

Pörtner, H.O., 2010. Oxygen- and capacity-limitation of thermal tolerance: a matrix for integrating climate-related stressor effects in marine ecosystems. J. Exp. Biol. 213, 881–893. http://dx.doi.org/10.1242/jeb.037523.

Pörtner, H.O., Bock, C., Reipschläger, A., 2000. Modulation of the cost of pHi regulation during metabolic depression: a ^{31}P-NMR study in invertebrate (*Sipunculus nudus*) isolated muscle. J. Exp. Biol. 203, 2417–2428.

Pörtner, H.O., Karl, D.M., Boyd, P.W., Cheung, W.W.L., Lluch-Cota, S.E., Nojiri, Y., Schmidt, D.N., Zavialov, P.O., 2014. Ocean systems. In: Field, C.B., Barros, V.R., Dokken, D.J., Mach, K.J., Mastrandrea, M.D., Bilir, T.E., Chatterjee, M., Ebi, K.L., Estrada, Y.O., Genova, R.C., Girma, B., Kissel, E.S., Levy, A.N., MacCracken, S., Mastrandrea, P.R., White, L. (Eds.), Climate Change 2014: Impacts, Adaptation, and Vulnerability. Part A: Global and Sectoral Aspects. Contribution of Working Group II to the Fifth Assessment Report of the Intergovernmental Panel on Climate Change. Cambridge University Press, Cambridge and New York, NY, pp. 411–484.

Ragg, N.L.C., Taylor, H.H., 2006. Heterogeneous perfusion of the paired gills of the abalone *Haliotis iris* Martyn 1784: an unusual mechanism for respiratory control. J. Exp. Biol. 209, 475–483. http://dx.doi.org/10.1242/jeb.02035.

Robinson, C.J., 2016. Evolution of the 2014–2015 sea surface temperature warming in the central west coast of Baja California, Mexico, recorded by remote sensing. Geophys. Res. Lett. 43, 7066–7071. http://dx.doi.org/10.1002/2016GL069356.

Rosenblum, E.S., Viant, M.R., Braid, B.M., Moore, J.D., Friedman, C.S., Tjeerdema, R.S., 2005. Characterizing the metabolic actions of natural stresses in the California red abalone, *Haliotis rufescens* using ^{1}H NMR metabolomics. Metabolomics 1, 199–209. http://dx.doi.org/10.1007/s11306-005-4428-3.

Sheedy, J.R., Lachambre, S., Gardner, D.K., Day, R.W., 2016. ^{1}H-NMR metabolite profiling of abalone digestive gland in response to short-term starvation. Aquac. Int. 24, 503–521. http://dx.doi.org/10.1007/s10499-015-9941-4.

Stramma, L., Schmidtko, S., Levin, L.a., Johnson, G.C., 2010. Ocean oxygen minima expansions and their biological impacts. Deep-Sea Res. I Oceanogr. Res. Pap. 57, 587–595. http://dx.doi.org/10.1016/j.dsr.2010.01.005.

Sunday, J.M., Bates, A.E., Dulvy, N.K., 2012. Thermal tolerance and the global redistribution of animals. Nat. Clim. Chang. 2, 686–690. http://dx.doi.org/10.1038/nclimate1539.

Taylor, H.H., Ragg, N.L.C., 2005. Extracellular fluid volume, urine filtration rate and haemolymph mixing time in the abalone, *Haliotis iris* Martyn: a comparison of 51Cr-EDTA and ^{14}C-inulin as extracellular markers. Mar. Freshw. Res. 56, 1117–1126. http://dx.doi.org/10.1071/MF05122.

Tikunov, A.P., Johnson, C.B., Lee, H., Stoskopf, M.K., Macdonald, J.M., 2010. Metabolomic investigations of American oysters using ^{1}H-NMR spectroscopy. Mar. Drugs 8, 2578–2596. http://dx.doi.org/10.3390/md8102578.

Venter, L., Loots, D.T., Vosloo, A., Jansen van Rensburg, P., Lindeque, J.Z., 2016. Abalone growth and associated aspects: now from a metabolic perspective. Rev. Aquac. 1–23. http://dx.doi.org/10.1111/raq.12181.

Verberk, W.C.E.P., Sommer, U., Davidson, R.L., Viant, M.R., 2013. Anaerobic metabolism at thermal extremes: a metabolomic test of the oxygen limitation hypothesis in an aquatic insect. Integr. Comp. Biol. 53, 609–619. http://dx.doi.org/10.1093/icb/ict015.

Verberk, W.C.E.P., Bartolini, F., Marshall, D.J., Pörtner, H.-O., Terblanche, J.S., White, C.R., Giomi, F., 2016. Can respiratory physiology predict thermal niches? Ann. N. Y. Acad. Sci. 1365, 73–88. http://dx.doi.org/10.1111/nyas.12876.

Viant, M.R., Rosenblum, E.S., Tjeerdema, R.S., 2003. NMR-based metabolomics: a powerful approach for characterizing the effects of environmental stressors on organism health. Environ. Sci. Technol. 37, 4982–4989. http://dx.doi.org/10.1021/es034281x.

Vosloo, D., Vosloo, A., Morillion, E.J., Samuels, J.N., Sommer, P., 2013. Metabolic readjustment in juvenile South African abalone (*Haliotis midae*) acclimated to combinations of temperature and dissolved oxygen levels. J. Therm. Biol. 38, 458–466. http://dx.doi.org/10.1016/j.jtherbio.2013.07.001.

Wu, H., Southam, A.D., Hines, A., Viant, M.R., 2008. High-throughput tissue extraction protocol for NMR- and MS-based metabolomics. Anal. Biochem. 372, 204–212. http://dx.doi.org/10.1016/j.ab.2007.10.002.

Xia, J., Sinelnikov, I.V., Han, B., Wishart, D.S., 2015. MetaboAnalyst 3.0—making metabolomics more meaningful. Nucleic Acids Res. 43, W251–7. http://dx.doi.org/10.1093/nar/gkv380.

Zaba, K.D., Rudnick, D.L., 2016. The 2014–2015 warming anomaly in the Southern California Current System observed by underwater gliders. Geophys. Res. Lett. 43, 1241–1248. http://dx.doi.org/10.1002/2015GL067550.

Zittier, Z.M.C., Bock, C., Lannig, G., Pörtner, H.O., 2015. Impact of ocean acidification on thermal tolerance and acid–base regulation of *Mytilus edulis* (L.) from the North Sea. J. Exp. Mar. Biol. Ecol. 473, 16–25. http://dx.doi.org/10.1016/j.jembe.2015.08.001.

Supplementary table I: Water parameter during the experiments with green abalone. In experimental tank (Exp) water temperature was increase 3°C per night with a final step of 2ºC, while Control (Ctrl) tank remained at 18°C. Values are means ± S.D.

	Temperature (°C)		Oxygen (% sat)		pH_{NBS}		pCO_2 (µatm)		Total alcalinity (umol/kg)	
Day	Exp	Ctrl	Exp	Ctrl	Exp	Ctrl	Exp	Ctrl	Exp	Ctrl
Experiment 1										
1	17.99 ± 0.14	17.93 ± 0.11	99.93 ± 0.32	99.1 ± 0.37	7.90	8.08	416.89	261.55	1264.34	1287.13
2	20.86 ± 0.09	18.05 ± 0.20	98.96 ± 0.37	98.73 ± 0.49	7.95	8.09	385.83	256.28	1321.02	1308.70
3	23.61 ± 0.07	18.14 ± 0.12	98.60 ± 0.39	101 ± 0.64	7.96	8.08	382.08	267.96	1314.25	1327.18
4	26.49 ± 0.09	18.16 ± 0.16	100 ± 0.77	101 ± 0.42	8.00	8.11	357.56	247.54	1349.37	1333.34
5	29.51 ± 0.07	18.28 ± 0.12	98.71 ± 0.37	102.3 ± 0.42	7.90	8.12	480.09	242.18	1349.37	1339.51
6	31.37 ± 0.05	18.43 ± 0.09	94.34 ± 0.48	101.4 ± 0.53	7.95	8.12	436.65	241.04	1388.80	1330.88
Experiment 2										
1	17.99 ± 0.08	18.43 ± 0.11	51.58 ± 0.53	58.68 ± 1.93	7.88	7.93	444.55	373.39	1276.23	1220.12
2	20.88 ± 0.13	18.68 ± 0.10	59.63 ± 8.96	59.02 ± 12.2	7.91	8.12	414.12	238.69	1260.84	1307.63
3	23.52 ± 0.08	18.51 ± 0.09	53.26 ± 6.05	49.81 ± 6.22	7.90	8.08	451.94	268.51	1311.32	1315.01
4	26.71 ± 0.08	18.60 ± 0.11	52.72 ± 4.23	49.82 ± 7.13	7.98	8.15	369.48	220.26	1308.86	1313.78
5	29.59 ± 0.08	18.88 ± 0.16	48.29 ± 3.20	41.22 ± 9.53	7.93	8.15	433.33	220.28	1313.78	1311.31
6	31.34 ± 0.13	19.14 ± 0.28	38.19 ± 11.0	28.45 ± 19.3	8.01	8.28	356.22	150.49	1350.11	1324.25
Experiment 3										
1	17.81 ± 0.12	18.47 ± 0.06	99.9 ± 0.41	100.8 ± 0.38	7.59	7.55	916.34	1048.59	1261.02	1269.11
2	20.85 ± 0.13	18.61 ± 0.13	100 ± 0.27	99.9 ± 0.51	7.38	7.44	1559.87	1334.27	1258.53	1272.84
3	23.84 ± 0.08	19.20 ± 0.26	101.1 ± 0.32	96.87 ± 0.30	7.42	7.47	1534.35	1251.87	1259.13	1275.33
4	26.54 ± 0.49	19.25 ± 0.30	100.4 ± 0.33	100.47 ± 0.35	7.56	7.51	1079.04	1154.90	1267.24	1285.28
5	29.78 ± 0.08	18.92 ± 0.09	100.6 ± 0.37	100.6 ± 0.31	7.55	7.52	1181.15	1128.04	1291.50	1302.70
6	31.84 ± 0.10	19.28 ± 0.12	100.7 ± 0.35	100.6 ± 0.62	7.48	7.52	1384.49	1125.95	1270.60	1300.21
Experiment 4										
1	18.12 ± 0.08	18.68 ± 0.22	51.40 ± 0.64	45.41 ± 1.54	7.51	7.51	1152.10	1180.81	1295.03	1323.27
2	21.11 ± 0.09	18.17 ± 0.14	50.20 ± 6.60	45.34 ± 8.12	7.59	7.48	983.23	1248.89	1296.98	1317.75
3	24.04 ± 0.06	18.11 ± 0.12	54.02 ± 0.60	47.12 ± 2.93	7.56	7.52	1066.95	1165.25	1298.28	1338.52
4	27.0 ± 0.06	18.36 ± 0.10	51.83 ± 0.86	49.62 ± 3.28	7.49	7.51	1307.10	1191.62	1295.03	1327.16
5	29.93 ± 0.07	18.55 ± 0.09	50.19 ± 0.60	49.58 ± 2.10	7.47	7.48	1473.34	1282.67	1332.03	1331.38
6	31.93 ± 0.07	18.45 ± 0.06	50.53 ± 0.55	45.91 ± 1.10	7.53	7.51	1290.95	1176.95	1340.80	1335.93

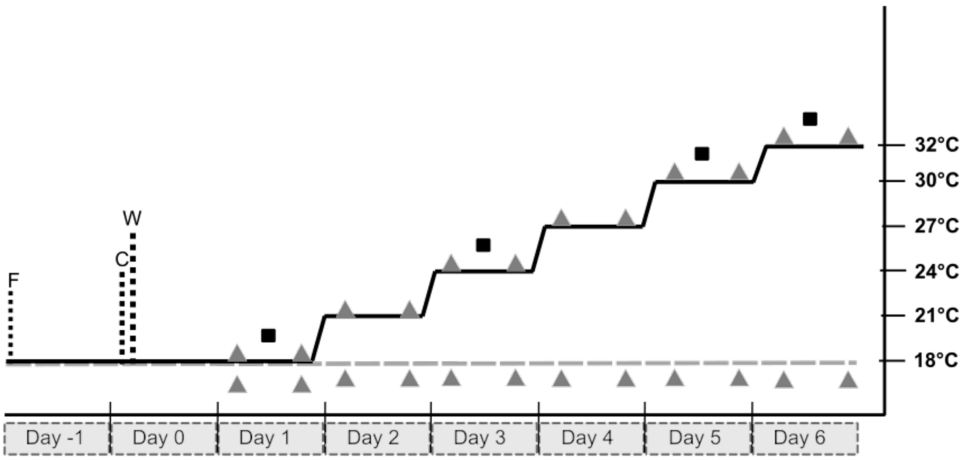

Supplementary figure 1: Graphic representation of the experimental design: Red line indicates the temperature (°C) for the experimental group; blue line indicates the temperature (°C) for the control group; triangles indicates the oxygen consumption measurements (section 2.2), squares indicates tissue sampling for metabolic profile (section 2.3). F indicates the start of fasting; C indicates the point where organisms were placed inside the respiration chambers (section 2.2); W indicates the point where water parameters were adjusted according to the experiment (section 2.2).

3.2 Publication II

Assessment of muscular energy metabolism and heat shock response of the green abalone *Haliotis fulgens* (Gastropoda:Philipi) at extreme temperatures combined with acute hypoxia and hypercapnia

Miguel A. Tripp-Valdez, Christian Bock, Gisela Lannig, Nils Koschnick, Hans O. Pörtner & Magnus Lucassen

2019

Comparative Biochemestry and Physiology. Part B

Comparative Biochemistry and Physiology, Part B 227 (2019) 1–11

Contents lists available at ScienceDirect

Comparative Biochemistry and Physiology, Part B

journal homepage: www.elsevier.com/locate/cbpb

Assessment of muscular energy metabolism and heat shock response of the green abalone *Haliotis fulgens* (Gastropoda: Philipi) at extreme temperatures combined with acute hypoxia and hypercapnia

Miguel A. Tripp-Valdez[a,*], Christian Bock[a], Gisela Lannig[a], Nils Koschnick[a], Hans O. Pörtner[a,b], Magnus Lucassen[a]

[a] Integrative Ecophysiology, Alfred Wegener Institute Helmholtz Centre for Polar and Marine Research, Am Handelshafen 12, D-27570 Bremerhaven, Germany
[b] University Bremen, Bibliothekstraße 1, 28359, Germany

ARTIC LE I NFO

Keywords:
^{1}H NMR spectroscopy
Citrate synthase
CT_{max}
Hsp70
Lactate dehydrogenase
Tauropine
Tauropine dehydrogenase

ABSTRAC T

The interaction between ocean warming, hypoxia and hypercapnia, suggested by climate projections, may push an organism earlier to the limits of its thermal tolerance window. In a previous study on juveniles of green abalone (*Haliotis fulgens*), combined exposure to hypoxia and hypercapnia during heat stress induced a lowered critical thermal maximum (CT_{max}), indicated by constrained oxygen consumption, muscular spams and loss of attachment. Thus, the present study investigated the cell physiology in foot muscle of *H. fulgens* juveniles exposed to acute warming (18 °C to 32 °C at +3 °C day^{-1}) under hypoxia (50% air saturation) and hypercapnia (~1000 µatm PCO_2), alone and in combination, to decipher the mechanisms leading to functional loss in this tissue. Under exposure to either hypoxia or hypercapnia, citrate synthase (CS) activity decreased with initial warming, in line with thermal compensation, but returned to control levels at 32 °C. The anaerobic enzymes lactate and tauropine dehydrogenase increased only under hypoxia at 32 °C. Under the combined treatment, CS overcame thermal compensation and remained stable overall, indicating active mitochondrial regulation under these conditions. Limited accumulation of anaerobic metabolites indicates unchanged mode of energy production. In all treatments, upregulation of Hsp70 mRNA was observed already at 30 °C. However, lack of evidence for Hsp70 protein accumulation provides only limited support to thermal denaturation of proteins. We conclude that under combined hypoxia and hypercapnia, metabolic depression allowed the *H. fulgens* musculature to retain an aerobic mode of metabolism in response to warming but may have contributed to functional loss.

1. Introduction

The increasing concentration of atmospheric CO_2 over the last century has resulted in a warming trend of the ocean which, in hand with an increasing frequency and intensity of extreme warming events, affects many marine organisms and ecosystems (Cai et al., 2014; Pörtner et al., 2014). According to the concept of the oxygen- and ca-pacity-limited thermal tolerance (OCLTT; Pörtner, 2002; Pörtner et al., 2017), transition to sublethal temperature constraints beyond *pejus* (T*p*) is indicated by the progressive decline in venous PO_2 and the progressively constrained aerobic metabolic scope of the mitochondria. This finally lead to a transition to anaerobic metabolism at a specific critical temperature (T*c*; Pörtner, 2002; Pörtner et al., 2017). Beyond T*c*, organisms are able to widen the passive range of thermal tolerance by increasing anaerobic metabolic capacity, inducing molecular protection mechanisms and by a minimization of metabolic costs through metabolic depression (Pörtner et al., 2017).

Green abalone (*Haliotis fulgens*: Philipi 1845) is a marine gastropod with high economic importance along the Pacific coast of the Baja California Peninsula, Mexico (Morales-Bojorquez et al., 2008). Within its distribution range, overfishing in combination with environmental extremes such as strong El Niño events, reduced oxygen availability or high PCO_2 levels in seawater have threatened abalone natural populations (Guzman del Proo et al., 2003; Morales-Bojorquez et al., 2008; Micheli et al., 2012; Somero et al., 2016). As future projections suggest that these factors will interact more frequently in marine ecosystems (Pörtner et al., 2014), it is necessary to investigate their interaction when addressing the vulnerability of abalone species to climate change.

In our previous study (Tripp-Valdez et al., 2017), juveniles of *H. fulgens* were exposed to a warming ramp under hypoxia (50% air

* Corresponding author.
E-mail address: mtripp@awi.de (M.A. Tripp-Valdez).

https://doi.org/10.1016/j.cbpb.2018.08.009
Received 11 June 2018; Received in revised form 24 August 2018; Accepted 29 August 2018
Available online 06 September 2018

saturation), hypercapnia (1000 μatm PCO_2) and both factors combined, based on realistic oxygen declines occurring along the Baja California Peninsula (Micheli et al., 2012) and PCO_2 values predicted by the end of the century (Pörtner et al., 2014). Whole-organism measurements showed that hypercapnia stimulated oxygen consumption (MO_2), whereas hypoxia elicited a shift in a temperature dependent breakpoint in MO_2 recordings to lower temperature, associated with the accumulation of anaerobic end products in gill and hepatopancreas. These findings suggest a downward shift in Tc. This response was even stronger under hypoxia and hypercapnia combined; abalone MO_2 dropped strongly during transition to the highest temperature, accom-panied by decreasing concentrations of anaerobic metabolites in gill, by the onset of muscular spams, loss of attachment, and mortality (Tripp-Valdez et al., 2017).

The onset of muscular spams and loss of righting are in line with the loss of integration of physiological functions that defines the critical thermal maximum (CT_{max}; Lutterschmidt and Hutchison, 1997; Diaz et al., 2006; Madeira et al., 2012). Previous investigations in *H. fulgens* juveniles from Mexico reported a CT_{max} at 33.6 °C under environmental oxygen and PCO_2 conditions (Diaz et al., 2006). This implies that warming stress under combined hypoxia and hypercapnia not only induced a downward shift in *H. fulgens* Tc according to the OCLTT concept (indicated by the onset of anaerobiosis in gill and hepatopancreas), but also in the CT_{max} threshold.

The central nervous system is known to be highly temperature sensitive in animals; temperature-induced failure of gap-junction, in hand increased membrane fluidity may elicit the onset of muscular failure at CT_{max} (White, 1983; Lutterschmidt and Hutchison, 1997; Dunphy et al., 2018). These mechanisms usually take place at the edge or outside the range of the aerobic power budget (Pörtner et al., 2017), and thus are not directly correlated to oxygen-dependent thermal limits (T*p*, T*c*). However, reduced oxygen availability resulted in a downward shift of CT_{max} in fish (Healy and Schulte, 2012) and invertebrate species (Verberk et al., 2013), suggesting an association between insufficient aerobic metabolism and CT_{max}, but this association remains obscure (Pörtner et al., 2017).

In this context, the ability of an organism to induce protection mechanisms upon thermal stress such as *e.g.* heat shock proteins (Hsp; Feder and Hofmann, 1999) prevents macromolecular damage and foster extended thermal tolerance and whole-organism maximum thermal limits (Tomanek, 2008; Bahrndorff et al., 2009; Fangue et al., 2011; Han et al., 2017). Studies with marine fishes and mollusks de-scribe a close link between metabolic perturbation and Hsp induction during thermal stress; hypoxemia, limited aerobic capacity, enhanced anaerobic potential, accumulation of anaerobic intermediates or dis-rupted ATP homeostasis preceded or developed in parallel to the in-duction of Hsp70 (Viant et al., 2003; Feidantsis et al., 2009; Anestis et al., 2010; Katsikatsou et al., 2012). Metabolic perturbations during strong environmental hypoxia or hypercapnia are also known to induce molecular protection mechanism, even at stable temperatures (*e.g.*Anestis et al., 2010; Harms et al., 2014). Therefore, the development of a strong temperature-induced systemic hypoxemia at T*c* may be causative of Hsp70 induction (Feidantsis et al., 2009; Anestis et al., 2010; Katsikatsou et al., 2012). At transcriptional level, Hsp70 induction may occur at lower temperatures than T*c* (Han et al., 2017), possibly at a putative T*p*, when systemic hypoxemia begins to develop (Pörtner et al., 2017), and thus on a warming ramp, already prior to the detectable accumulation of Hsp proteins (Bahrndorff et al., 2009).

Abalone species exhibit high anaerobic capacity, particularly in the musculature, which produces large amounts of the anaerobic end products lactate and tauropine during severe environmental and functional hypoxia (Omolo et al., 2003; Venter et al., 2016). We therefore hypothesize that a downward shift in CT_{max} in *H. fulgens* juveniles is associated to i) the additional factors hypoxia and hypercapnia causing a shift in the use of anaerobic mechanisms of energy supply towards lower temperatures; and ii) the onset of cellular disturbances in muscle occurring at lower temperatures under combined hypoxia and hypercapnia, linked to the induction of protection mechanisms through members of the Hsp70 family.

To test these hypotheses, we investigated the cellular metabolic status and the molecular stress response in muscle tissue of thermally challenged *H. fulgens* under hypoxia (50% air saturation), hypercapnia (1000 μatm PCO_2) and both factors combined, thereby using muscle tissue from the same experiment as described in Tripp-Valdez et al. (2017). Cellular metabolic status was estimated from enzyme activities (citrate synthase, lactate dehydrogenase, tauropine dehydrogenase), and from the accumulation of anaerobic end products. The onset of the molecular stress response was estimated from gene expression patterns of six genes of the Hsp70 family and from immunoblot analysis with a heterologous Hsp70 antibody.

2. Material and methods

2.1. Experimental design and tissue collection

All investigations were performed on muscle tissues sampled during our experiment described in Tripp-Valdez et al. (2017). Briefly, juveniles of green abalone (*Haliotis fulgens*; 20–30 mm shell length) were provided by a fishery cooperative in Bahia Tortugas, Mexico, and brought to the Centro de Investigaciones Biológicas del Noroeste, Mexico, where they were kept at 18 °C for 73 days. Temperature, salinity and pH_{NBS} were monitored daily with HOBO® pendant data loggers, an optic refractometer (Extech Instruments, Waltham, MA, USA) and a pH sensor (Neptune Systems, CA, USA), respectively. During acclimation, green abalone were fed with an artificial diet (see Tripp-Valdez et al., 2017 for details) and visual inspection of the gonad showed no sign of sexual maturation. Following the incubation period, animals were placed in a flow-through aquarium connected to a header tank with a flow of 2.5 L min^{-1} under four different experimental conditions: Experiment 1 (Control; 100% air saturation; 400 μatm PCO_2), experiment 2 (Hypoxia; 50% air saturation; 400 μatm PCO_2), experiment 3 (Hypercapnia; 100% air saturation; ~1000 μatm PCO_2) and experiment 4 (Combination; 50% air saturation; ~1000 μatm PCO_2). The following day and thereafter, water temperature was increased from 18 °C to 32 °C at 3 °C steps every night (00:00 ± 1 h) with a final increment step of 2 °C. After 12 h ± 1 h of each temperature increment step ten animals were randomly taken at 18 °C, 24 °C, 30 °C and 32 °C. As described in Tripp-Valdez et al. (2017) animals at 32 °C under combined hypoxia and hypercapnia began to display muscular failure. However, for this last sampling step, we used only animals that were still attached to the walls of the tank, although they were considerably weaker and could be easily removed compared to animals of the other treatments. The muscle section from each animal including foot and adductor muscle was dissected, snap-frozen in liquid nitrogen and kept at −80 °C. Before the analyses, each muscle sample was ground to fine powder under liquid nitrogen using a Cryogrinder (OPS diagnostics, Lebanon, NJ, USA).

2.2. Determination of enzyme activity

Ground tissue subsamples were mixed in 10 volumes (w:v) of ice-cold extraction buffer (50 mM imidazole-HCl, 1 mM EDTA, 2 mM $MgCl_2$, pH 7.4) and sonicated for 5 min at 0 °C in a Branson Sonifier 450 (output control 8, duty cycle 50%). Homogenates were centrifuged at 4 °C for 20 min at 13000*g* and supernatant was transferred to a new tube and kept on ice for immediate assays.

Activities of tauropine dehydrogenase (EC. 1.5.1.23) and lactate dehydrogenase (EC. 1.1.1.27) were estimated according to Hickey and Wells (2003) in a total volume of 1 mL reaction buffer. Firstly, background activity was estimated followed by the addition of pyruvate to start the reaction. Activity was calculated from the oxidation of NADH monitored at 340 nm. Final tauropine dehydrogenase activity was

determined by subtracting the lactate dehydrogenase activity. Citrate synthase (EC. 2.3.3.1) activity was determined according to Sidell et al. (1987) with modifications in 1 mL buffer. Activity was recorded following the absorbance at 412 nm after the addition of oxaloacetate to start the reaction. Preliminary trials were made to test the optimal concentration of reagents.

All enzyme activities were measured at 18 °C and 32 °C in a UV/VIS spectrophotometer (Beckman, Fullerton, CA, USA) with a thermostated cell holder. Each sample was measured in duplicate with different concentrations of the extract to ensure linearity. Activities were standardized to fresh tissue weight.

To assess whether additional pyruvate reductases contribute to the anaerobic potential in green abalone muscle, activities of octopine dehydrogenase (EC. 1.1.1.11), strombine dehydrogenase (EC. 1.5.1.22), alanopine dehydrogenase (EC. 1.5.1.17) and lysopine dehydrogenase (EC. 1.5.1.16) were measured. For this, only three samples from muscle at 18 °C from the control experiment were used at an assay temperature of 18 °C. Final activity was calculated by subtracting lactate dehydrogenase activity.

The final composition of the reaction mixtures for enzyme activities were as listed:

Tauropine dehydrogenase: 80 mmol L^{-1} imidazole-HCl pH 7.4, 1 mmol L^{-1} ethylenediaminetetraacetic acid (EDTA), 1 mmol L^{-1} $MgCl_2$, 0.15 mmol L^{-1} nicotinamide adenine dinucleotide (NADH), 80 mmol L^{-1} taurine, 2.5 mmol L^{-1} pyruvate. ε_{340} = 6.22 mmol L^{-1} cm^{-1}.
Lactate dehydrogenase: 80 mmol L^{-1} imidazole-HCl pH 7.4, 1 mmol L^{-1} EDTA, 1 mmol L^{-1} $MgCl_2$, 0.15 mmol L^{-1} NADH, 2.5 mmol L^{-1} pyruvate. ε_{340} = 6.22 mmol L^{-1} cm^{-1}.
Octopine dehydrogenase: 80 mmol L^{-1} imidazole-HCl pH 7.4, 1 mmol L^{-1} EDTA, 1 mmol L^{-1} $MgCl_2$, 0.15 mmol L^{-1} NADH, 5 mmol L^{-1} arginine, 2.5 mmol L^{-1} pyruvate. ε_{340} = 6.22 mmol L^{-1} cm^{-1}.
Strombine dehydrogenase: 80 mmol L^{-1} imidazole-HCl pH 7.4, 1 mmol L^{-1} EDTA, 1 mmol L^{-1} $MgCl_2$, 0.15 mmol L^{-1} NADH, 200 mmol L^{-1} glycine, 2.5 mmol L^{-1} pyruvate. ε_{340} = 6.22 mmol L^{-1} cm $^{-1}$.
Alanopine dehydrogenase: 80 mmol L^{-1} imidazole-HCl pH 7.4, 1 mmol L^{-1} EDTA, 1 mmol L^{-1} $MgCl_2$, 0.15 mmol L^{-1} NADH, 100 mmol L^{-1} alanine, 2.5 mmol L^{-1} pyruvate. ε_{340} = 6.22 mmol L^{-1} cm^{-1}.
Lysopine dehydrogenase: 80 mmol L^{-1} imidazole-HCl pH 7.4, 1 mmol L^{-1} EDTA, 1 mmol L^{-1} $MgCl_2$, 0.15 mmol L^{-1} NADH, 100 mmol L^{-1} lysine, 2.5 mmol L^{-1} pyruvate. ε_{340} = 6.22 mmol L^{-1} cm $^{-1}$.
Citrate synthase: 80 mmol L^{-1} Tris-HCl pH 8.0, 0.2 mmol L^{-1} 5,5′-dithio-bis-(2-nitrobenzoic acid; DTNB), 0.3 mmol L^{-1} acetyl-CoA, 0.5 mmol L^{-1} oxaloacetate. ε_{412} = 13.61 mmol L^{-1} cm^{-1}.

2.3. Nuclear magnetic resonance (NMR) spectroscopy

Succinate, lactate, tauropine, ATP/ADP and valine were quantified in ground muscle subsamples using ^{1}H NMR spectroscopy from polar metabolite extractions according to Wu et al. (2008). Briefly, preweighed frozen tissue was mixed with 4 mL g^{-1} of ice-cold methanol and 0.85 mL g^{-1} water and sonicated for 5 min at 0 °C in a Branson Sonifier 450 (output control 8, duty cycle 50%), followed by the addition of 4 mL g^{-1} ice-cold chloroform and 2 mL g^{-1} water. The homogenate was vortexed, incubated on ice for 10 min and centrifuged at 4 °C for 10 min at 3000g. The upper methanol layer with polar metabolites was transferred into a new 1.5 mL tube and dried overnight in a centrifugal vacuum concentrator (RVC 2−18, Martin Christ Freeze dryers, GmbH, Germany) at room temperature. Dried samples were resuspended in D_2O containing 0.05% trimethylsilyl propionate (TSP; Sigma-Aldrich, St. Louis, USA) to a final concentration of 0.3 g mL^{-1} of the initial tissue weight. After mixing, an aliquot of 50 μL was transferred into a 4 mm standard HRMAS (high-resolution magic angle spinning) zirconia rotor. The ^{1}H-HRMAS NMR spectra were acquired with a 9.4 T Avance III HD 400 WB spectrometer (Bruker Biospin GmbH, Germany) using a Nuclear Overhauser Enhancement Spectro-scopy sequence with low-power water-signal presaturation (NOESY) with the following parameters: flip angle 90°, acquisition time 3.98 s, relaxation delay 4 s, sweep width 8223.7 Hz, 64 scans with 4 dummy scans. All spectra were acquired using TopSpin 3.2 (Bruker Biospin GmBH, Germany) and imported to the software Chenomx NMR suit 8.0 (Chenomx Inc., Edmonton, Canada) using the included libraries for metabolite identification and relative quantification. All Fourier-transformed spectra were baseline corrected and calibrated to the internal reference (TSP at 0.0 ppm) with an exponential broadening of 0.5 Hz (see Tripp-Valdez et al. (2017) for details on metabolite identification and quantification).

Tauropine accumulation constitutes a good indicator of anaerobic glycolysis in adductor muscle as it results from the activity of tauropine dehydrogenase in abalone species (Venter et al., 2016), however, the chemical shift of tauropine in ^{1}H NMR spectra has not been described. To identify the tauropine peak in green abalone muscle extracts, we conducted a brief analysis using the product of the tauropine dehydrogenase enzyme activity assay described in section 2.2. Tauropine dehydrogenase catalyzes the reductive condensation of pyruvate and taurine with NADH as coenzyme resulting in tauropine and NAD^+ (Gäde, 1986). Therefore, under conditions of taurine saturation, any increase of NADH would result in enrichment of tauropine. Accordingly, using four increasing concentrations of NADH and a fixed amount of taurine, the corresponding ^{1}H NMR signals of tauropine should arise accordingly (see supplementary material 1). A representative ^{1}H NMR spectrum of *H. fulgens* muscle indicating the analyzed metabolites is displayed in Fig. 1.

2.4. Hsp70 mRNA sequence determination and phylogenetic analysis

Gene sequences for Hsp70 expression analysis were obtained from a *de novo* transcriptome assembly of *Haliotis fulgens* juveniles from Baja California (unpublished). Briefly, total RNA sequencing was performed in an Illumina MiSeq platform (2 × 300 bp paired-end). The transcriptome was assembled using Trinity (Haas et al., 2013) and resulting transcripts were annotated using BLAST against SwissProt database. Six Hsp70 isoforms were selected for the analysis based on their sequence similarity to known Hsp70 family members (Supplementary material 2). A phyloge-netic analysis was made to assess the homology of the six *H. fulgens* Hsp70 genes with other abalone species, as well as with other marine mollusks and with model vertebrate species. *In silico* sequence translation and ORF identification of the Hsp70 was made with the Expasy translate tool (http://web.expasy.org/translate/). Multiple sequence alignment was

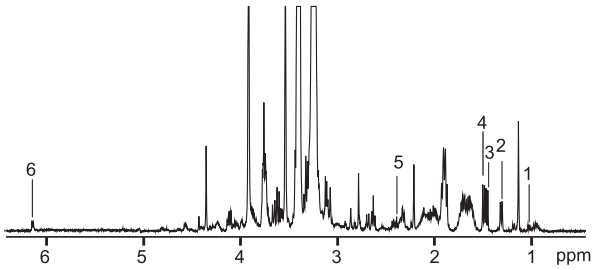

Fig. 1. Representative one-dimensional ^{1}H NMR spectrum from green abalone muscle extracts. Compounds of interest are as indicated: 1) valine; 2) lactate; 3) alanine (not analyzed in this study); 4) tauropine; 5) succinate; 6) ATP/ADP.(For interpretation of the references to colour in this figure legend, the reader is referred to the web version of this article.)

performed with the ClustalW method and a Neighbor-Joining tree was constructed from the aligned sequences with 1000 bootstrap replicates using the Jones-Taylor-Thornton (JTT) model with MEGA7 (Kumar et al., 2016). The phylogenetic tree was rooted using the Heat shock protein SSA1 sequence from *Saccharomyces cerevisiae*.

2.5. Total RNA isolation and quantitative real-time PCR analysis of Hsp70 genes

Approximately 20 mg of frozen muscle subsample was homogenized in 1 mL QIAzol lysis reagent (Qiagen) by one cycle of 20 s at 6500 rpm using Precellys 24 (Bertin Technologies, France). After incubation for 5 min at room temperature, RNA was isolated by phase separation with chloroform and precipitated with isopropanol followed by two wash steps with 75% ethanol. The concentration of RNA was determined photometrically at 260 nm. Purity was determined from the ratios of 260/280 nm and 260/230 nm (NanoDrop ND-1000, Seqlab, Erlangen, Germany) and integrity was evaluated using capillary electrophoresis (Bioanalyzer, Agilent Technologies, Waldbronn, Germany). To exclude DNA contamination, 3 µg of total RNA was treated with the Turbo DNA-free Kit (Ambion, Darmstadt, Germany). cDNA synthesis was performed with 0.4 µg of DNA-free RNA using the High-Capacity Reverse Transcription Kit (Applied Biosystems, Darmstadt, Germany) following the manufacturer's instructions.

Primers were designed with the software Primer Express® 3.0 using the default parameters for the Taqman quantification method (Applied Biosystems, Darmstadt, Germany). Actin, E3 ubiquitin-protein ligase and 60s ribosomal protein were selected as potential reference genes as these constitute commonly used reference and has been previously tested in *Haliotis* species (López-Landavery et al., 2014).

PCR was conducted in a ViiA 7 Real-Time PCR System (Applied Biosystems) using SYBR Green PCR Master Mix (Applied Biosystems). Each reaction contained 2 ng of cDNA in a final volume of 20 µL with a primer concentration of 300 nM each. Samples were run in duplicates and repeated samples were used to assess inter-plate variability. Efficiency curves were constructed using five serial dilutions of template cDNA (from 2 ng to 0.02 pg cDNA) including a no-template control (NTC) and a template without reverse transcriptase (−RT) to test possible contamination of DNA. A melting curve was performed immediately after amplification to corroborate the specificity of primers.

2.6. Immunoblot analysis

Immunoblot analysis of Hsp70 was performed for the control, hypercapnia and combined experiments due to limited availability of muscle tissue. Ground muscle subsamples were homogenized in 10 volumes (w:v) of ice-cold extraction buffer (50 mM imidazole-HCl, 1 mM EDTA, 2 mM $MgCl_2$, pH 7.4) by one cycle of 20 s at 5500 rpm using Precellys 24 (Bertin Technologies, France). Homogenates were centrifuged at 4 °C and 13,000*g* for 20 min, and the supernatant was transferred to a new tube. Protein concentration of the tissue extracts was determined according to Bradford (1976) with BSA as standard. Immunoblotting of 15 µL of crude protein extract was done with polyvinylidene difluoride membranes (Bio-Rad, Munich, Germany) as described earlier (Deigweiher et al., 2008), after fractionating by SDS-PAGE on 10% polyacrylamide gels according to Laemmli (1970). For immunodetection of Hsp70, the monoclonal antibody 3A3 (MA3-006; Thermo Fisher Scientific, Germany) was used as the primary antibody and as secondary antibody a goat anti-mouse/anti-mouse IgG conjugated with horse radish peroxidase (Pierce Rockford, IL, USA). Sig-nals were visualized with the ECL Advanced Western blotting detection reagent (GE Healthcare, Munich, Germany) and recorded by a cooled charge-coupled device camera (LAS-1000: Fuji, Tokyo, Japan). Signal intensity was calculated using the AIDA Image Analyzer v. 3.52 (Raytest, Straubenhardt, Germany) software. A pool of samples was loaded on each gel as a standard. All Hsp70 levels were normalized relative to the standard and related to total protein content (µg) of each tissue sample.

2.7. Data analysis

All data processing and statistical analysis were performed in R (R Core Team, 2015). A two-way ANOVA was used to test the effect of experimental conditions (control, hypoxia, hypercapnia and combined), temperature (18 °C, 24 °C, 30 °C, 32 °C) at sampling time and their interaction on enzyme activity (section 2.2) and for the ^{1}H NMR analysis (section 2.3). Normality was tested with a Shapiro-Wilk test while homogeneity of variances was assessed through Bartlett's test and visual inspection of the model's residuals. Data were log transformed where large deviations from homoscedasticity were found. Mean differences in significant main effects were assessed with a Tukey's honest significant deviance (HSD) test using the HSD.test function from the package *Agricolae*. If the interaction term was significant, *post hoc* interaction analysis was performed with the package *phia*. A three-way ANOVA was used for enzyme activity data (section 2.2) to test the interaction effect between experimental conditions, temperature at sampling and assay temperature (18 °C and 32 °C).

Statistical analysis of PCR data was performed with the package *MCMC.qpcr*. This converts Cq values into natural logarithms of relative abundance while correcting for the efficiency of amplification (Matz et al., 2013). The model was therefore performed under the “classic” method, normalized by the harmonic mean of expression values of the reference genes (Vandesompele et al., 2002). Relative gene abundance is reported as posterior means with 95% credible intervals, which are the Bayesian analog to confidence intervals. Pairwise differences between groups were calculated controlling for multiple comparisons with the p.adjust function in R. Stability of the reference genes was assessed through the package *SLqPCR*, which implements the algorithm of geNorm into R and confirmed by running a “naive” model with *MCMC.qpcr* (not shown). Given the low sample size, statistical analysis from western blot were made only for the hypercapnia experiment. A one-way ANOVA was made after testing for normality and homoscedasticity.

3. Results

3.1. Metabolic condition: enzyme activity

Aerobic and anaerobic metabolic capacities from *H. fulgens* muscle samples were assessed through citrate synthase (CS), lactate dehydrogenase (LDH) and tauropine dehydrogenase (TDH) enzyme activity assays.

The three-way ANOVA indicated no significant interaction between assay temperature (18 °C and 32 °C), sampling temperature and experimental condition on any of the tested enzymes (CS: $F_{9,\ 158} = 0.674$, $P = 0.731$; LDH: $F_{9,\ 157} = 0.586$, $P = 0.807$; TDH: $F_{9,\ 160} = 0.1$, $P = 0.99$). Therefore, only results from the 18 °C assay temperature are shown in Fig. 2 while the calculated Q_{10}'s between the 18 °C and 32 °C assay temperatures are shown in Table 1.

Overall, CS had the lowest activity among analyzed enzymes (Fig. 2A), followed by LDH (Fig. 2B) and TDH, which showed the highest activities (Fig. 2C). Nonetheless, the Q_{10} between 18 and 32 °C measurements was 3.11 ± 0.40 for LDH indicating the highest thermal response, whereas CS and TDH displayed quite moderate Q_{10} values of 1.48 ± 0.121 and 1.32 ± 0.10, respectively (Table 1).

Changes in enzyme activity induced by the warming ramp were notable for CS, where a significant decline in capacity occurred with warming from 18 °C up to 30 °C (Tukey: $P < 0.05$) under control, hypoxia and hypercapnia (Fig. 2A). In these experiments, the observed decline was followed by a reestablishment of initial capacities with further warming up to 32 °C. However, this pattern was not observed under the combined treatment (hypoxic hypercapnia) and activity remained constant despite increasing temperature (Fig. 2A). LDH and

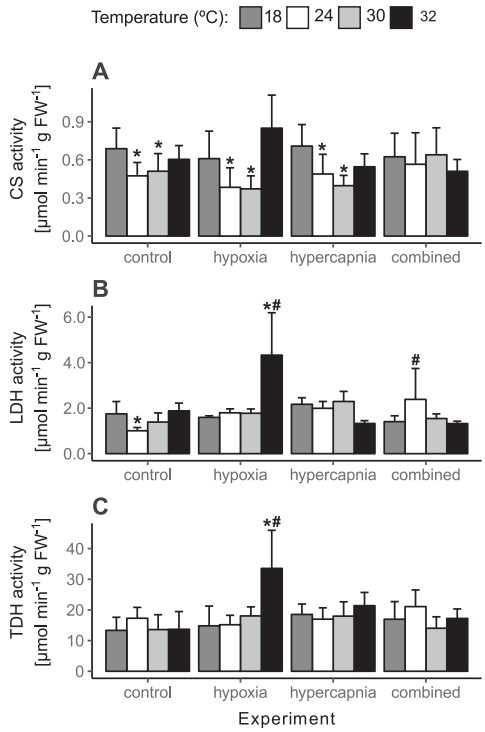

Fig. 2. Maximum activity of A) citrate synthase (CS); B) lactate dehydrogenase (LDH) and C) tauropine dehydrogenase (TDH) per g fresh weight in muscle tissue of *Haliotis fulgens* at the 18 °C assay temperature during the warming ramp under control (normoxic normocapnia), hypoxia (hypoxic normocapnia), hypercapnia (normoxic hypercapnia) and combined (hypoxic hypercapnia) exposures. * indicates data significantly different from the initial incubation temperature (18 °C) at the same experimental condition. # indicates significant differences to control conditions at same incubation temperature. n = 5–6. Values are means ± S.D.

Table 1
Calculated Q_{10} values from the enzyme activities measured at 18 °C and 32 °C assay temperature during a warming ramp (section 2.2). CS: citrate synthase, LDH: lactate dehydrogenase, TDH: tauropine dehydrogenase.

Experiment	Temperature (°C)	Q_{10}		
		CS	LDH	TDH
Control	18	1.59 ± 0.06	3.23 ± 0.34	1.35 ± 0.07
	24	1.46 ± 0.1*	3.34 ± 0.13	1.38 ± 0.05
	30	1.47 ± 0.02	3.26 ± 0.22	1.3 ± 0.06
	32	1.57 ± 0.1	2.93 ± 0.15*	1.41 ± 0.12
Hypoxia	18	1.51 ± 0.12	3.05 ± 0.17	1.25 ± 0.08
	24	1.35 ± 0.1	3.04 ± 0.16	1.31 ± 0.07
	30	1.43 ± 0.12	2.94 ± 0.11	1.31 ± 0.05
	32	1.49 ± 0.07	2.55 ± 0.09*	1.19 ± 0.1
Hypercapnia	18	1.61 ± 0.07	2.61 ± 0.13	1.29 ± 0.07
	24	1.5 ± 0.12	3.01 ± 0.13*	1.28 ± 0.08
	30	1.34 ± 0.1*	2.74 ± 0.16	1.36 ± 0.09
	32	1.51 ± 0.11	3.36 ± 0.22*	1.34 ± 0.07
Combined	18	1.48 ± 0.06	3.26 ± 0.26	1.35 ± 0.11
	24	1.54 ± 0.11	3.63 ± 1.02	1.32 ± 0.07
	30	1.43 ± 0.18	3.26 ± 0.4	1.25 ± 0.03*
	32	1.54 ± 0.09	3.54 ± 0.28	1.42 ± 0.07

The * indicates significant differences from the initial temperature (18 °C) at their corresponding treatment.

Table 2
Maximum activity of additional pyruvate dehydrogenase per g of fresh weight of muscle of *Haliotis fulgens* at 18 °C. Values are mean ± S.D. n = 3.

Enzyme	Activity (µmol min^{-1} g FW^{-1})
Tauropine dehydrogenase	12.65 ± 1.61
Lysopine dehydrogenase	2.36 ± 0.24
Lactate dehydrogenase	2.33 ± 0.55
Alanopine dehydrogenase	0.94 ± 0.02
Strombine dehydrogenase	0.36 ± 0.10
Octopine dehydrogenase	0.13 ± 0.07

TDH as proxies for anaerobic capacities responded similarly to temperature increments: Warming under control, hypercapnic and combined treatments did not induce changes in both enzymes, whereas warming under hypoxia caused capacities of both enzymes to increase at 32 (LDH, Fig. 2B; TDH, Fig. 2C). A moderate, albeit significant increment in LDH activity was only observed at 24 °C in the combined experiment (Fig. 2B), which was absent for TDH (Fig. 2C).

Additional pyruvate reductases with potential relevance in anaerobic glycolysis were tested at 18 °C (Table 2). Tauropine dehydrogenase had the highest activity values in this test (12.65 ± 1.61 µmol min^{-1} g FW^{-1}; n = 3), while lysopine dehydrogenase and lactate dehydrogenase showed similar values (2.36 ± 0.24 and 2.33 ± 0.55 µmol min^{-1} g FW^{-1}, respectively; n = 3) followed by alanopine dehydrogenase (0.92 ± 0.02 µmol min^{-1} g FW^{-1}; n = 3), strombine dehydrogenase (0.36 ± 0.10 µmol min^{-1} g FW^{-1}; n = 3) and lastly by octopine dehy-drogenase (0.13 ± 0.07 µmol min^{-1} g FW^{-1}; n = 3).

3.2. Metabolic condition: anaerobic end products

Tauropine was identified as a double peak at 1.5 ppm, next to the double peak of alanine (Fig. 1). The analysis of the ^{1}H NMR metabolic profiles (Fig. 3) revealed no accumulation of lactate and tauropine, the main end products of anaerobic glycolysis, under any experimental con-dition in muscle tissue. Instead, a significant reduction of lactate was ob-served under the combined treatment at 32 °C while a significant reduc-tion of tauropine was observed from 30 °C onward (Tukey: $P < 0.05$). Succinate, the main end product of mitochondrial anaerobiosis, displayed a significant reduction at 32 °C under hypercapnia in isolation as well as under the combined exposure (Tukey: $P < 0.05$). ATP/ADP levels re-mained unchanged during the warming protocol under all experimental condition. In contrast, valine displayed a warming-induced accumulation: In the control experiment, a significant accumulation of valine was ob-served from 30 °C onwards (Tukey: $P < 0.05$). The same pattern was observed under hypercapnia alone and under the combined conditions. Under hypoxia, no increase in valine besides considerable variation be-yond 30 °C could be observed.

3.3. Heat shock response: phylogenetic analysis of Hsp70 genes

The deduced protein sequences of potential Hsp70 genes, derived from the transcriptome, were between 431 and 655 amino acids long. Phylogenetic analysis revealed high similarity with sequences from other species; with the exception of members of the 12A family, all *H. fulgens* Hsp70 contained the signature sequences of the Hsp70 family: IDLGTTYS, DLGGGTFD, TVPAYVFN, NEPTAA and GP[T/N][I/V]EEVD (data not shown). The resulting phylogenetic tree located Hsp70 C4 in the same branch with other constitutive isoforms from vertebrate and invertebrate species (Fig. 4; group I) while Hsp70 B2, Hsp70 A2 and Hsp70i were in the same branch with other Hsp70 inducible forms (Fig. 4; group II). The tree also revealed a clear distinction of members of the Hsp70 12A, including vertebrates and invertebrate species,

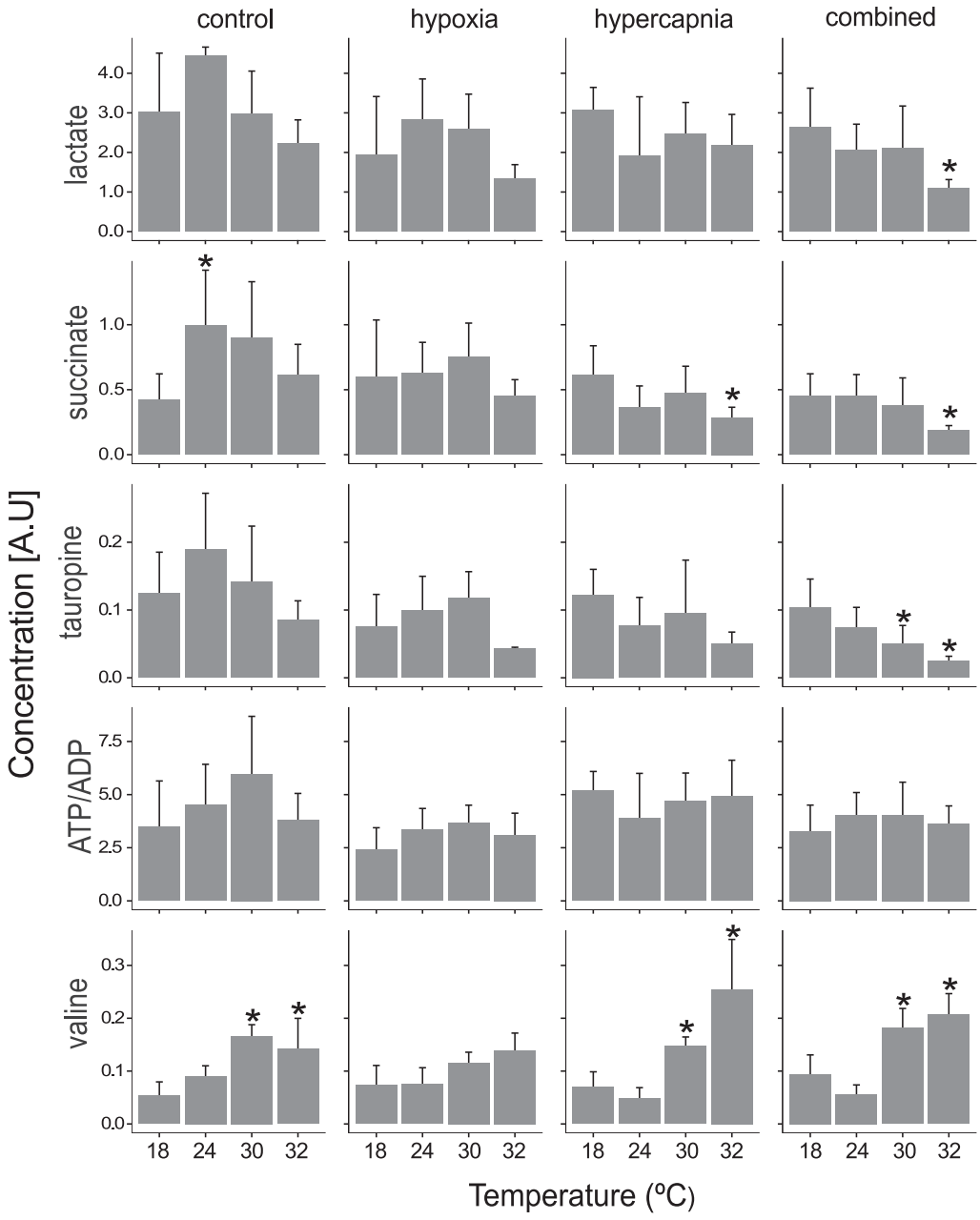

Fig. 3. Concentrations of lactate, succinate, tauropine, ATP/ADP and valine in muscle tissue of *Haliotis fulgens* during the warming ramp. * indicates significant differences with initial temperature (18 °C) at their respective experimental condition. Control: normoxic normocapnia; hypoxia: hypoxic normocapnia; hypercapnia: normoxic hypercapnia; combined: hypoxic hypercapnia. n = 6. Values are means ± S.D.

where the *H. fulgens* genes Hsp70 13 and Hsp70 12A were located inside this branch (Fig. 4; group III).

3.4. Heat shock response: Hsp70 gene expression

Expression profiles of the six genes member of the Hsp70 family confirmed the presence of both constitutive and inducible forms (Fig. 5; Supplementary material 2). Hsp70 12A expression levels remained at baseline levels throughout the warming ramp (Fig. 5A). Similarly, Hsp70 C4 showed a slight but not significant induction with temperature (Fig. 5B). The remaining genes showed a coordinated expression pattern with a significant upregulation observed at 30 °C ($P < 0.01$) and above (Fig. 5). Hsp70i showed the highest inducibility: starting with lower initial relative expression compared to the reference genes and other *H. fulgens* Hsp70 genes, a strong upregulation up to three orders of magnitude ($P < 0.001$) was observed from 30 °C onwards (Fig. 5F). Overall, the multiple comparison tests indicated no effect of the different experimental conditions on the temperature-induced expression profile of the analyzed genes; only Hsp70 A2 at 32 °C showed significantly higher expression values under hypercapnia

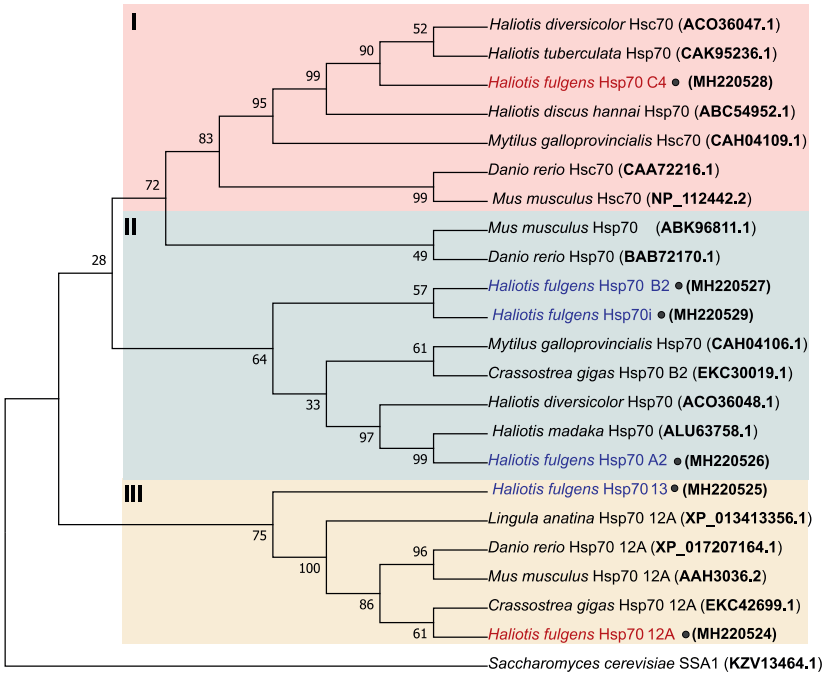

Fig. 4. Phylogenetic relationship between the six analyzed *Haliotis fulgens* Hsp70 translated proteins with vertebrate and invertebrate Hsp70s (section 2.4). Sequences from this study are indicated with the symbol • and highlighted in blue if it displayed significant heat inducibility or in red if it displayed no significant heat inducibility (section 3.4; Fig. 5). (For interpretation of the references to colour in this figure legend, the reader is referred to the web version of this article.)

compared to the control experiment at the same temperature ($P < 0.01$; Fig. 5D).

3.5. Heat shock response: Hsp70 protein expression

The monoclonal antibody raised against mouse Hsp70 and used in this study detected a single band in *H. fulgens* muscle at approximately 70 kDa (data not shown). The small sample size and the lack of one experimental condition (hypoxia) constrained the interpretations of Hsp70 protein regulation with warming. Nonetheless, the observed pattern of Hsp70 per µg of protein (Fig. 6) suggests that Hsp70 protein expression followed a pattern different from gene expression, where the concentration of Hsp70 proteins remained stable regardless of the increasing temperature.

4. Discussion

The aim of this study was to deepen our understanding on the cellular mechanisms defining the muscular response, malfunction and molecular damage of green abalone (*Haliotis fulgens*) to changes in temperature under hypoxia and hypercapnia alone and in combination, which may involve impairments of aerobic metabolism, involvement of anaerobic mechanisms, and induction of thermal protection by the induction of Hsp70s in muscle tissue. Following the onset temperature of the specific physiological trait (energy metabolism, cellular protection, metabolites, muscle spasm) we tried to unravel why the exposure to warming under combined hypoxia and hypercapnia resulted in the observed muscular failure.

4.1. Cellular metabolic condition

Our first hypothesis was that the observed muscular failure and loss of attachment in thermally challenged *H. fulgens* under combined hypoxia and hypercapnia is related to a limited aerobic and anaerobic capacity for energy production. However, our ^{1}H NMR metabolic profile of muscle showed no evidence of anaerobiosis, regardless of the experimental conditions. Abalone musculature is well known to be highly dependent on oxygen reserves and anaerobic glycolysis during strong environmental hypoxia and functional hypoxia (Omolo et al., 2003; Venter et al., 2016). Therefore, the lack of muscular anaerobiosis indicates that the development of warming-induced hypoxemia was prevented in muscle, whereas the metabolically more active tissues such as gill and hepatopancreas displayed higher energetic demand with the concomitant onset of anaerobiosis (Tripp-Valdez et al., 2017). This matches with previous observations in marine mollusk where muscle displayed lower sensitivity to warming stress than other soft tissues like gill or mantle (Anestis et al., 2008).

Citrate synthase (CS) catalyzes the first step in the tricarboxylic acid cycle (TCA) and plays a central role in several metabolic pathways connecting carbohydrate, lipid, and protein metabolism for aerobic ATP synthesis. Therefore, changes in CS will reflect a response in the aerobic capacity and possibly a different use of fuels following thermal acclimation (Lucassen et al., 2003; Windisch et al., 2011). Under control, hypoxic and hypercapnic condition, CS activity declined with increasing temperature between 24 °C and 30 °C indicating rapid compensatory adjustments to warming-induced kinetic stimulation and removal of excess capacity in the warmth (Pörtner, 2002; Lucassen et al., 2003; Martinez et al., 2016). Rapid compensatory adjustment in mitochondrial capacities has previously been described in the Antarctic eelpout (*Pachycara brachycephalum*) exposed to acute heat stress, where tissue specific CS activity declined by ~29% from the first day of thermal exposure (Windisch et al., 2011). In *H. fulgens* muscle, however, further warming to 32 °C in the control, hypoxic and hypercapnic experiments, stimulated CS maximum capacity to similar values as observed at the initial temperature, with moderately higher values under the hypoxic treatment.

Previous investigations on *H. fulgens* acclimated within their natural thermal range (14 °C – 27 °C) demonstrated that the Arrhenius break temperature for mitochondrial function of *H. fulgens* is close to 40 °C (Dahlhoff and Somero, 1993) which is above the maximum temperature tested in present study. Therefore, modulation of CS at high temperatures may indicate an active regulatory response of mitochondrial capacity to thermal stress overcoming the compensatory adjustments at medium temperatures.

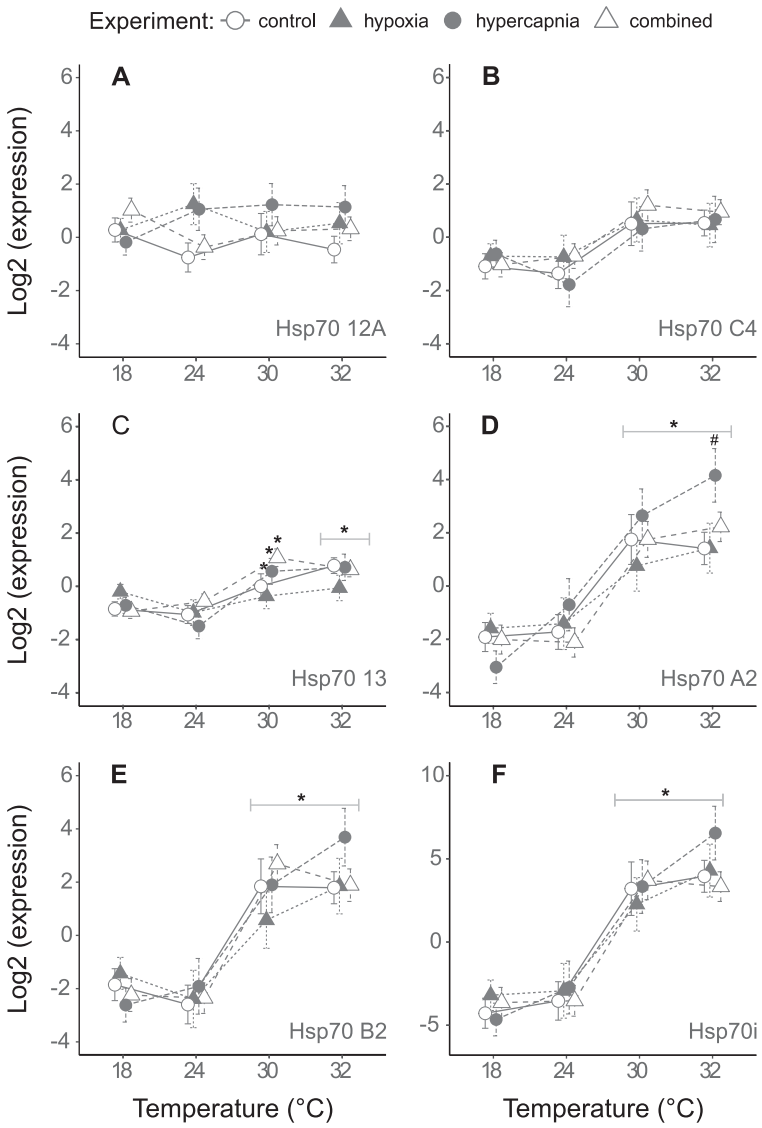

Fig. 5. Gene expression pattern of six isoforms from the Hsp70 family during the warming ramp under control (normoxic normocapnia), hypoxia (hypoxic normocapnia), hypercapnia (normoxic hypercapnia) and combined (hypoxic hypercapnia) exposures. A) Hsp7012A, B) Hsp70C4, C) Hsp7013, D) Hsp70A2, E) Hsp70B2, F) Hsp70i. * indicates significant differences with initial temperature (18 °C) from same experiments (multiple test). # denotes significant differences with same temperature at control experiment (multiple test). n = 4–6 (n = 2 in Control, 30 °C). Values are posterior means ± 95% credible intervals (section 2.5).

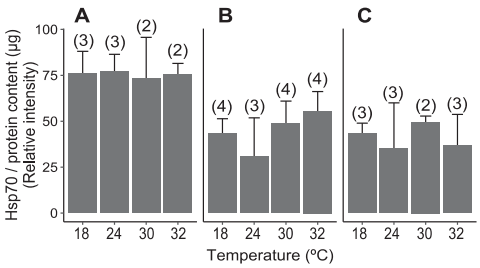

Fig. 6. Relative abundance of Hsp70 normalized by protein content in *Haliotis fulgens* muscle during the warming ramp under A) control (normoxic normocapnia); B) hypercapnia (normoxic hypercapnia); and C) combined exposures (hypoxic hypercapnia). n is indicated in parenthesis. Values are mean ± S.D.

Stimulation of mitochondrial capacity have been attributed to systemic signals related to acute insufficiency of the energetic metabolism such as low ATP levels or accumulation of adenosine (Eckerle et al., 2008; Vosloo et al., 2013b). A similar mechanism may have stimulated CS capacity in the musculature of *H. fulgens* juveniles at extreme temperature (32 °C), when warming stress was accompanied by hypoxia and hypercapnia in isolation. However, mitochondrial stimulation against thermal compensation was shifted to lower temperatures during combined exposure to hypoxia and hypercapnia. Further investigations are necessary to test this hypothesis and to unravel the mechanisms that stimulate mitochondrial capacity.

In juveniles of *H. midae*, exposure to thermal stress elicited increased rates of ammonia excretion over decreasing oxygen consumption rates resulting in declining O:N ratios (Vosloo et al., 2013b). Similarly, *H. midae* adults exposed to acute heat stress increased their

rates of ammonia excretion coupled with lower lactate levels in hemolymph (Vosloo et al., 2013a). Together, these observations denote a reduction of the glycolytic flux and a higher reliance of protein degradation to access the carbon skeletons from the released amino acids as an alternative fuel for aerobic ATP production (Vosloo et al., 2013a; Venter et al., 2016).

Although direct evidence of increased use of proteins for aerobic energy production is not available in this study due to limited tissue amount, accumulation of valine in *H. fulgens* musculature upon three out of four treatments (Fig. 3) may be related to a change in protein turnover rates. Valine is an essential amino acid in animals and intracellular free valine pool can be related to process of protein synthesis and protein degradation: in rat liver, accumulation of valine results from endogenous protein degradation (Khairallah and Mortimore, 1976). Valine accumulation has been additionally observed in gill and muscle of marine gastropods under hypoxic and thermal stress as well as during functional hypoxia (Lu et al., 2016; Dunphy et al., 2018; Venter et al., 2018). Therefore, valine accumulation likely indicates altered protein turnover at extreme temperature in *H. fulgens*, in line with the previous observations in *H. midae,* where the use of amino acids allowed to sustain aerobic energy production (Vosloo et al., 2013a; Vosloo et al., 2013b).

In muscle of fish and limpets, enhanced glycolytic capacity at thermal extremes are associated with higher dependence of carbohydrate metabolism, reflecting an increased role of anaerobic metabolism to cover energetic demands (Feidantsis et al., 2009; Windisch et al., 2011; Han et al., 2017). In *H. fulgens*, muscular glycolytic potential depicted by the capacities of lactate dehydrogenase (LDH) and tauropine dehydrogenase (TDH) was stimulated only at the highest temperature under the hypoxia treatment (Fig. 2B, C). However, lactate and tauropine were not accumulated at any stage, and the depletion of lactate, tauropine, and succinate observed at the warmest temperature under combined hypoxia and hypercapnia even indicate a reduced glycolytic flux at extreme conditions.

The significant depletion of anaerobic intermediates in muscle takes place in a similar way as in gill and precedes a drop in whole animal metabolic rate at 32 °C (Tripp-Valdez et al., 2017). This suggests that the organism went into hypometabolic state at extreme temperature likely to sustain reduced but oxygen-based energy production. In the quahog (*Arctica islandica*) the reduction of metabolic oxygen demand allowed mitochondria to sustain aerobic energy production without affecting specific activities of anaerobic enzymes, such as LDH (Strahl et al., 2011). A higher reliance on proteins instead of carbohydrates to fuel TCA together with a hypometabolic state could enable the pre-valence of low levels of aerobic capacity, (Vosloo et al., 2013a), which is reflected in *H. fulgens* under the combined treatment possibly also explaining the lack of regulation of LDH and TDH in this treatment. Upon metabolic depression, however, a reduced capacity to compensate additional cellular disturbances, such as intra- or extra-cellular acidosis may have caused insufficient functioning in muscle and contributed to the observed muscular fatigue and failure (Pörtner et al., 1996), but clearly, this aspect needs further investigation.

Interestingly, the low Q_{10} in the range of 18 °C to 32 °C of TDH compared to LDH activities indicate that TDH is already at its highest capacity at control temperature, whereas LDH may function as an emergency system with higher potential to increase maximal activity in response to acute thermal stimulation, both in fully oxygenated waters and under hypoxia. Glycolytic potential by means of additional opine dehydrogenases tested in this study (octopine-, strombine-, alanopine and lysopine dehydrogenase) can be neglected as the observed low activity may predominately resulted from the non-specific reaction of TDH (Omolo et al., 2003).

4.2. Heat shock response

The phylogenetic analyses and the observed gene expression patterns highlight the challenges in proper functional Hsp70 classification simply based on similarity: Hsp70 C4 clustered with other cognate forms from vertebrates and invertebrates (Fig. 4; group I) and showed no significant induction with temperature; however, Hsp70 C4 relative expression did not stay at baseline levels with increasing temperatures, the observed fold change was similar to that of the inducible form Hsp70 13 (Fig. 5B; Supplementary material 2). Our observation suggests that constitutive isoforms are also involved in the protection against heat stress, in line with previous observations in the abalone *H. tuberculata* (Farcy et al., 2007), where the analyzed Hsp70 gene (CAK95236.1; Fig. 4) was constitutively expressed at control temperature but displayed temperature inducibility. In contrast, Hsp70 12A in *H. fulgens* was relatively stable and showed no apparent temperature induction irrespective of the experimental conditions (Fig. 5A), but it clustered together with inducible forms from vertebrates and invertebrates. The *H. fulgens* Hsp70i and Hsp70 B2 clustered together and form a separate branch in the phylogenetic tree together with inducible isoforms from other mollusks (Fig. 4). Both isoforms were highly inducible but differed with respect to their control levels, as Hsp70i started from very low expression levels at control conditions but passed all other isoforms at high temperature. This points to specific functional roles of the two isoforms in heat shock response, besides their close phylogenetic relationship. The high induction observed in Hsp70i could represent a real emergency system and may thus help to guide consecutive studies to detect sensitive responses to warming in other mollusks.

All inducible forms of *H. fulgens* Hsp70s were highly induced by temperature, showing an abrupt upregulation already at 30 °C where other physiological traits such as metabolite concentrations were still unaffected. Previous investigations had suggested a possible association between Hsp70 induction and CT_{max} (Fangue et al., 2011), but the gene expression patterns of Hsp70 in this study were the same regardless of the experimental conditions, meaning that induction of Hsp70 mRNA cannot be directly related to the reduced maximum thermal limit and muscular failure seen in the combined treatment.

In a broader context, the range of temperature experienced by *H. fulgens* in their natural habitat usually lies between 14° and 27 °C (Dahlhoff and Somero, 1993), and an optimum growth temperature was estimated with about 25 °C for the population from the Baja California Peninsula (Diaz et al., 2006). Temperatures of 30 °C and above are not usually found in the habitat of the studied green abalone but have been observed during strong El Niño events (Guzman del Proo et al., 2003). Due to the experimental design of this study with only four temperature steps, the exact induction temperature of the heat shock response could not been resolved, but it falls in the range of the common natural maximum of 27 °C or slightly above. Consequently, transcriptional Hsp70 upregulation reflects a preparative defense mechanism to increase hardiness against extreme temperatures (Bahrndorff et al., 2009) as those naturally ocurring during severe El Niño events (Guzman del Proo et al., 2003).

At first, the unchanged dynamics of almost all Hsp70 isoforms with hypoxia and hypercapnia was surprising, as several studies on diverse tissues from mollusks and arthropods demonstrated that hypoxia and hypercapnia triggered a heat shock response even at constant temperature (Anestis et al., 2010; Harms et al., 2014). However, in all cases, a decreased energy charge and low body fluid oxygenation may constitute the stimulus to induce Hsp70 mRNA, as suggested previously (Anestis et al., 2010). In *H. fulgens* juveniles, whole-organism metabolic rate and accumulation of anaerobic metabolites in gill and hepatopancreas indicate a warming-induced reduction in fluid oxygenation in both tissues. However, a more delayed metabolic response in muscle compared to gill and the prevalence of an aerobic metabolic mode in muscle may have prevented the onset of the heat shock response at lower temperature in this tissue. Nonetheless, the slight but significantly stronger upregulation of Hsp70 A2 under hypercapnia at 32 °C warrants further investigation of the effect of hypercapnia in fine-

tuning of the heat shock response.

Assessment of Hsp70 protein induction was considerably limited in this study (we were not able to test it in the hypoxia experiment). Nonetheless, immunoblot analyses using the heterologous antibody against mouse Hsp70 gave no evidence of protein induction. This result is not surprising as the dynamics of transcriptional induction of Hsp70 genes may not be directly paralleled by protein synthesis (Bahrndorff et al., 2009; Farcy et al., 2007; Morris et al., 2013), and the stepwise design of the present study may imply an attenuation between mRNA and protein expression. Furthermore, energetic shortage may also prevent or attenuate the direct translation of the mRNA into protein. Besides, methodological aspects must be considered, as the immunoblot analysis using the heterologous antibody against mouse Hsp70 (MA3-006) revealed a single band only. In a study with the oyster *Crassostrea gigas*, the same antibody as the one used in this study could detect two Hsp isomers following a heat stress treatment (cognate isomer Hsp77 and inducible isomer Hsp69) (Yang et al., 2016). Therefore, we cannot exclude the possibility that blot analysis in our study only detected the cognate isoform or a mixture of several isoforms in a way that the summed signal remained constant.

Overall, our findings indicate that mRNA induction of several Hsp70s play an important role in the abalone thermal response. However, we found no evidence that thermal stress with additional hypoxia and hy-percapnia alone or in combination induced an earlier activation of pro-tection mechanisms or at higher levels than temperature alone. Consequently, it is unlikely that the observed reduction in the whole-or-ganism thermal limits with warming under combined hypoxia and hy-percapnia is related to higher rates of protein damage in muscle.

5. Conclusions

Results from the present study indicate lower thermal sensitivity of green abalone musculature than other tissues such as gill and hepato-pancreas analyzed in our previous work, as in muscle an aerobic ca-pacity for energy production prevailed during the warming protocol under all experimental conditions. Regulation of muscular mitochon-drial capacity, as seen in the depression of citrate synthase capacity, indicated a compensatory adjustment during warming under control condition and during warming under solely hypoxia and hypercapnia. A reduction in oxygen demand supported avoidance of anaerobic me-tabolism in muscle until at the highest temperature (32 °C). These changes possibly come with a higher reliance on protein degradation as energy fuel. However, the depletion of anaerobic metabolites (lactate, tauropine and succinate) in muscle together with the lack of upregu-lation of the glycolytic capacity for anaerobic energy production during warming under combined hypoxia and hypercapnia suggest that aba-lone musculature switched to a metabolically depressed state as a re-sponse to the strong environmental stress. Gene expression analysis of members of the Hsp70 family demonstrated a coordinated upregulation of four out of six analyzed genes with warming. This indicates early initiation of the heat shock response, possibly without expression of functional protein. An association between Hsp70 induction and the onset of muscular spams characterizing CT_{max} is thus not supported by this study. We suggest that due to metabolic depression, *H. fulgens* muscle displayed lower sensitivity to warming stress than other tissues – as observed in our previous study– at the expense of functional loss. Investigations of additional processes such as neuromuscular failure, extracellular acidosis, or increased membrane fluidity are needed to elucidate the cellular mechanisms associated with muscular failure and the downward shift in whole-organism thermal thresholds in *H. fulgens* juveniles during exposure to environmental hypoxia and hypercapnia.

Acknowledgments

We thank Gilberto González Soriano, Julio Felix Dominguez and Rosa Linda Salgado García from CIBNOR for the support during the experiments in Mexico; Martín Gerardo Ruíz, from the Sociedad Cooperativa de Producción Pesquera de Bahía Tortugas S.C. de R.L. and their personnel for kindly providing the organisms; Jutta Jürgens from AWI for the assistance in the molecular analyses. Financial support to Miguel A. Tripp-Valdez was granted by fellowship of the Deutscher Akademischer Austauschdienst (DAAD) program: 57076385. This work is a contribution to the research program PACES II of the AWI.

Appendix A. Supplementary data

Supplementary data to this article can be found online at https://doi.org/10.1016/j.cbpb.2018.08.009.

References

Anestis, A., Pörtner, H.O., Lazou, A., Michaelidis, B., 2008. Metabolic and molecular stress responses of sublittoral bearded horse mussel *Modiolus barbatus* to warming sea water: implications for vertical zonation. J. Exp. Biol. 211, 2889–2898. https://doi.org/10.1242/jeb.016782.

Anestis, A., Pörtner, H.O., Michaelidis, B., 2010. Anaerobic metabolic patterns related to stress responses in hypoxia exposed mussels *Mytilus galloprovincialis*. J. Exp. Mar. Biol. Ecol. 394, 123–133. https://doi.org/10.1016/j.jembe.2010.08.008.

Bahrndorff, S., Mariën, J., Loeschcke, V., Ellers, J., 2009. Dynamics of heat-induced thermal stress resistance and hsp70 expression in the springtail, *Orchesella cincta*. Funct. Ecol. 23, 233–239. https://doi.org/10.1111/j.1365-2435.2009.01541.x.

Bradford, M.M., 1976. A rapid and sensitive method for the quantitation of microgram quantities of protein utilizing the principle of protein-dye binding. Anal. Biochem. 72, 248–254. https://doi.org/10.1016/0003-2697(76)90527-3.

Cai, W., Borlace, S., Lengaigne, M., van Rensch, P., Collins, M., Vecchi, G., Timmermann, A., Santoso, A., McPhaden, M.J., Wu, L., England, M.H., Wang, G., Guilyardi, E., Jin, F.-F., 2014. Increasing frequency of extreme El Niño events due to greenhouse warming. Nat. Clim. Chang. 5, 1–6. https://doi.org/10.1038/nclimate2100.

Dahlhoff, E., Somero, G.N., 1993. Effects of temperature on mitochondria from abalone (Genus *Haliotis*) - adaptive plasticity and its limits. J. Exp. Biol. 185, 151–168.

Deigweiher, K., Koschnick, N., Pörtner, H.-O., Lucassen, M., 2008. Acclimation of ion regulatory capacities in gills of marine fish under environmental hypercapnia. Am. J. Phys. Regul. Integr. Comp. Phys. 295, R1660–R1670. https://doi.org/10.1152/ajpregu.90403.2008.

Diaz, F., Re, A.D., Medina, Z., Re, G., Valdez, G., Valenzuela, F., 2006. Thermal preference and tolerance of green abalone *Haliotis fulgens* (Philippi, 1845) and pink abalone *Haliotis corrugata* (Gray, 1828). Aquac. Res. 37, 877–884. https://doi.org/10.1111/j.1365-2109.2006.01506.x.

Dunphy, B.J., Ruggiero, K., Zamora, L.N., Ragg, N.L.C., 2018. Metabolomic analysis of heat-hardening in adult green-lipped mussel (Perna canaliculus): a key role for succinic acid and the GABAergic synapse pathway. J. Therm. Biol. 74, 37–46. https://doi.org/10.1016/j.jtherbio.2018.03.006.

Eckerle, L.G., Lucassen, M., Hirse, T., Pörtner, H.-O., 2008. Cold induced changes of adenosine levels in common eelpout (*Zoarces viviparus*): a role in modulating cytochrome c oxidase expression. J. Exp. Biol. 211, 1262–1269. https://doi.org/10.1242/jeb.013474.

Fangue, N.A., Osborne, E.J., Todgham, A.E., Schulte, P.M., 2011. The onset temperature of the heat-shock response and whole-organism thermal tolerance are tightly correlated in both laboratory-acclimated and field-acclimatized tidepool sculpins (*Oligocottus maculosus*). Physiol. Biochem. Zool. Ecol. Evol. Approaches 84, 341–352.

Farcy, E., Serpentini, A., Fiévet, B., Lebel, J.-M., 2007. Identification of cDNAs encoding HSP70 and HSP90 in the abalone *Haliotis tuberculata*: transcriptional induction in response to thermal stress in hemocyte primary culture. Comp. Biochem. Physiol. B Biochem. Mol. Biol. 146, 540–550. https://doi.org/10.1016/j.cbpb.2006.12.006.

Feder, M.E., Hofmann, G.E., 1999. Heat-shock proteins, molecular chaperones, and the stress response: evolutionary and ecological physiology. Annu. Rev. Physiol. 61, 243–282. https://doi.org/10.1146/annurev.physiol.61.1.243.

Feidantsis, K., Pörtner, H.O., Lazou, A., Kostoglou, B., Michaelidis, B., 2009. Metabolic and molecular stress responses of the gilthead seabream *Sparus aurata* during long-term exposure to increasing temperatures. Mar. Biol. 156, 797–809. https://doi.org/10.1007/s00227-009-1135-z.

Gäde, G., 1986. Purification and properties of tauropine dehydrogenase from the shell adductor muscle of the ormer, *Haliotis lamellosa*. Eur. J. Biochem. 160, 311–318. https://doi.org/10.1111/j.1432-1033.1986.tb09973.x.

Guzman del Proo, S.A., Palau, L.C., Perez, J.B., Laguna, J.C., Fragoso, R.H., 2003. Effects of the "El Niño" event on the recruitment of benthic invertebrates in Bahia Tortugas, Baja California Sur. Geofis. Int. 42, 429–438.

Haas, B.J., Papanicolaou, A., Yassour, M., Grabherr, M., Blood, P.D., Bowden, J., Couger, M.B., Eccles, D., Li, B., Lieber, M., MacManes, M.D., Ott, M., Orvis, J., Pochet, N., Strozzi, F., Weeks, N., Westerman, R., William, T., Dewey, C.N., Henschel, R., Leduc, R.D., Friedman, N., Regev, A., 2013. De novo transcript sequence reconstruction from RNA-seq using the Trinity platform for reference generation and analysis. Nat. Protoc. 8, 1494–1512. https://doi.org/10.1038/nprot.2013.084.

Han, G., Zhang, S., Dong, Y., 2017. Anaerobic metabolism and thermal tolerance: the importance of opine pathways on survival of a gastropod after cardiac dysfunction. Integr. Zool. 12, 361–370. https://doi.org/10.1111/1749-4877.12229.

Harms, L., Frickenhaus, S., Schiffer, M., Mark, F.C., Storch, D., Held, C., Pörtner, H.-O., Lucassen, M., 2014. Gene expression profiling in gills of the great spider crab *Hyas araneus* in response to ocean acidification and warming. BMC Genomics 15, 789. https://doi.org/10.1186/1471-2164-15-789.

Healy, T.M., Schulte, P.M., 2012. Factors affecting plasticity in whole-organism thermal tolerance in common killifish (*Fundulus heteroclitus*). J. Comp. Physiol. B 182, 49–62. https://doi.org/10.1007/s00360-011-0595-x.

Hickey, A.J.R., Wells, R.M.G., 2003. Thermal constraints on glycolytic metabolism in the New Zealand abalone, *Haliotis iris*: the role of tauropine dehydrogenase. New Zeal. J. Mar. Freshw. Res. 37, 723–731. https://doi.org/10.1080/00288330.2003.9517202.

Katsikatsou, M., Anestis, A., Pörtner, H.O., Vratsistas, A., Aligizaki, K., Michaelidis, B., 2012. Field studies and projections of climate change effects on the bearded horse mussel *Modiolus barbatus* in the Gulf of Thermaikos, Greece. Mar. Ecol. Prog. Ser. 449, 183–196. https://doi.org/10.3354/meps09550.

Khairallah, E.A., Mortimore, G.E., 1976. Assessment of protein turnover in perfused rat liver. Evidence for amino acid compartmentation from differential labeling of free and tRNA-gound valine. J. Biol. Chem. 251, 1375–1384.

Kumar, S., Stecher, G., Tamura, K., 2016. MEGA7: molecular evolutionary genetics analysis version 7.0 for bigger datasets. Mol. Biol. Evol. 33, 1870–1874. https://doi.org/10.1093/molbev/msw054.

Laemmli, U.K., 1970. Cleavage of structural proteins during the assembly of the head of the bacteriophage T4. Nature 227, 680–685.

López-Landavery, E.A., Portillo-López, A., Gallardo-Escárate, C., Del Río-Portilla, M.A., 2014. Selection of reference genes as internal controls for gene expression in tissues of red abalone *Haliotis rufescens* (Mollusca, Vetigastropoda; Swainson, 1822). Gene 549, 258–265. https://doi.org/10.1016/j.gene.2014.08.002.

Lu, J., Shi, Y., Wang, S., Chen, H., Cai, S., Feng, J., 2016. NMR-based metabolomic analysis of Haliotis diversicolor exposed to thermal and hypoxic stresses. Sci. Total Environ. 545–546, 280–288. https://doi.org/10.1016/j.scitotenv.2015.12.071.

Lucassen, M., Schmidt, A., Eckerle, L.G., Pörtner, H.O., 2003. Mitochondrial proliferation in the permanent vs. temporary cold: enzyme activities and mRNA levels in Antarctic and temperate zoarcid fish. Am. J. Physiol. Integr. Comp. Physiol. 285, R1410–R1420. https://doi.org/10.1152/ajpregu.00111.2003.

Lutterschmidt, W.I., Hutchison, V.H., 1997. The critical thermal maximum: data to support the onset of spasms as the definitive end point. Can. J. Zool. 75, 1553–1560. https://doi.org/10.1139/z97-782.

Madeira, D., Narciso, L., Cabral, H.N., Vinagre, C., 2012. Thermal tolerance and potential impacts of climate change on coastal and estuarine organisms. J. Sea Res. 70, 32–41. https://doi.org/10.1016/j.seares.2012.03.002.

Martinez, E., Porreca, A.P., Colombo, R.E., Menze, M.A., 2016. Tradeoffs of warm adaptation in aquatic ectotherms: live fast, die young? Comp. Biochem. Physiol. -Part A Mol. Integr. Physiol. 191, 209–215. https://doi.org/10.1016/j.cbpa.2015.07.014.

Matz, M.V., Wright, R.M., Scott, J.G., 2013. No control genes required: bayesian analysis of qRT-PCR data. PLoS ONE 8, e71448. https://doi.org/10.1371/journal.pone.0071448.

Micheli, F., Saenz-Arroyo, A., Greenley, A., Vazquez, L., Espinoza Montes, J.A., Rossetto, M., De Leo, G.A., 2012. Evidence that marine reserves enhance resilience to climatic impacts. PLoS ONE e40832, 7. https://doi.org/10.1371/journal.pone.0040832.

Morales-Bojorquez, E., Orieta Mucino-Diaz, M., Alfonso Velez-Barajas, J., 2008. Analysis of the decline of the abalone fishery (*Haliotis fulgens* and *H. corrugata*) along the westcentral coast of the Baja California peninsula. Mexico. J. Shellfish Res. 27, 865–870. https://doi.org/10.2983/0730-8000(2008)27{[}865:AOTDOT]2.0.CO;2.

Morris, J.P., Thatje, S., Hauton, C., 2013. The use of stress-70 proteins in physiology: a reappraisal. Mol. Ecol. 22, 1494–1502. https://doi.org/10.1111/mec.12216.

Omolo, S.O., Gade, G., Cook, P.A., Brown, A.C., 2003. Can the end products of anaerobic metabolism, tauropine and D-lactate, be used as metabolic stress indicators during transport of live South African abalone *Haliotis Midae*? Afr. J. Mar. Sci. 25, 301–309. https://doi.org/10.2989/18142320309504019.

Pörtner, H.-O., 2002. Climate variations and the physiological basis of temperature dependent biogeography: systemic to molecular hierarchy of thermal tolerance in animals. Comp. Biochem. Physiol. A. Mol. Integr. Physiol. 132, 739–761.

Pörtner, H.-O., Finke, E., Lee, P.G., 1996. Metabolic and energy correlates of intracellular pH in progressive fatigue of squid (*L. brevis*) mantle muscle. Am. J. Phys. 271, R1403–R1414.

Pörtner, H.-O., Karl, D.M., Boyd, P.W., Cheung, W.W.L., Lluch-Cota, S.E., Nojiri, Y., Schmidt, D.N., Zavialov, P.O., 2014. Ocean systems. In: Field, C.B., Barros, V.R., Dokken, D.J., Mach, K.J., Mastrandrea, M.D., Bilir, T.E., Chatterjee, M., Ebi, K.L., Estrada, Y.O., Genova, R.C., Girma, B., Kissel, E.S., Levy, A.N., MacCracken, S., Mastrandrea, P.R., White, L. (Eds.), Climate Change 2014: Impacts, Adaptation, and Vulnerability. Part A: Global and Sectoral Aspects. Contribution of Working Group II to the Fifth Assessment Report of the Intergovernmental Panel on Climate Change. Cambridge University Press, Cambridge and New York, NY, pp. 411–484.

Pörtner, H.-O., Bock, C., Mark, F.C., 2017. Oxygen- and capacity-limited thermal tolerance: bridging ecology and physiology. J. Exp. Biol. 220, 2685–2696. https://doi.org/10.1242/jeb.134585.

Sidell, B.D., Driedzic, W.R., Stowe, D.B., Johnston, A., 1987. Biochemical correlations of power development and metabolic fuel preferenda in fish hearts. Physiol. Zool. 221–232.

Somero, G.N., Beers, J.M., Chan, F., Hill, T.M., Klinger, T., Litvin, S.Y., 2016. What changes in the carbonate system, oxygen, and temperature portend for the Northeastern Pacific Ocean: a physiological perspective. Bioscience 66, 14–26. https://doi.org/10.1093/biosci/biv162.

Strahl, J., Dringen, R., Schmidt, M.M., Hardenberg, S., Abele, D., 2011. Metabolic and physiological responses in tissues of the long-lived bivalve *Arctica islandica* to oxygen deficiency. Comp. Biochem. Physiol. - A Mol. Integr. Physiol. 158, 513–519. https://doi.org/10.1016/j.cbpa.2010.12.015.

Tomanek, L., 2008. The importance of physiological limits in determining biogeographical range shifts due to global climate change: The heat-shock response. Physiol. Biochem. Zool. 81, 709–717. https://doi.org/10.1086/590163.

Tripp-Valdez, M.A., Bock, C., Lucassen, M., Lluch-Cota, S.E., Sicard, M.T., Lannig, G., Pörtner, H.-O., 2017. Metabolic response and thermal tolerance of green abalone juveniles (*Haliotis fulgens*: Gastropoda) under acute hypoxia and hypercapnia. J. Exp. Mar. Biol. Ecol. 497, 11–18. https://doi.org/10.1016/j.jembe.2017.09.002.

Vandesompele, J., De Preter, K., Pattyn, F., Poppe, B., Van Roy, N., De Paepe, A., Speleman, F., 2002. Accurate normalization of real-time quantitative RT-PCR data by geometric averaging of multiple internal control genes. Genome Biol. 3. https://doi.org/10.1186/gb-2002-3-7-research0034.

Venter, L., Loots, D.T., Vosloo, A., Jansen Van Rensburg, P., Lindeque, J.Z., 2016. Abalone growth and associated aspects: now from a metabolic perspective. Rev. Aquac. 1–23. https://doi.org/10.1111/raq.12181.

Venter, L., Loots, D.T., Mienie, L.J., Jansen van Rensburg, P.J., Mason, S., Vosloo, A., Lindeque, J.Z., 2018. The cross-tissue metabolic response of abalone (*Haliotis midae*) to functional hypoxia. Biol. Open 7, bio031070. https://doi.org/10.1242/bio.031070.

Verberk, W.C.E.P., Sommer, U., Davidson, R.L., Viant, M.R., 2013. Anaerobic metabolism at thermal extremes: a metabolomic test of the oxygen limitation hypothesis in an aquatic insect. Integr. Comp. Biol. 53, 609–619. https://doi.org/10.1093/icb/ict015.

Viant, M.R., Werner, I., Rosenblum, E.S., Gantner, A.S., Tjeerdema, R.S., Johnson, M.L., 2003. Correlation between heat-shock protein induction and reduced metabolic condition in juvenile steelhead trout (*Oncorhynchus mykiss*) chronically exposed to elevated temperature. Fish Physiol. Biochem. 29, 159–171. https://doi.org/10.1023/B:FISH.0000035938.92027.81.

Vosloo, A., Laas, A., Vosloo, D., 2013a. Differential responses of juvenile and adult South African abalone (Haliotis midae Linnaeus) to low and high oxygen levels. Comp. Biochem. Physiol. A. Mol. Integr. Physiol. 164, 192–199. https://doi.org/10.1016/j.cbpa.2012.09.002.

Vosloo, D., Vosloo, A., Morillion, E.J., Samuels, J.N., Sommer, P., 2013b. Metabolic readjustment in juvenile South African abalone (Haliotis midae) acclimated to combinations of temperature and dissolved oxygen levels. J. Therm. Biol. 38, 458–466. https://doi.org/10.1016/j.jtherbio.2013.07.001.

White, R.L., 1983. Effects of acute temperature change and acclimation temperature on neuromuscular function and lethality in crayfish. Physiol. Zool. 56, 174–194. https://doi.org/10.1086/physzool.56.2.30156050.

Windisch, H.S., Kathover, R., Pörtner, H.-O., Frickenhaus, S., Lucassen, M., 2011. Thermal acclimation in Antarctic fish: transcriptomic profiling of metabolic pathways. AJP Regul. Integr. Comp. Physiol. 301, R1453–R1466. https://doi.org/10.1152/ajpregu.00158.2011.

Wu, H., Southam, A.D., Hines, A., Viant, M.R., 2008. High-throughput tissue extraction protocol for NMR- and MS-based metabolomics. Anal. Biochem. 372, 204–212. https://doi.org/10.1016/j.ab.2007.10.002.

Yang, C.-Y., Sierp, M.T., Abbott, C.A., Li, Y., Qin, J.G., 2016. Responses to thermal and salinity stress in wild and farmed Pacific oysters *Crassostrea gigas*. Comp. Biochem. Physiol. Part A Mol. Integr. Physiol. 201, 22–29. https://doi.org/10.1016/j.cbpa.2016.06.024.

Supplementary 1

Identification of tauropine peak in ^{1}H-NMR spectra from *H. fulgens* muscle extracts.

S.1.1 Enzyme activity

Three subsamples of *Haliotis fulgens* muscle from control experiment (normoxic normocapnia) at 18 °C were used for determination of tauropine dehydrogenase activity as described in section 2.2 in the manuscript. For each sample, three different concentration of NADH was used: 0.15 mmol L^{-1}, 0.30 mmol L^{-1} and 0.50 mmol L^{-1}. Taurine concentration remained constant at 80 mmol L^{-1} and samples without the addition of taurine (for lactate dehydrogenase determination) and without addition of pyruvate (no reaction) were run in parallel as controls. All assays were conducted at 18°C until all NADH was oxidized.

S.1.2 Metabolite extraction

An aliquot of 200 µl from the resulting reaction in S.1.1 was transfer into a new 1.5 ml tube. Polar metabolites were extracted following a modified method for fluids (Blackwell, A. et al., 2013. *Agilient Technologies Inc.* Technical Overview 5991-3528EN. USA). Briefly, 2 parts of ice-cold methanol and one part of ice-cold chloroform was added to the aliquot and vortexed for 10 s. This was followed by the addition of one part water and one part chloroform to a final solution ratio of 2:2:1.8. The homogenate was vortexed for 10 s and centrifuged at 4 °C for 10 min at 3000g. Supernatant was transfer to a new 1.5 ml tube and dried overnight in a centrifugal vacuum concentrator (RVC 2-18, Martin Christ Freeze dryers, GmbH, Germany) at room temperature.

S.1.3. NMR spectroscopy and post processing

Dried polar extract was re-suspended with 200µL D_2O containing 1% Thrymethylsilyl propionate (TSP; Sigma-Aldrich, St. Louis, USA) and a 50µL aliquot was transferred into a 4 mm zirconia rotor. The ^{1}H-HRMAS NMR was acquired using the NOESY sequence with the following parameters: flip angle 90°, acquisition time 3.98 s, relaxation delay 4 s, sweep width 8223.7 Hz, 64 scans with 4 dummy scans. All spectra were imported to the software Chenomx NMR suit 8.0 (Chenomx Inc., 2014) for metabolite identification.

S.1.4. Tauropine identification

Figure S.1 show a section of the ^{1}H-HRMAS NMR spectra. An increasing double peak at 1.5 ppm matches with the increasing concentration of NADH (R^2 = 0.88; P=0.001) in the enzyme activity reaction and its lacking in the reaction were taurine or pyruvate was not added.

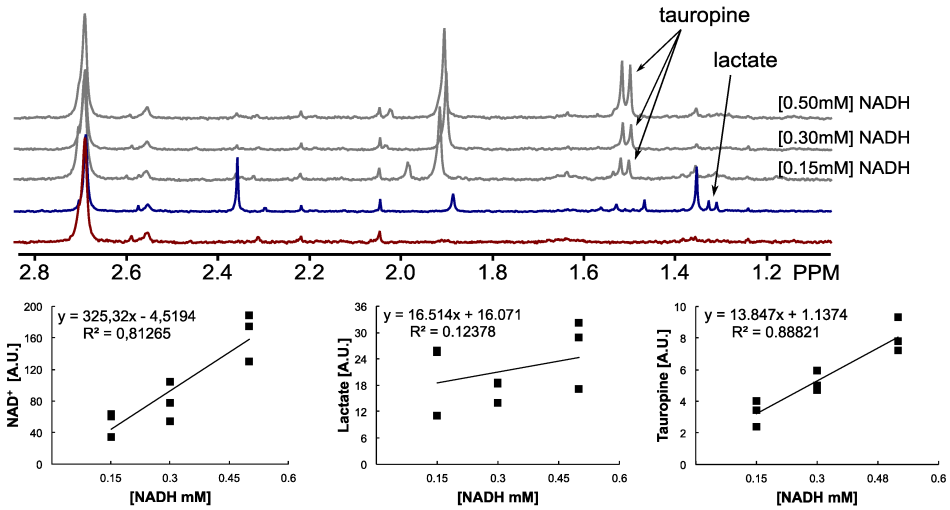

Fig. S1: Identification of tauropine peak in ^{1}H-NMR spectra. The upper panel shows spectra sections from the polar metabolite extraction of the end-product of tauropine dehydrogenase reaction. The red spectrum corresponds to the reaction without the addition of pyruvate (see section 2.2 in the manuscript), hence the reaction cannot start and neither lactate nor tauropine is present. In the blue spectrum, no taurine was added to the reaction; only lactate is produced. Grey spectra show reactions with 80 mmol L^{-1} taurine and increasing concentrations of NADH (0.15, 0.30 and 0.50 mmol L^{-1}) resulting in increasing height of the tauropine peak. The correlation between NADH concentration with NAD^{+} (peak not shown), lactate, and tauropine is shown in the lower panel.

S.1.5. Tauropine peak validation

To validate the results from the ^{1}H-NMR analysis, we used an online tool to predict chemical shift in 1D NMR spectrum from a given compound (http://www.nmrdb.org/new_predictor). The chemical structure (Fig. S2) was obtained from the Chemical Entities of Biological Interest (ChEBI) dictionary (https://www.ebi.ac.uk/chebi/init.do) and analyzed in the spectrum predictor using a frequency of 400, a line width of 1 Hz and 64k points. Predicted spectrum indicate a double peak at 1.348 ppm which is in line with the observed double peak in our green abalone muscle analysis (Fig. S1). Note that predicted spectrum does not consider differences in pH or additional factors affecting the chemical shift, which explains why we observed this double peak at 1.5 ppm (Fig. 1 in the manuscript). Additional peaks were predicted (Fig. S2), but these are in a region were other compounds are overlapping the signal in the muscle extracts (>3 ppm).

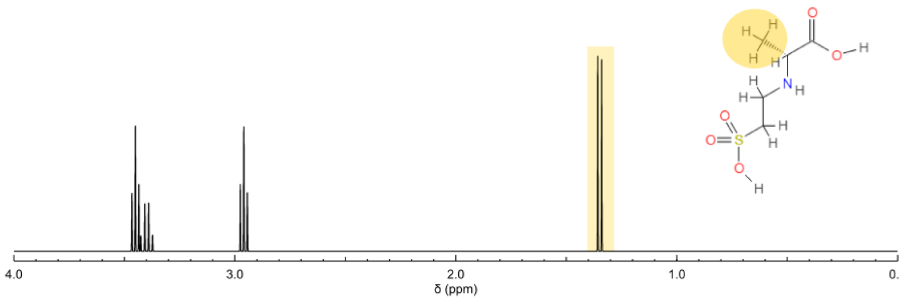

Fig. S2: Tauropine chemical structure and predicted ^{1}H-NMR spectrum. Regions in yellow indicate the part of the molecule that results in the observed double peak in the green abalone muscle metabolic profiles.

Supplementary material 2

Hsp70 and reference gene primer sets for *Haliotis fulgens*. * Primer efficiency was estimated using the R package MCMC.qpcr. + Maximum fold change observed trough warming under all experimental conditions (control, hypoxia, hypercapnia, combination).

Gene	Blastx Hit	Evalue	Primer name	Primer sequence	E*	Maximum FC+	Accession
Actine	ACT_PLAMG	$7.00E^{-84}$	Actine_F	GCCCCAAGCACAATGAAGAT	1.98	-	MH220512
			Actine_R	CGATCCAGACGGAGTATTTCCT			
E3 ubiquitin-protein ligase	MYCB2_HUMAN	0.00	E3UL_F	GGTCGTCTGATGTGTACTGCTTTG	1.94	-	MH220513
			E3UL_R	AGGTAGATCCGCCCCACATT			
60s Ribosomal protein	RL5_STYCL	$4.00E^{-155}$	RP5_F	TCCGTGCTTACCTGGACATTG	2.02	-	MH220514
			RP5_R	AAGCTCCAAACACCCTTGCA			
Hsp70 A2	HSP72_ANOAL	0.00	Hsp70A2_F	CAACGCACGTGCCATGA	2.05	89.85	MH220526
			Hsp70A2_R	CAGAGTTCTCTTGGCACGTTCAC			
Hsp70 12A	HS12A_MOUSE	0.00	Hsp7012A_F	CTGTGGAGGCGGGACAGT	1.99	1.66	MH220524
			Hsp7012A_R	TAGCCTTGTAGAGCTCCGTCAGT			
Hsp70 B2	HSP74_ANOAL	0.00	Hsp70B2_F	GGTAACAGGACAACACCAAGTTATGT	2.06	81.07	MH220527
			Hsp70B2_R	CGCAGCGTCACCTAAAAGTCT			
Hsp70 cognate 4	HSP7D_MANSE	0.00	Hsp70C4_F	GGAAGTCCAGGACCTGCTACTG	2.01	6.02	MH220528
			Hsp70C4_R	CACCAGCGGTCTCAATACCA			
Hsp70 13-like	HSP13_HUMAN	$3.00E^{-152}$	Hsp7013_F	GACTTGGTGGGCAGGACTTC	2.00	6.28	MH220525
			Hsp7013_R	TCTCGATGGCGTCCTTCAG			
Hsp70 inducible	HSP70_ONCTS	0.00	Hsp70i_F	CGTCTTGACCGGTGACACAA	1.95	2603	MH220529
			Hsp70i_R	GAGGCGCAAGGTCGACTAGT			

3.3 Publication III

De novo transcriptome assembly and gene expression profile of thermally challenged green abalone (*Haliotis fulgens*: Gastropoda) under acute hypoxia and hypercapnia.

Miguel A. Tripp-Valdez, Lars Harms, Hans O. Pörtner, M. Teresa Sicard & Magnus Lucassen

submitted

Marine Genomics

De novo transcriptome assembly and gene expression profile of thermally challenged green abalone (*Haliotis fulgens*: Gastropoda) under acute hypoxia and hypercapnia.

Miguel A. Tripp-Valdez[a,*], Lars Harms[a], Hans O. Pörtner[a,b], M. Teresa Sicard[c], Magnus Lucassen[a]

[a] *Integrative Ecophysiology, Alfred Wegener Institute Helmholtz Centre for Polar and Marine Research, Am Handelshafen12, D-27570 Bremerhaven, Germany*
[b] *University Bremen, Bibliothekestrasse 1, 28359, Germany*
[c] *Centro de Investigaciones Biolgicas del Noroeste (CIBNOR), Instituto Politcnico Nacional, 195, La Paz, Baja California Sur 23096, Mexico*

Abstract

Transcriptional regulation constitutes a rapid response of marine organisms facing stressful environmental conditions, such as the concomitant exposure to warming, ocean acidification and hypoxia under climate change. In previous studies, we investigated whole-organism physiological patterns and cellular metabolism in gill and muscle of the marine gastropod *Haliotis fulgens* in response to increasing temperature (18 °C to 32 °C at +3 °C per day) under hypoxia (50% air saturation), hypercapnia (1,000 µatm PCO_2) and both factors combined. Here, we report investigations of the molecular responses of *H. fulgens* to temperature and identify mechanisms concomitantly affected by hypoxia and hypercapnia. A *de novo* transcriptome assembly was effective in inspecting the global response to a changing environment. Furthermore, quantitative PCR and correlation network analysis of genes involved in the molecular response were used to unravel the correlations between gene expression patterns under the different experimental conditions. The analysis of the green abalone transcriptome under extreme combined conditions revealed a strong up-regulation of molecular chaperones, antioxidant genes, and apoptosis inhibitors, indicating a strong upregulation of damage prevention and repair systems at sustained cellular energy production. The correlation networks identified a shift from the expression of genes involved in energy metabolism (down-regulated) to the up-regulation of Hsp70 during warming under all experimental conditions in gill and muscle. However, warming under hypoxia and hypercapnia kept mRNA levels of citrate synthase in both tissues unchanged, suggesting an emphasis on maintaining mitochondrial activity due to an unidentified regulatory mechanism.

Keywords: Cellular stress response, climate change, gastropod, gene expression, RNA-seq

1. Introduction

With the continuous rise in atmospheric concentration of CO_2, marine ecosystems are undergoing changes in seawater temperature and in the concentrations of oxygen and carbon dioxide beyond their natural variability, threatening marine organisms and potentially affecting the structure and functioning of ecosystems (Pörtner et al., 2014; Henson et al., 2017). To persist under such changes in the physical environment, organisms must be responsive through physiological and cellular adjustments which are based on changes in molecular processes including altered gene expression (Hochachka and Somero, 2002; Meistertzheim et al., 2007; Kassahn et al., 2009; Tomanek and Zuzow, 2010).

The cellular stress response (CSR) constitutes a highly conserved set of proteins involved in preventing and repairing DNA and protein damage, cell cycle arrest or apoptosis, prevention of oxidative damage, and adjustment of the cellular energy metabolism (Kültz, 2005). Therefore, a rapid induction of the CSR during an environmental challenge shifts the cellular state of organisms from a state of growth to one of damage prevention and repair, allowing to momentarily increase its tolerance towards the environmental insult (Kultz, 2003; Kültz, 2005; Buckley et al., 2006).

With the development of transcriptional profiling tools, such as cDNA microarrays and RNA-Seq technology, it is now possible to explore a large pool of genes involved in the CSR during an environmental challenge (Podrabsky and Somero, 2004; Buckley et al., 2006; Todgham and Hofmann, 2009; Desalvo et al., 2010; Harms et al., 2014; Han et al., 2016) and to identify candidate genes as early indicators of stress (Farcy et al., 2009; Shiel et al., 2017). The molecular chaperones (e.g. heat shock proteins; Hsp) are usually the most strongly induced genes during thermal stress (Buckley et al., 2006; Farcy et al., 2009; Shiel et al., 2015; Han et al., 2016); Nonetheless, acute heat stress (hours) in a eurythermic fish (*Gilichtys mirabilis*) revealed over 200 genes that were rapidly induced or repressed. Many of those involved in protein biosynthesis, cell proliferation, and apoptosis displayed different patterns in gill and muscle (Buckley et al., 2006). Changes in gene expression levels representing energy metabolism are another common feature during thermal stress. During an acute heat challenge in the limpet *Cellena toreuma*, gene induction of alanopine dehydrogenase and the hypoxia inducible factor (*HIF*) in muscle indicated the development of warming-induced tissue hypoxemia and onset of anaerobic metabolism (Han et al., 2016). However, in light of

*Alfred Wegener Institute, Am Handelshafen12, D-27570
Email address: mtripp@awi.de (Miguel A. Tripp-Valdez)

ongoing climate change it is important to consider that the presence of combined multiple environmental drivers may result in interactive effects and modify the gene expression dynamics of individual drivers (Chapman et al., 2011; Rathburn et al., 2013; Harms et al., 2014).

Abalone (Haliotis sp) are marine gastropods with high commercial value worldwide. Overexploitation, pouching, habitat degradation and climate change have contributed to strong declines in abalone fisheries (Cook, 2016). The increasing interest to improve abalone fishery and aquaculture is reflected in the rising number of transcriptomic studies during the last decade, where de novo transcriptomes were produced for *H. rufescens* (Valenzuela-Muñoz et al., 2012; Valenzuela-Miranda et al., 2015), *H. discus hannai* (Choi et al., 2015; Nam et al., 2016), *H. midae*, *H. tuberculata* (Harney et al., 2016) and *H. laevigata* (Shiel et al., 2015), focusing on the identification of genes related to development and higher growth rates (Huang et al., 2012; Choi et al., 2015; Picone et al., 2015; Valenzuela-Miranda et al., 2015), the immune response (Nam et al., 2016) and temperature stress markers (Shiel et al., 2015, 2017). However, transcriptomic studies under environmental multi-stressor conditions are still scarce. A reference transcriptome from green abalone (*H. fulgens*), one of the most important species in the abalone fishery in Mexico (Morales-Bojorquez et al., 2008), has also not been available. As warming will more frequently interact with additional drivers such as hypoxia and hypercapnia, with negative consequences for organismal physiology (Somero et al., 2016), a transcriptome would provide valuable tools to assist green abalone management.

In a previous study, the physiological response and metabolic changes from thermally challenged *H. fulgens* juveniles were investigated in animals exposed to an acute warming ramp under conditions of normoxia, hypoxia, hypercapnia and the latter two factors combined (Tripp-Valdez et al., 2017). Warming under hypercapnia stimulated the whole-organism oxygen consumption, whereas hypoxia increased abalone heat sensitivity, as the warming-induced rise in oxygen consumption became limited and anaerobic metabolites accumulated in gill and hepatopancreas. Warming under combined hypoxia and hypercapnia, however, induced a hypometabolic state at extreme temperatures (32 °C) which was accompanied by the depletion of metabolites in the gill and the onset of muscular spams and loss of attachment, indicating a downward shift in the upper thermal limits (Tripp-Valdez et al., 2017). A consecutive study gave further insight into the abalones muscle cellular state, indicating upregulation of the maximum capacity of citrate synthase, which occurred at a lower temperature under combined hypoxia and hypercapnia. At the same time anaerobic metabolite accumulation (lactate, tauropine, and succinate) did not occur, suggesting that the muscle retained aerobic potential for energy production over the warming protocol in all experimental conditions (Tripp-Valdez et al., 2019).

Altogether, hypoxia and hypercapnia, as single stressors and if combined, changed the thermal limits of *H. fulgens*, but tissues displayed different thermal sensitivities and metabolic responses. We hypothesize that transcriptional responses to warming, particularly in genes involved in the CSR, also display tissue-specific expression patterns and are affected by hypoxia, hypercapnia and the combination of both. Therefore, this study aimed to test the suitability of a *de novo* transcriptome assembly for analysing the transcriptomic response of thermally challenged *H. fulgens* under combined hypoxia (50% air saturation) and hypercapnia (1,000 µatm PCO_2). Subsequently, tissue-specific (gill and muscle) and treatment-specific (hypoxia, hypercapnia and both factors combined) gene expression patterns were investigated by constructing correlation networks from specific genes involved in the CSR processes such as energy metabolism, oxidative stress, molecular protection (chaperones), and oxygen sensing.

2. Materials and Methods

2.1. Experimental animal

Juveniles of *H. fulgens* were provided by a fishery cooperative from the Baja California Peninsula, Mexico and brought to Northwestern Center for Biological Research (CIBNOR), Mexico. After 73 days acclimation to 18 °C, animals were exposed to the experimental conditions described in our previous study (Tripp-Valdez et al., 2017). Briefly, abalones were placed in a flow-through aquarium connected to a header tank with a flow of 2.5 L min^{-1} under four different experimental conditions: control (100% air saturation; 400 µatm PCO_2), hypoxia (50% air saturation; 400 µatm PCO_2), hypercapnia (100% air saturation; 1,000 µatm PCO_2) and combination (50% air saturation; 1,000 µatm PCO_2). Conditions were achieved by injecting food grade N_2, CO_2 or both directly into the header tank. Dissolved oxygen in seawater was controlled by online monitoring using a needle-type O_2 sensor (Presens, GmbH, Regensburg, Germany), in addition, twice-daily measurements of pH_{NBS}, total alkalinity, temperature, and salinity were used to calculate water pCO_2 as described in (Tripp-Valdez et al., 2017). The warming protocol consisted in daily increments of temperature from 18 °C to 32 °C at 3 °C steps every night (00:00 ± 1 h) with a final increment by 2 °C. Twelve hours after each temperature increase, abalone subsamples were randomly taken at 18 °C, 24 °C, 30 °C and 32 °C. Gill, mantle, hepatopancreas, and muscle (adductor and foot) were excised from each animal, snap-frozen in liquid nitrogen and stored at -80 °C until RNA isolation. Gonad inspection of experimental animals showed no signs of sexual maturation.

2.2. Library preparation and Illumina sequencing

Libraries were prepared with RNA from gill, mantle and hepatopancreas tissue from one unstressed individual (18 °C; normoxic normocapnia) and one stressed individual (32 °C; hypoxic hypercapnia). Approximately 20 mg of frozen tissue was homogenized in 1 mL QIAzol lysis reagent (Qiagen) by one cycle of 20 s at 5,500 rpm using a Precellys 24 (Bertin Technologies, France). After incubation for 5 min at room temperature, total RNA from individual tissues were isolated using RNeasy® Mini Kit (Qiagen) according to the manufacturers protocol. RNA concentrations were determined photometrically at 260 nm. Purity was determined from the ratios

Table 1: Primer sets for the analysed genes using qPCR

Gene	Primer name	Primer sequence	Efficiency	Accession
E3 Ubiquitin protein ligase	E3UL	F-GGTCGTCTGATGTGTACTGCTTTG R-AGGTAGATCCGCCCCACATT	1.94	MH220513
60s Ribosomal Protein L5	RP5	F-TCCGTGCTTACCTGGACATTG R-AAGCTCCAAACACCCTTGCAT	2.02	MH220514
Aspartate aminotransferase (mitochondrial)	AspAT	F-AGGAGTGGTTGGTGGATGTCA R-CAGCTTCGTTCTCATGCTGATG	1.94	MH220515
Cytochrome c oxidase, subunit III	COXIII	F-TGGAATCCGGTTGCTACATAGAA R- TGAAGCCCCTTTCACAATCG	1.92	MH220516
Enolase	ENO	F- CGTGGAAACCCCACTGTTG R- GCACGGAACAGGCCATTTT	1.94	MH220517
Glyceraldehyde-3-phosphate dehydrogenase	GAPDH	F- GGCGTGAACCACACCAAGTA R- CAGGAGGCGTTGCTGACAA	2.05	MH220518
Hexokinase	HK	F- TCAAGTACGTCTGCACCCTCAT R- CCCAGCCGCTGAAAGGA	1.95	MH220519
Citrate Synthase, mitochondrial	CS	F- CGCCATCACCGCTCTCA R- TGTTGACACCTTCTGCGTATGC	2.07	MH220520
Phosphoenolpyruvate carboxykinase	PEPCK	F- GGGCGCACCATGTATGTGA R- TGGACATGGGCGATCCA	2.07	MH220521
Pyruvate kinase	PK	F- TGCTGTAGAGGCGTCCTTCTC R - CCCGAGGTTGTGATGACGAT	2.04	MH220522
Long-chain-fatty-acid CoA ligase 3	LCF	F- AGTACATGGGAGCCCAACCA R- TCGGCTCGGGTGAGTGA	2.05	MH220523
Hsp70 12A	Hsp70 12A	F- CTGTGGAGGCGGGACAGT R- TAGCCTTGTAGAGCTCCGTCAGT	1.99	MH220524
Hsp70 13 like	Hsp70 13	F- GACTTGGTGGGCAGGACTTC R- TCTCGATGGCGTCCTTCAG	2.00	MH220525
Hsp70 A2	Hsp70 A2	F- CAACGCACGTGCCATGA R- CAGAGTTCTCTTGGCACGTTCAC	2.05	MH220526
Hsp70 B2	Hsp70 B2	F- GGTAACAGGACAACACCAAGTTATGT R- CGCAGCGTCACCTAAAAGTCT	2.06	MH220527
Hsp70 Cognate 4	Hsp70 C4	F- GGAAGTCCAGGACCTGCTACTG R- CACCAGCGGTCTCAATACCA	2.01	MH220528
Hsp70 inducible	Hsp70i	F- CGTCTTGACCGGTGACACAA R- GAGGCGCAAGGTCGACTAGT	1.95	MH220529
Hypoxia-inducible factor-1a	HIF	F- CGAGATGCGGCCAGATG R- GCCAACTCGTAAAACACCTCTGT	1.99	MH220530
Glutathione-S-transferase	GST	F- TTCAACGCCCGTGGATTC R- TCCTGCCAAGGCAAACAGA	1.95	MH220532
Glutathione reductase	GLR	F- CGACGTGCATTGGATGTCA R- CGCATCGAGGAACCAGGTAAT	2.29	MH220533
Superoxide dismutase	SOD	F- AAGATCCCCTGGAGGCTACAA R- CCCAGACATCGATGCCAAA	2.06	MH220534

of 260/280 nm and 260/230 nm with a NanoDrop ND-1000 (Seqlab, Erlangen, Germany) and integrity was assessed using capillary electrophoresis (Bioanalyzer, Agilent Technologies, Waldbron, Germany). Three micrograms of total RNA were treated with the turbo DNA-free Kit (Ambion). RNA from individual tissues was pooled in equal amounts from the unstressed and the stressed individuals and mRNA was isolated by poly(A)+ enrichment. After RNA fragmentation, a cDNA library (Vertis Biotechnology, Freising, Germany) was prepared by synthesis of the random-primed first strand, followed by strand-specific ligation of sequencing adapter to the 3′ and 5′ ends of the first strand. The resulting library was size-fractioned and normalized by depletion of redundant cDNA copies. Sequencing of the libraries was performed on an Illumina MiSeq system: Paired-end 2x 300 bp according to the manufacturers protocol.

2.3. Transcriptome assembly

Reads from the sequenced libraries were concatenated and quality trimmed using Trimmomatic version 0.30 (Bolger et al.,

2014) with the following parameters: leading: 5, trailing: 5, sliding window: 4:15, and minlen: 30. The final quality of the sequences was assessed with fastQC version 0.10.01 (Andrews, 2012). *In silico* normalization was performed for the trimmed sequences and the transcriptome was assembled using Trinity version 2.0.4 (Grabherr et al., 2011) with default parameters. To reduce the risk of assembly artifacts, contigs with low abundance were excluded from the analysis. Abundance estimation was made with the RNA Sequence Expected Maximization method, RSEM version 1.2.11 (Li and Dewey, 2011) with a Transcripts per kilobase million (TPM) cut-off of 1, using Bowtie v. 1.0.0 (Langmead et al., 2009) to align the reads to the Trinity transcripts. Additionally, redundant sequences were removed with CD-HIT-V4.6.1 (Li and Godzik, 2006) with a 95% identity cut-off. The transcriptome of *H. fulgens* was annotated using the Trinotate pipeline version 2.0 (https://trinotate.github.io/), comprising protein prediction (Transdecoder; http:// transdecoder.github.io/), BLAST homology searches against the SwissProt database, identification of protein domains (HMMER), prediction of signal peptides (Pfam) and further annotation with GO and eggNOG databases.

As only two samples were used in this study (one unstressed and one stressed), a comprehensive differential expression analysis was constrained. Nevertheless, a GO enrichment analysis was performed to get a general insight into the processes affected by the experimental condition. Firstly, abundance estimation was made for both libraries with RSEM v. 1.2.11 and Bowtie v. 1.0.0. Thereafter, a counts matrix was constructed for each library and EdgeR (Robinson et al., 2009) was used to test for differentially expressed transcripts, employing a dispersion value of 0.1. Transcripts with fold changes ≥ 2 and P value ≤ 0.001 were used for a GO enrichment analysis and statistically tested for over- and under-representation of GO terms using GOseq v.3.6 (Young et al., 2010) as implemented in the trinity pipeline (https://github.com/trinityrnaseq/trinityrnaseq/wiki). Finally, enriched GO terms from both individuals were mapped to a reduced set of Gene ontologies using the GOslim classification method implemented in CateGOrizer v. 3.218 (Hu et al., 2008) with consolidated single occurrence.

2.4. *Gene expression analysis with qPCR and correlation networks*

To Investigate differences in transcriptional regulation patterns of the cellular stress response (CSR) in gill and muscle under the different experimental condition, we selected a set of 20 genes belonging or associated to the CSR including energy metabolism, molecular chaperones (Hsp70), redox and detoxification system, and oxygen sensing (Table 1; Kültz 2005).

Twenty micrograms of frozen tissue were homogenized in 1 mL QIAzol lysis reagent (Qiagen) by one cycle of 20 s at 5,500 rpm (gill) or 6,500 rpm (muscle) using a Precellys 24 (Bertin Technologies, France). After incubation for 5 min at room temperature, total RNA was isolated by phase separation with chloroform and precipitated with isopropanol, followed by two wash steps with 75% ethanol. Determination of total RNA

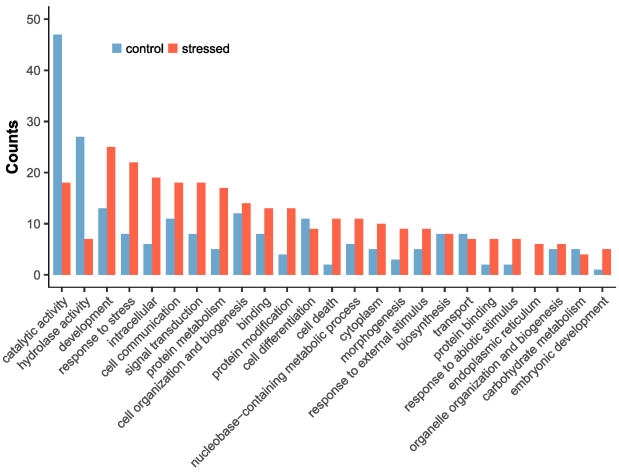

Figure 1: Enriched gene ontology (GO) terms in the unstressed (18 °C; normoxic normocapnia) and stressed (32 °C; hypoxic hypercapnia) samples. The top 25 categories and their counts for each sample are shown

concentration, purity, and integrity, as well as cDNA synthesis and reverse transcription was performed as in section 2.2.

All qPCR were conducted in a ViiA 7 Real-Time PCR System (Applied Biosystems, Darmstadt, Germany) using SYBR Green PCR Master Mix (Applied Biosystems, Darmstadt, Germany). Primers were designed with the software PrimerExpress® using the default parameters for the TaqMan Quantification method. Each reaction contained 2 ng of cDNA in 20 µL final volume with a primer concentration of 300 nM. Primer efficiencies was validated by five serial dilutions from 2 ng to 0.02 pg cDNA. Each plate for qPCR included a negative control and a template without reverse transcriptase (-RT) to test for possible DNA contamination and unspecific amplification, and repeated samples to assess inter-plate variability. A melting curve was performed immediately after amplification to corroborate the specificity of the primers.

Statistical analysis of qPCR data was performed for each tissue (gill and muscle) separately with the package MCMC.qpcr (Matz et al. 2013; Supplementary material 1). This method employs a Bayesian Markov Chain Monte Carlo algorithm to fit a single linear mixed model to the complete set of genes. We included Experiment (control, hypoxia, hypercapnia, and combined) and Temperature (18 °C, 24 °C, 30 °C, and 32 °C) as fixed factors plus their interaction (two-way design). This was run under the classic model, which follows the multigene normalization procedure dividing all the gene expression values by the harmonic mean of the reference genes (Vandesompele et al., 2002). 60S ribosomal protein L5 (*RPL5*) and E3 ubiquitin protein ligase (*E3UL*) were used as reference genes based on our previous study (Tripp-Valdez et al., 2019). Relative abundance is reported as posterior means with 95% credible intervals. Pairwise t-test between groups were calculated controlling for multiple comparisons (False Discovery Rate).

Correlation networks were constructed from a pairwise Spearmans correlation matrix of relative gene expression values using an R-script previously described (Hüning et al., 2013). As

normalized gene expression values cannot be extracted from the model employed by MCMC.qpcr, gene expression values for the correlation matrices were analysed through the ΔΔCT method (Livak and Schmittgen, 2001) using the harmonic mean of *RPL5* and *E3UL* as reference. Networks were constructed for gill and muscle at each of the experimental conditions using a force-directed layout. To simplify networks and improve their interpretation, only the correlations with a Spearmans $\rho > 0.7$ are displayed (The respective gene-specific expression profiles are depicted in the supplementary material 1).

2.5. Transcriptome validation and additional response to warming under combined hypoxia and hypercapnia

To test the suitability of the *H. fulgens* transcriptome assembly for exploring additional processes associated to the cellular stress response, we investigated the correlation between the changes in gene expression from the control condition (18 °C, normoxic normocapnia) toward the most stressful condition (32 °C; hypoxic hypercapnia) displayed by the transcriptome assembly and by the qPCR results from gill and muscle. TPM values were extracted from the count matrices of the unstressed and stressed libraries (section 2.3) and used to calculate the log2 fold changes. This was compared to the calculated log2 fold change in gene expression from the MCMC.qpcr model for the control and the most stressful treatment for gill and muscle. By using the fold change in TPM values, we investigated further changes in the abundance of additional genes involved in the CSR, with a focus on genes involved in the antioxidant system, molecular chaperones, protein degradation, energy metabolism and programmed cell death.

3. Results

3.1. de novo transcriptome assembly

Illumina sequencing of the normalized libraries from one unstressed abalone (18 °C; normoxia; normocapnia) and one stressed abalone (32 °C; hypoxia; hypercapnia) generated 31,022,126 paired-end reads. Initial de novo assembly from both libraries produced 582,114 contigs, with an average contig length of 695.29 bp. After discarding the redundant contigs and those with low expression levels, the assembly was reduced to 95,098 contigs with an average length of 704.62 bp and an N50 of 1,134 bp (Table 2). A total of 13,481 transcripts (14.17%) were annotated following Blastx against the Swiss-Prot database, from which 383 are derived from mollusk species and 102 from Haliotis species.The Transcriptome Shotgun Assembly (TSA) has been deposited at DDBJ/EMBL/GenBank under the accession GGVS00000000. The version described in this paper is the first version: **GGVS01000000**. The raw Sequence Reads (SRA) for the two biological samples has been deposited under the accessions **SRR7096023** & **SRR7096024**.

The explorative GO functional enrichment analysis demonstrated that several biological processes were affected by the experimental conditions (Fig. 1). Most notably, genes involved in catalytic activity were strongly under-represented in the animals exposed to 32 °C and hypoxic hypercapnia, while terms related to the stress response, cell communication, signal transduction and protein metabolism were over-represented. Additionally, the stressed organism displayed increased activities of genes related to programmed cell death (Fig. 1).

Table 2: Statistics of the *H. fulgens* transcriptome assembly

Statistic	Unfiltered assembly	Filtered assembly
Number of contigs	582, 114	95, 098
Average contig length (bp)	695.29	704.44
N50	929	1, 134
Total assembled bases	404, 738, 326	66, 990, 780
Annotated sequences SwissProt (E^{-6})	-	13, 481 (14.17%)

3.2. Gene expression patterns: qPCR results

Patterns of gene expression were investigated for 20 genes related to the cellular stress response using the MCMC.qpcr model for gill and muscle. Overall, models from both tissues demonstrate a coordinated induction of the heat shock proteins (Hsp70s) under all experimental conditions, whereas genes involved in energy metabolism and antioxidant response displayed tissue-specific and treatment-specific expression patterns. In our previous studies with the same *H. fulgens* samples we found evidence of regulation of the mitochondrial and glycolytic capacities as well as a strong heat shock response in muscle (Tripp-Valdez et al., 2019); therefore, here we focus on the results of the MCMC.qpcr model for citrate synthase (*CS*), pyruvate kinase (*PK*), phosphoenolpyruvate carboxykinase (*PEPCK*), *Hsp70i*, and the hypoxia inducible factor (*HIF*). Gene expression results for all remaining genes are shown in supplementary material 1.

In both tissues, *CS* displayed a warming-induced down-regulation pattern under control, hypoxia and hypercapnia treatments (Fig. 2A-C). In the combined treatment (Fig. 2D), *CS* didn't show any significant changes with temperature. A down-regulation pattern for *PK* was observed under all treatments (Fig. 2E-H), however, a stronger response could be seen in gill tissue in the combined treatment (Fig. 2H), where a significant decrease was already detected at 24 °C. *PEPCK* showed a tissue-dependent pattern, as it was up-regulated in gills during warming in all treatments, but it remained unchanged in muscle (Fig. 2I-L). Strong up-regulation was observed for *Hsp70i* under all experimental conditions in both tissues. However, *Hsp70i* in gill displayed a stronger response to warming under hypercapnic (Fig. 2O) and combined (Fig. 2P) treatments with a significant induction at 24 °C, while this occurred at 30 °C under all treatments in muscle. Finally, *HIF* was down-regulated in gill (Fig. 2Q-T), a trend which was non-significant under hypercapnia, whereas up-regulation occurred in muscle, although

this was significant only in the control (Fig. 2Q) and combined (Fig. 2T) treatments at 32 °C.

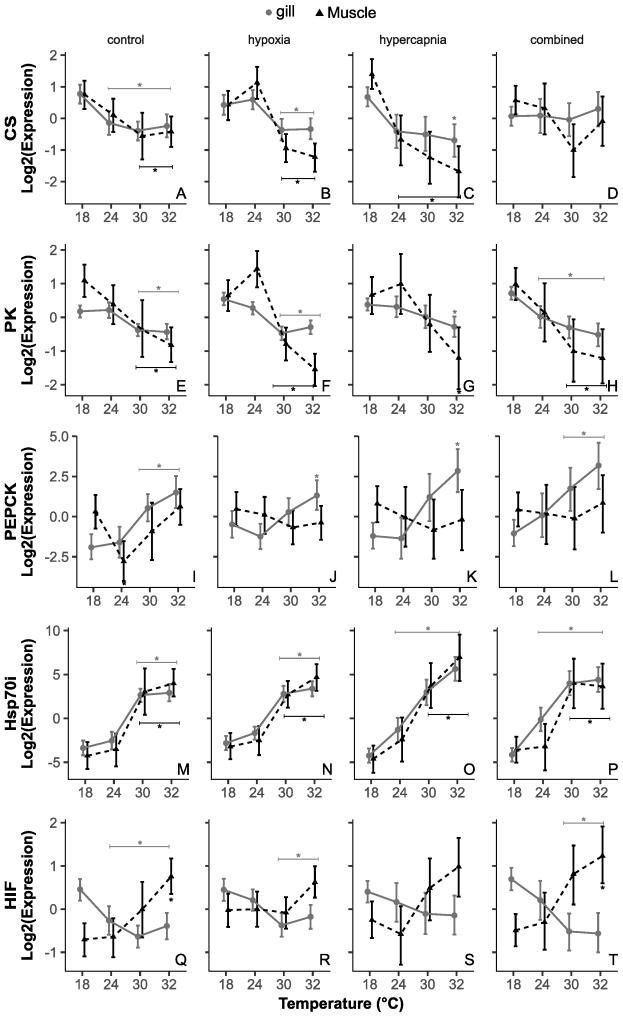

Figure 2: Enriched gene ontology (GO) terms in the unstressed (18 °C; normoxic normocapnia) and stressed (32 °C; hypoxic hypercapnia) samples. The top 25 categories and their counts for each sample are shown

3.3. Gene expression patterns: correlation networks

In both tissues, there is an evident separation of two clusters formed from genes involved in energy metabolism on the one side, characterized by down-regulation, and chaperones and antioxidant genes on the other side, being up-regulated (Figs. 3 and 4). Nonetheless, tissue-specific differences were present in all networks: In gill, the chaperone cluster is more tightly connected under all treatments; glutathione-S-transferase (*GST*) is connected to the chaperone cluster; *PK* and *PEPCK* are inversely connected to each other (see below); and *HIF* is linked to the energy metabolism cluster (Fig. 3). In muscle, chaperones are more loosely connected; *GST* and *PEPCK* do not display strong correlation to any cluster ($\rho < 0.7$) and therefore, they are absent in the networks; and *HIF* is linked to the chaperone cluster (Fig. 4).

In both gill and muscle, the correlation networks additionally displayed modifications due to the presence of the additional factors hypoxia, hypercapnia, and their combination. Changes displayed in gill were more evident in the hypoxic treatment (Fig. 3B) as fewer elements are present in the network; *PK* is connecting the chaperones and energy clusters and is directly connected to *HIF*. In the hypercapnic treatment (Fig. 3C) and in the combined treatment (Fig. 3D), *PK* doesnt play a central role but is still directly connected to *HIF*.

Alterations in gill energy metabolism are further demonstrated by the interaction between *PK* and *PEPCK*: In the control treatment (Fig. 3A) and the hypercapnic treatment (Fig. 3C), *PEPCK* and *PK* are directly connected to each other with an inverse correlation. Under the combined treatment, however, *PEPCK* and *PK* are linked to each other by *HIF* (Fig. 3D), and under the hypoxic treatment, *PEPCK* is absent in the network ($\rho < 0.7$; Fig. 3B). Finally, *CS* shows a direct connection with energy metabolism, particularly with *PK*, under the control (Fig. 3A) and hypoxic (Fig. 3B) treatments, however, under the hypercapnic treatment (Fig. 3C) *CS* doesnt display a direct connection with the energy metabolism cluster and is absent in the combined treatment ($\rho < 0.7$; Fig. 3D). Moreover, glutathione reductase (*GLR*) is displayed only in the hypoxia (Fig. 3B) and combined (Fig. 3D) treatments and is absent in the remaining treatments.

Changes in the gene correlation patterns in muscle were less robust than in gill. However, the hypoxia treatment also displayed major changes, as genes representing energy metabolism were more tightly connected (Fig. 4B) than in other treatments.

3.4. Transcriptomic responses to warming under combined hypoxia and hypercapnia

The comparison of gene expression changes between the unstressed (18 °C; normoxic normocapnia) and stressed (32 °C; hypoxia; hypercapnia) conditions in the transcriptome and in the qPCR showed high correlation in both tissues ($R^2 = 0.77$ in gill and $R^2 = 0.73$ in muscle; Fig. 5) which reflects shared trends in gene expression for most of the analysed genes (Table 3). This suggests that relative changes in transcript abundance (TPM values) are well suited to explore additional changes in our de novo transcriptome assembly.

Exploration of additional genes demonstrated that genes involved in redox regulation and molecular chaperones were mostly affected in the sample exposed to combined drivers, particularly genes related to the glutathione system (Fig. 6A). Genes involved in protein degradation displayed a diverse pattern with high up-regulation of *caspase-8* and *LON* protease and a strong down-regulation of *cathepsin-L* (Fig. 6C). The down-regulation of energy metabolism related genes observed by qPCR is further confirmed here as additional genes involved in carbohydrate metabolism displayed a general down-regulation pattern (Fig. 6D). Finally, several genes involved in cell death and apoptosis were found upregulated under the combined drivers, such as the apoptosis inhibitors (*IAP* and *BIRCs*),

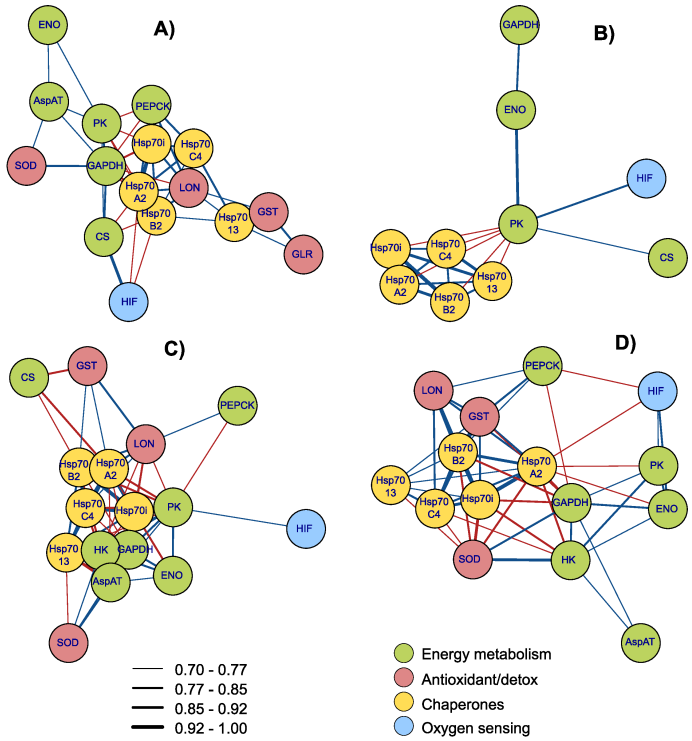

Figure 3: : Correlation network of genes in *H. fulgens* gill in response to warming under A) normoxic normocapnia, B) hypoxic normocapnia, C) normoxic hypercapnia, and D) hypoxic hypercapnia treatments. Line width of vertices correspond to Spearmans ρ value. Blue line indicates positive correlation. Red line indicates negative correlation.

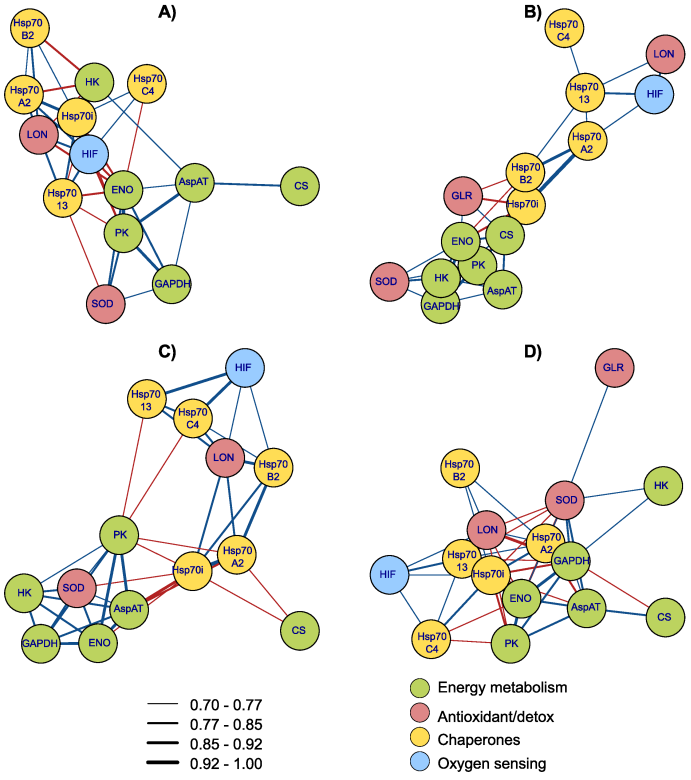

Figure 4: : Correlation network of genes in *H. fulgens* muscle in response to warming under A) normoxic normocapnia, B) hypoxic normocapnia, C) normoxic hypercapnia, and D) hypoxic hypercapnia treatments. Line width of vertices correspond to Spearmans ρ value. Blue line indicates positive correlation. Red line indicates negative correlation.

the tumor necrosis factor and the programmed cell death genes (*PDCD-2*; Fig. 6E).

4. Discussion

In this study, we developed a de novo transcriptome assembly from Haliotis fulgens juveniles to investigate transcriptional changes in the cellular stress response in organisms exposed to acute thermal stress under hypoxia (50% air saturation), hypercapnia (1,000 µatm PCO_2) and both factors combined. The general applicability of the transcriptome for monitoring responses to environmentally relevant events was tested by validating the exemplary transcriptomic responses of distinct libraries by quantitative expression data (qPCR) of candidate genes covering several cellular functions.

4.1. Description of the H. fulgens molecular response through the transcriptome assembly

The transcriptome assembly from normalized libraries resulted in 95,098 contigs after removing redundant contigs and those with low expression. The resulting number of contigs, as well as the average contig length (704.44 bp), the N50 (1,134 bp) and the percentage of annotated sequences (14.17%) fall in the range reported for other abalone species using Illumina technologies (Franchini et al., 2011; Shiel et al., 2015; Harney et al., 2016). The shared trend in the direction of gene expression indicated by transcript abundance (TPM) and those obtained with the qPCR analysis (Fig. 5; Table 3) validate the use of our transcriptome to do a preliminary assessment of molecular responses of *H. fulgens* to temperature with and without additional challenges. A complete correlation between the TPM and qPCR fold changes is not expected in this study because i) we used a normalization step during the library preparation which should attenuate the absolute abundance, especially of highly abundant transcripts; ii) we used only one library per treatment; and iii) libraries were prepared from a pool of different tissues (gill, mantle and hepatopancreas), thus transcript abundances were likely influenced by tissues that were not analysed by qPCR (*e.g.* in *GAPDH*, *HK*, and *Hsp70 12A*). Nonetheless, the distinct expression patterns across treatments seem to be preserved.

The observed changes in expression in genes belonging to the cellular stress response (Fig. 6) indicate an overall reduction in energy metabolism, while molecular chaperones and the antioxidant system were up-regulated. This pattern of gene regulation is in accordance with changes in cellular condition towards damage prevention (Kültz, 2005; Buckley et al., 2006; Kassahn et al., 2009). In a parallel study, we discussed the strong inducibility of the mRNA of Hsp70 family members in *H. fulgens* muscle (Tripp-Valdez et al., 2019). Here we show that additional Hsps (*Hsp10*, *Hsp60*, *Hsp95* and, to a less extent, *Hsp75*) are also involved in the abalone stress response. Therefore, use of additional Hsp other than Hsp70 as stress indicators in abalone may be promising to decipher stress- and tissue-specific responses with higher resolution.

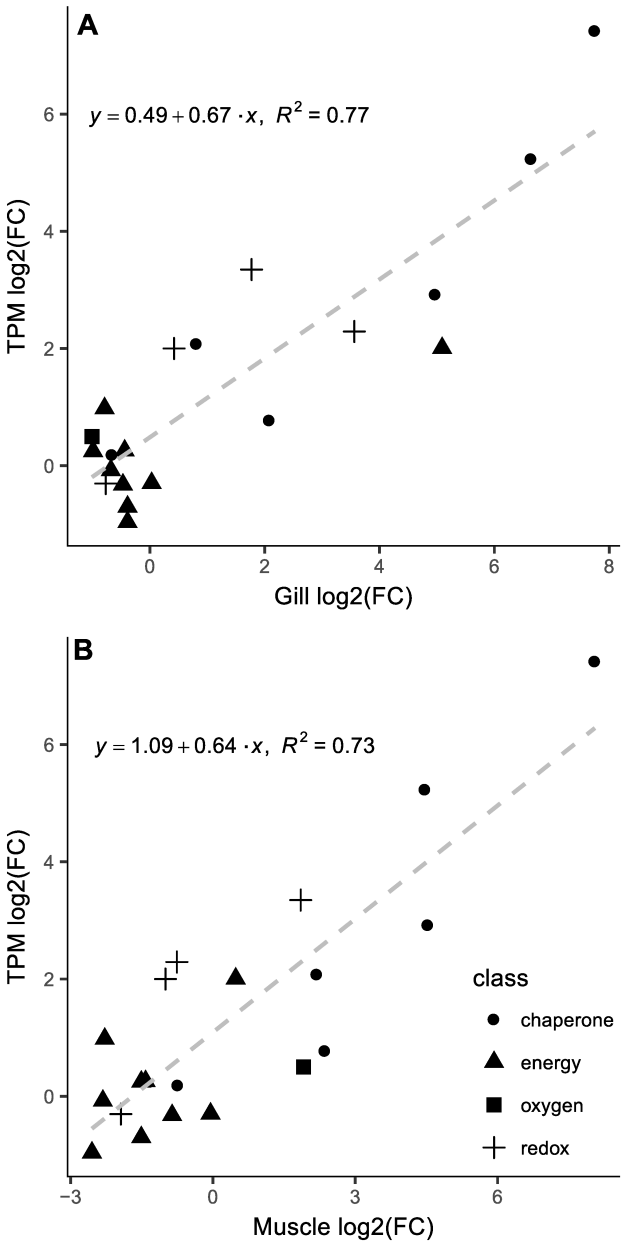

Figure 5: Transcriptome (TPM) versus qPCR log2fold changes in gene expression between unstressed (18 C; normoxic normocapnia) and stressed (32 C; hypoxic hypercapnia) conditions in A) gill and B) muscle.

The strong up-regulation of aldehyde dehydrogenase (*ALDH8A1*), together with the up-regulation of several members of the glutathione system seems to reflect a response to increased oxidative stress upon warming, especially when combined with hypoxia and hypercapnia. Reduced cellular oxygen levels, resulting from strong environmental hypoxia or warming-induced systemic hypoxemia, can enhance mitochondrial production of reactive oxygen species, which can subsequently induce protein damage (Kassahn et al., 2009). En-

zymes such as superoxide dismutase (SOD), glutathione reductase (GLR), glutathione-S-transferase (GST), glutathione peroxidase (Gpx) and catalase, among others, collectively reduce the negative effects of by-products of oxidative damage (Hermes-Lima and Zenteno-Savín, 2002). Particularly, higher levels of *GST* mRNA were correlated with higher mitochondrial oxidative activity and granulocytes concentration in the oyster *Crassostrea gigas* after short-term emersion (3 h), suggesting an activation of glutathione turnover in response to increased oxidative metabolism (Sussarellu et al., 2012). Similarly, high levels of *LON* protease, which is localized in the mitochondrial matrix, are related to the prevention of damaged protein accumulation under stressful conditions (Koppen and Langer, 2007). Therefore, up-regulation of *LON* protease and *GST* mRNA detected in *H. fulgens* from this study (both by transcriptome and PCR) indicates the induction of mechanisms protecting macromolecular structures against oxidative damage and to enable the detoxification of by-products. Moreover, the high induction of *ALDH8A1*, in addition to *GST*, could indicate higher rates of lipid peroxidation (Hermes-Lima and Zenteno-Savín, 2002), but this aspect needs further investigation. The increased reliance by the animals on the glutathione machinery and the heat shock proteins to mitigate thermal and accompanying oxidative stress could explain the reduced levels of *Cu-Zn SOD* and *Mn SOD* observed in *H. fulgens*, as has been previously described in *H. discus* exposed to acute thermal challenges (De Zoysa et al., 2009).

The RNA-Seq analysis also demonstrated up-regulation of several genes involved in the apoptotic process. From the analyzed genes displayed in Fig. 6, the inhibitor of apoptosis 2 (*IAP2*) and the baculoviral IAP repeat-containing protein 2 (*BIRC-2*) were highly up-regulated in the stressed animal. Genes belonging to the inhibitor of apoptosis family maintain a balance between cell proliferation and cell death by inhibiting the activity of caspases (Qu et al., 2015). Accordingly, a coordinated up-regulation of heat shock proteins and inhibitors of apoptosis constitutes an antiapoptotic system which could reduce cell turnover rates, giving more time to the cell repair machinery to work against the warming-induced damage (Gracey et al., 2008).

4.2. Warming-induced patterns of gene expression under hypoxia, hypercapnia, and both factor combined

In our previous studies with *H. fulgens* based on the same samples, we already demonstrated that thermal tolerance and cellular energy metabolism in gill and muscle were altered when the thermal challenge is accompanied by additional hypoxia, hypercapnia or both factors combined (Tripp-Valdez et al., 2017). In the following, we focus on specific patterns of the responsiveness and underlying molecular networks of key functional traits for both tissues. From our previous analyses, we identified contrasting cellular metabolic responses to thermal stress in gill and muscle, as enhanced anaerobic activity in gill could be depicted from the accumulation of succinate, alanine and lactate during warming under hypoxia, hypercapnia and the combined treatments (Tripp-Valdez et al., 2017), whereas muscle didn't display a significant accumulation of succinate, lactate or tauropine (Tripp-Valdez et al., 2019). In this study, gill and muscle displayed a down-regulation of *PK*, however, *PEPCK* in gill was up-regulated. Both enzymes control a metabolic bifurcation point at phosphoenolpyruvate, channeling it for aerobic oxidation to the tricarboxylic acid cycle (TCA) through pyruvate (*PK*) or to an anaerobic mitochondrial pathway via oxaloacetate (*PEPCK*) leading to an accumulation of succinate (Grieshaber et al., 1994). Consequently, the increasing levels of *PEPCK* in gill may correspond to a higher potential for anaerobic energy production and transcriptional adjustment to favour the synthesis of succinate, in line with the significant accumulation of this anaerobic end product in gill (Tripp-Valdez et al., 2017). Unfortunately, we were not able to produce successful primers to investigate the mRNA levels of lactate dehydrogenase and tauropine dehydrogenase, which are important components in abalone anaerobic metabolism (Venter et al., 2016). Nevertheless, enzyme capacities of both enzymes important for NAD^+ restoration were found high but unchanged in abalone muscle during all treatments (Tripp-Valdez et al., 2019).

The expression patterns of *HIF* in gill and muscle (Fig. 2) suggest different sensitivities and trade-offs in the oxidative state of the different tissues. It has been shown that *HIF-1a* and *HIF-1b* are regulated at both transcriptional and posttranscriptional level (Ma and Haddad, 2000). *HIF* plays an important role in the activation of glycolysis and several other pro-

Table 3: Estimated log2 fold change (FC) between the unstressed (18 °C; normoxic normocapnia) and stressed (32 °C; hypoxic hypercapnic) conditions comparing the Transcripts Per Kilobase Million (TPM) values from the transcriptome assembly (section 2.3) and the gene expression values from the qPCR analysis for gill and muscle (section 2.4). Numbers in bold indicate discordant regulation patterns between transcriptome and both gill and muscle qPCR results.

	Transcriptome	qPCR	
Gene	TPM log2(FC)	Gill log2(FC)	Muscle log2(FC)
AspAT	-0.70	-0.39	-1.51
COXIII	**0.26**	-0.44	-1.42
ENO	-0.96	-0.39	-2.55
GAPDH	**0.98**	-0.79	-2.28
HEX	**0.25**	-0.99	-1.51
CS	-0.32	-0.47	-0.86
PK	-0.08	-0.68	-2.32
LCF	-0.30	0.03	-0.05
Hsp70 12A	**0.19**	-0.66	-0.74
Hsp70 13	2.08	0.81	2.19
Hsp70 A2	2.92	4.97	4.53
Hsp70 B2	5.23	6.64	4.47
Hsp70 C4	0.77	2.08	2.36
Hsp70i	7.42	7.75	8.05
HIF-1a	0.50	-1.01	1.91
LON	3.35	1.77	1.85
GLR	2.00	0.42	-1.00
GST	2.29	3.56	-0.76
SOD	-0.30	-0.77	-1.94

cesses related to energy production under reduced oxygen levels in the cell (Ma and Haddad, 2000; Semenza, 2001), and transcriptional up-regulation of *HIF-1a* was associated with the development of warming-induced cellular hypoxia and enhancement of anaerobic metabolism (Han et al., 2016). In *H. fulgens* muscle, *HIF* up-regulation was highly correlated with the heat shock proteins (Fig. 4), however, as gill displayed a very similar Hsp70 expression pattern (Fig. 3), it is unlikely that *HIF* was involved in this response. As abalone musculature is known to receive low cardiac output, especially during conditions of high oxygen demand (Venter et al., 2016), abalone musculature is more frequently exposed to anaerobic situations than gills. Therefore, the observed pattern of *HIF* up-regulation may correspond to a fast response mechanism to cellular hypoxia inherent to the abalone muscle.

Network responses in gill and muscle demonstrated that acute temperature stress, alone and combined with additional factors (hypoxia and hypercapnia), induced a coordinated down-regulation of gene expression patterns for ATP restoring systems. This contrasts previous findings in fish and invertebrates, where acute and chronic heat stress stimulated mRNA levels of genes involved in glycolysis and TCA, interpreted to reflect the need of sustained ATP production during heat stress (Buckley et al., 2006; Meistertzheim et al., 2007; Han et al., 2016; Goncalves et al., 2017). The observed pattern in *H. fulgens*, however, seems to indicate a warming-induced reconfiguration of protein synthesis from energy production mechanisms to those involved in the stress response. As abalone species are known to switch metabolic fuels during strong environmental stress, it is conceivable that an activation of genes involved in carbohydrate metabolism is not required to be part of the thermal reaction norm. Reduced expression of genes involved in carbohydrate metabolism was seen in organisms from the combined treatments, in parallel to a warming-induced reduction of the glycolytic flux in gill and muscle together with a drop in whole-organism metabolic rate reflecting a reduction of energy demanding processes (Tripp-Valdez et al., 2017, 2019).

In contrast to the genes involved in carbohydrate metabolism, *CS* displayed unchanged mRNA levels under all drivers combined (Fig. 2D). Maximum capacity of this enzyme in *H. fulgens* muscle was measured in our previous study (Tripp-Valdez et al., 2019) and followed a trend similar to mRNA levels: in the control, hypoxia, and hypercapnia treatments, warming caused a decline in enzyme capacity which returned to initial levels at the warmest temperature step (32 °C); but under the combined experiment, CS remained unchanged at all temperatures. As CS catalyzes the first step of TCA, introducing carbon chains from carbohydrate, protein and fatty acid degradation, it constitutes a good indicator of mitochondrial capacities. The data suggest that thermal compensation (*i.e.* a decline of mitochondrial capacities) occurred during moderate warming under control, hypoxic and hypercapnic treatments, but severe warming (32 °C) reversed this trend. Warming under the combined treatment, however, resulted in functional and transcriptional adjustments of mitochondrial capacity over the whole temperature ramp. High rates of cytosolic ATP breakdown have been associated with compensatory adjustments in mitochondrial content and function, including transcriptional upregulation of mitochondrial enzymes (Eckerle et al., 2008; Kassahn et al., 2009). In this context, energetic deficits may result from the depressed metabolic rate and may have triggered transcriptional compensation to sustain levels of aerobic capacity. Similar observations of mitochondrial adjustments and shifts in metabolic fuels have been described in *H. midae* juveniles and adults: Warm acclimated *H. mideae* juveniles displayed up-regulation of two cytochrome c oxidase subunits (*COXI* and *COXII*) in muscle, possibly indicating enhanced mitochondrial capacity, paralleled by a higher reliance on protein as a substrate to fuel the TCA (Vosloo et al., 2013), whereas acute warming in adults induced a reduction of muscular glycolytic flux, evidenced by a reduction in lactate levels and higher rates of protein degradation, indicated by increased nitrogen excretion citepVosloo2010.

5. Conclusions

The de novo transcriptome assembly for juveniles of *H. fulgens* described in this work proved to be a powerful tool to access the transcriptional changes in abalone exposed to thermal extremes under hypoxia and hypercapnia. Although two individuals were used to construct the transcriptome assembly (one unstressed individual and one stressed individual), the contrasting conditions and the pooling of multiple tissues (gill, hepatopancreas, and mantle) ensured that a wide range of cellular processes was covered by the transcriptome. Despite the representation of various tissues, the transcriptome was a reasonable first step to identify new candidate genes and diverse processes involved. The overall transcription changes indicate a shift in emphasis from mechanisms associated with energy production to those supporting damage prevention and repair; in parallel, a higher induction of molecular chaperones (*e.g.* Hsp) and antioxidant enzymes (*e.g. ALDH8A1*and *GST*) is likely reflecting high rates of protein damage and degradation. Further analyses of correlation networks in gill and muscle allowed us to explore the underlying molecular response in each tissue and to identify the modulation of thermal reaction norms by the different experimental settings. The most robust changes in the warming-induced network connections were observed in gills, particularly under hypoxia, concerning carbohydrate metabolism. Moreover, we observed a warming-induced strengthening of *CS* gene expression only under combined hypoxia and hypercapnia which is in line with the pattern of CS enzyme capacities found in our previous study. Therefore, we suggest that during warming stress, a systemic control of mitochondrial activity and mRNA levels sets in at a lower temperature under combined hypoxia and hypercapnia than under hypoxia or hypercapnia as individual drivers. In the transcriptome, additional genes involved in the cellular responses to stress could be identified, including the strong up-regulation of genes related to the inhibition of apoptosis as well as genes related to programmed cell death. As most genes of the classical CSR behaved in quite similar ways in all treatments, a more detailed transcriptome-wide expression analysis of specific tissues seems promising to differentiate the responses with higher resolution and to identify the most sensitive traits involved in

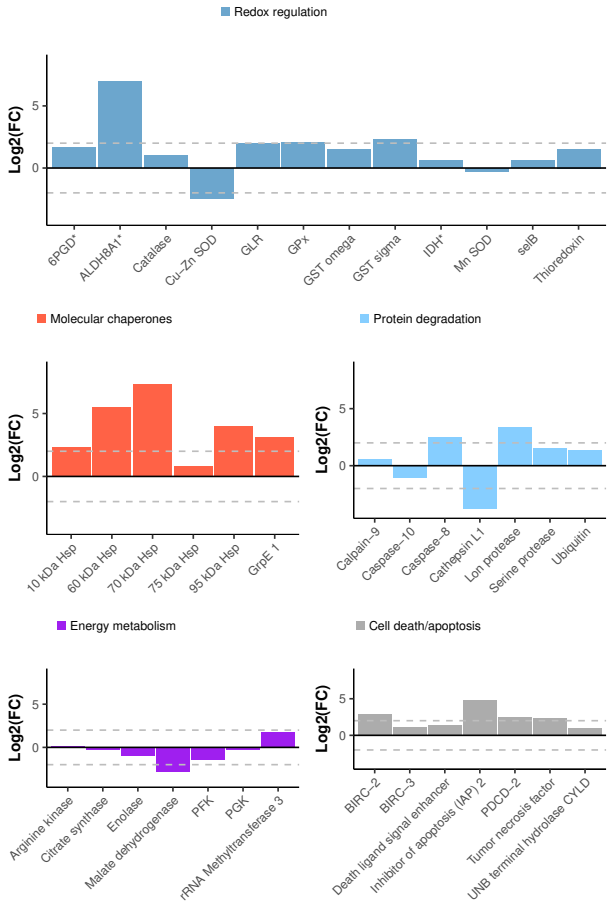

Figure 6: Estimated fold change (FC) from the Transcripts Per Kilobase Million (TPM) values for genes associated with redox regulation (A), molecular chaperones (B), protein degradation (C), energy metabolism (D) and programmed cell death/apoptosis (E). TPM values from the unstressed and stressed samples were obtained following the transcript abundance estimation through RSEM method (section 2.3). 6PDG, 6-phosphogluconate dehydrogenase; ALDH8A1, aldehyde dehydrogenase family 8; Cu-Zn SOD, copper-zinc superoxide dismutase; GLR, glutathione reductase; GPx, glutathione peroxidase; GST, glutathione-S-transferase; IDH, isocitrate dehydrogenase; Mn SOD, manganese superoxide dismutase; selB, Selenocysteine-specific elongation factor; Hsp, heat shock protein; PFK, 6-phosphofructokinase; PGK, Phosphoglycerate kinase; BIRC, baculoviral IAP repeat-containing protein; PDCD-2, programmed cell death protein-2. * indicates genes that are also important for energy metabolism

muscular and organismic failure observed under the combined treatment. In any case, transcriptional changes from the analyzed genes in this study support observations at the cellular level from our previous studies, such as the tissue-specific potential for succinate production and mitochondrial stimulation under combined hypoxia and hypercapnia. Consequently, the current transcriptome provides an extensive source of genetic information not only for green abalone but also for other gastropods facing environmental challenges and climate change.

6. Acknowledgments

We thank Gilberto González Soriano and Rosa Linda Salgado García from the Ecophysiology Lab in CIBNOR for their support during the experiments and samples shipping to Alfred Wegener Institute (AWI); to Martín Gerardo Ruíz, from the Sociedad Cooperativa de Producción Pesquera de Bahía Tortugas S.C. de R.L. for providing the organisms; Jutta Jürgens and Kerstin Oetjen from AWI for their assistance in library sequencing and molecular analyses. Financial support to Miguel A. Tripp-Valdez was granted by the fellowship of the Deutscher Akademischer Austauschdienst (DAAD) program: 57076385. This work is a contribution to the research program PACES II of the AWI.

References

Andrews, S., 2012. FastQC: a quality control tool for high throughput sequence data. URL: http://www.bioinformatics.babraham.ac.uk/projects/fastqc/.

Bolger, A.M., Lohse, M., Usadel, B., 2014. Trimmomatic: A flexible trimmer for Illumina sequence data. Bioinformatics 30, 2114–2120. doi:10.1093/bioinformatics/btu170.

Buckley, B.A., Gracey, A., Somero, G., 2006. The cellular response to heat stress in the goby Gillichthys mirabilis: a cDNA microarray and protein-level analysis. Journal of Experimental Biology 209, 2660–2677. URL: http://jeb.biologists.org/cgi/doi/10.1242/jeb.02292, doi:10.1242/jeb.02292.

Chapman, R.W., Mancia, A., Beal, M., Veloso, A., Rathburn, C., Blair, A., Holland, a.F., Warr, G.W., Didinato, G., Sokolova, I.M., Wirth, E.F., Duffy, E., Sanger, D., 2011. The transcriptomic responses of the eastern oyster, Crassostrea virginica, to environmental conditions. Molecular ecology 20, 1431–49. URL: http://www.ncbi.nlm.nih.gov/pubmed/21426432, doi:10.1111/j.1365-294X.2011.05018.x.

Choi, M.J., Kim, G.D., Kim, J.M., Lim, H.K., 2015. Differentially-expressed genes associated with faster growth of the pacific abalone, *Haliotis discus hannai*. International Journal of Molecular Sciences 16, 27520–27534. doi:10.3390/ijms161126042.

Cook, P.A., 2016. Recent Trends in Worldwide Abalone Production. Journal of Shellfish Research 35, 581–583. URL: http://www.bioone.org/doi/10.2983/035.035.0302, doi:10.2983/035.035.0302.

De Zoysa, M., Whang, I., Lee, Y., Lee, S., Lee, J.S., Lee, J., 2009. Transcriptional analysis of antioxidant and immune defense genes in disk abalone *Haliotis discus discus*, during thermal, low-salinity and hypoxic stress. Comparative Biochemistry and Physiology - B Biochemistry and Molecular Biology 154, 387–395. doi:10.1016/j.cbpb.2009.08.002.

Desalvo, M.K., Sunagawa, S., Voolstra, C.R., Medina, M., 2010. Transcriptomic responses to heat stress and bleaching in the elkhorn coral *Acropora palmata*. Marine Ecology Progress Series 402, 97–113. doi:10.3354/meps08372.

Eckerle, L.G., Lucassen, M., Hirse, T., Pörtner, H.O., 2008. Cold induced changes of adenosine levels in common eelpout *Zoarces viviparus*: a role in modulating cytochrome c oxidase expression. The Journal of experimental biology 211, 1262–9. URL: http://www.ncbi.nlm.nih.gov/pubmed/18375851, doi:10.1242/jeb.013474.

Farcy, E., Voiseux, C., Lebel, J.M., Fi?vet, B., 2009. Transcriptional expression levels of cell stress marker genes in the Pacific oyster *Crassostrea gigas* exposed to acute thermal stress. Cell Stress and Chaperones 14, 371–380. URL: http://link.springer.com/10.1007/s12192-008-0091-8, doi:10.1007/s12192-008-0091-8.

Franchini, P., van der Merwe, M., Roodt-Wilding, R., 2011. Transcriptome characterization of the South African abalone *Haliotis midae* using sequencing-by-synthesis. BMC research notes 4, 59. URL: http://www.biomedcentral.com/1756-0500/4/59, doi:10.1186/1756-0500-4-59.

Goncalves, P., Thompson, E.L., Raftos, D.A., 2017. Contrasting impacts of ocean acidification and warming on the molecular responses of CO_2-resilient oysters. BMC Genomics 18, 431. URL: http://bmcgenomics.

biomedcentral.com/articles/10.1186/s12864-017-3818-z, doi:10.1186/s12864-017-3818-z.

Grabherr, M.G., Haas, B.J., Yassour, M., Levin, J.Z., Thompson, D.A., Amit, I., Adiconis, X., Fan, L., Raychowdhury, R., Zeng, Q., Chen, Z., Mauceli, E., Hacohen, N., Gnirke, A., Rhind, N., di Palma, F., Birren, B.W., Nusbaum, C., Lindblad-Toh, K., Friedman, N., Regev, A., 2011. Full-length transcriptome assembly from RNA-Seq data without a reference genome. Nature Biotechnology 29, 644–652. URL: http://www.nature.com/doifinder/10.1038/nbt.1883, doi:10.1038/nbt.1883.

Gracey, A.Y., Chaney, M.L., Boomhower, J.P., Tyburczy, W.R., Connor, K., Somero, G.N., 2008. Rhythms of gene expression in a fluctuating intertidal environment. Current biology : CB 18, 1501–7. URL: http://www.ncbi.nlm.nih.gov/pubmed/18848447, doi:10.1016/j.cub.2008.08.049.

Grieshaber, M.K., Hardewig, I., Kreutzer, U., Portner, H., 1994. Physiological and Metabolic Responses to Hypoxia in Invertebrates. Reviews of Physiology, Biochemistry and Pharmacology 125. doi:doi.org/10.1007/BFb0030909.

Han, G., Zhang, S., Dong, Y., 2016. Anaerobic metabolism and thermal tolerance: the importance of opine pathways on survival of a gastropod after cardiac dysfunction. Integrative Zoology URL: http://doi.wiley.com/10.1111/1749-4877.12229, doi:10.1111/1749-4877.12229.

Harms, L., Frickenhaus, S., Schiffer, M., Mark, F.C., Storch, D., Held, C., Pörtner, H.O., Lucassen, M., 2014. Gene expression profiling in gills of the great spider crab *Hyas araneus* in response to ocean acidification and warming. BMC genomics 15, 789. URL: http://www.biomedcentral.com/1471-2164/15/789, doi:10.1186/1471-2164-15-789.

Harney, E., Dubief, B., Boudry, P., Basuyaux, O., Schilhabel, M.B., Huchette, S., Paillard, C., Nunes, F.L.D., 2016. De novo assembly and annotation of the European abalone *Haliotis tuberculata* transcriptome. Marine Genomics 28, 11–16. URL: http://dx.doi.org/10.1016/j.margen.2016.03.002, doi:10.1016/j.margen.2016.03.002.

Henson, S.A., Beaulieu, C., Ilyina, T., John, J.G., Long, M., Séférian, R., Tjiputra, J., Sarmiento, J.L., 2017. Rapid emergence of climate change in environmental drivers of marine ecosystems. Nature Communications 8, 14682. URL: http://www.nature.com/doifinder/10.1038/ncomms14682, doi:10.1038/ncomms14682.

Hermes-Lima, M., Zenteno-Savín, T., 2002. Animal response to drastic changes in oxygen availability and physiological oxidative stress. Comparative Biochemistry and Physiology - C Toxicology and Pharmacology 133, 537–556. doi:10.1016/S1532-0456(02)00080-7.

Hochachka, P., Somero, G.N., 2002. Biochemical adaptation: Mechanism and process in physiological evolution. Oxford University Press.

Hu, Z.L., Bao, J., Reecy, J., 2008. CateGOrizer: A Web-Based Program to Batch Analyze Gene Ontology Classification Categories. Online Journal of Bioinformatics 9, 108–112. URL: http://users.comcen.com.au/{~}journals/geneontologyabs2008.htm.

Huang, Z.X., Chen, Z.S., Ke, C.H., Zhao, J., You, W.W., Zhang, J., Dong, W.T., Chen, J., 2012. Pyrosequencing of *Haliotis diversicolor* Transcriptomes: Insights into Early Developmental Molluscan Gene Expression. PLoS ONE 7, 1–12. doi:10.1371/journal.pone.0051279.

Hüning, A.K., Melzner, F., Thomsen, J., Gutowska, M.a., Krämer, L., Frickenhaus, S., Rosenstiel, P., Pörtner, H.O., Philipp, E.E.R., Lucassen, M., 2013. Impacts of seawater acidification on mantle gene expression patterns of the Baltic Sea blue mussel: implications for shell formation and energy metabolism. Marine Biology 160, 1845–1861. URL: http://link.springer.com/10.1007/s00227-012-1930-9http://www.springerlink.com/index/10.1007/s00227-012-1930-9, doi:10.1007/s00227-012-1930-9.

Kassahn, K.S., Crozier, R.H., Pörtner, H.O., Caley, M.J., 2009. Animal performance and stress: Responses and tolerance limits at different levels of biological organisation. Biological Reviews 84, 277–292. doi:10.1111/j.1469-185X.2008.00073.x.

Koppen, M., Langer, T., 2007. Protein Degradation within Mitochondria: Versatile Activities of AAA Proteases and Other Peptidases. Critical Reviews in Biochemistry and Molecular Biology 42, 221–242. URL: http://www.tandfonline.com/doi/full/10.1080/10409230701380452, doi:10.1080/10409230701380452.

Kultz, D., 2003. Evolution of the cellular stress proteome: from monophyletic origin to ubiquitous function. Journal of Experimental Biology 206, 3119–3124. URL: http://jeb.biologists.org/cgi/doi/10.1242/jeb.00549, doi:10.1242/jeb.00549.

Kültz, D., 2005. Molecular and Evolutionary Basis of the Cellular Stress Response. Annual Review of Physiology 67, 225–257. URL: http://www.annualreviews.org/doi/10.1146/annurev.physiol.67.040403.103635, doi:10.1146/annurev.physiol.67.040403.103635.

Langmead, B., Trapnell, C., Pop, M., Salzberg, S.L., 2009. Ultrafast and memory-efficient alignment of short DNA sequences to the human genome. Genome Biology 10. doi:10.1186/gb-2009-10-3-r25.

Li, B., Dewey, C.N., 2011. RSEM: accurate transcript quantification from RNA-Seq data with or without a reference genome. BMC Bioinformatics 12, 323. URL: http://bmcbioinformatics.biomedcentral.com/articles/10.1186/1471-2105-12-323, doi:10.1186/1471-2105-12-323, arXiv:NIHMS150003.

Li, W., Godzik, A., 2006. Cd-hit: A fast program for clustering and comparing large sets of protein or nucleotide sequences. Bioinformatics 22, 1658–1659. doi:10.1093/bioinformatics/btl158.

Livak, K.J., Schmittgen, T.D., 2001. Analysis of Relative Gene Expression Data Using Real-Time Quantitative PCR and the 2ΔΔCT Method. Methods 25, 402–408. URL: http://linkinghub.elsevier.com/retrieve/pii/S1046202301912629, doi:10.1006/meth.2001.1262, arXiv:1003.3921v1.

Ma, E., Haddad, G.G., 2000. Cell and molecular responses to hypoxic stress. Environmental Stressors and Gene Responses 1, 89.

Matz, M.V., Wright, R.M., Scott, J.G., 2013. No Control Genes Required: Bayesian Analysis of qRT-PCR Data. PLoS ONE 8, e71448. URL: http://www.plosone.org/article/info:doi/10.1371/journal.pone.0071448{#}pone-0071448-g010http://dx.plos.org/10.1371/journal.pone.0071448, doi:10.1371/journal.pone.0071448.

Meistertzheim, A.L., Tanguy, A., Moraga, D., Thébault, M.T., 2007. Identification of differentially expressed genes of the Pacific oyster *Crassostrea gigas* exposed to prolonged thermal stress. FEBS Journal 274, 6392–6402. URL: http://doi.wiley.com/10.1111/j.1742-4658.2007.06156.x, doi:10.1111/j.1742-4658.2007.06156.x.

Morales-Bojorquez, E., Orieta Mucino-Diaz, M., Alfonso Velez-Barajas, J., 2008. Analysis of the decline of the abalone fishery (*Haliotis fulgens* and *H. corrugata*) along the westcentral coast of the Baja California peninsula, Mexico. Journal of Shellfish Research 27, 865–870. doi:10.2983/0730-8000(2008)27{[}865:AOTDOT]2.0.CO;2.

Nam, B.H., Jung, M., Subramaniyam, S., Yoo, S.I., Markkandan, K., Moon, J.Y., Kim, Y.O., Kim, D.G., An, C.M., Shin, Y., Jung, H.J., Park, J.H., 2016. Transcriptome analysis revealed changes of multiple genes involved in *Haliotis discus hannai* innate immunity during vibrio parahemolyticus infection. PLoS ONE 11, 1–16. doi:10.1371/journal.pone.0153474.

Picone, B., Rhode, C., Roodt-Wilding, R., 2015. Transcriptome profiles of wild and cultured South African abalone, *Haliotis midae*. Marine Genomics 20, 3–6. URL: http://dx.doi.org/10.1016/j.margen.2015.01.002http://linkinghub.elsevier.com/retrieve/pii/S1874778715000033, doi:10.1016/j.margen.2015.01.002.

Podrabsky, J.E., Somero, G.N., 2004. Changes in gene expression associated with acclimation to constant temperatures and fluctuating daily temperatures in an annual killifish *Austrofundulus limnaeus*. Reactions 207, 2237–2254. doi:10.1242/jeb.01016.

Pörtner, H.O., Karl, D., Boyd, P., Cheung, W.W., Lluch-Cota, S.E., Nojiri, Y., Schmidt, D., Zavialov, P., 2014. Ocean systems, in: Field, C., Barros, V., Dokken, D., Mach, K., Mastrandrea, M., Bilir, T., Chatterjee, M., Ebi, K., Estrada, Y., Genova, R., Girma, B., Kissel, E., Levy, A., MacCracken, S., Mastrandrea, P., White, L. (Eds.), Climate change 2014: impacts, adaptation, and vulnerability. Part A: global and sectoral aspects. Contribution of working group II to the Fifth assessment report of the intergovernmental panel on climate change. Cambridge University Press, Cambridge and New York, NY, pp. 411 – 484.

Qu, T., Zhang, L., Wang, W., Huang, B., Li, Y., Zhu, Q., Li, L., Zhang, G., 2015. Characterization of an inhibitor of apoptosis protein in *Crassostrea gigas* clarifies its role in apoptosis and immune defense. Developmental & Comparative Immunology 51, 74–78. URL: http://linkinghub.elsevier.com/retrieve/pii/S0145305X15000348, doi:10.1016/j.dci.2015.02.011.

Rathburn, C.K., Sharp, N.J., Ryan, J.C., Neely, M.G., Cook, M., Chapman, R.W., Burnett, L.E., Burnett, K.G., 2013. Transcriptomic responses of juvenile Pacific whiteleg shrimp, *Litopenaeus vannamei*, to hypoxia and hypercapnic hypoxia. Physiological genomics 45, 794–807. URL: http://physiolgenomics.physiology.org/content/45/17/

794.long, doi:10.1152/physiolgenomics.00043.2013.

Robinson, M.D., McCarthy, D.J., Smyth, G.K., 2009. edgeR: A Bioconductor package for differential expression analysis of digital gene expression data. Bioinformatics 26, 139–140. doi:10.1093/bioinformatics/btp616.

Semenza, G.L., 2001. HIF-1, O_2, and the 3 PHDs: How animal cells signal hypoxia to the nucleus. Cell 107, 1–3. doi:10.1016/S0092-8674(01)00518-9.

Shiel, B.P., Hall, N.E., Cooke, I.R., Robinson, N.A., Strugnell, J.M., 2015. De Novo Characterisation of the Greenlip Abalone Transcriptome (Haliotis laevigata) with a Focus on the Heat Shock Protein 70 (HSP70) Family. Marine Biotechnology 17, 23–32. URL: http://link.springer.com/10.1007/s10126-014-9591-y, doi:10.1007/s10126-014-9591-y.

Shiel, B.P., Hall, N.E., Cooke, I.R., Robinson, N.A., Strugnell, J.M., 2017. Epipodial tentacle gene expression and predetermined resilience to summer mortality in the commercially important greenlip abalone, *Haliotis laevigata*. Marine Biotechnology , 191–205URL: http://link.springer.com/10.1007/s10126-017-9742-z, doi:10.1007/s10126-017-9742-z.

Somero, G.N., Beers, J.M., Chan, F., Hill, T.M., Klinger, T., Litvin, S.Y., 2016. What changes in the carbonate system, oxygen, and temperature portend for the Northeastern Pacific Ocean: A Physiological Perspective. BioScience 66, 14–26. URL: https://academic.oup.com/bioscience/article-lookup/doi/10.1093/biosci/biv162, doi:10.1093/biosci/biv162.

Sussarellu, R., Fabioux, C., Camacho Sanchez, M., Le Goïc, N., Lambert, C., Soudant, P., Moraga, D., 2012. Molecular and cellular response to short-term oxygen variations in the Pacific oyster *Crassostrea gigas*. Journal of Experimental Marine Biology and Ecology 412, 87–95. doi:10.1016/j.jembe.2011.11.007.

Todgham, A.E., Hofmann, G.E., 2009. Transcriptomic response of sea urchin larvae *Strongylocentrotus purpuratus* to CO2-driven seawater acidification. The Journal of experimental biology 212, 2579–94. URL: http://www.ncbi.nlm.nih.gov/pubmed/19648403, doi:10.1242/jeb.032540.

Tomanek, L., Zuzow, M.J., 2010. The proteomic response of the mussel congeners *Mytilus galloprovincialis* and *M. trossulus* to acute heat stress: implications for thermal tolerance limits and metabolic costs of thermal stress. Journal of Experimental Biology 213, 3559–3574. URL: http://www.ncbi.nlm.nih.gov/pubmed/20889836http://jeb.biologists.org/cgi/doi/10.1242/jeb.041228, doi:10.1242/jeb.041228.

Tripp-Valdez, M.A., Bock, C., Lannig, G., Koschnick, N., Pörtner, H.O., Lucassen, M., 2019. Assessment of muscular energy metabolism and heat shock response of the green abalone Haliotis fulgens (Gastropoda: Philipi) at extreme temperatures combined with acute hypoxia and hypercapnia. Comparative Biochemistry and Physiology Part B: Biochemistry and Molecular Biology 227, 1–11. URL: https://linkinghub.elsevier.com/retrieve/pii/S1096495918301118, doi:10.1016/j.cbpb.2018.08.009.

Tripp-Valdez, M.A., Bock, C., Lucassen, M., Lluch-Cota, S.E., Sicard, M.T., Lannig, G., Pörtner, H.O., 2017. Metabolic response and thermal tolerance of green abalone juveniles (*Haliotis fulgens*: Gastropoda) under acute hypoxia and hypercapnia. Journal of Experimental Marine Biology and Ecology 497, 11–18. URL: http://www.sciencedirect.com/science/article/pii/S0022098116303744, doi:10.1016/j.jembe.2017.09.002.

Valenzuela-Miranda, D., Del Río-Portilla, M.A., Gallardo-Escárate, C., 2015. Characterization of the growth-related transcriptome in California red abalone *Haliotis rufescens* through RNA-Seq analysis. Marine Genomics 24, 199–202. URL: http://linkinghub.elsevier.com/retrieve/pii/S1874778715000860, doi:10.1016/j.margen.2015.05.009.

Valenzuela-Muñoz, V., Bueno-Ibarra, M.A., Escárate, C.G., 2012. Characterization of the transcriptomes of *Haliotis rufescens* reproductive tissues. Aquaculture Research , 1–15doi:10.1111/are.12044.

Vandesompele, J., De Preter, K., Pattyn, F., Poppe, B., Van Roy, N., De Paepe, A., Speleman, F., 2002. Accurate normalization of real-time quantitative RT-PCR data by geometric averaging of multiple internal control genes. Genome Biology 3. URL: http://www.ncbi.nlm.nih.gov/pubmed/12184808{%}5Cnhttp://www.pubmedcentral.nih.gov/articlerender.fcgi?artid=PMC126239http://genomebiology.biomedcentral.com/articles/10.1186/gb-2002-3-7-research0034, doi:10.1186/gb-2002-3-7-research0034, arXiv:1465-6906.

Venter, L., Loots, D.T., Vosloo, A., Jansen van Rensburg, P., Lindeque, J.Z., 2016. Abalone growth and associated aspects: Now from a metabolic perspective. Reviews in Aquaculture , 1–23doi:10.1111/raq.12181.

Vosloo, D., Vosloo, A., Morillion, E.J., Samuels, J.N., Sommer, P., 2013. Metabolic readjustment in juvenile South African abalone *H*aliotis midae acclimated to combinations of temperature and dissolved oxygen levels. Journal of Thermal Biology 38, 458–466. doi:10.1016/j.jtherbio.2013.07.001.

Young, M.D., Wakefield, M.J., Smyth, G.K., Oshlack, A., 2010. Gene ontology analysis for RNA-seq: accounting for selection bias. Genome Biology 11. doi:10.1186/gb-2010-11-2-r14.

Supplementary material 1: gene expression pattern identified by qPCR. in gill and muscle during warming under normoxic normocapnia (control), hypoxic normocapnia (hypoxia), normoxic hypercapnia (hypercapnia) and hypoxic hypercapnia (combined) treatments. * indicates significant differences in gill (above error bars) and muscle (below error bars) with initial temperature (18 ºC) from same experiments (multiple test). # denotes significant differences from values at the same temperature in the warming only protocol (multiple test). n = 4 – 6 (n= 2 in muscle/Control/30°C). Values are posterior means ± 95% credible intervals.

Antioxidant:

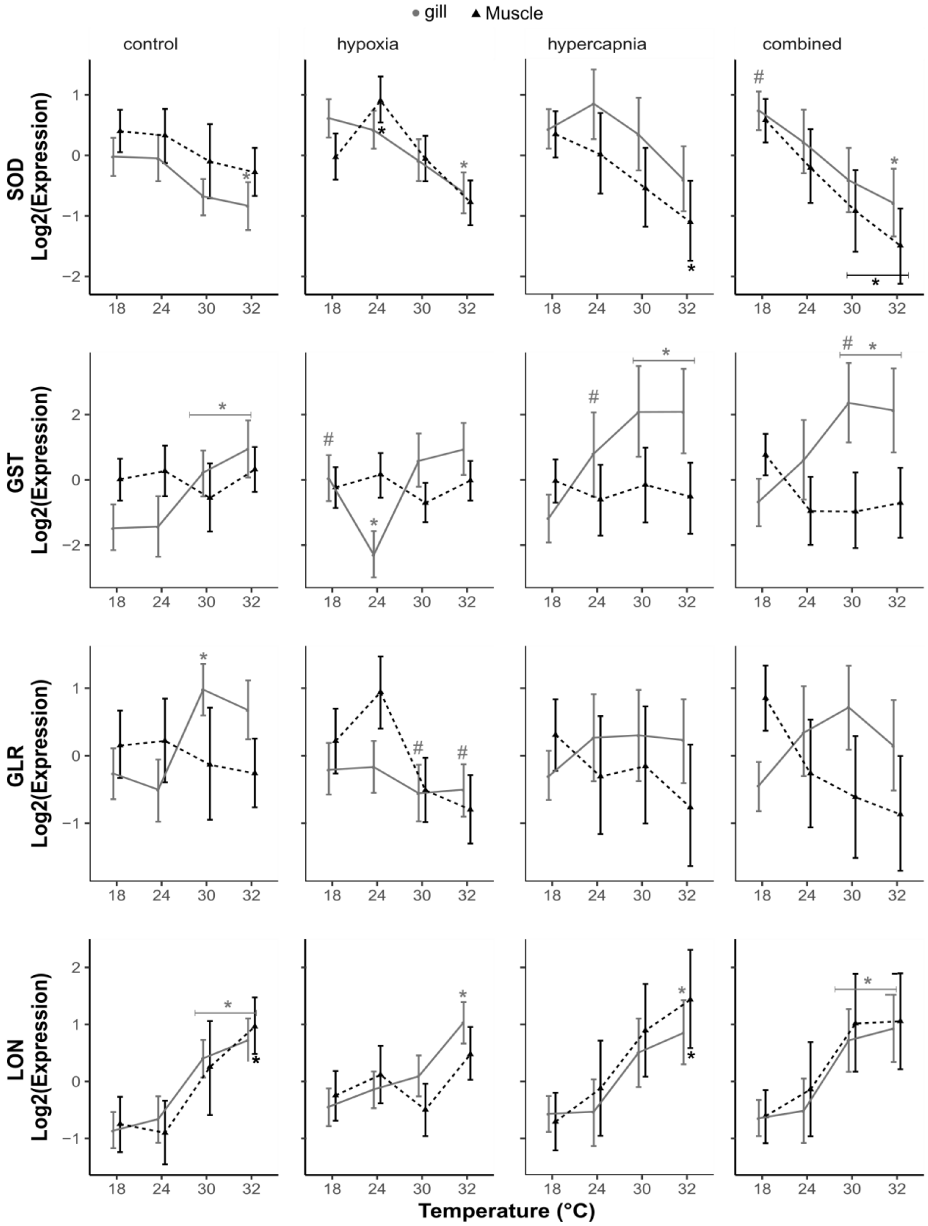

Energy metabolism

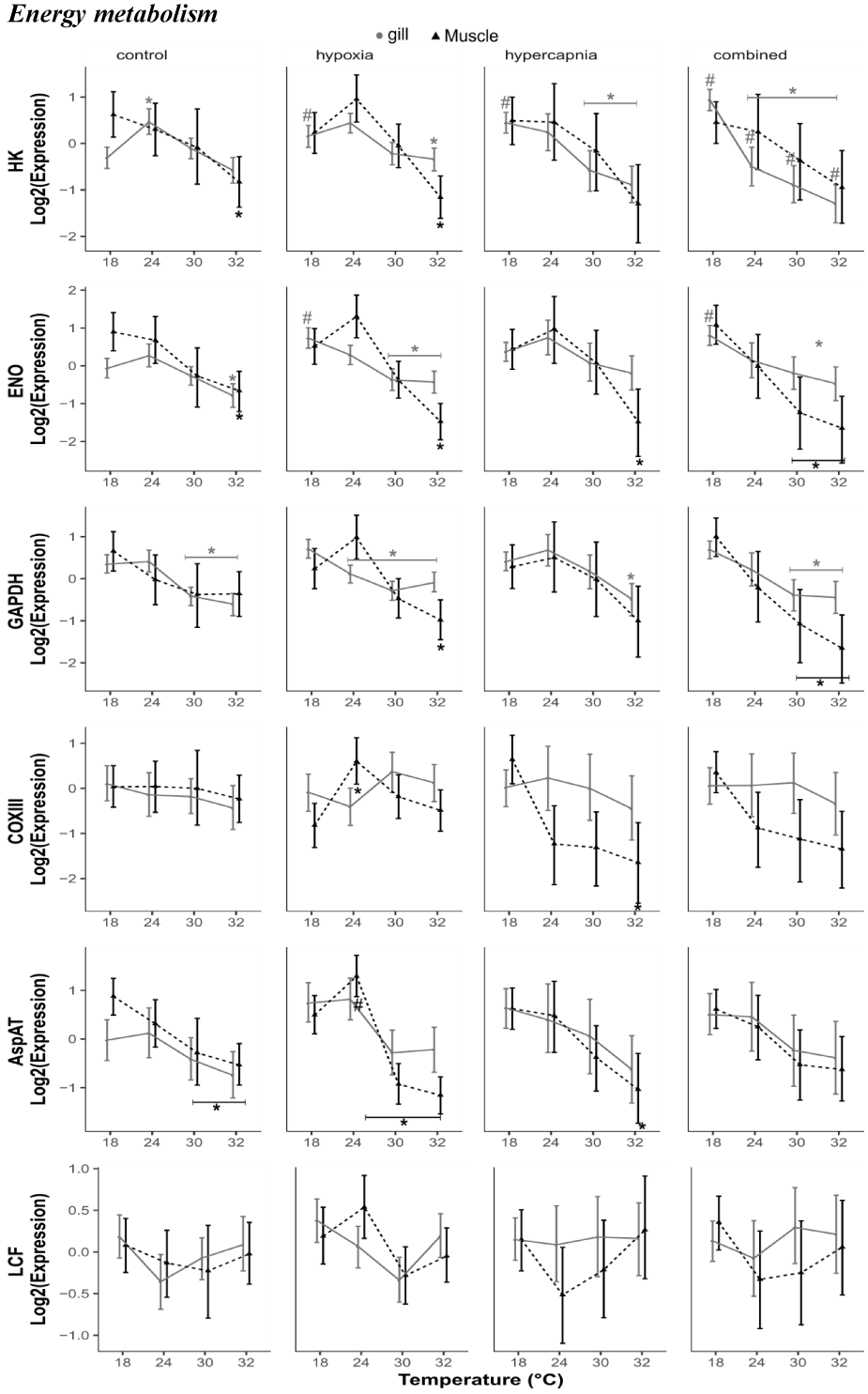

Molecular chaperones

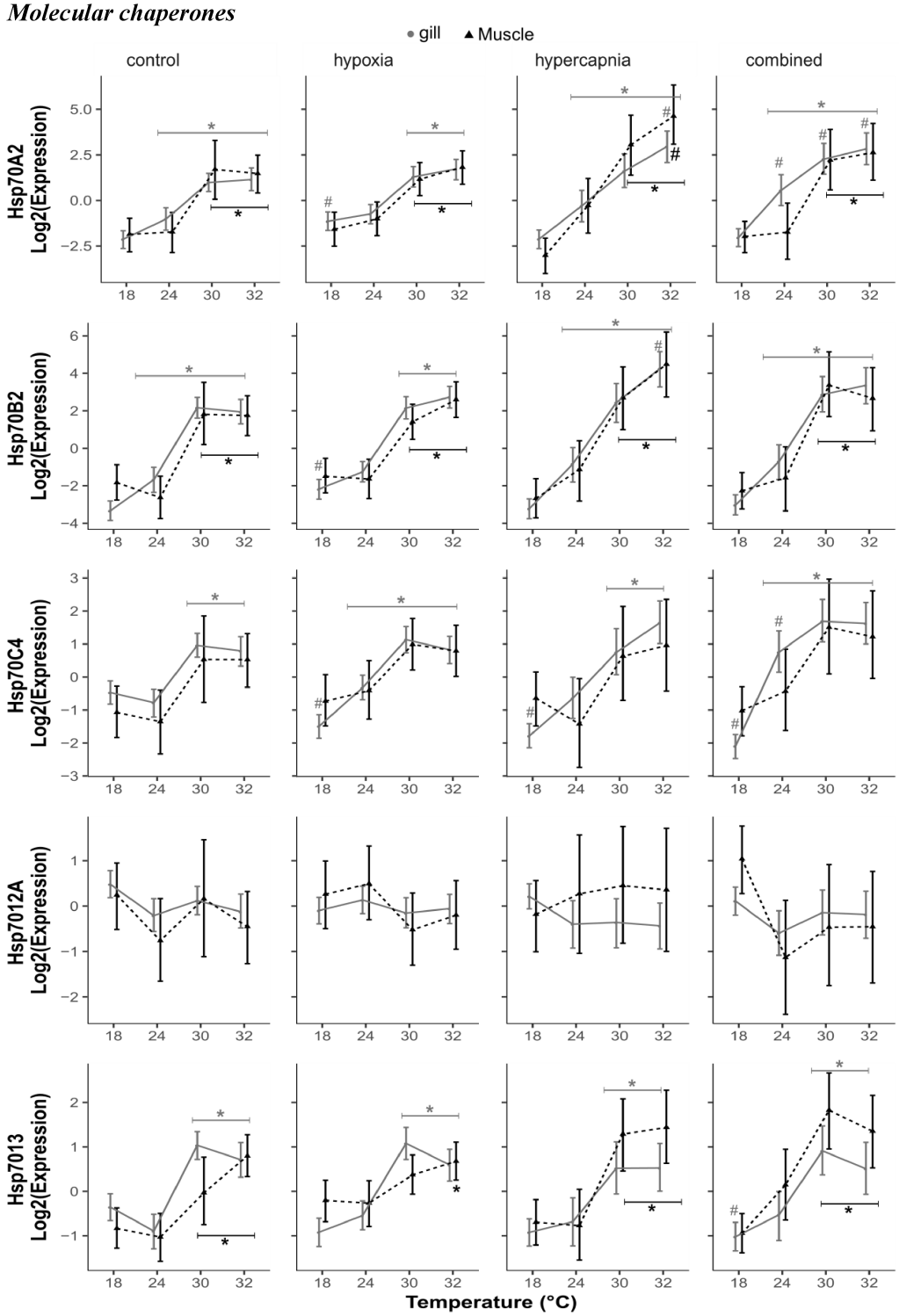

CHAPTER 4

DISCUSSION

The present thesis aimed to investigate whether exposure to reduced oxygen availability and high PCO_2 induce negative effects on the *H. fulgens* metabolic condition leading to a downward shift of the upper thermal limits. The studies demonstrate that acute hypoxia and hypercapnia, as single stressors and in combination, modify the thermal sensitivity in juveniles of green abalone with impacts at systemic, cellular, and molecular levels. Therefore, this thesis highlights the importance of addressing the impacts of multiple drivers simultaneously when investigating the sensitivity of marine organisms to climate change.

The integration of different levels of biological organization constitutes a key element in this thesis: impacts in MO_2 described in Publication I already indicate impacts on the whole-organism aerobic capacity due to the different experimental conditions. However, the NMR-based metabolic profiles of gill, hepatopancreas, and muscle (Publications I and II) together with the gene expression networks for gill and muscle (Publication III) also indicate that metabolic impacts were not only driver-dependent (hypoxia, hypercapnia, and both factors combined) but also tissue-dependent. This is of high relevance when addressing the impacts of environmental insults using molecular or biochemical indicators (e.g. heat shock proteins or antioxidant response).

The impacts of hypoxia and hypercapnia in the *H. fulgens* metabolic response is described through the three manuscripts derived from the thesis. In this chapter, I will deepen the discussion from an integrative perspective and I will address additional results which deserve further analysis, such as i) why hypoxia and hypercapnia, as individual stressors and in combination, did not induce metabolic impacts in the abalone at unchanged temperature? ii) which is the role of cardiac capacity in setting the *H. fulgens* thermal limitation; iii) how is the interplay of the metabolic conditions from the analyzed tissues during warming with and without additional drivers, iv) which mechanisms were involved in setting the metabolically depressed condition in abalone exposed to combined warming, hypoxia and hypercapnia, and finally v) which is the ecological relevance of the findings from this thesis?

4.1 The metabolic rate at an unchanged temperature

The OCLTT concept places the first line of thermal limitations at the whole-organism level and it becomes effective by limited capacities of oxygen supply mechanisms (e.g. cardiovascular systems) to meet the temperature-induced cellular oxygen demand. Therefore, assessment of the metabolic activity by means of oxygen consumption (MO_2) constitutes a sensitive indicator of restricted whole-organism aerobic metabolism during environmental warming and during the interaction between warming and additional drivers such as hypoxia and hypercapnia/low pH (Le Moullac et al., 2007b; Walther et al., 2009; Lannig et al., 2010; Schiffer et al., 2012; Zittier et al., 2015).

Abalone species are considered to be oxyregulators and a positive correlation between MO_2 and environmental temperature has been described in many species, including *H. fulgens* (García-Esquivel et al., 2007). In Publication I, changes in the temperature-dependent exponential increase of MO_2 during the warming protocol under hypoxia, hypercapnia and both factors combined (Publication I: Figure 1) evidenced an impacted aerobic metabolism in *H. fulgens* juveniles.

However, an additional finding from the *H. fulgens* MO_2 recordings in this work is the unchanged MO_2 in organisms from the control tanks from each experiment, which deserves a deeper analysis (Publication I: Figure 1). As described in section 2.2, each experiment was accompanied by a control group which was exposed to the same conditions of seawater oxygen and PCO_2 (hypoxia, hypercapnia, and combined hypoxia and hypercapnia) as the experimental tank but at constant temperature (Fig. 2.2). At such conditions, *H. fulgens* MO_2 remained unchanged during the experiment suggesting no effect of hypoxia and hypercapnia, as single stressors and in combination, when thermal stress is not present.

As stated above, abalone species maintain oxygen consumption over a range of environmental oxygen levels, but when oxygen availability is below the minimum to cover oxygen demand, the organisms become conformers and anaerobic metabolism is required to sustain ATP dependent processes (de Zwaan and Wijsman, 1976; Pörtner, 2010). In *H. midae* juveniles, long-term exposure (one month) to moderate hypoxia (~83% air saturation) did not induce changes in MO_2 (Vosloo et al., 2013a). Similarly, adult *H. laevigata* displayed unaffected MO_2 when they were exposed for 57 days to moderate hypoxia (above 81% air saturation). However, a reduction in MO_2 by 50% was observed after exposure to lower oxygen levels (68% air saturation) which was accompanied by a reduction in somatic growth rates (Harris, 1999). In *H. fulgens*, little information is available regarding their critical oxygen thresholds. An unpublished work made at CIBNOR found that juveniles of *H. fulgens* from Bahia Tortugas acclimated at 17 °C showed a decline of 40% in MO_2 when they were exposed to severe

hypoxia (1 mgO_2 L^{-1}; ~10% air saturation) but MO_2 returned to control levels after 30 hours [1]. These findings indicate that oxygen levels of 50% air saturation used in the present thesis are still well above the critical threshold where *H. fulgens* can no longer regulate its oxygen consumption. The mechanisms used by *H. fulgens* to maintain oxygen uptake might be similar to those described for *H. iris*, including an increase in branchial blood flow, enhanced water flow over the shell and endogenous ventilation by cilia of the gill lamellae (Ragg and Taylor, 2006).

The effects of hypercapnia/low pH on marine organisms have been the focus of attention in recent years. An assessment of high CO_2 tolerance across multiple taxa led to the conclusion that acid-base regulatory capacity is a crucial factor explaining sensitivity to hypercapnic exposure. Notably, taxa with high metabolic rates and high levels of mobility or activity seem to have the higher acid-base regulatory capacity and, therefore, more tolerance to hypercapnia (Melzner et al., 2009). Accordingly, the inability to compensate acidotic shifts in extracellular pH (pH_e) during hypercapnic exposure has been demonstrated to induce metabolic depression (Pörtner et al., 1998).

As abalones are benthic organisms with low metabolic rate, they are likely to be more susceptible to hypercapnia given a less developed ion-exchange mechanism (Michaelidis et al., 2005; Melzner et al., 2009; Gazeau et al., 2013). In this thesis, *H. fulgens* exposed to hypercapnic conditions displayed non-significant but slightly lower MO_2 values at the acclimation temperature (18 ºC); however, organisms in the control tank which were exposed to hypercapnia for six days without the thermal challenge did not show any evidence of impacted metabolic activity (Publication I: Figure 1C). This result is similar to observations in marine bivalves, where short-term hypercapnic exposure (days) had no impact on aerobic metabolic rates at acclimation temperature (Lannig et al., 2010; Zittier et al., 2015). Nevertheless, studies on abalone species described reduced fitness, growth and calcification rates after long-term exposure to hypercapnia/low pH (Kim et al., 2013; Cunningham et al., 2016; Li et al., 2018). Moreover, a previous study with *H. iris* found no effect of long-term hypercapnic exposure (100 days at 1,000 µatm PCO_2) in MO_2, but somatic growth and shell length were reduced 2 – 3 fold compared to the control group (Cunningham et al., 2016). The authors from this study concluded that the physiological allocation of resources and metabolic rates were maintained at an expense of reduced calcification and increased shell dissolution. In line with these findings, shell dissolution under hypercapnia (3.82 mm Hg; 5,000 µatm PCO_2) in *Mytilus galloprovincialis* facilitated compensation of temporary acid-base disturbances (Michaelidis et al., 2005). A similar mechanism would allow *H. fulgens* to tolerate the short-

[1] Calderón-Liévanos, S. 2015. Respuestas fisiológicas del abulón azul (*Haliotis fulgens*) por efecto combinado de hipoxia y estrés térmico. Centro de Investigaciones Biológicas del Noroeste. México. Corresponding: scalderon@cibnor.mx

term (six days) hypercapnic exposure in this study without inducing metabolic depression. Further investigations are needed to elucidate whether long-term exposure of *H. fulgens* to hypercapnic conditions induce shell dissolution or reduced growth rates to compensate acid-base disturbances.

Given that an organism responds to strong hypoxia and high PCO_2 by metabolic down-regulation, hypoxia combined with hypercapnia should emphasize metabolic depression (Pörtner et al., 2005). Such additive effects were observed in several marine invertebrate species from the upwelling ecosystems of the Chilean coast in which exposure to hypoxia (2 mgO_2 L^{-1}) and high CO_2 (~1,000 µatm PCO_2) induced lower metabolic rates than the exposure to single drivers (Steckbauer et al., 2015). In marine bivalves, additive and synergistic negative effects of simultaneous presence of hypoxia and hypercapnia/low pH has been observed, with reduced growth rates and higher mortality rates than under hypoxia and hypercapnia as single stressors (Gobler et al., 2014; Clark and Gobler, 2016), possibly reflecting an overlap of the physiological mechanisms impacted by both drivers.

Nevertheless, and in line with the results from hypoxia and hypercapnia as single stressors, *H. fulgens* exposed to combined hypoxia and hypercapnia at an unchanged temperature maintained their MO_2 stable through the six days course of the experiment (Publication I: Figure 1D). This finding implies that at the acclimation temperature, the interaction between both drivers did not have an immediate impact on aerobic metabolism and likely in the mechanisms contributing to metabolic depression such as a reduction in pH_e (Pörtner et al., 1998; Cheng et al., 2004; Storey and Storey, 2004). However, it is important to mention that tissue metabolic profiles from these specimes exposed to hypoxia and hypercapnia at stable temperature were not analyzed due to time and biological material limitations. Therefore, it is not possible to exclude negative impacts on the cellular metabolic state which elicited the observed constraints in MO_2 even at moderate temperature in organism exposed to the warming protocol (Publication I: Fig. 1D).

4.2 The cardiac response of *H. fulgens* during thermal stress

According to the OCLTT concept, the heart and ventilation rates and outputs in relation to oxygen demand define the temperature range of aerobic performance. Consequently, a warming-induced rise in oxygen demand is initially met by enhanced ventilation and heart rate (Frederich and Pörtner, 2000; Walther et al., 2009). Previous investigations in abalone demonstrated that HR and stroke volume increased in parallel to MO_2, with little effect from moderate hypoxia (70% air saturation; Alter et al. 2017) whereas cardiac performance can be negatively impacted by additional drivers, such as hypercapnia in crustaceans (Walther et al., 2009). In this thesis,

measurements of heart rate were performed in juveniles of *H. fulgens* to evaluate the potential impacts of the experimental conditions on the cardiac performance. The protocol, however, was unsuccessful and reliable measurements were obtained from a very limited number of individuals only and not included in the publications.

Figure 4.1 shows the hourly average of HR (in beats per minutes; BPM) from four animals. At a stable temperature in the control experiment (normoxic normocapnia; purple dots), HR displays a slightly decreasing trend with time. With warming, however, HR increased immediately after each temperature increment (dashed lines) and, while initial values seem to be lower in the organism from hypercapnia experiment (normoxic hypercapnia; black dots), it follows similar patterns as for the two abalone from the combined experiment (hypoxic hypercapnia; red and blue dots). It is worth to notice that organisms from the combined experiment (red and blue dots) show high fluctuation in HR above 27 °C. It is not clear why organisms from these trials died immediately after the last warming step while the rest of the organism from the experiments (in the respiration chambers and in the external tank) were able to persist longer (see Publication I for details). Possibly, the attached sensor on the shells represented an additional cost to the organisms or prevented them to increase water flow to the gills.

While the limited results from this analysis do not allow to get any robust conclusion, the higher variation in BPM in both specimens from the combined experiment above 27 °C compared to the specimen from the hypercapnic experiment may represent cardiac arrhythmia, resulting in lower capacities for oxygen delivery to the tissues, in line with the OCLTT concept. More replicates are needed to corroborate these findings and relate a lower cardiac capacity during thermal stress under combined hypoxia and hypercapnia with the onset of metabolic depression to persist in such conditions.

4.3 The cellular metabolic response

4.3.1 Interplay of tissues

Abalone are well known for their high anaerobic potential which allows them to survive relatively long periods (hours) in anoxia (Bowen, 1984; Omolo et al., 2003). The accumulation of anaerobic end products (e.g. lactate, succinate, alanine) in gill and hepatopancreas confirmed the warming-induced tissue hypoxemia and stimulation of anaerobiosis when aerobic metabolism was constrained (discussed in Publication I). However, further investigation in muscle metabolic condition (Publication II) and gene expression patterns in gill and muscle (Publication III) indicate tissue-specific thermal sensitivities and biochemical responses.

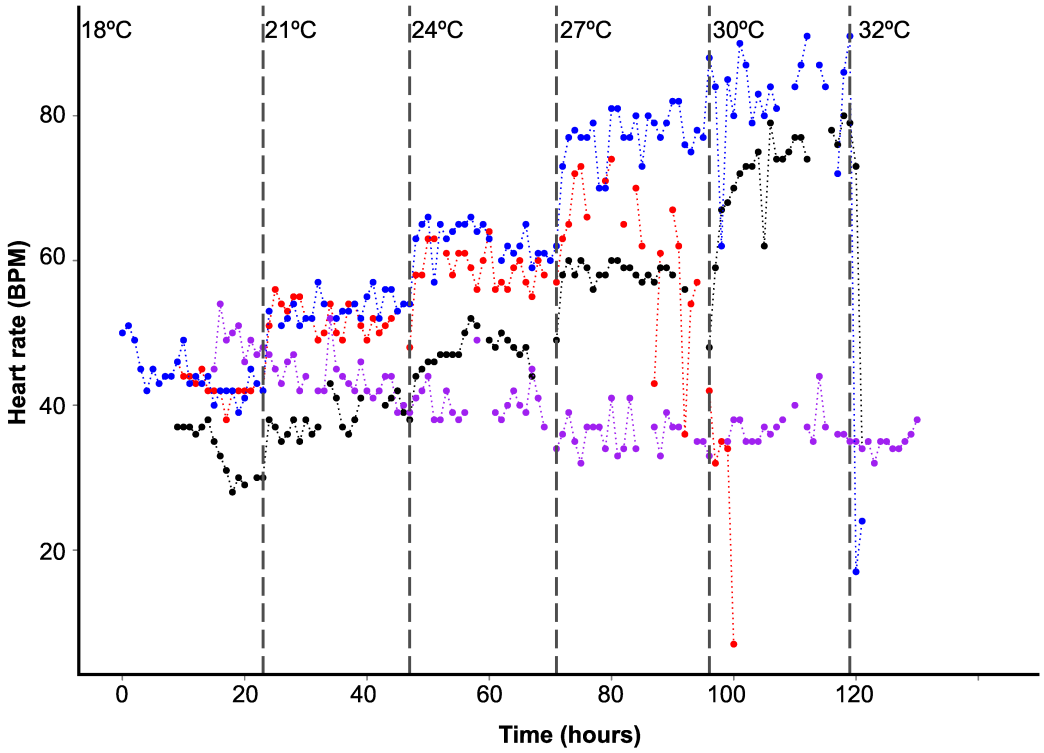

Figure 4.1 Hourly average of heart rate in beats per minute from *H. fulgens* under the experimental conditions. The dashed vertical lines indicates the increments of temperature. Purple: animal at unchanged temperature (18 °C) under normoxic normocapnia; black: animal at increasing temperature under normoxic hypercapnia; red and blue: animals at increasing temperature under hypoxic hypercapnia.

As discussed in Publications II and III, the responses by the analyzed tissues indicate different thermal sensitivities, where muscle seems to be more tolerant to the experimental conditions and retains aerobic potential over the entire thermal challenge. A delayed response and lower thermal sensitivity in muscle has been already described in marine mollusks (Anestis et al., 2010; Lu et al., 2016), but it is worth mentioning that in both cases, the response of muscle was delayed but it was similar to other tissues (gill or mantle), while in *H. fulgens* in this study muscular response follows a different pattern as gill and hepatopancreas.

A recent study on the metabolic response from different tissues in *H. midae* during functional and environmental hypoxia (Venter et al., 2018a,b) constitutes a good reference to compare the tissue-specific responses to this study: Under functional and environmental hypoxia, all investigated tissues in *H. midae* (including gill, adductor muscle, and foot muscle) displayed the activation of the glucose/aspartate – succinate pathway to sustain NAD^+ levels, and also displayed accumulation of lactate and tauropine (Venter et al., 2018a,b). In both cases, the authors concluded that shuttling of compounds between the different tissues played an important

role in setting the observed metabolic profiles, where compounds from hypoxic tissues are moved to regions that have access to oxygen. In the present study with *H. fulgens*, transport of compounds from muscle to gill, where they could be metabolized or release outside the body is unlikely as metabolic profiles of gill and muscle do not conform to a shuttling pattern (Venter et al., 2018a). The hepatopancreas, on the contrary, showed a constant accumulation of most analyzed metabolic products which became evident during warming under combined hypoxia and hypercapnia (Publication I: Figure 4). The hepatopancreas accumulated significantly metabolites after a decline of several metabolites in both gill and muscle, which may indicate a shuttling of metabolites to this tissue.

The metabolite pettern in gill from thermally challenged *H. fulgens* conform a systemic-hypoxemia response with an onset of anaerobiosis when mitochondrial respiration becomes inadequate. On the contrary, the oxygen storage capacity in abalone musculature (Wells et al., 1998), in addition with the higher capacity of muscle for ATP synthesis via phosphoarginine (Morash and Alter, 2015) and the reduction of the glycolytic flux which is observed in abalone under thermal and hypoxic stress (Omolo et al., 2003; Vosloo et al., 2013b) might have allowed this tissue to retain the aerobic mode for energy production during the warming protocol under all experimental conditions.

4.3.2 Metabolomic and gene expression patterns

While gill and muscle displayed different metabolic states, the integration of transcriptomic information (e.g. gene expression) made it possible to elucidate the metabolic thermal reaction norm of *H. fulgens* (Fig. 4.2 and Fig. 4.3). Both tissues followed a very similar trend: declining levels of genes involved in carbohydrate metabolism, including pyruvate kinase (*PK*), hexokinase (*HK*), glyceraldehyde-3-phosphate dehydrogenase (*GAPDH*), and enolase (*ENO*) reflect thermal compensation of enzyme activity, as higher capacities in the warmth due to the Q_{10} effect might allow for a reduced gene expression and/or protein concentration (Schiffer et al., 2014). Instead, phosphoenolpyruvate carboxykinase (*PEPCK*) increased in gill (Fig. 4.2) and remained unchanged in muscle (Fig. 4.3) which indicates an essential role of *PEPCK* as compensation mechanism during thermal stress and the observed pattern of *PEPCK* mRNA may correspond to transcriptional adjustments to favor the synthesis of the anaerobic end product succinate.

A similar transcriptomic study, which can be used as a reference, was made for the intertidal limpet *Cellana toreuma* exposed to an acute warming protocol (0.1 °C min^{-1}). In this species, mRNA levels of alanopine dehydrogenase and *PEPCK* increased with temperature, but other glycolytic genes such as *HK*, *GAPDH*, and *ENO* behave similar (Han et al., 2017). The up-regulation of glycolytic genes conforms to a Pasteur effect (i.e. an increase in glycolytic flux

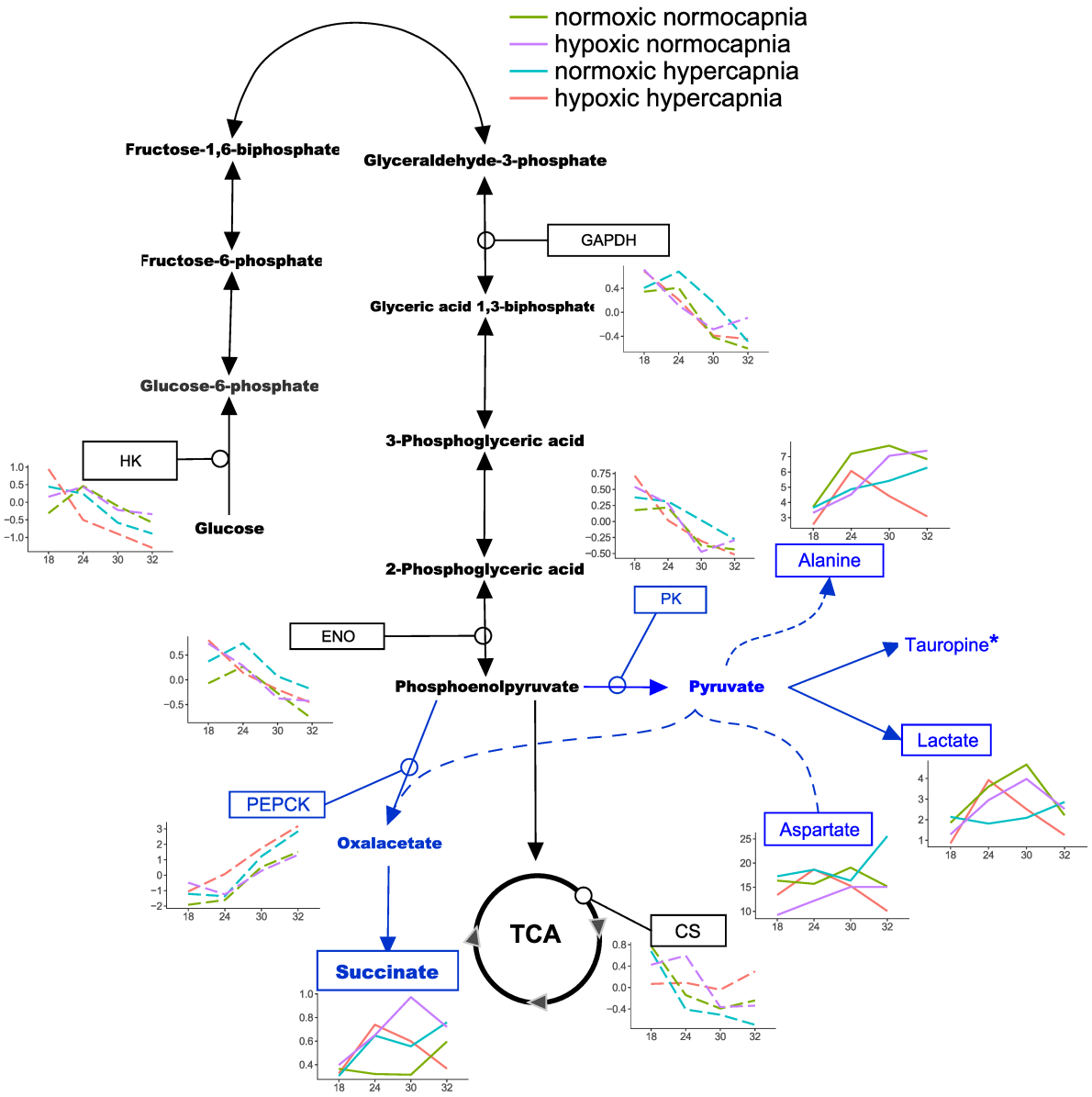

Figure 4.2 Warming-induced patterns of metabolite concentrations (solid lines) and gene expression (dashed lines) of key metabolites and genes (names in boxes) involved in glycolytic pathways in abalone gill samples. * Not detected in this tissue. Data derived from Publications I, II, and III.

driven by temperature (Brooks and Storey, 1997). In *H. fulgens*, gene expression data suggest that temperature does not induce a strong Pasteur effect as seen in the limpet. This is further confirmed by the cellular metabolic state in muscle: although muscle poses high anaerobic enzyme capacities (LDH and TDH), the lack of accumulation of end products indicate little flux through these anaerobic pathways (Publication II).

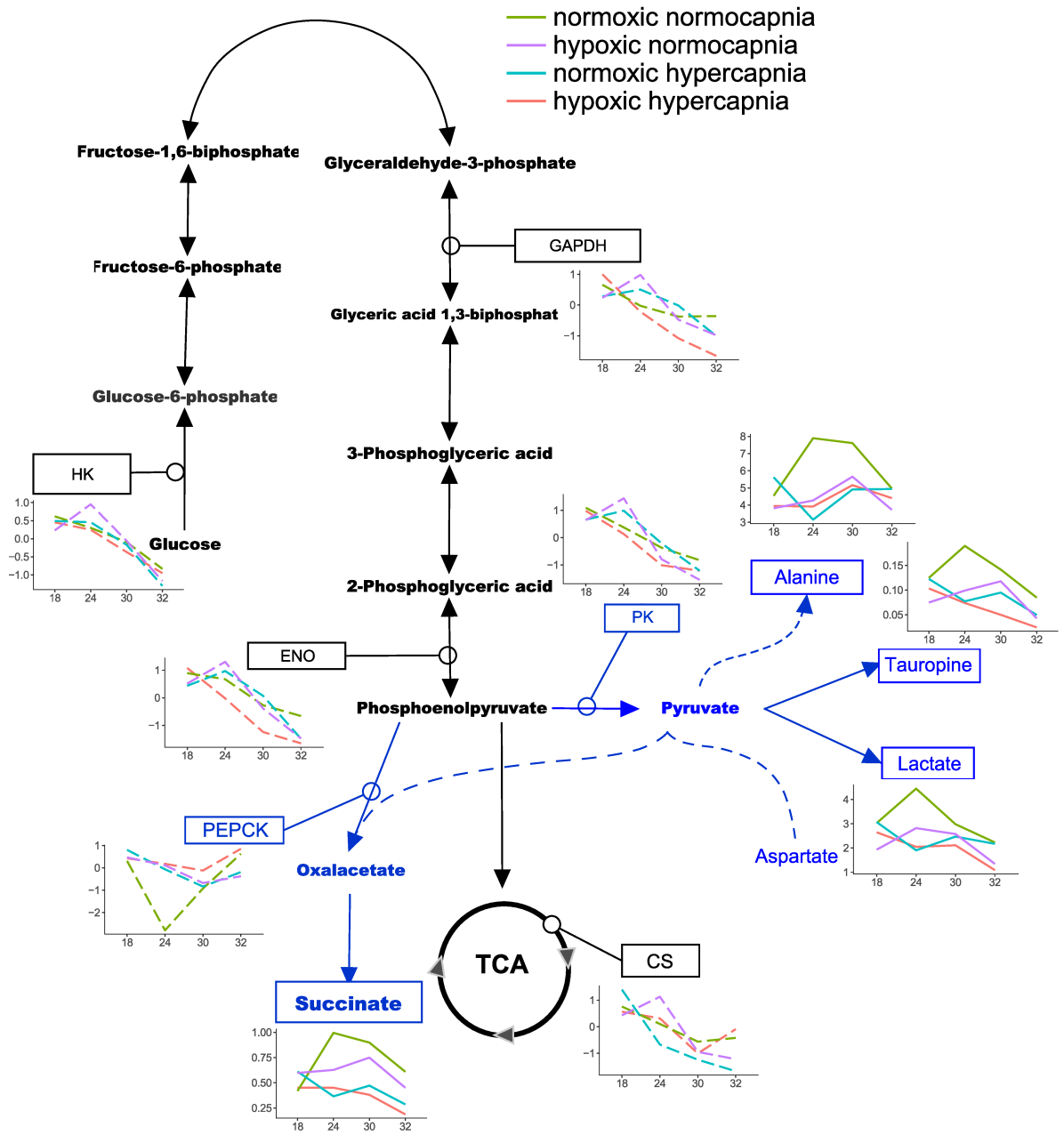

Figure 4.3 Warming-induced patterns of metabolite concentrations (solid lines) and gene expression (dashed lines) of key metabolites and genes (names in boxes) involved in glycolytic pathways in abalone muscle samples. Data derived from Publications I, II, and III.

4.3.3 Mitochondrial capacity and valine metabolism

Adjustments in mitochondrial function and capacity are usually investigated by CS and COX enzyme capacities and mRNA levels (Lucassen, 2006; Eckerle et al., 2008; Windisch et al., 2011; Vosloo et al., 2013b; Schiffer et al., 2014). As discussed in Publications II and III, one

of the key findings was the regulation of mitochondrial capacity as indicated by CS enzyme activity in muscle and mRNA levels in gill and muscle.

It has been suggested that mitochondrial metabolism in abalone species is low compared to more active mollusk species, and they most likely have a low number of mitochondria per cell (Venter et al., 2016). However, previous investigations have demonstrated a high capacity to retain mitochondrial function and structure along a wide range of temperature, especially as *H. fulgens* can be found in the intertidal (Dahlhoff and Somero, 1993). This can be confirmed from the cellular metabolic state of the investigated tissues in this study: the transient accumulation of anaerobic metabolites in gills was likely the result of an overshoot of energy demand during warming, which had to be compensated by alternative means of energy production or by physiological adjustments to increase oxygen uptake (*e.g.* increased gill perfusion; Ragg and Taylor 2006); however, *H. fulgens* did not switch towards a fully anaerobic ATP production. Accordingly, the animals were able to increase their metabolic rate with warming under most experimental conditions (except at the highest temperature under combined hypoxia and hypercapnia, which will be discussed later). Oysters *Crassostrea gigas* exposed to hypoxic conditions (1.7 mgO_2 L^{-1}; ~20% air saturation) for 6 h, were able to maintain at least 40% of normoxic respiration capacities through involvement of several adjustments of the respiratory chain which can occur very quickly in response to natural oxygen fluctuations (Sussarellu et al., 2013).

While CS enzyme capacities and mRNA showed modulation with warming, *COXIII* mRNA levels remained mostly unchanged with warming under all experimental conditions (Fig. 4.4). COX catalyzes the transfer of electrons from reduced cytochrome c to molecular oxygen as the final step of the respiratory chain and thus plays a key role in forming the electrochemical gradient for ATP production (Li and Deng, 2006). Increased *COX* mRNA levels could indicate compensation for reduced mitochondrial capacities to maintain standard metabolic rate (Vosloo et al., 2013a; Harms et al., 2014). Moreover, increase in CS capacities and constant COX would indicate a relative increase in matrix over membrane functions in mitochondria (Lucassen, 2006). This would imply that mitochondrial adjustments observed in *H. fulgens* (Publication II) are directed towards enhancement of TCA functions in relation to a constant capacity of the respiratory chain. Caution must be taken, however, as transcriptional control of *COX* gene expression does not necessary occur through mitochondrial encoded *COXIII*, but might be regulated by nuclear-encoded subunits or by post-translational control (Lucassen, 2006).

Enhanced capacities of matrix enzymes over membrane enzymes are assumed to support anabolic process. I hypothesize that the observed modulation of CS capacities (Fig. 4.4) is largely driven by a shift in metabolic fuels to sustaining the TCA. Evidence for this can be found in studies with *H. midae*, where increased nitrogen excretion under acute and chronic

warming stress indicates higher rates of protein degradation and use of the released amino acids as an energy source (Vosloo et al., 2013c,a). In times when energy levels are low or when there is a surplus of proteins or amino acids in the system, protein is used as an energy source with the formation of two end products: the carboxy acid and ammonia (Venter et al., 2016).

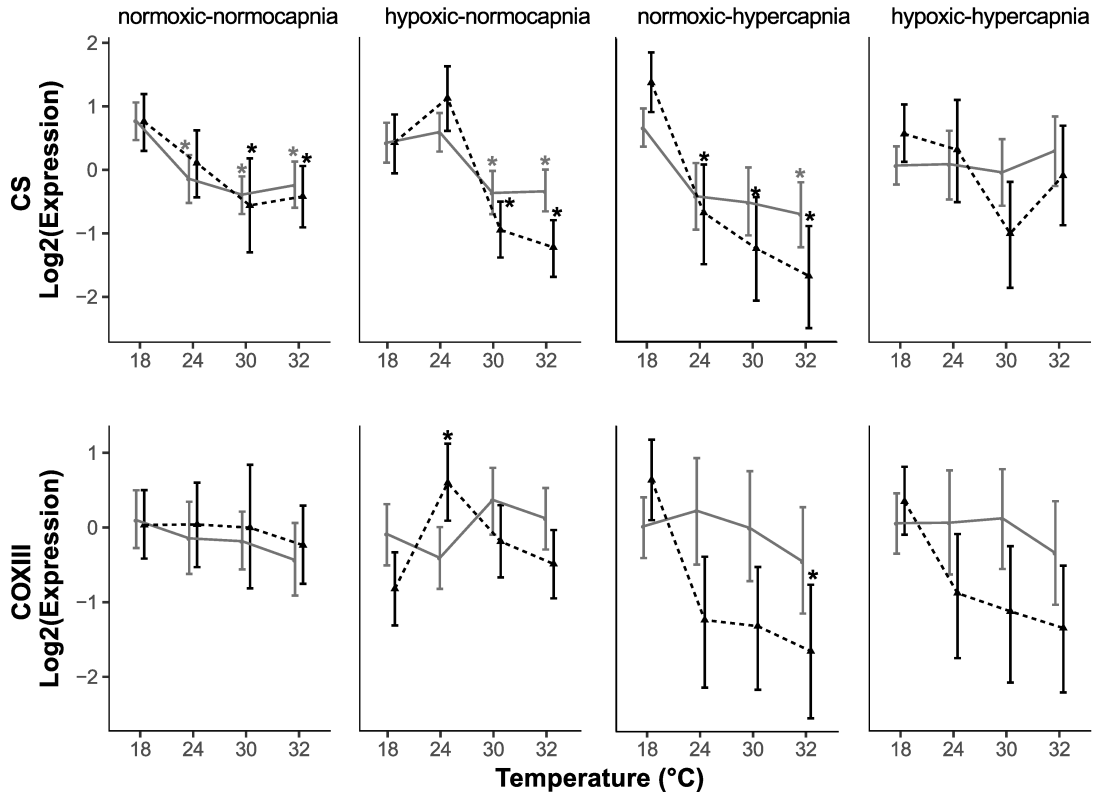

Figure 4.4 Gene expression for citrate synthase (*CS*) and cytochrome c oxidase subunit III(*COXIII*) in *H. fulgens* gill (grey lines) and muscle (black lines) derived from Publication III. The * indicates significant differences with the respective data at initial condition (18 °C).

As ammonia excretion was not measured in this study, the most reliable indicator of increased protein degradation is the accumulation of amino acids displayed by the ^{1}H-NMR metabolic profiles, particularly of valine. Valine is an essential amino acid, but there is evidence that certain organisms can synthesize valine from pyruvate (Rothstein and Tomlinson, 1962). This pathway, however, seems to be absent in mollusks (e.g. Livingstone 1983; Grieshaber et al. 1994). In rat liver, valine can be used as indicator of protein turnover rates, as valine accumulation resulted mostly from endogenous protein degradation (Khairallah and Mortimore, 1976). Moreover, valine accumulation has been related to impacted energy metabolism during

thermal stress in several marine mollusks (Rosenblum et al., 2005; Li et al., 2015; Clark et al., 2017; Lu et al., 2016; Dunphy et al., 2018).

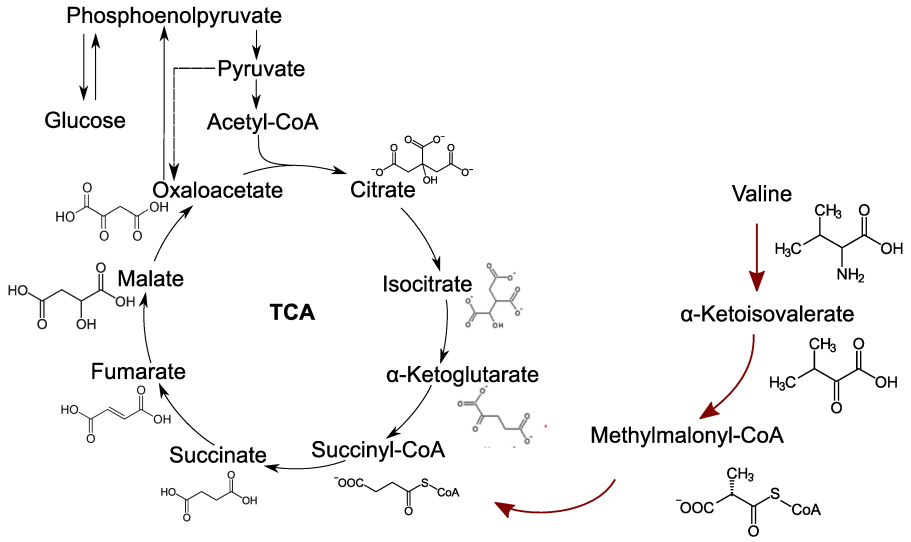

Figure 4.5 Overview of valine catabolism to form succinyl-CoA (after Brosnan and Letto 1991).

Valine can enter directly the TCA through the formation of succinyl-CoA (Fig. 4.5) for terminal oxidation or be converted to glucose via gluconeogenesis, which in vertebrates occur in the liver and kidney (Brosnan and Letto, 1991). From our studies, we cannot conclude whether valine feeds directly into the TCA or is converted to glucose, but the accumulation pattern in gill is wort noting: in this tissue, warming under combined hypoxia and hypercapnia induced valine accumulation at 24 °C and the content remained stable with further warming (Fig. 4.6D), whereas in the other experimental conditions (control, hypoxia, and hypercapnia) valine continued to accumulate (Fig. 4.6). As valine accumulation is related to increased rates of protein degradation (Khairallah and Mortimore, 1976), the constant level of valine in gill may indicate that metabolic depression, induced by the combined stressors conditions, halted the rates of protein breakdown in this tissue keeping valine levels constant.

4.4 Temperature-induced metabolic depression under combined hypoxia and hypercapnia

The simultaneous presence of warming, hypoxia, and hypercapnia led to a strong narrowing of the abalone's thermal window, which cannot be predicted from each factor in isolation: declining MO_2 rates at the highest temperature (Publication I: Figure 1D) was paralleled by declining levels of amino acids, osmolytes, and anaerobic metabolites in gill (Publication I: Figure 3) and muscle (Publication II: Figure 3), and by a lack of potential of muscle glycolytic

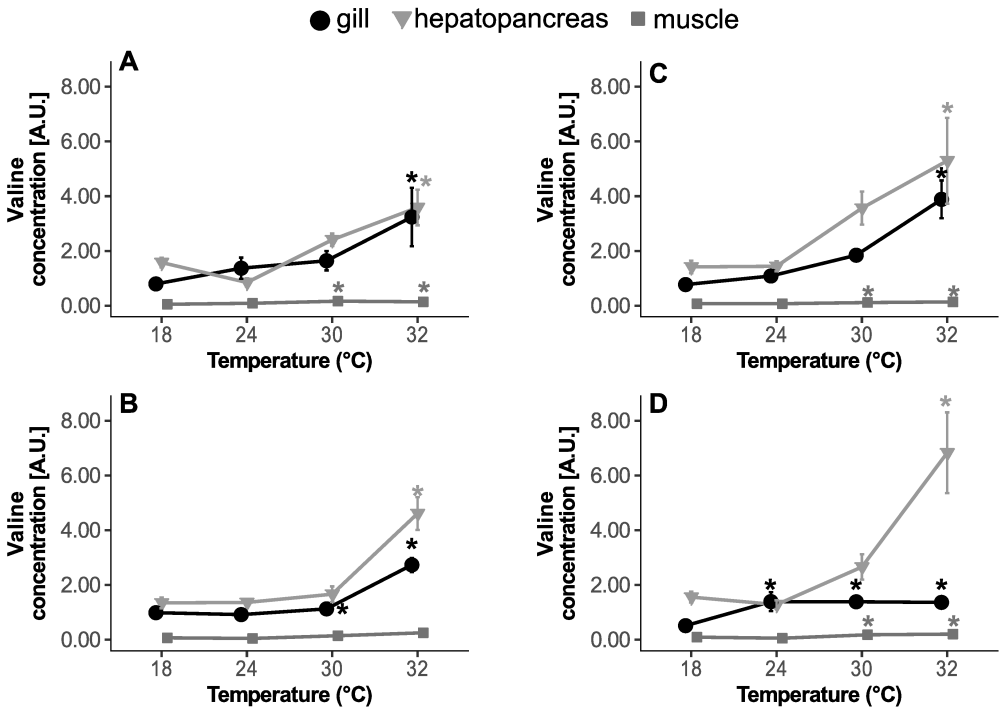

Figure 4.6 Valine accumulation with warming in the *H. fulgens* analyzed tissues under A) normoxic normocapnia, B) hypoxic normocapnia, C) normoxic hypercapnia, and D) hypoxic hypercapnia. The * indicate significant differences with the respective data at initial condition (18 °C). Data derived from Publication I and II

capacity to increase with warming (Publication II: Figure 2). These impacts in the metabolic condition finally led to a downward shift of the maximum thermal limit indicated by the onset of muscular failure (Publication I).

The drop in MO_2 and in most of the analyzed metabolites in gill and muscle (Fig. 4.2 and Fig. 4.3) likely indicates that animals underwent metabolic depression to reduce ATP turnover. This process involves down-regulation of protein synthesis and down-regulation or modification of certain metabolic enzymes to conserve energy. The reduction of mRNA levels and enzyme activities of PK sets the initial step in metabolic reorganization leading to metabolic rate depression (Storey and Storey, 2004; Le Moullac et al., 2007b; Anestis et al., 2008, 2010). Likewise, the repression of genes involved in the TCA and ETS is also an indication of depressed metabolism (van der Meer et al., 2005). Similarly, *PK* mRNA levels in *H. fulgens* gill and muscle displayed a warming-induced down-regulation pattern (Figs 4.2 and 4.3). But as discussed in section 4.3.2 this pattern most likely reflects a basic compensatory adjustment to temperature of regardless of additional drivers, as this pattern was observed under all experimental conditions, including the control experiment where there was no evidence of anaerobiosis or constrained metabolic rate. Moreover, previous investigations with *C. gigas*

exposed to prolonged hypoxia have demonstrated that immediate regulation of PK enzyme ocurred by allosteric effectors such as alanine, and mRNA control was reflected at a later stage (Le Moullac et al., 2007b,a).

Enhanced use of amino acids to fuel TCA would retain the aerobic mode of energy production (Section 4.3.3), but at low levels (Vosloo et al., 2013a). This would explain the limited capacity of MO_2 to increase with warming under combined hypoxia and hypercapnia, which finally failed at 32 °C (Publication I: Figure 2D). As argued in Publication II, the hypometabolic state increased sensitivity of the animals to additional mechanisms, such as impacted neuromuscular functioning or osmotic imbalance, which may have resulted in the observed muscular failure. Temperature is known to induce neural failure (White, 1983; Lutterschmidt and Hutchison, 1997) and a recent study demonstrated that an acute thermal challenge (3 h) induced loss of neural control by reduced GABAergic synapse activity in mussels *Perna canaliculus* (Dunphy et al., 2018). The same mechanisms are affected by increased seawater PCO_2/acidification (Moya et al., 2016), thus, the combination of extreme warming, hypoxia, and hypercapnia may have imposed additional constraints in synapse activity.

As discussed in section 4.1, intra- and extra-cellular pH could play a major role in the development of the hypometabolic state. During warming and during hypoxic stress, accumulation of anaerobic compounds (e.g. lactate) results in tissue acidification which, in turn, have a negative impact on the functioning of cellular enzymes (Storey and Storey, 2004) possibly leading to a decrease of muscular performance and fatigue (Pörtner et al., 1996). In *H. diversicolor*, exposure to hypoxic conditions (2.11 $mgO_2\ L^{-1}$for 96 h) resulted in a reduction of hemolymph pH by 72% of the initial values (Cheng et al., 2004). Blue mussels (*Mytilus edulis*) exposed to a temperature ramp under high PCO_2 (1,120 µatm PCO_2) developed a stronger extracellular acidosis than mussels exposed to only warming stress (Zittier et al., 2015). Although pH_e was not measured in this study, seems likely that the synergistic effect of hypoxia, hypercapnia, and warming induced changes in pH_e beyond the abalone's buffer capacity resulting in a strong cellular acidosis at moderate temperature. This hypothesis could explain the metabolic perturbations observed at 24 °C ingill as a tissue with low buffering capacity (Michaelidis et al., 2005); the observed increase in MO_2 values at 30 °C as an attempt to compensate for the higher energy demands (Schiffer et al., 2012, 2014); and finally the metabolic arrest and muscular failure at the warmest temperature stress (Pörtner et al., 1996). However, the metabolic profiles of muscle did not show any accumulation of anaerobic metabolites (Publication II: Fig. 3). It is known that abalone musculature possesses a good pH buffering capacity, which is related to the high pyruvate reductase activity and its capacity to perform a burst of anaerobic muscle work during locomotion, heavy wave pressure, and escape from predators (Wells and Baldwin,

1995; Wells et al., 1998). Therefore, the tissue-specific acidosis and buffer capacity is an aspect that warrants future investigation.

A final remark on the induction of metabolic depression at moderate temperature under multiple drivers can be derived from the transcriptomic analysis: the up-regulation of genes involved in oxidative stress and lipid peroxidation (Publication III: Figure 6) suggest that these factors might also be involved in the depressed metabolic state and loss of muscle integrity. Heat stress increases the number of abnormal proteins in the cell, resulting in the induction of the heat shock proteins (Hsp), but also increase lipid peroxidation and reactive oxygen species (Meistertzheim et al., 2007; Madeira et al., 2018; Sokolova, 2018). The rise in lipid peroxidation suggests cell membrane disruption with possible induction of apoptosis and negative impacts in the mitochondrial complex enzymes, leading to a progressive physiological and energetic depression (Madeira et al., 2018; Sokolova, 2018). In *H. fulgens*, warming-induced expression patterns of the Hsp70 isoforms were mostly unaffected by the experimental conditions in gill and muscle. But genes involved in the antioxidant response showed tissue-specific and experiment-specific expression patterns, suggesting a different response to oxidative stress. Moreover, the transcriptome analysis also suggests increasing protection mechanism for lipid peroxidation in an animal at the most stressful condition (32 °C; hypoxic hypercapnia; Publication III: Figure 6), but these genes were not analyzed with qPCR under all experimental conditions, thus, requiring a thorough statistical assessment.

4.5 Environmental implications

The results from this thesis provide evidence for a high thermal tolerance of *H. fulgens* but additional factors such as hypoxia and hypercapnia increase warming sensitivity. While temperatures as high as 32 °C are not common at the collection site of the abalone juveniles, oxygen levels as low as 2 mgO_2 L^{-1} (~20% air saturation) are frequently registered along the California Current with negative impacts on abalone natural populations (Micheli et al., 2012; Boch et al., 2018).

A recent study with natural populations of *H. fulgens* from the Pacific Coast of the Baja California Peninsula provided evidence for an interactive effect of elevated temperatures and reduced oxygen availability on abalone performance, with higher mortality rates and reduced growth rates in a year where high temperatures (>20 °C) where accompanied by a higher frequency of days with reduced oxygen (<4.6 mgO_2 L^{-1}) compared to a year with less hypoxic events (Boch et al., 2018). In this same study, abalone from the field were transported to controlled lab facilities and exposed to warming conditions, demonstrating high survival and a high acclimation capacity to short-term increases in temperature. The authors concluded that

hypoxic events are more likely than anomalous high temperatures to cause depressed growth in juvenile abalone in natural systems (Boch et al., 2018).

The results from this thesis confirm the high capacity of *H. fulgens* to tolerate short-term increments of temperature. Upon thermal challenge, green abalone is able to increase their oxygen uptake and to sustain an aerobic mode of energy production. Additionally, *H. fulgens* juveniles showed a rapid and coordinated molecular response to stress (Publication III), particularly from the Hsp70s, which were up-regulated already at 30 °C. The induction temperature for Hsp (T_{on}) has been found to occur close to the upper critical temperature at which mortality starts to rise (Anestis et al., 2007; Tomanek and Zuzow, 2010). In this short-term experiment, induction of Hsp70 is not related to the maxima thermal limits (CT_{max}; Publication II), but it may represent a preventive mechanism when the temperatures reach suboptimal levels. This is exemplified in Fig. 4.7: according to the transcriptomic analysis, Hsp70 was significantly up-regulated in gill and muscle at 30 °C, but T_{on} occurs likely at a lower temperature than 30 °C and not deteccted due to the attenuation in detection due to the sampling protocol of this study (Publications II and III). During strong El Niño events, like the 1997-1998 and the 2015-2016 events, there is a higher frequency of temperatures near T_{on}, which would trigger the heat shock response. Moreover, an unpublished work with *H. fulgens* juveniles from Bahia Tortugas acclimated at 20 °C demonstrated that animals exposed to 29 °C for 14 days had a higher MO_2 and lower growth, feeding, and excretion rates than specimens acclimated at lower temperatures [2]. This matches with previous studies suggesting an optimum growth for *H. fulgens* from California is in the range of 20 – 28 °C (Leighton et al., 1981).

The rapid temperature-induced up-regulation of genes involved in the CSR, mainly the heat shock proteins and genes from the antioxidant system imply that more transcripts are available for a rapid protein translation. These mechanisms likely allow *H. fulgens* to survive extreme temperature events, such as El Niño, where temperatures above 28 °C or 30 °C occur for several days, depending on the geographical location (Guzman del Proo et al., 2003; Ponce-Díaz et al., 2004; Vilchis et al., 2005; Boch et al., 2018). However, this short-term physiological adaptation is generally expensive and possibly not an effective strategy to deal with long-term effects (Pörtner and Knust, 2007; Martinez et al., 2016). At sublethal temperatures, the compensatory responses related to the CSR use the energetic surplus which is otherwise used for somatic and reproductive growth, compromising the ecological performance of a population (Sokolova, 2013; Pörtner et al., 2017). While *H. fulgens* population from Baja California Peninsula could be resistant to temperature extremes, long-term warming trends, as expected with climate

[2] Velasco-Echavarría, H. 2014. Marco ambiental y capacidad de recuperación ante estress térmico del ablón azul (*H. fulgens* provenientes de la zona de Bahia Tortugas, B.C.S. Centro de Investigaciones Biológicas del Noroeste. Corresponding: himilce.velasco@gmail.com

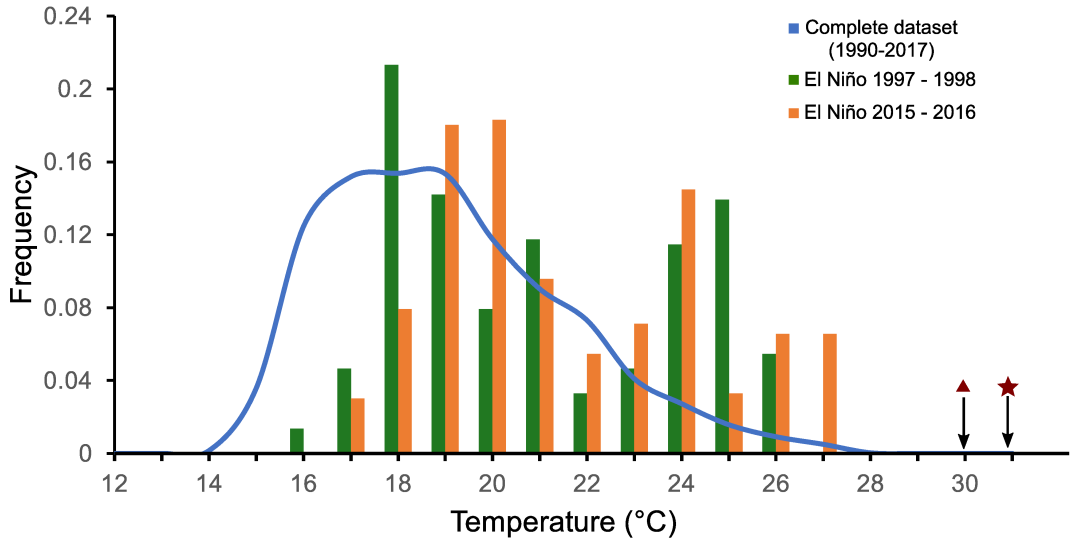

Figure 4.7 Frequency of temperature records in the region close to Bahia Tortugas (27.625N, 114.875W) derived from the NOAA high-resolution Blended Analysis Data (http://www.esrl.noaa.gov/psd/) with daily mean SST values from January 1990 to January 2017. The blue line indicates temperature frequency from the whole dataset, whereas the green and orange bars indicate temperature frequency during the strongest El Niño events during the period (1997-1998 and 2015-2016, respectively). The ▲ indicates the temperature at which Hsp70 upregulation is already observed in *H. fulgens* tissues (Publication III). The ★ indicate the highest *in situ* temperature record in Bahia Tortugas during El Niño 1997-1998, according to Guzman del Proo et al. (2003).

change, could be detrimental if this is paralleled by increasing frequency and intensity of El Niño events (Cai et al., 2014).

The above-mentioned effects of temperature are more detrimental under reduced oxygen availability, which is expected to occur more frequently in the near future due to increased stratification or due to shoaling of deep seawater with low oxygen concentrations. In this thesis, moderate hypoxia (50% air saturation) already constrained aerobic capacity at 27 °C (Publication I). Abalone sensitivity to hypoxia has been related to impacted antioxidant capacity (Vosloo et al., 2013b), as a high antioxidant activity prepares the organism for the oxidative stress during reoxygenation (Hermes-Lima and Zenteno-Savín, 2002). The gene expression correlation networks for the hypoxia treatment in gill demonstrates an altered expression pattern of genes involved in the antioxidant system compared to the other treatments (Publication III: Figure 3). These alterations involve a higher glutathione-S-transferase (*GST*) relative expression at the initial condition (Publication III: Supplementary material 1) compared to the control treatment (normoxia), and lower levels of glutathione reductase (*GLR*) at warmest temperature compared to the control treatment (normoxia). While the alterations in these genes were minor in this short-term experiment, it is possible that the combination of excessive

mitochondrial reactive oxygen species (ROS) production during warming exposure, in addition to longer exposure to moderate hypoxia or acute exposure to much lower oxygen levels, as observed in natural populations (*e.g.* < 2 mgO_2 L^{-1}; Micheli et al. 2012; Boch et al. 2018), could induce stronger oxidative stress resulting in increased mortality (Boch et al., 2018). As a remark, the observed changes in antioxidant genes under hypoxia were not present during warming under combined hypoxia and hypercapnia (Publication III: Supplementary material 1), which may indicate some compensatory interaction between hypoxia and hypercapnia, or an overload favoring an hypometabolic response causing reduced transcriptomic inducibility (section 4.4).

In this thesis, hypercapnic exposure induced less impacts in green abalone than hypoxia, but it is evident that the simultaneous presence of both hypoxia and hypercapnia had a major impact on the abalone metabolic state and thermal tolerance. Currently, there is no long-term record of seawater PCO_2/pH fluctuations in the natural habitat of the investigated population. However, the increasing interaction of warming, hypoxia and acidified water is already a major threat in many marine ecosystems with negative economic impacts (Pörtner et al., 2014; Gattuso et al., 2015; Somero et al., 2016; Hodgson et al., 2018). As portrayed in this thesis, the simultaneous presence of reduced oxygen and high PCO_2 compromise the abalone metabolic state at temperatures which are well inside the optimum for growth (24 – 27 °C). A depressed metabolic state and higher rates of protein utilization imply a reduced performance and likely a reduced capacity to withstand additional pressure, such as bacterial infections, which are known to cause mass mortalities events in natural populations of green abalone along the Baja California Peninsula and the coasts from California (García-Esquivel et al., 2007; Moore et al., 2009).

4.6 Conclusions and future perspectives

Juveniles of *H. fulgens* proved to be tolerant to short-term (six days) exposure to rising temperatures up to 32 °C as well as reduced oxygen (50% air saturation) and high PCO_2 (1,000 µatm PCO_2) at unchanged temperature, respectively. But exposure to hypoxia and hypercapnia, in isolation and if combined, modified the thermal response and induced impacts in the cellular metabolic state. In line with the OCLTT concept, these results confirmed our initial hypothesis that hypoxia and hypercapnia induced downwards shifts in the abalone thermal limits by constraints in aerobic capacity and changes in the energy metabolism, such as metabolic depression.

As individual stressors, hypoxia induced the largest impacts in the aerobic capacity and in the cellular metabolic state with rising temperatures, and this matches with field observations,

where naturally occurring episodes of hypoxia resulted in higher negative impacts on gree abalone than the effect of temperature alone. Hypercapnia had a stimulatory effect with a higher thermal sensitivity of MO_2 and energy demand compared to animals exposed to warming as the only driver. The synergistic negative impacts from the combination of hypoxia and hypercapnia resulted in a strong narrowing of the thermal limits. However, it was not possible to fully elucidate the impacted mechanism resulting in the observed onset of muscular failure and mortality at 32 °C. As there is no evidence of increased structural damage or lethal energy deficiency in muscle under this treatment, further investigations are needed to assess whether the impacts of multiple drivers affect the extra- or intra- cellular pH or neural function beyond the impacts observed during warming as a single driver.

The present thesis uses an integrative approach to deepen our understanding of impacted mechanisms involved in the reduction of the abalone's thermal tolerance, and to find suitable indicators for increased vulnerability upon exposure to multiple environmental drivers. In order to draw a more detailed picture, I will present the conclusions for the key metabolic and cellular responses analyzed in this thesis which displayed sensitivity to the different experimental conditions (Table 4.1)

Metabolic rate

Oxygen consumption as a measure of whole-organism metabolic rate followed the expectations derived from the OCLTT concept and proved to be a sensitive indicator for metabolic perturbations and limitations in aerobic performance. The highest Q_{10} in MO_2 measurements during warming from 18 °C to 32 °C under hypoxia (Q_{10} = 2.86 ± 0.99) and warming under hypercapnia (Q_{10} = 3.29 ± 0.94) compared to warming under normoxia and normocapnia (Q_{10} = 1.72 ± 0.60) evidenced increased thermal sensitivity under the presence of these additional drivers, whereas the decrease in MO_2 values during warming under combined hypoxia and hypercapnia (Q_{10}= 1.23 ± 0.45) indicate a synergistic impact from both drivers and a metabolically depressed state. Previous studies with *H. midae* questioned whether an increased metabolic rate with temperature is indicative of a new homeostatic state or a condition that may ultimately result in death (Vosloo et al., 2013a). But in this study, the integration of the cellular metabolic state demonstrated that increased MO_2 is accompanied by anaerobiosis and higher rates of protein degradation, which allow to conclude that this new metabolic state would result in reduced performance and, likely, reduced growth rates if exposure to experimental conditions are sustained for longer.

Cellular metabolic state

The accumulation of anaerobic metabolites, such as lactate and succinate in gill and hepatopancreas was more evident when rising temperatures is accompanied by hypoxia and combined hypoxia and hypercapnia. But in contrast to previous studies where reduction of aerobic capacity finally leads to an accumulation of anaerobic metabolites (Frederich and Pörtner 2000; Zittier et al. 2015), the onset of anaerobiosis in *H. fulgens* gill was only transient and absent in muscle. Firstly, rising temperature under hypoxia likely triggered physiological mechanisms, such an increase in gill irrigation or higher movement of cilia in the gill lamellae which support increased oxygen uptake to sustain an aerobic mode for energy production. Secondly, with the simultaneous presence of warming, hypoxia, and hypercapnia the reduced aerobic capacity was rather sustained by depression of metabolism, involving a decrease of glycolytic capacity and change in metabolic fuels.

Assessment of CS enzyme capacities in addition with mRNA levels provided additional evidence for regulation of aerobic capacity. With warming under combined hypoxia and hypercapnia, CS enzyme capacity and *CS* and *COXIII* mRNA levels did not increase their basal levels but overcame the temperature compensation adjustments that were observed in the other treatments. Due to their rapid response to temperature and sensitivity to additional drivers, CS enzyme capacity and *CS* and *COXIII* mRNA levels demonstrated to be promising indicators of metabolic impacts during environmental stress.

Impacts in the free amino acids pool, particularly on the concentration of valine, was an important indicator of the cellular metabolic state in *H. fulgens* tissues under the different experimental conditions. In this study, I hypothesize that valine accumulation is involved in a shift in fuel utilization and in the observed adjustments of the mitochondrial capacities (using proteins instead of carbohydrates to run the TCA), as this is a well-described response of abalone during both acute and chronic thermal stress. Futures studies should confirm this mechanism by measuring whole-organism nitrogen excretion and tissue-specific protein content. As the branched chain amino acid pool and protein synthesis are essential components the immune system (Calder, 2006), and valine accumulation in this study displayed an experiment-dependent pattern, this amino acid could be helpful in assessing the sensitivity of *H. fulgens* to temperature and disease outbreaks.

Transcriptomic analysis

Induction of the CSR proved to be a sensitive indicator of warming stress. As denoted by the patterns of gene expression, the most prominent changes were observed in the analyzed

Hsp70 isoforms, where a strong up-regulation is observed already at 30 °C. This likely denotes that this temperature is close to the upper thermal limits and matches with the anomalously high temperatures registered in their natural habitat inducing high mortalities. But unlike other studies where the induction temperature of the heat shock response was reduced due to hypoxia or hypercapnia (Anestis et al., 2010; Schiffer et al., 2012; Harms et al., 2014), the heat shock response in *H. fulgens* was mostly unaffected by these drivers.

Gene up-regulation of the heat shock response seems to be an important component of the *H. fulgens* thermotolerance, but as the assessment of Hsp70 protein induction was restricted in this study (Publication II), future assessment should address the Hsp70 protein induction and their modification by hypoxia and hypercapnia. Induction of the Hsp proteins is an energetically expensive process, therefore, increase in Hsp70 protein levels may be observed during a recovery period after the heat shock only (Bahrndorff et al., 2009). Nevertheless, induction of Hsp70 gene expression was an effective indicator of thermal stress but was insensitive to additional metabolic impacts resulting from hypoxia and hypercapnia as has been seen for other indicators, such as CS, anaerobic metabolites, and valine.

Several additional processes affected by the experimental conditions were detected by the de novo transcriptome assembly, including the antiapoptotic response as an important component of the CSR. Due to time constraints, genes involved in this process could finally not be included in the quantitative (qPCR) analysis, but these genes represent good candidate genes to test if the highly detrimental condition from the combination of multiple drivers trigger a stronger antiapoptotic response, which then could be related to the downward shift of the upper thermal limit (CT_{max}), or whether they follow the same temperature-induction pattern as the Hsp70 genes, regardless of additional drivers.

The cellular and molecular analysis in this thesis highlighted the contrasting metabolic state and expression patterns from certain genes between different tissues (e.g. *HIF*, *PEPCK*). This should be considered carefully when analyzing the thermal sensitivity of marine species. In this work, it was decided to focus on the more metabolically active tissues with contrasting functions such as respiration, digestion and attachment (gill, hepatopancreas, and muscle, respectively) for the cellular and molecular analyses, whereas the epipodium, which has a sensory function (Fig. 2.3), was not used. But recent evidence demonstrates that this tissue follows similar metabolic response as muscle or gill during functional and environmental hypoxia (Venter et al., 2018a,b). Therefore, the use of epipodial tissue could be a powerful tool for future assessment of the cellular state of abalone, as this tissue is easily accessible, and it's not needed to sacrifice the animal, making it possible to take samples from animals directly in the field.

As a corollary, *H. fulgens* juveniles withstand short periods of high environmental temperature or reduced oxygen levels, but upon an increasing interaction between multiple drivers

Table 4.1 Key metabolic and cellular responses in green abalone juveniles exposed to a warming ramp under control (normoxic normocapnia), hypoxia (hypoxic normocapnia), hypercapnia (normoxic hypercapnia), and combined (hypoxic hypercapnia) conditions. Cells in blue indicate depletion/downregulation of the paramter whereas cells in red indicate accumulation/upregulation of the parameter. White cells indicates unchanged values of the parameter. The number in each cell indicates the temperature (in °C) at which up- or downregulation was observed. The ↷ and ↶ indicate that the parameter returned to initial levels after the observed up- or downregulation, respectively

Parameter	Tissue	Experiment			
		Control	Hypoxia	Hypercapnia	Combined
Whole-organism					
Constraints in MO_2		–	27	–	30
Muscular failure		–	–	–	32
Cellular metabolic state					
Anaerobic end-products	Gill	–	Lac-24; Suc-30	Suc-32	Lac / Suc-24 ↷
	Muscle	Suc-24 ↷	–	–	–
Valine	Gill	32	30	32	24
	Muscle	30	–	32	32
Enzyme capacities					
LDH	Muscle	–	32	–	24 ↷
TDH	Muscle	–	32	–	–
CS	Muscle	24 (↶ at 32)	24 (↶ at 32)	24 (↶ at 32)	–
Gene expression					
CS	Gill	24	30	32	–
	Muscle	30	30	24	–
PEPCK	Gill	30	32	32	30
	Muscle	24 ↶	–	–	–
PK	Gill	30	30	32	24
	Muscle	30	30	32	30
Hsp70i	Gill	30	30	24	24
	Muscle	30	30	30	30

in their natural environment, the metabolic state is shifted towards damage control, restricted energy production and protein synthesis. Consequently, natural populations of green abalone will most likely show reduced performance and higher susceptibility to diseases promoting mass mortalities.

In this thesis, the integration of physiology, metabolomics and transcriptomics demonstrated to be a powerful tool to investigate the impacted physiological mechanism during environmental extremes. With this integrative approach, it was possible to identify a set of sensitive traits from all different levels which can be effectively used in future studies assessing the impacts of the ongoing climate change in natural populations of abalone, with respect to the combination of multiple drivers and increasing frequency of extremes. Future studies investigating the long-term effects of high temperature, hypoxia, and hypercapnia are needed to investigate the abalone's acclimation potential and to confirm whether the rise in energy demand observed with warming results in lower performance, reduced size or higher susceptibility to diseases

REFERENCES

Aggio, R. B., Ruggiero, K., and Villas-Bôas, S. G. (2010). Pathway activity profiling (papi): From the metabolite profile to the metabolic pathway activity. *Bioinformatics*, 26(23):2969–2976.

Alter, K., Andrewartha, S. J., Morash, A. J., Clark, T. D., Hellicar, A. D., León, R. I., and Elliott, N. G. (2017). Hybrid abalone are more robust to multi-stressor environments than pure parental species. *Aquaculture*, 478(September):25–34.

Anestis, A., Lazou, A., Pörtner, H. O., and Michaelidis, B. (2007). Behavioral, metabolic, and molecular stress responses of marine bivalve *Mytilus galloprovincialis* during long-term acclimation at increasing ambient temperature. *American journal of physiology. Regulatory, integrative and comparative physiology*, 293(2):R911–21.

Anestis, A., Portner, H. O., Lazou, A., and Michaelidis, B. (2008). Metabolic and molecular stress responses of sublittoral bearded horse mussel *Modiolus barbatus* to warming sea water: implications for vertical zonation. *Journal of Experimental Biology*, 211(17):2889–2898.

Anestis, A., Pörtner, H. O., and Michaelidis, B. (2010). Anaerobic metabolic patterns related to stress responses in hypoxia exposed mussels *Mytilus galloprovincialis*. *Journal of Experimental Marine Biology and Ecology*, 394(1-2):123–133.

Bahrndorff, S., Mariën, J., Loeschcke, V., and Ellers, J. (2009). Dynamics of heat-induced thermal stress resistance and hsp70 expression in the springtail, *Orchesella cincta*. *Functional Ecology*, 23(2):233–239.

Bakun, A., Black, B. A., Bograd, S. J., García-Reyes, M., Miller, A. J., Rykaczewski, R. R., and Sydeman, W. J. (2015). Anticipated Effects of Climate Change on Coastal Upwelling Ecosystems. *Current Climate Change Reports*, 1(2):85–93.

Boch, C., Micheli, F., AlNajjar, M., Monismith, S., Beers, J., Bonilla, J., Espinoza, J., Vazquez, L., and Woodson, C. (2018). Local oceanographic variability influences the performance of juvenile abalone under climate change. *Scientific Reports*, (215):1–12.

Bowen, C. (1984). Facultative anaerobiosis in *Haliotis*(ormer/abalone): Pyruvate kinase and phosphoenolpyruvate carboxykinase activities. *Comparative Biochemistry and physiology*, 77B(I):197–200.

Brooks, S. and Storey, K. (1997). Glycolytic controls in estivation and anoxia: A comparison of metabolic arrest in land and marine molluscs. *Comparative Biochemistry and Physiology Part A: Physiology*, 118(4):1103–1114.

Brosnan, M. E. and Letto, J. (1991). Interorgan metabolism of valine. *Amino Acids*, 1(1):29–35.

Buckley, B. A., Gracey, A., and Somero, G. (2006). The cellular response to heat stress in the goby *Gillichthys mirabilis*: a cDNA microarray and protein-level analysis. *Journal of Experimental Biology*, 209(14):2660–2677.

Cai, W., Borlace, S., Lengaigne, M., van Rensch, P., Collins, M., Vecchi, G., Timmermann, A., Santoso, A., McPhaden, M. J., Wu, L., England, M. H., Wang, G., Guilyardi, E., and Jin, F.-F. (2014). Increasing frequency of extreme El Niño events due to greenhouse warming. *Nature Climate Change*, 5(2):1–6.

Calder, P. C. (2006). Branched-Chain Amino Acids and Immunity. *The Journal of Nutrition*, 136(1):288S–293S.

Chen, N., Luo, X., Gu, Y., Han, G., Dong, Y., You, W., and Ke, C. (2016). Assessment of the thermal tolerance of abalone based on cardiac performance in *Haliotis discus hannai*, *H. gigantea* and their interspecific hybrid. *Aquaculture*, 465:258–264.

Cheng, W., Liu, C.-H., Cheng, S.-Y., and Chen, J.-C. (2004). Effect of dissolved oxygen on the acid–base balance and ion concentration of Taiwan abalone *Haliotis diversicolor supertexta*. *Aquaculture*, 231(1-4):573–586.

Clark, H. R. and Gobler, C. J. (2016). Diurnal fluctuations in CO_2 and dissolved oxygen concentrations do not provide a refuge from hypoxia and acidification for early-life-stage bivalves. *Marine Ecology Progress Series*, 558:1–14.

Clark, M. S., Sommer, U., Sihra, J. K., Thorne, M. A., Morley, S. A., King, M., Viant, M. R., and Peck, L. S. (2017). Biodiversity in marine invertebrate responses to acute warming revealed by a comparative multi-omics approach. *Global change biology*, 23(1):318–330.

Cook, P. A. (2016). Recent Trends in Worldwide Abalone Production. *Journal of Shellfish Research*, 35(3):581–583.

Cox, K. W. (1962). *California Abalones, Family Haliotidae*. Fish bulletin. Department of Fish and Game, the Resources Agency, State of California.

Cunningham, S. C., Smith, A. M., and Lamare, M. D. (2016). The effects of elevated pCO_2 on growth, shell production and metabolism of cultured juvenile abalone, *Haliotis iris*. *Aquaculture Research*, 47(8):2375–2392.

Dahlhoff, E. and Somero, G. N. (1993). Effects of Temperature on Mitochondria from Abalone (Genus *Haliotis*) - Adaptive Plasticity and Its Limits. *Journal of Experimental Biology*, 185:151–168.

de Zwaan, A. and Wijsman, T. C. (1976). Anaerobic metabolism in bivalvia (Mollusca) Characteristics of anaerobic metabolism. *Comparative Biochemistry and Physiology Part B: Comparative Biochemistry*, 54(3):313–323.

Diaz, F., Re, A. D., Medina, Z., Re, G., Valdez, G., and Valenzuela, F. (2006). Thermal preference and tolerance of green abalone *Haliotis fulgens* (Philippi, 1845) and pink abalone *Haliotis corrugata* (Gray, 1828). *Aquaculture Research*, 37(9):877–884.

Dickson, A. and Millero, F. (1987). A comparison of the equilibrium constants for the dissociation of carbonic acid in seawater media. *Deep Sea Research*, 34(10):1733–1743.

Dickson, A. G. (1990). Thermodynamics of the dissociation of boric acid in synthetic seawater from 273.15 to 318.15 K. *Deep Sea Research Part A, Oceanographic Research Papers*, 37(5):755–766.

Dunphy, B. J., Ruggiero, K., Zamora, L. N., and Ragg, N. L. (2018). Metabolomic analysis of heat-hardening in adult green-lipped mussel (*Perna canaliculus*): A key role for succinic acid and the GABAergic synapse pathway. *Journal of Thermal Biology*, 74(February):37–46.

Eckerle, L. G., Lucassen, M., Hirse, T., and Pörtner, H. O. (2008). Cold induced changes of adenosine levels in common eelpout (*Zoarces viviparus*): a role in modulating cytochrome c oxidase expression. *The Journal of experimental biology*, 211(Pt 8):1262–9.

Farcy, E., Voiseux, C., Lebel, J.-M., and Fivet, B. (2009). Transcriptional expression levels of cell stress marker genes in the Pacific oyster *Crassostrea gigas* exposed to acute thermal stress. *Cell Stress and Chaperones*, 14(4):371–380.

Feder, M. E. and Hofmann, G. E. (1999). Heat-shock proteins, molecular chaperones, and the stress response: evolutionary and ecological physiology. *Annual review of physiology*, 61(c):243–82.

Feely, R. a., Sabine, C. L., Hernandez-Ayon, J. M., Ianson, D., and Hales, B. (2008). Evidence for upwelling of corrosive "acidified" water onto the continental shelf. *Science*, 320(5882):1490–2.

Feidantsis, K., Pörtner, H. O., Lazou, A., Kostoglou, B., and Michaelidis, B. (2009). Metabolic and molecular stress responses of the gilthead seabream *Sparus aurata* during long-term exposure to increasing temperatures. *Marine Biology*, 156(4):797–809.

Frederich, M. and Pörtner, H. O. (2000). Oxygen limitation of thermal tolerance defined by cardiac and ventilatory performance in spider crab, *Maja squinado*. *American journal of physiology. Regulatory, integrative and comparative physiology*, 279(5):R1531–8.

Gäde, G. (1983). Energy metabolism of arthropods and mollusks during environmental and functional anaerobiosis. *Journal of Experimental Zoology*, 228(3):415–429.

García-Esquivel, Z., Montes-Magallón, S., and González-Gómez, M. a. (2007). Effect of temperature and photoperiod on the growth, feed consumption, and biochemical content of juvenile green abalone, *Haliotis fulgens*, fed on a balanced diet. *Aquaculture*, 262(1):129–141.

Gattuso, J.-P., Magnan, A., Billé, R., Cheung, W. W., Howes, E. L., Joos, F., Allemand, D., Bopp, L., Cooley, S. R., Eakin, C. M., et al. (2015). Contrasting futures for ocean and society from different anthropogenic CO_2 emissions scenarios. *Science*, 349(6243):aac4722.

Gazeau, F., Parker, L. M., Comeau, S., Gattuso, J.-P., O'Connor, W. A., Martin, S., Pörtner, H.-O., and Ross, P. M. (2013). Impacts of ocean acidification on marine shelled molluscs. *Marine Biology*, 160(8):2207–2245.

Gobler, C. J., DePasquale, E. L., Griffith, A. W., and Baumann, H. (2014). Hypoxia and acidification have additive and synergistic negative effects on the growth, survival, and metamorphosis of early life stage bivalves. *PLoS ONE*, 9(1).

Grieshaber, M. K., Hardewig, I., Kreutzer, U., and Portner, H. (1994). Physiological and Metabolic Responses to Hypoxia in Invertebrates. *Reviews of Physiology, Biochemistry and Pharmacology*, 125.

Guzman del Proo, S. A., Palau, L. C., Perez, J. B., Laguna, J. C., and Fragoso, R. H. (2003). Effects of the "El Niño" event on the recruitment of benthic invertebrates in Bahia Tortugas, Baja California Sur. *Geofisica Internacional*, 42(3):429–438.

Haas, B. J., Papanicolaou, A., Yassour, M., Grabherr, M., Blood, P. D., Bowden, J., Couger, M. B., Eccles, D., Li, B., Lieber, M., MacManes, M. D., Ott, M., Orvis, J., Pochet, N., Strozzi, F., Weeks, N., Westerman, R., William, T., Dewey, C. N., Henschel, R., LeDuc, R. D., Friedman, N., and Regev, A. (2013). De novo transcript sequence reconstruction from RNA-seq using the Trinity platform for reference generation and analysis. *Nature Protocols*, 8(8):1494–1512.

Han, G., Zhang, S., and Dong, Y. (2017). Anaerobic metabolism and thermal tolerance: the importance of opine pathways on survival of a gastropod after cardiac dysfunction. *Integrative Zoology*, 12:361–370.

Harms, L., Frickenhaus, S., Schiffer, M., Mark, F. C., Storch, D., Held, C., Pörtner, H.-O., and Lucassen, M. (2014). Gene expression profiling in gills of the great spider crab *Hyas araneus* in response to ocean acidification and warming. *BMC genomics*, 15(1):789.

Harris, J. O. (1999). Low dissolved oxygen reduces growth rate and oxygen consumption rate of juvenile greenlip abalone , *Haliotis laevigata* Donovan. *Aquaculture*, 174:265–278.

Harris, J. O., Burke, C. M., Edwards, S. J., and Johns, D. R. (2005). Effects of oxygen supersaturation and temperature on juvenile greenlip, *Haliotis laevigata* Donovan, and blacklip, *Haliotis rubra* Leach, abalone. *Aquaculture Research*, 36(14):1400–1407.

Hauri, C., Gruber, N., Plattner, G., Alin, S., Feely, R., Hales, B., and Wheeler, P. (2009). Ocean Acidification in the California Current System. *Oceanography*, 22(4):60–71.

Healy, T. M. and Schulte, P. M. (2012). Factors affecting plasticity in whole-organism thermal tolerance in common killifish (*Fundulus heteroclitus*). *Journal of Comparative Physiology B*, 182(1):49–62.

Heise, K. (2006). Oxidative stress during stressful heat exposure and recovery in the North Sea eelpout *Zoarces viviparus* L. *Journal of Experimental Biology*, 209(2):353–363.

Henson, S. A., Beaulieu, C., Ilyina, T., John, J. G., Long, M., Séférian, R., Tjiputra, J., and Sarmiento, J. L. (2017). Rapid emergence of climate change in environmental drivers of marine ecosystems. *Nature Communications*, 8(5020):14682.

Hermes-Lima, M. and Zenteno-Savín, T. (2002). Animal response to drastic changes in oxygen availability and physiological oxidative stress. *Comparative Biochemistry and Physiology - C Toxicology and Pharmacology*, 133(4):537–556.

Hochachka, P. and Somero, G. N. (2002). *Biochemical adaptation: Mechanism and process in physiological evolution*. Oxford University Press.

Hodgson, E. E., Kaplan, I. C., Marshall, K. N., Leonard, J., Essington, T. E., Busch, D. S., Fulton, E. A., Harvey, C. J., Hermann, A., and McElhany, P. (2018). Consequences of spatially variable ocean acidification in the California Current: Lower pH drives strongest declines in benthic species in southern regions while greatest economic impacts occur in northern regions. *Ecological Modelling*, 383(May):106–117.

Ioannou, S., Anestis, A., Pörtner, H. O., and Michaelidis, B. (2009). Seasonal patterns of metabolism and the heat shock response (HSR) in farmed mussels *Mytilus galloprovincialis*. *Journal of Experimental Marine Biology and Ecology*, 381(2):136–144.

Jacox, M. G., Hazen, E. L., Zaba, K. D., Rudnick, D. L., Edwards, C. A., Moore, A. M., and Bograd, S. J. (2016). Impacts of the 2015-2016 El Niño on the California Current System: Early assessment and comparison to past events. *Geophysical Research Letters*, 43(13):7072–7080.

Jorgensen, D. D., Ware, S. K., and Redmond, J. R. (1984). Cardiac output and tissue blood flow in the abalone, *Haliotis cracherodii* (Mollusca, Gastropoda). *Journal of Experimental Zoology*, 231(3):309–324.

Kassahn, K. S., Crozier, R. H., Pörtner, H. O., and Caley, M. J. (2009). Animal performance and stress: Responses and tolerance limits at different levels of biological organisation. *Biological Reviews*, 84(2):277–292.

Katsikatsou, M., Anestis, A., Pörtner, H., Vratsistas, A., Aligizaki, K., and Michaelidis, B. (2012). Field studies and projections of climate change effects on the bearded horse mussel *Modiolus barbatus* in the Gulf of Thermaikos, Greece. *Marine Ecology Progress Series*, 449:183–196.

Khairallah, E. A. and Mortimore, G. E. (1976). Assessment of protein turnover in perfused rat liver. Evidence for amino acid compartmentation from differential labeling of free and tRNA-gound valine. *Journal of Biological Chemistry*, 251(5):1375–1384.

Kim, T. W., Barry, J. P., and Micheli, F. (2013). The effects of intermittent exposure to low pH and oxygen conditions on survival and growth of juvenile red abalone. *Biogeosciences Discussions*, 10(2):3559–3576.

Lannig, G., Eilers, S., Pörtner, H. O., Sokolova, I. M., and Bock, C. (2010). Impact of ocean acidification on energy metabolism of oyster, *Crassostrea gigas*—Changes in metabolic pathways and thermal response. *Marine Drugs*, 8(8):2318–2339.

Le Moullac, G., Bacca, H., Huvet, A., Moal, J., Pouvreau, S., and Van Wormhoudt, A. (2007a). Transcriptional regulation of pyruvate kinase and phosphoenolpyruvate carboxykinase in the adductor muscle of the oyster *Crassostrea gigas* during prolonged hypoxia. *Journal of Experimental Zoology Part A: Ecological Genetics and Physiology*, 307A(7):371–382.

Le Moullac, G., Quéau, I., Le Souchu, P., Pouvreau, S., Moal, J., René Le Coz, J., and François Samain, J. (2007b). Metabolic adjustments in the oyster *Crassostrea gigas* according to oxygen level and temperature. *Marine Biology Research*, 3(5):357–366.

Leighton, D. L., Byhower, M. J., Kelly, J. C., Hooker, G. N., and Morse, D. E. (1981). Acceleration of development and growth in young green abalone (*Haliotis fulgens*) using warmed effluent seawater. *Journal of the World Mariculture Society*, 12(1):170–180.

Lewis, E. and Wallace, D. W. R. (1998). Program Developed for CO_2 System Calculations. ORNL/CDIAC-105. Carbon Dioxide Information Analysis Center, Oak Ridge National Laboratory, U.S. Department of Energy, Oak Ridge, Tennessee.

Li, J., Mao, Y., Jiang, Z., Zhang, J., Fang, J., and Bian, D. (2018). The detrimental effects of CO_2-driven chronic acidification on juvenile Pacific abalone (*Haliotis discus hannai*). *Hydrobiologia*, 809(1):297–308.

Li, S., Liu, C., Huang, J., Liu, Y., Zheng, G., Xie, L., and Zhang, R. (2015). Interactive effects of seawater acidification and elevated temperature on biomineralization and amino acid metabolism in the mussel *Mytilus edulis*. *Journal of Experimental Biology*, pages 3623–3631.

Li, Y. and Deng, J.-s. P. J.-h. (2006). Cytochrome c oxidase subunit IV is essential for assembly and respiratory function of the enzyme complex. *Journal of Bioenergetics and Biomembranes*, 38:283–291.

Livingstone, D. R. (1983). Invertebrate and vertebrate pathways of anaerobic metabolism: evolutionary considerations. *Journal of the Geological Society*, 140(1):27–37.

Lu, J., Shi, Y., Wang, S., Chen, H., Cai, S., and Feng, J. (2016). NMR-based metabolomic analysis of *Haliotis diversicolor* exposed to thermal and hypoxic stresses. *Science of the Total Environment*, 545-546:280–288.

Lucassen, M. (2006). Mitochondrial mechanisms of cold adaptation in cod (*Gadus morhua* L.) populations from different climatic zones. *Journal of Experimental Biology*, 209(13):2462–2471.

Lucassen, M., Schmidt, A., Eckerle, L. G., and Pörtner, H. (2003). Mitochondrial proliferation in the permanent vs. temporary cold: enzyme activities and mRNA levels in Antarctic and temperate zoarcid fish. *American Journal of Physiology-Regulatory Integrative and Comparative Physiology*, 285(6):R1410–R1420.

Lutterschmidt, W. I. and Hutchison, V. H. (1997). The critical thermal maximum: data to support the onset of spasms as the definitive end point. *Canadian Journal of Zoology*, 75(February 1997):1553–1560.

Madeira, C., Mendonça, V., Flores, A. A. V., Diniz, M. S., and Vinagre, C. (2018). High thermal tolerance does not protect from chronic warming – A multiple end-point approach using a tropical gastropod, *Stramonita haemastoma*. *Ecological Indicators*, 91(April):626–635.

Martinez, E., Porreca, A. P., Colombo, R. E., and Menze, M. A. (2016). Tradeoffs of warm adaptation in aquatic ectotherms: Live fast, die young? *Comparative Biochemistry and Physiology -Part A : Molecular and Integrative Physiology*, 191:209–215.

Matz, M. V., Wright, R. M., and Scott, J. G. (2013). No Control Genes Required: Bayesian Analysis of qRT-PCR Data. *PLoS ONE*, 8(8):e71448.

Mehrbach, C., Culberson, C. H., Hawley, J. E., and Pytkowicx, R. M. (1973). Measurement of the apparent dissociation constants of carbonic acid in seawater at atmospheric pressure. *Limnology and Oceanography*, 18(6):897–907.

Meistertzheim, A.-L., Tanguy, A., Moraga, D., and Thébault, M.-T. (2007). Identification of differentially expressed genes of the Pacific oyster *Crassostrea gigas* exposed to prolonged thermal stress. *FEBS Journal*, 274(24):6392–6402.

Melzner, F., Gutowska, M. a., Langenbuch, M., Dupont, S., Lucassen, M., Thorndyke, M. C., Bleich, M., and Pörtner, H.-O. (2009). Physiological basis for high CO_2 tolerance in marine ectothermic animals : pre-adaptation through lifestyle and ontogeny? *Biogeosciences*, 6(6):2313–2331.

Michaelidis, B., Ouzounis, C., Paleras, A., and Pörtner, H. (2005). Effects of long-term moderate hypercapnia on acid-base balance and growth rate in marine mussels *Mytilus galloprovincialis*. *Marine Ecology Progress Series*, 293(Lackner 2003):109–118.

Micheli, F., Saenz-Arroyo, A., Greenley, A., Vazquez, L., Espinoza Montes, J. A., Rossetto, M., and De Leo, G. a. (2012). Evidence that marine reserves enhance resilience to climatic impacts. *PloS one*, 7(7):e40832.

Moore, J. D., Juhasz, C. I., Robbins, T., and Vilchis, L. I. (2009). Green abalone, *Haliotis fulgens* infected with the agent of withering syndrome do not express disease signs under a temperature regime permissive for red abalone, *Haliotis rufescens*. *Marine biology*, 156(11):2325–2330.

Morales-Bojórquez, E., Muciño-Díaz, M. O., and Vélez-Barajas, J. A. (2008). Analysis of the decline of the abalone fishery (*Haliotis fulgens* and *H. corrugata*) along the westcentral coast of the Baja California peninsula, Mexico. *Journal of Shellfish Research*, 27(4):865–870.

Morash, A. J. and Alter, K. (2015). Effects of environmental and farm stress on abalone physiology: perspectives for abalone aquaculture in the face of global climate change. *Reviews in Aquaculture*, 7:1 – 27.

Morris, J. P., Thatje, S., and Hauton, C. (2013). The use of stress-70 proteins in physiology: a re-appraisal. *Molecular Ecology*, 22(6):1494–1502.

Moya, A., Howes, E. L., Lacoue-Labarthe, T., Forêt, S., Hanna, B., Medina, M., Munday, P. L., Ong, J. S., Teyssié, J. L., Torda, G., Watson, S. A., Miller, D. J., Bijma, J., and Gattuso, J. P. (2016). Near-future pH conditions severely impact calcification, metabolism and the nervous system in the pteropod *Heliconoides inflatus*. *Global Change Biology*, 22(12):3888–3900.

Omolo, S., Gade, G., Cook, P. a., and Brown, a. C. (2003). Can the end products of anaerobic metabolism, tauropine and D-lactate, be used as metabolic stress indicators during transport of live South African abalone *Haliotis Midae*? *African Journal of Marine Science*, 25(May 2013):301–309.

Papetti, C., Lucassen, M., and Pörtner, H. O. (2016). Integrated studies of organismal plasticity through physiological and transcriptomic approaches: Examples from marine polar regions. *Briefings in Functional Genomics*, 15(5):365–372.

Piano, A., Asirelli, C., Caselli, F., and Fabbri, E. (2002). Hsp70 expression in thermally stressed *Ostrea edulis*, a commercially important oyster in Europe. *Cell stress & chaperones*, 7(3):250–257.

Ponce-Díaz, G., Serviere-Zaragoza, E., Racotta, I. S., Reynoso-Granados, T., Mazariegos-Villarreal, A., Monsalvo-Spencer, and Lluch-Belda, D. (2004). Growth and tissue biochemical composition of *Haliotis fulgens* at elevated temperatures in Baja California under two dried brown algal diets. *Journal of Shellfish Research*, 23(4):1051.

Pörtner, H. O. (2002). Climate variations and the physiological basis of temperature dependent biogeography: systemic to molecular hierarchy of thermal tolerance in animals. *Comparative biochemistry and physiology. Part A, Molecular & integrative physiology*, 132(4):739–61.

Pörtner, H. O. (2010). Oxygen- and capacity-limitation of thermal tolerance: a matrix for integrating climate-related stressor effects in marine ecosystems. *The Journal of experimental biology*, 213(6):881–93.

Pörtner, H. O., Bock, C., and Mark, F. C. (2017). Oxygen- and capacity-limited thermal tolerance: bridging ecology and physiology. *The Journal of Experimental Biology*, 220(15):2685–2696.

Pörtner, H. O., Bock, C., and Reipschläger, A. (2000). Modulation of the cost of pHi regulation during metabolic depression: a ^{31}P-NMR study in invertebrate (*Sipunculus nudus*) isolated muscle. *The Journal of experimental biology*, 203(Pt 16):2417–28.

Pörtner, H. O., Finke, E., and Lee, P. G. (1996). Metabolic and energy correlates of intracellular pH in progressive fatigue of squid (*L. brevis*) mantle muscle. *The American journal of physiology*, 271(5 Pt 2):R1403–14.

Pörtner, H. O. and Grieshaber, M. K. (1993). Critical PO_2 (s) in oxyconforming and oxyregulating animals: gas exchange, metabolic rate and the mode of energy production. In *The vertebrate gas transport cascade adaptations to environment and mode of life (JEPW Bicudo, ed) CRC Press, Boca Raton FL*, pages 330–357.

Pörtner, H. O., Karl, D., Boyd, P., Cheung, W. W., Lluch-Cota, S. E., Nojiri, Y., Schmidt, D., and Zavialov, P. (2014). Ocean systems. In Field, C., Barros, V., Dokken, D., Mach, K., Mastrandrea, M., Bilir, T., Chatterjee, M., Ebi, K., Estrada, Y., Genova, R., Girma, B., Kissel, E., Levy, A., MacCracken, S., Mastrandrea, P., and White, L., editors, *Climate change 2014: impacts, adaptation, and vulnerability. Part A: global and sectoral aspects. Contribution of working group II to the Fifth assessment report of the intergovernmental panel on climate change*, pages 411 – 484. Cambridge University Press, Cambridge and New York, NY.

Pörtner, H. O. and Knust, R. (2007). Climate Change Affects Marine Fishes Through the Oxygen Limitation of Thermal Tolerance. *Science*, 315(5808):95–97.

Pörtner, H. O., Langenbuch, M., and Michaelidis, B. (2005). Synergistic effects of temperature extremes, hypoxia, and increases in CO_2 on marine animals: From Earth history to global change. *Journal of Geophysical Research*, 110(C9):C09S10.

Pörtner, H. O., Reipschlager, a., and Heisler, N. (1998). Acid-base regulation, metabolism and energetics in *Sipunculus nudus* as a function of ambient carbon dioxide level. *Journal of Experimental Biology*, 201(1):43–55.

Ragg, N. L. C. and Taylor, H. H. (2006). Heterogeneous perfusion of the paired gills of the abalone *Haliotis iris* Martyn 1784: an unusual mechanism for respiratory control. *Journal of Experimental Biology*, 209(3):475–483.

Rodríguez-Valencia, J., Caballero-Alegría, F., and Castro-González, J. (2004). Temporal trends (1989–1999) in populations of *Haliotis fulgens* and *H. corrugata* (Gastropoda: Haliotidae) from Cedros Island, Baja California, Mexico. *Ciencias Marinas*, 30(3):489–501.

Rosenblum, E. S., Viant, M. R., Braid, B. M., Moore, J. D., Friedman, C. S., and Tjeerdema, R. S. (2005). Characterizing the metabolic actions of natural stresses in the California red abalone, *Haliotis rufescens* using ^{1}H NMR metabolomics. *Metabolomics*, 1(2):199–209.

Rothstein, M. and Tomlinson, G. (1962). Nematode biochemistry. II. Biosynthesis of amino acids. *BBA - Biochimica et Biophysica Acta*, 63(3):471–480.

Schiffer, M., Harms, L., Lucassen, M., Mark, C. C., Pörtner, H. O., and Storch, D. (2014). Temperature tolerance of different larval stages of the spider crab *Hyas araneus* exposed to elevated seawater PCO_2. *Frontiers in Zoology*, 11(1).

Schiffer, M., Harms, L., Pörtner, H. O., Lucassen, M., Mark, F. C., and Storch, D. (2012). Tolerance of *Hyas araneus* zoea I larvae to elevated seawater PCO_2 despite elevated metabolic costs. *Marine Biology*, 160(8):1943–1953.

Searcy-Bernal, R., Ramade-Villanueva, M. R., and Altamira, B. (2010). Current Status of Abalone Fisheries and Culture in Mexico. *Journal of Shellfish Research*, 29(3):573–576.

Shepherd, S. A., Guzmán del Próo, S. A., Turrubiates, J., Belmar, J., Baker, J. L., and Sluczanowski, P. R. (1991). Growth, Size at Sexual Maturity, and Egg-Per_Recruit Analysis of the Abalone *Haliotis fulgens* in Baja California. *The Veliger*, 34(4):324–330.

Simpfendörfer, R. W., Vial, M. V., López, D. A., Verdala, M., and González, M. L. (1995). Relationship between the aerobic and anaerobic metabolic capacities and the vertical distribution of three intertidal sessile invertebrates: *Jehlius cirratus* (Darwin) (Cirripedia), *Perumytilus purpuratus* (Lamarck) (Bivalvia) and *Mytilus chilensis*. *Comparative Biochemistry and Physiology – Part B: Biochemistry and Molecular Biology*, 111(4):615–623.

Sokolova, I. (2018). Mitochondrial adaptations to variable environments and their role in animals' stress tolerance. *Integrative and Comparative Biology*, (June):1–13.

Sokolova, I. M. (2013). Energy-limited tolerance to stress as a conceptual framework to integrate the effects of multiple stressors. *Integrative and comparative biology*, 53(4):597–608.

Somero, G. N. (2002). Thermal Physiology and Vertical Zonation of Intertidal Animals: Optima, Limits, and Costs of Living. *Integrative and Comparative Biology*, 42(4):780–789.

Somero, G. N. (2004). Adaptation of enzymes to temperature: Searching for basic "strategies". *Comparative Biochemistry and Physiology - B Biochemistry and Molecular Biology*, 139(3 SPEC.ISS.):321–333.

Somero, G. N. (2005). Linking biogeography to physiology: Evolutionary and acclimatory adjustments of thermal limits. *Frontiers in zoology*, 2(1):1.

Somero, G. N., Beers, J. M., Chan, F., Hill, T. M., Klinger, T., and Litvin, S. Y. (2016). What Changes in the Carbonate System, Oxygen, and Temperature Portend for the Northeastern Pacific Ocean: A Physiological Perspective. *BioScience*, 66(1):14–26.

Steckbauer, A., Ramajo, L., Hendriks, I. E., Fernandez, M., Lagos, N. A., Prado, L., and Duarte, C. M. (2015). Synergistic effects of hypoxia and increasing CO_2 on benthic invertebrates of the central Chilean coast. *Frontiers in Marine Science*, 2(July):1–12.

Stillman, J. H. and Armstrong, E. (2015). Genomics are transforming our understanding of responses to climate change. *BioScience*, 65(3):237–246.

Storey, K. B. and Storey, J. (2004). Oxygen limitation and metabolic rate depression. In Storey, K. B., editor, *Functional Metabolism: Regulation and Adaptation*, pages 415–442. John Wiley & Sons, Inc.

Strobel, A., Leo, E., Pörtner, H. O., and Mark, F. C. (2013). Elevated temperature and pCO_2 shift metabolic pathways in differentially oxidative tissues of *Notothenia rossii*. *Comparative Biochemistry and Physiology - B Biochemistry and Molecular Biology*, 166(1):48–57.

Sussarellu, R., Dudognon, T., Fabioux, C., Soudant, P., Moraga, D., and Kraffe, E. (2013). Rapid mitochondrial adjustments in response to short-term hypoxia and re-oxygenation in the Pacific oyster, *Crassostrea gigas*. *Journal of Experimental Biology*, 216(9):1561–1569.

Taylor, H. H. and Ragg, N. L. C. (2005). Extracellular fluid volume, urine filtration rate and haemolymph mixing time in the abalone, *Haliotis iris* Martyn: A comparison of 51Cr-EDTA and 14C-inulin as extracellular markers. *Marine and Freshwater Research*, 56(8):1117–1126.

Tomanek, L. and Zuzow, M. J. (2010). The proteomic response of the mussel congeners *Mytilus galloprovincialis* and *M. trossulus* to acute heat stress: implications for thermal tolerance limits and metabolic costs of thermal stress. *Journal of Experimental Biology*, 213(20):3559–3574.

Turi, G., Lachkar, Z., Gruber, N., and Münnich, M. (2016). Climatic modulation of recent trends in ocean acidification in the California Current System. *Environmental Research Letters*, 11(1):014007.

van der Meer, D. L. M., van den Thillart, G. E. E. J. M., Witte, F., de Bakker, M. A. G., Besser, J., Richardson, M. K., Spaink, H. P., Leito, J. T. D., and Bagowski, C. P. (2005). Gene expression profiling of the long-term adaptive response to hypoxia in the gills of adult zebrafish. *American Journal of Physiology-Regulatory, Integrative and Comparative Physiology*, 289(5):R1512–R1519.

Venter, L., Loots, D. T., Mienie, L. J., Jansen van Rensburg, P. J., Mason, S., Vosloo, A., and Lindeque, J. Z. (2018a). The cross-tissue metabolic response of abalone (*Haliotis midae*) to functional hypoxia. *Biology Open*, 7(3):bio031070.

Venter, L., Loots, D. T., Mienie, L. J., Jansen van Rensburg, P. J., Mason, S., Vosloo, A., and Lindeque, J. Z. (2018b). Uncovering the metabolic response of abalone (*Haliotis midae*) to environmental hypoxia through metabolomics. *Metabolomics*, 14(4):49.

Venter, L., Loots, D. T., Vosloo, A., Jansen van Rensburg, P., and Lindeque, J. Z. (2016). Abalone growth and associated aspects: Now from a metabolic perspective. *Reviews in Aquaculture*, pages 1–23.

Verberk, W. C. E. P., Sommer, U., Davidson, R. L., and Viant, M. R. (2013). Anaerobic metabolism at thermal extremes: A metabolomic test of the oxygen limitation hypothesis in an aquatic insect. *Integrative and Comparative Biology*, 53(4):609–619.

Viant, M. R., Rosenblum, E. S., and Tjeerdema, R. S. (2003). NMR-Based Metabolomics: A powerful approach for characterizing the effects of environmental stressors on organism health. *Environmental Science & Technology*, 37(21):4982–4989.

Vilchis, L. I., Tegner, M. J., Moore, J. D., Friedman, C. S., Riser, K. L., Robbins, T. T., and Dayton, P. K. (2005). Ocean Warming Effects on Growth, Reproduction, and Survivorship of Southern California Abalone. *Ecological Applications*, 15(2):469–480.

Vosloo, A., Laas, A., and Vosloo, D. (2013a). Differential responses of juvenile and adult South African abalone (*Haliotis midae* Linnaeus) to low and high oxygen levels. *Comparative biochemistry and physiology. Part A, Molecular & integrative physiology*, 164(1):192–9.

Vosloo, D., van Rensburg, L., and Vosloo, A. (2013b). Oxidative stress in abalone: The role of temperature, oxygen and l-proline supplementation. *Aquaculture*, 416-417:265–271.

Vosloo, D., Vosloo, A., Morillion, E. J., Samuels, J. N., and Sommer, P. (2013c). Metabolic readjustment in juvenile South African abalone (*Haliotis midae*) acclimated to combinations of temperature and dissolved oxygen levels. *Journal of Thermal Biology*, 38(7):458–466.

Walther, K., Sartoris, F. J., Bock, C., and Pörtner, H. O. (2009). Impact of anthropogenic ocean acidification on thermal tolerance of the spider crab *Hyas araneus*. *Biogeosciences*, 6(10):2207–2215.

Wells, R. M. and Baldwin, J. (1995). A comparison of metabolic stress during air exposure in two species of New Zealand abalone, *Haliotis iris* and *Haliotis australis*: implications for the handling and shipping of live animals. *Aquaculture*, 134(3-4):361–370.

Wells, R. M. G., Baldwin, J., Speed, S. R., and Weber, R. E. (1998). Haemocyanin function in the New Zealand abalones *Haliotis iris* and *H. australis*: relationships between oxygen-binding properties, muscle metabolism and habitat. *Marine and Freshwater Research*, 49(2):143.

White, R. L. (1983). Effects of Acute Temperature Change and Acclimation Temperature on Neuromuscular Function and Lethality in Crayfish. *Physiological Zoology*, 56(2):174–194.

Whitehead, A. (2012). Comparative genomics in ecological physiology: toward a more nuanced understanding of acclimation and adaptation. *Journal of Experimental Biology*, 215(6):884–891.

Windisch, H. S., Frickenhaus, S., John, U., Knust, R., Pörtner, H. O., and Lucassen, M. (2014). Stress response or beneficial temperature acclimation: Transcriptomic signatures in Antarctic fish (*Pachycara brachycephalum*). *Molecular Ecology*, 23(14):3469–3482.

Windisch, H. S., Kathover, R., Portner, H. O., Frickenhaus, S., and Lucassen, M. (2011). Thermal acclimation in Antarctic fish: transcriptomic profiling of metabolic pathways. *AJP: Regulatory, Integrative and Comparative Physiology*, 301(5):R1453–R1466.

Wu, H., Southam, A. D., Hines, A., and Viant, M. R. (2008). High-throughput tissue extraction protocol for NMR- and MS-based metabolomics. *Analytical Biochemistry*, 372(2):204–212.

Zittier, Z. M., Bock, C., Lannig, G., and Pörtner, H. O. (2015). Impact of ocean acidification on thermal tolerance and acid–base regulation of *Mytilus edulis* (L.) from the North Sea. *Journal of Experimental Marine Biology and Ecology*, 473:16–25.

APPENDIX A

QUALITY ASSESMTEMNT OF THE *H. fulgens* TRANSCRIPTOME ASSEMBLY

Quality of the raw paired end sequences was assessed with fastQC v.0.10.01 (Andrews, 2012) resulting in 31,022,126 sequences with a minimum length of 35 and maximum of 301 (Fig. S2A-B; Table SI). After sequence processing with Trimmomatic-0.30 (Bolger et al., 2014); see Publication III for parameters, final quality of the sequences increased (Fig. S2C-D) and the number of sequences was reduced to 27,783,263 with a minimum sequence length of 50 and maximum of 291 (Table SI).

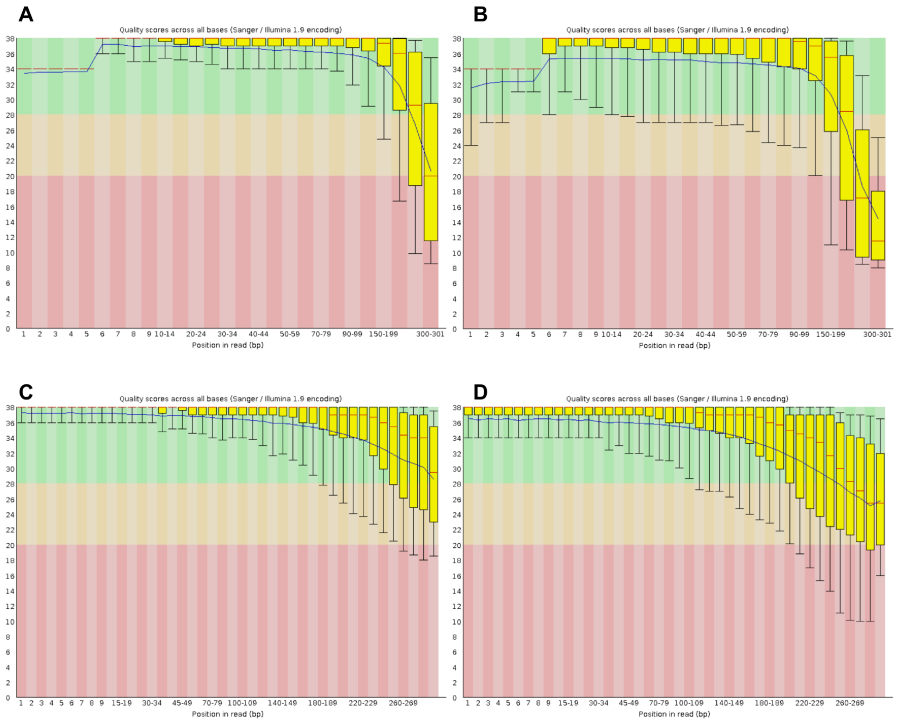

Figure A.1 Quality control of the paired end raw sequences (A-B) and paired end trimmed sequences (C-C).

After filtering for low abundance contigs and removing redundant sequences (see Publication III for details), the resulting transcriptome assembly contained 95,098 contigs with an average length of 704.44 and N50 of 1,134. Such values fall in the range of published de novo transcriptomes for other abalone and mollusk species (Table SII).

Table A.1 Quality control of the raw and trimmed sequences

Sequencing statistics	Raw data	Trimmed data
Total sequences	31, 022, 126	27, 783, 263
Minimum sequence length	35	50
Maximum sequence length	301	291
%GC	43	42

APPENDIX B

de novo TRANSCRIPTOME ASSEMBLY VALIDATION

Comparative table of *H. fulgens* asssembly with other *Haliotis* and similar species.

Table B.1 Summary of transcriptome assemblies for abalone and other mollusk species

Species	Taxonomy	Sequencer	Assembler	N50	Mean Length (BP)	Number of contigs	Reference
H. fulgens	Gastropoda	Illumna MiSeq	Trinita 2.0.4	1,134	704.4	95, 098	This study
H. midae	Gastropoda	454 GS FLX (Roche)	CLC Genomic Workbench v.7	NA	379	31,491	1
H. diversicolor	Gastropoda	454 GS FLX (Roche)	Newbler v.2.3	NA	300.1	9,567	2
H. laevigata	Gastropoda	Illumina Hiseq2000	Trinity 10.5.2012	1,313	NA	104,885	3
H. midae	Gastropoda	Illumina GAIIx	CLC Genomic Workbench v.4	356	260	21,761	4
H. rufescens	Gastropoda	454 GS FLX (Roche)	CLC Genomic Workbench v.7	910	790	44, 312	5
Reishia clavigera	Gastropoda	Illumina GAIIx	Trinity 10.25.2012	582	499	197,324	6
Nerita elanotragus	Gastropoda	PGM	Trinity	258	293	10, 886	7
Patinopecten yessoensis	Bivalvia	Illumina Hiseq2000	Trinity	2,296	1,120	135, 963	8
Cyclina snensis	Bivalvia	Illumina MiSeq	Trinity 2013.06.08	1,670	980	70, 079	9

References:

1. Picone B, Rhode C, Roodt-Wilding R. Transcriptome profiles of wild and cultured South African abalone, *Haliotis midae*. *Mar Genomics*. 2015;20(January):3-6.

2. Huang ZX, Chen Z Sen, Ke CH, et al. Pyrosequencing of *Haliotis diversicolor* Transcriptomes: Insights into Early Developmental Molluscan Gene Expression. *PLoS One*. 2012;7(12):1-12.

3. Shiel BP, Hall NE, Cooke IR, Robinson NA, Strugnell JM. De Novo Characterisation of the Greenlip Abalone Transcriptome (*Haliotis laevigata*) with a Focus on the Heat Shock Protein 70 (HSP70) Family. *Mar Biotechnol*. 2015;17(1):23-32. doi:10.1007/s10126-014-9591-y.

4. Franchini P, van der Merwe M, Roodt-Wilding R. Transcriptome characterization of the South African abalone *Haliotis midae* using sequencing-by-synthesis. *BMC Res Notes*. 2011;4(1):59.

5. Valenzuela-Miranda D, Del Río-Portilla MA, Gallardo-Escárate C. Characterization of the growth-related transcriptome in California red abalone (*Haliotis rufescens*) through RNA-Seq analysis. *Mar Genomics*. 2015;24(MAY):199-202.

6. Nam BH, Jung M, Subramaniyam S, et al. Transcriptome analysis revealed changes of multiple genes involved in *Haliotis discus hannai* innate immunity during vibrio parahemolyticus infection. *PLoS One*. 2016;11(4):1-16.

7. Amin S, Prentis PJ, Gilding EK, Pavasovic A. Assembly and annotation of a non-model gastropod (*Nerita melanotragus*) transcriptome: a comparison of De novo assemblers. *BMC Res Notes*. 2014;7(1):488. doi:

8. Sun X, Yang A, Wu B, Zhou L, Liu Z. Characterization of the mantle transcriptome of Yesso scallop (*Patinopecten yessoensis*): Identification of genes potentially involved in biomineralization and pigmentation. *PLoS One*. 2015;10(4):

9. Pan B, Ren Y, Gao J, Gao H. De novo RNA-seq analysis of the venus clam, *cyclina sinensis*, and the identification of immune-related genes. *PLoS One*. 2015;10(4):1-13.

ACKNOWLEDGEMENTS

My sincere gratitude to Prof. Hans O. Pörtner for the opportunity to develop my work in the group despite our littler previous interaction, and for all the fruitful discussion and advice along these years. To Magnus Lucassen, for his great support and guidance through practical and theoretical work, and especially, his trust in me to develop my own ideas.

To Christian Bock, for his guidance during all my metabolomics analysis, which was a completely new world for me. I'm also especially gratefully to Gisela Lannig for all her support, the teaching, and for all the positive thoughts during my most stressful moments.

Furthermore, I would like to thank the technicians from the Integrative Ecophysiology section for all the support and invaluable help through the different aspects of my thesis: To Rolf Wittig for his assistance during my NMR analysis; to Isabel Ketelesen for helping me during my very first approach to measure metabolic rate; to Anette Tillman for her advises during my work in the Extraction- and Cell- labs; to Jutta Jörgens for her support during the library construction; to Nils Kochnik for his support and assistance in pretty much all the aspects of my work; and last but not least, to Fredy Velez for his huge support in- and outside the Institute. Gracias, compadre!

To the Ph.D. students from the section: Khadda, Lena, Laura, Basti, and Flemming for the discussions, language translations, and friendship through all these years. Special thanks to the ghosts from the IEP, Kristina and Elettra, for the warm company during the late hours work.

I would like to thank Teresa Sicard and Salvador Lluch for making it possible to get live animals for the project and for their support during my work in Mexico. To Gilberto González Soriano and Julio Félix Dominguez for their assistance in the experimental set-up, and to Rosa Linda Salgado García for her huge help during the experiments and transport of the frozen samples to Germany. I would like to thank Martín Gerardo Ruíz, from the Sociedad Cooperativa de Producción Pesquera de Bahía Tortugas, S.C. de R.L. and their personnel for kindly providing the animals for the project.

I thank my family for their unconditional support and motivation and for always being there for me.

To my wife, for accepting this challenge with me and being there by my side all the time, despite the distance.

Financial support during my stay in Germany was granted by the Deutscher Akademischer Austauschdienst (DAAD), Program 57076385

Erklärung

Miguel A. Tripp Valdez
Priv. Paraiso 738
La Paz, Baja California Sur
Mexico

La Paz, Baja California Sur, Mexico. 05.11.2018

Erklärung gemäß § 6(5) der Promotionsordnung der Universität Bremen für die mathematischen, natur-und ingenieurwissenschaftlichen Fachbereiche

Hiermit erkläre ich, Miguel A. Tripp Valdez, dass ich die Arbeit mit dem Titel:

"**Effects of hypoxia and hypercapnia on thermal tolerance: an integrative assessment on the green abalone (*Haliotis fulgens*).**"

1. Ohne unerlaubte fremde Hilfe angefertigt habe.
2. Keine anderen als die von mir angegebenen Quellen und Hilfsmittel benutzt habe.
3. Die den benutzen Werken wörtlich oder inhaltlich entnommenen Stellen als solche kenntlich gemacht habe.

Miguel Ángel Tripp Valdez